Geometry, Kinematics, and Rigid Body Mechanics in Cayley-Klein Geometries

vorgelegt von
"Master of Science" Mathematiker
Charles Gunn
Portsmouth, Virginia, USA

Von der Fakultät II - Mathematik und Naturwisssenschaften
der Technischen Universität Berlin
zur Erlangung des akademischen Grades
Doktor der Naturwissenschaften

genehmigte Dissertation

Promotionsausschuss:

Vorsitzender: Prof. Dr. Stefan Felsner
Berichter/Gutachter: Prof. Dr. Ulrich Pinkall
Berichter/Gutachter: Prof. Dr. Johannes Wallner

Tag der wissenschaftlichen Aussprache: 21 September, 2011

Berlin 2011
D 83

Preface

This thesis arose out of a desire to understand and simulate rigid body motion in 2- and 3-dimensional spaces of constant curvature.The results are arranged in a theoretical part and a practical part. The theoretical part first constructs necessary tools – a family of real projective Clifford algebras – which represent the geometric relations within the above-mentioned spaces with remarkable fidelity. These tools are then applied to represent kinematics and rigid body dynamics in these spaces, yielding a complete description of rigid body motion there. The practical part describes simulation and visualization results based on this theory.

Historically, the contents of this work flow out of the stream of 19^{th} century mathematics due to Chasles, Möbius, Plücker, Klein, and others, which successfully applied new methods, mostly from projective geometry, to the problem of rigid body motion. The excellent historical monograph [Zie85] coined the name *geometric mechanics* expressly for this domain[1]. Its central concepts belong to the geometry of lines in three-dimensional projective space. The theoretical part of the thesis is devoted to formulating and occasionally extending these concepts in a modern, metric-neutral way using the real Clifford algebras mentioned above.

Autobiographically, the current work builds on previous work ([Gun93]) which explored visualization of three-dimensional manifolds modeled on one of these three constant curvature spaces. The dream of extending this geometric-visualization framework to include physics in these spaces – analogous to how in the past two decades the mainstream euclidean visualization environments have been gradually extended to include physically-based modeling – was a personal motivation for undertaking the research which led to this thesis.

[1] although today there are other meanings for this term.

Audience

The thesis is written with a variety of audiences in mind. In the foreground is the desire to present a rigourous, self-contained, metric-neutral elaboration of the mathematical results, both old and new. It is however not written for the specialist alone. For those interested only in the euclidean theory I have attempted to make it accessible to readers without background or interest in the non-euclidean thread. To be self-contained, many preliminary results from projective geometry and linear and multi-linear algebra are stated, with references to proofs in the literature. To be accessible, most of the results are stated and proved only for the dimensions $n = 2$ and $n = 3$, even when a general proof might present no extra difficulty. The exposition includes many examples, particularly euclidean ones, in which the reader can familiarize himself with the content. I have attempted at the ends of chapters to provide a guide to original literature for those interested in exploring further. Finally, as a firm believer in the value of pictures, I have tried to illustrate the text wherever possible.

Outline

Chapter 1 introduces the important themes of the thesis via the well-known example of the Euler top, and shows how by generalizing the Euler top one is led to the topic of the thesis. In addition to reviewing the key ingredients of rigid body motion, it contrasts the historical approaches of Euler and Poinsot to the problem, and relates these to the approach taken here. It discusses the appropriate algebraic representation for the mathematical problems being considered. It shows how quaternions can be used to represent the Euler top, and specifies a set of properties which an algebraic structure should possess in order to serve the same purpose for the extended challenge posed by the thesis.

Chapter 2 introduces the non-metric foundations of the thesis. The geometric foundation is provided by real projective geometry. From this is constructed the Grassmann, or exterior, algebra, of projective space. A distinction is drawn between the Grassmann algebra and its dual algebra; the latter plays a more important role in this thesis than the former. We discuss Poincaré duality, which yields an algebra isomorphism between these two algebras, allowing access to the exterior product of the one algebra within the dual algebra without any metric assumptions.

Chapter 3 introduces the mathematical prerequisites for metric geometry. This begins with a discussion of quadratic forms in a real vector space V and associated quadric surfaces in projective space $\mathbf{P}(\mathsf{V})$. A class of *admissable* quadric surfaces are identified – which include non-degenerate and "slightly" degenerate quadric surfaces – which form the focus of the the subsequent development.

Chapter 4 begins with descriptions of how to construct the elliptic, hyperbolic, and euclidean planes using a quadric surface in $\mathbb{R}P^2$ (also known as a conic section in this case), before turning to a more general discussion of Cayley-Klein spaces and Cayley-Klein geometries. We establish results on Cayley-Klein spaces based on the admissable

quadric surfaces of Chapter 3 – which are amenable to the techniques described in the rest of the thesis.

In Chapter 5 the results of the preceding chapters are applied to the construction of real Clifford algebras, combining the outer product of the Grassmann algebra with the inner product of the Cayley-Klein space. We show that for Cayley-Klein spaces with admissable quadric surfaces, this combination can be successfully carried out. For the 3 Cayley-Klein geometries in our focus, we are led to base this construction on the *dual* Grassmann algebras. We discuss selected results on $n-$dimensional Clifford algebras before turning to the 2- and 3-dimensional cases.

Chapter 6 investigates in detail the use of the Clifford algebra structures from Chapter 5 to model the metric planes of euclidean, elliptic, and hyperbolic geometry.[2] The geometric product is exhaustively analyzed in all it variants. Following this are metric-specific discussions for each of the three planes. The implementation of direct isometries via conjugation operators with special algebra elements known as rotors is then discussed, and a process for finding the logarithm of any rotor is demonstrated. A typology of these rotors into 6 classes is introduced based on their fixed point sets.

Taking advantage of the results of Chapter 6 wherever it can, Chapter 7 sets its focus on the role of non-simple bivectors, a phenomenon not present in 2D, and one which plays a pervasive role in the 3D theory. This is introduced with a review of the line geometry of $\mathbb{R}P^3$, translated into the language of Clifford algebras used here. Classical results on line complexes and null polarities – both equivalent to bivectors – are included. The geometric products involving bivectors are exhaustively analyzed. Then, the important 2-dimensional subalgebra consisting of scalars and pseudoscalars is discussed and function analysis based on it is discussed. Finally, the *axis* of a rotor is introduced and explored in detail. These tools are then applied to solve for the logarithm of a rotor in the 3D case also. We discuss the exceptional isometries of Clifford translations (in elliptic space) and euclidean translations in detail. Finally, we close with a discussion of the continuous interpolation of a metric polarity. We demonstrate a solution which illustrates the power and flexibility of these Clifford algebra to deal with challenging geometric problems.

Having established and explored the basic tools for metric geometry provided by these algebras, Chapter 8 turns to kinematics. The basic object is an isometric motion: a continuous path in the rotor group beginning at the identity. Taking derivatives in this Lie group leads us to the Lie algebra of bivectors. The results of Chapter 7 allow us to translate familiar results of Lie theory into this setting with a minimum of machinery. We analyse the vector field associated to a bivector, considered as an instantaneous velocity state. In deriving a transformation law for different coordinate systems we are led to the Lie bracket, in the form of the commutator product of bivectors. Finally, for noneuclidean metrics, we discuss the dual formulation of kinematics in which the role of point and plane, and of rotation and translation, are reversed.

The final theoretical chapter, Chapter 9, treats rigid body dynamics in the 3D setting. This begins with a metric-neutral treatment of statics. Movement appears via newtonian particles, whose velocity and impulse are defined in a metric-neutral way purely in terms

[2] The decision to begin with the 2D case rather directly with the 3D was based on the conviction that this path offers significant pedagogical advantages due to the unfamiliarity of many of the underlying concepts.

of bivectors and the metric quadric. Rigid bodies are introduced as collections of such particles. The inertia tensor is defined and shown to be a symmetric bilinear form on the space of bivectors. We introduce a second Clifford algebra, on the space of bivectors, whose inner product is derived from this inertia tensor. We derive Euler equations for rigid body motion, and indicate how to solve them. Finally, we discuss the role of external forces and discuss work and power in this context.

Chapter 10 provides a brief introduction to dual euclidean geometry and its associated Clifford algebra. It begins by showing that the set of four geometries: euclidean, dual euclidean, elliptic and hyperbolic, form an unified family closed under dualization. It compares the dual euclidean plane to the euclidean plane via some elementary examples, and indicates some interesting research possibilities for this geometry.

Once these theoretical results have been established, experimental results based on this theory are presented in Chapter 11. The focus is on the non-euclidean spaces, with the euclidean results being mainly useful as quality control. First the two-dimensional case is handled. A variety of qualitative behaviors are presented and discussed with reference to the theoretical results already presented. Then the three-dimensional case is handled, and some behaviors not seen in the 2D case are shown and discussed. The presentation of these results is accompanied by a description of visualization strategies and tools developed to assist in the presentation and analysis of the results, in both 2D and 3D.

The concluding chapter, Chapter 12, reflects on the results presented and provides an overview of innovative aspects, ranging from concrete to methodological.

Acknowledgements

This work owes its existence to many people, a few of whom I want to thank by name: my parents, Charles and Virginia† Gunn, encouraged me to develop my inborn interests and supported me in countless ways; Thomas Brylawski, Ph. D., (1944-2007), Professor of Mathematics at the University of North Carolina at Chapel Hill, was the advisor of my master's project there and tireless encourager of my slumbering capacities; and my wife Edeltraud and daughter Lucia, who have patiently accompanied me on the odyssey of this thesis over the past 8 years. I wish to thank my thesis advisor Ulrich Pinkall for his expert and tolerant guidance. Also, without support from the DFG Research Center Matheon in the academic year 2010-2011, the thesis would not have been possible in its present form.

Finally, thanks to all the mathematicians living and dead whose works flowed into this project. Most of the better parts of this thesis are certainly due to their impulses; the parts due to me will have served their purpose if they bring these impulses a step further in a scientific sense and a step wider, to a larger audience.

Berlin, August, 2011

Contents

Chapter 1
Preview: the Euler Top

One of the main goals of this thesis, as sketched in the Forward, is to provide a modern understanding of rigid body motion in the 3-dimensional non-euclidean spaces of elliptic and hyperbolic geometry. A natural starting point for this investigation is provided by the well-known example of the *Euler top*, one of the simplest non-trivial examples of rigid body motion. This is a rigid body in three-dimensional euclidean space, constrained to move around its center of mass, and not subject to any external forces. Not only does this example serve to identify the key components of the analysis of rigid body motion; we will show below (Sect. 9.5.2) that the content of this thesis is a natural extension of the Euler top when one removes the constraint that the motion has a fixed point. Furthermore, the differing approaches to the Euler top represented by Euler and Poinsot, also throws an important light on the choice of methods adopted in this thesis.

The discussion here is not intended to be mathematically rigorous. Readers for which the material is unfamiliar are encouraged to consult standard literature on rigid body mechanics such as [Arn78], Ch. 2. Proofs for all the results presented here can also be obtained from the thesis itself by re-introducing the constraint that the center of mass is fixed by the motion. See Section Sect. 9.5.2 for details. A much fuller account of the historical details presented here can be found in [Zie85].

1.1 Euler and the analytic approach

The question of rigid body mechanics entered the mathematical literature with the investigations of Euler and d'Alembert (working separately around 1760) [Zie85]. The problem which they solved was: given the mass distribution of the rigid body and its initial velocity, to find a path in the isometry group $SO(3)$ of rotations of $\mathbb{R}^3$, which describes the position of the body at each subsequent moment of time. Each obtained a complete description of the motion of an Euler top as the solution of a set of ordinary differential equations. The differential equations for the instantaneous velocity of the object became known as *Euler equations* of the motion. Lagrange (1788) introduced a more abstract setting in which the motion of the Euler top could be solved.

The key feature of all the analytic approach is that attention is focused on the isometry group of the rigid body rather than on the ambient space of the rigid body.[1] This is easy to overlook since the dimension of both spaces in the case of the Euler top is 3. As a result, the analytic solution does not immediately provide any detailed description of how the motion proceeds within the ambient space of the body.

1.1.1 Poinsot and the geometric approach

This unsatisfactory state of affairs was addressed and remedied by Poinsot in [Poi51] (English translation [Poi84]), based on a work first presented in 1834. This work, made possible by the dramatic developments in geometry at the turn of the 19^{th} century notably in the school led by Monge (1746-1818), is based on a geometric approach, in contrast to the analytic approach pioneered by Euler and Lagrange. Poinsot first describes his dissatisfaction with the results of the analytic approach:

> ...it must be allowed, that in all these solutions [of Euler, d'Alembert, and Lagrange], we see nothing but calculations, without having any clear idea of the rotation of the body. We may be able by calculations, more or less long and complicated, to determine the place of the body at the end of a given time; but we do not see at all how it arrives there. [[Poi84], p. 2]

and goes on to describe his alternative approach and its advantages:

> Therefore to furnish a clear idea of this rotatory motion, hitherto unrepresented, has been the object of my endeavors. The result is an entirely new solution to the problem of [the Euler top]: a genuine solution, inasmuch as it is palpable, and enables us to follow the motion of the body as clearly as the motion of a point. And if we would pass from this geometrical representation to calculation ... the formulae required for the purpose are direct and simple, each of them expressing a dynamical theorem of which we have a clear idea, and which proceeds at once to its object. [[Poi84], p. 3]

Finally, Poinsot reflects on the success of his method as being a result of a particular penetration of the phenomena with exactly the correct mathematical concepts:

> For we may remark generally of our mathematical researches, that these auxiliary quantities, these long and difficult calculations into which we are often drawn, are almost always proofs that we have not in the beginning considered the objects themselves so thoroughly and directly as their nature requires, since all is abridged and simplified, as soon as we place ourselves in a right point of view. [[Poi84], p. 4]

From this we can infer that the distinction between his method and that of his predecessors is not only *geometric vs. analytic*; it is just as much *concrete vs. abstract*. Poinsot's achievement is based on his focusing on the concrete conditions of the Euler top, and out of these concrete conditions, deriving a description that avoids the complexities inherent in the more abstract approach of Euler and Lagrange. His method is more comprehensive than the analytic one, since using it he was able to derive all the results obtained by Euler and Lagrange for the Euler top, but the opposite is not true.

---

[1] This is a modern formulation; the group concept had not yet been introduced in the 18^{th} century.

1.2 Ingredients of the motion of the Euler top

Before proceeding further we provide a quick review of the ingredients of these solutions of the Euler top. Fig. 1.1 shows a diagramatic representation of an Euler top at a particular instant of its motion. In this case the rigid body is represented by the yellow wireframe box, and consists of 8 particles positioned at the corners of the box. That it is a *rigid* body means that the distances of all particle pairs remains fixed under the motion. The other elements in the figure will be discussed in the subsequent discussion of Poinsot's contributions.

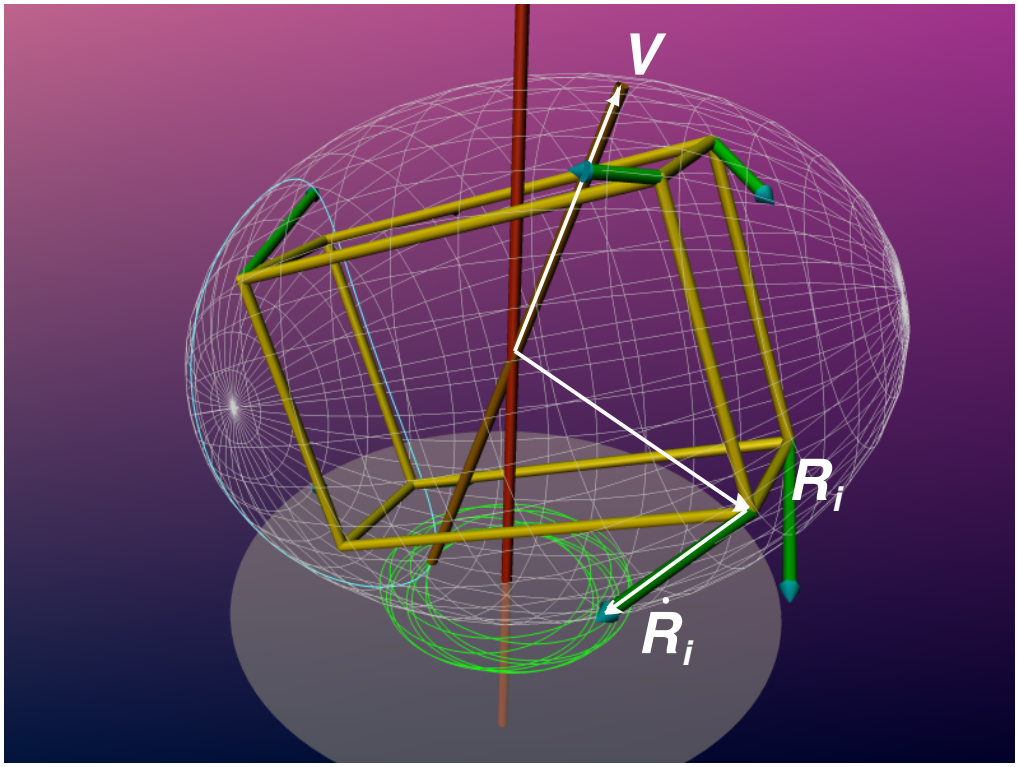

Fig. 1.1 The angular velocity $\mathbf{V}$ determines the linear velocity $\dot{\mathbf{R}}_i$ of the particle of the rigid body located at position $\mathbf{R}_i$.

The instantaneous motion of an Euler top is a rotation around an axis passing through the fixed point. Such an element is called an *angular velocity* and is represented by the bronze axis labeled $\mathbf{V}$. This angular velocity imparts to each particle $\mathbf{R}_i$ a direction and intensity of motion represented by the vector $\dot{\mathbf{R}}_i := \mathbf{V} \times \mathbf{R}_i$. The angular momentum of the particle is then obtained by $\mathbf{M}_i := m_i \mathbf{R} \times \dot{\mathbf{R}}_i$ where m_i is the mass of the particle at $\mathbf{R}_i$. One also defines the kinetic energy of the particle as $E_i := \frac{m}{2} \|\dot{\mathbf{R}}_i\|^2$. The absence of external forces implies that both $\mathbf{M}_i$ as well as E_i is a conserved quantity.

When one sums over all the particles in the body, one obtains aggregate momentum and kinetic energy for the body:

$$\mathbf{M} = \sum_i \mathbf{M}_i, \qquad E := \sum_i E_i$$

These are naturally also conserved quantities.

Expanding out the summation for the energy yields an expression which depends quadratically on the angular velocity $\mathbf{V}$. One can express this dependence in a symmetric bilinear form $\mathbf{A}$, the *inertia tensor* of the body, and arrive at the formula $E = \mathbf{A}(\mathbf{V}, \mathbf{V})$. This in turn provides a similar form for the momentum: $\mathbf{M} = \mathbf{A}(\mathbf{V})$. Here, the occurrence of $\mathbf{A}$ represents the *polarizing* operator associated to a symmetric bilinear form. This shows that the momentum is a dual vector with respect to the angular velocity.

By considering the fact that the momentum is conserved, one can derive the Euler equations for the angular velocity in the body:

$$\dot{\mathbf{V}}_c = \mathbf{A}^{-1}(\mathbf{V}_c \times \mathbf{M}_c) \tag{1.1}$$

To obtain the motion of the rigid body as a path $\mathbf{g}$ in the Lie group $SO(3)$, the rotations of $\mathbb{R}^3$, one can then integrate $\dot{\mathbf{g}}$ using the relation $\dot{\mathbf{g}} = \mathbf{g}\mathbf{V}_c$.

1.2.1 Poinsot description

The description above essentially reflects the thought-process of the Euler approach to the Euler top. [Poi51] provides a much fuller geometric description of this motion. The elements of this description are shown in Fig. 1.2. The angular velocity is assumed to be given. Then the angular momentum, defined as above by $\mathbf{M} = \mathbf{A}(\mathbf{V})$ is an element of the dual space, hence a plane; it is traditionally represented by the normal direction of this plane, in this case, the red vertical axis. For a given choice of $\mathbf{M}$, the set of all angular velocity $\mathbf{V}$ which yield the same kinetic energy E is a quadric surface called by Poinsot the *inertia ellipsoid*. It is shown as a white wireframe ellipsoid in the figure.

Poinsot provides a geometric understanding of how the angular velocity and angular momentum evolve in $\mathbb{R}^3$. The path of the angular velocity vector, as the rigid body moves, is called by Poinsot the *polhode* of the motion. Since the energy E is conserved, the polhode is constrained to lie on the surface of the inertia ellipsoid. On the other hand, conservation of the momentum vector in space implies conservation of its length in body coordinate system: $\|\mathbf{A}(\mathbf{V})\| = k$, which represents another, confocal ellipsoid. Hence the polhode is the intersection of these two ellipsoids, a closed quartic curve on the inertia ellipsoid. It is the cyan curve in the figure.

In the world coordinate system, where the momentum is fixed, the condition that $\langle \mathbf{V}, \mathbf{M} \rangle = E$ represents a plane perpendicular to the angular momentum, called by Poinsot the *invariant plane*, which appears in gray at the bottom of the figure. The green curve in the invariant plane is the path of the angular velocity in the world coordinate system, and was called by Poinsot the *herpolhode*. As the body moves, the angular velocity vector traces out the polhode on the inertia ellipsoid and the herpolhode on the

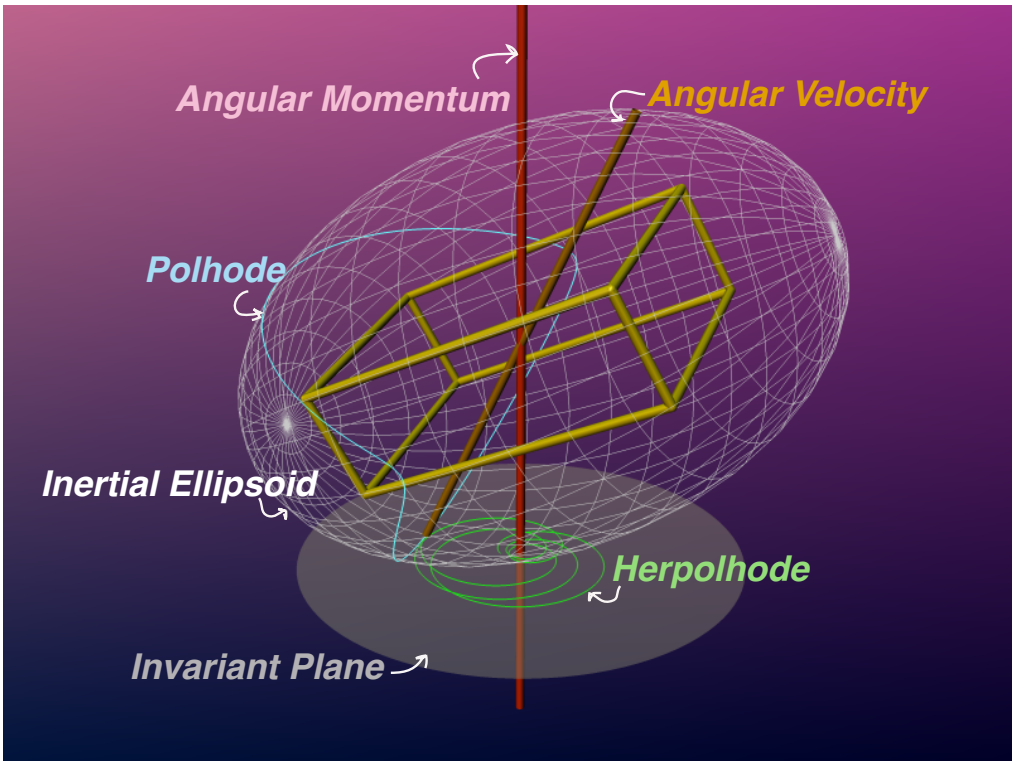

Fig. 1.2 The Poinsot description of the motion provides geometric interpretation to the elements of the analytic description of the motion.

invariant plane. This means that the inertia ellipsoid rolls on the invariant plane during the motion, its point of contact being the current angular velocity. The herpolhode is a quasi-periodic curve that, generically, fills in an annulus of the invariant plane, where the inner (outer) boundary circle of the annulus corresponds to angular velocities with minimum (maximum) speed.

1.2.2 Generalizing the Euler top

One obtains the theme of this thesis if one replaces the condition that the body has a fixed point, with the condition that the body is free to move in a (3-dimensional) space of constant curvature. The details of this claim are established in the introductory chapters of the thesis, where it is shown that there are three such spaces – euclidean, elliptic, and hyperbolic space. Furthermore, the isometry groups of these spaces are all 6-dimensional Lie groups which contain $SO(3)$ as a subgroup.

[Arn78], Appendix 2, provides a methodology to deduce and solve the Euler equations for rigid body motion in an abstract setting which includes the three spaces above. Arnold's approach works with any Lie group; the role of the inertia tensor is taken over

by a left-invariant metric on the corresponding Lie algebra. That is, if one has an inertia tensor, one obtains such a left-invariant metric; but one can in fact work with the wider class of left-invariant metrics and obtain and solve ODE's. This is a useful approach for a first solution.

However, all the objections raised by Poinsot to the analytic approach apply here to the Arnold approach. All the calculations take place in the 6-dimensional spaces of the Lie group and the Lie algebra. There is, *a priori*, no geometric insight into how the motion unfolds in the underlying 3-dimensional space where the rigid body and the observer are at home. Due to this limitation, the current thesis adopts the attitude of Poinsot, and sets the goal of providing a geometric description of the rigid body motion which as much as possible refers to geometric entities in the underlying 3-dimensional space where the motion occurs.

1.3 Algebraic representation

The goal of providing a Poinsot description of rigid body motion brings with it the question of what mathematical representation is best-fitted to achieve that goal. The historical work of Euler and Poinsot preceded the development of modern algebra. The majority of the current literature on rigid body motion employs linear algebra to represent the isometry groups and their action on the points of the ambient space of the body. The current work departs from that trend in its use of geometric (or Clifford) algebra for that purpose. The best way to motivate this choice is to return to the example of the Euler top and show how *quaternions* can be profitably used to model the rigid body motion. Then, after this excursion, we discuss the ways this algebraic structure needs to be extended to handle the spaces considered by this thesis.

1.3.1 Quaternions

William Rowan Hamilton discovered quaternions in 1843. Our aim here is not to provide an exhaustive account of quaternions, but just to present enough results to indicate the direction followed in the sequel.

Recall some facts about quaternions. Begin with $\mathbb{R}^4$ with basis $\{\mathbf{1}, \mathbf{i}, \mathbf{j}, \mathbf{k}\}$. Introduce a product structure on the basis elements:

$$\begin{gathered}\mathbf{1}^2 = 1; \quad \mathbf{i}^2 = \mathbf{j}^2 = \mathbf{k}^2 = -1 \\ \mathbf{1} \text{ commutes with } \mathbf{i}, \mathbf{j}, \text{ and } \mathbf{k}. \\ \mathbf{ij} = -\mathbf{ji}, \quad \mathbf{jk} = -\mathbf{kj}, \quad \mathbf{ki} = -\mathbf{ik}\end{gathered}$$

Extend this product by linearity to all of $\mathbb{R}^4$. This yields an associative, non-commutative algebra called the quaternions, written $\mathbb{H}$. $\mathbf{1}$ is the identity element.

Definition 1. For a quaternion $\mathbf{a} := a_0\mathbf{1} + a_1\mathbf{i} + a_2\mathbf{j} + a_3\mathbf{k}$:

- $\mathbf{a}_s := a_0\mathbf{1}$ is the *scalar* part of $\mathbf{a}$.

- $\mathbf{a}_v := a_1\mathbf{i} + a_2\mathbf{j} + a_3\mathbf{k}$ is the *vector* part of $\mathbf{a}$.
- If $\mathbf{a} = \mathbf{a}_v$, $\mathbf{a}$ is an *imaginary* quaternion; the set of imaginary quaternions is denoted $\mathbb{IH}$.
- For $\mathbf{a} = \mathbf{a}_s + \mathbf{a}_v$, $\overline{\mathbf{a}} := \mathbf{a}_s - \mathbf{a}_v$ is called the *conjugate* of $\mathbf{a}$.
- $\mathbf{a} \cdot \mathbf{b} = \mathbf{a}\overline{\mathbf{b}}$ is the *inner product* of $\mathbf{a}$ and $\mathbf{b}$.
- For non-zero $\mathbf{a}$, $\mathbf{a}^{-1} := \dfrac{\overline{\mathbf{a}}}{\mathbf{a} \cdot \mathbf{a}}$ is the *inverse* of $\mathbf{a}$.
- $\|\mathbf{a}\| := \sqrt{\mathbf{a}\overline{\mathbf{a}}}$ is the *norm* of $\mathbf{a}$.
- If $\|\mathbf{a}\| = 1$, $\mathbf{a}$ is a *unit* quaternion.

Remark 2. Verify that the definitions make sense. $\mathbf{a} \cdot \mathbf{b} \in \mathbb{R}\mathbf{1}$. The inverse satisfies $\mathbf{a}^{-1}\mathbf{a} = \mathbf{a}\mathbf{a}^{-1} = 1$.

The set of unit quaternions can be identified with the 3-dimensional sphere $\mathbf{S}^3$. We identify $\mathbb{IH}$ with $\mathbb{R}^3$ in the obvious way.

Let $\cdot$ and $\times$ be the inner and cross products, resp., on $\mathbb{R}^3$. Then for $\mathbf{g}, \mathbf{h} \in \mathbb{IH}$ one can verify directly that:

$$\mathbf{g}\mathbf{h} = -\mathbf{g} \cdot \mathbf{h} + \mathbf{g} \times \mathbf{h}$$

Thus, the quaternion product combines the inner product with the cross product of $\mathbb{R}^3$.

A unit quaternion $\mathbf{g}$ can be written as $\cos\theta + \sin\theta(\mathbf{u})$ where $\mathbf{u}$ is a unit imaginary quaternion satisfying $\mathbf{u}^2 = -1$. Then evaluate the exponential function as a power series to obtain:

$$\mathbf{g} = e^{\theta\mathbf{u}}$$

For $\theta \in [0, 2\pi)$, this is a bijective mapping $\mathbb{IH} \leftrightarrow \mathbf{S}^3$.

Consider the product $\underline{\mathbf{g}}(\mathbf{x}) := \mathbf{g}\mathbf{x}\mathbf{g}^{-1} = \mathbf{g}\mathbf{x}\overline{\mathbf{g}}$ for unit quaternion $\mathbf{g}$ and imaginary quaternion $\mathbf{x}$. Write $\mathbf{g} = \cos\theta + \sin\theta(\mathbf{u})$. Then one can show that $\underline{\mathbf{g}}$ is a rotation of $\mathbb{R}^3$ around the axis $\mathbf{u}$ of an angle 2θ. Under this mapping, $\underline{\mathbf{g}}$ and $\underline{-\mathbf{g}}$ give the same rotation. Hence, one obtains a map:

$$\mathbb{IH} \xrightarrow{e \text{ (1:1)}} \mathbf{S}^3 \xrightarrow{\underline{\mathbf{g}} \text{ (2:1)}} SO(3)$$

We review the prominent features of the configuration described above:

I. The quaternion product $\mathbf{g}\mathbf{h}$ combines a symmetric and an anti-symmetric part.
II. $\mathbb{IH}$ is a vector subspace of $\mathbb{H}$, and $\mathbf{S}^3$ is a sub-group of $\mathbb{H}$ such the exponential map $e : \mathbb{IH} \to \mathbf{S}^3$ is locally a bijection and globally a covering map. The nice properties of this map depend on the fact that the elements of $\mathbb{IH}$ have scalar square.
III. The map $\mathbf{S}^3 \to SO(3) : \mathbf{g} \to \underline{\mathbf{g}}$ is a 2:1 covering of the rotation group of $\mathbb{R}^3$.

1.3.2 The Euler top via quaternions

One can represent elements of $SO(3)$ and its Lie algebra via quaternions. The motion $\mathbf{g}$ becomes a path in $\mathbf{S}^3$; the angular velocity and momentum become elements of $\mathbb{IH}$. The Euler equations become:

$$\dot{\mathbf{g}} = \mathbf{g}\mathbf{V}_c$$
$$\dot{\mathbf{M}}_c = \frac{1}{2}(\mathbf{V}_c\mathbf{M}_c - \mathbf{M}_c\mathbf{V}_c)$$

Here all products are the quaternion product. We mention two advantages of the quaternion approach:

1. The representation of isometries is *geometric*: the axis of a rotation $\mathbf{r} \in \mathbf{S}^3$ is the imaginary part of $\mathbf{r}$.
2. The representation is *compact*: an isometry is represented by 4 real numbers. Compare this to the matrix approach, where 9 real numbers are required. This compactness has significant advantages in numerical applications, for example, in solving differential equations, since one has many fewer directions of moving away from the correct solution.

1.3.3 Quaternion-like algebras for spaces of constant curvature

Motivated by these advantages, the current thesis incorporates algebras, analogous to the quaternions, corresponding to the larger isometry groups of the spaces under investigation. It turns out to be possible to find algebras which not only fulfill properties analogous to I, II, and III above, but which possess further attractive properties.

These algebras are obtained by introducing a graded algebraic structure in which different grades represent different-dimensional subspaces. Such a graded algebra is called a *Grassmann algebra*. The next step involves adding an inner product, which reflects the underlying metric properties of the space, to yield a *Clifford algebra*. The full power of this approach to represent a variety of interesting spaces is only enabled when one works within projective space rather than vector space. These are the mathematical foundations which form the next four chapters of this study. There follow two chapters showing how to use these algebras to do geometry in 2- and 3-dimensional spaces of constant curvature. These tools then provide the basis for investigating kinematics and rigid body mechanics in these spaces (Chapter 8 and Chapter 9).

Chapter 2
Projective foundations

This chapter reviews the non-metric mathematical structures – projective space and exterior algebra – required for the rest of the thesis. The choice of results presented here is conditioned by the requirements of later chapters. Consequently, particular attention is paid to establishing the principle of duality.

2.1 Projective geometry

Real projective n-space Let V be a real vector space of dimension $(n+1)$, and V^* its dual space. Let $\langle \mathbf{u}, \mathbf{x} \rangle = \mathbf{u}(\mathbf{x})$ represent the scalar product on $\mathsf{V} \otimes \mathsf{V}^*$ given by the evaluation map of a dual vector (linear functional) applied to a vector.

Then the n-dimensional projective space $\mathbf{P}(\mathsf{V})$ is obtained from V by introducing an equivalence relation on vectors $\mathbf{x}, \mathbf{y} \in \mathsf{V} \setminus \{\mathbf{0}\}$ defined by: $\mathbf{x} \sim \mathbf{y} \iff \mathbf{x} = \lambda \mathbf{y}$ for some $\lambda \neq 0$. That is, points in $\mathbf{P}(\mathsf{V})$ correspond to lines through the origin in V. We sometimes write this equivalence relation $\mathbf{x} \equiv \mathbf{y}$ if two vectors represent the same projective point. See also Sect. 2.4 below.

Remark 3. For most of this work, $\mathsf{V} = \mathbb{R}^{n+1}$ (or $(\mathbb{R}^{n+1})^*$) and $\mathbf{P}(\mathsf{V}) = \mathbb{R}P^n$ (or $(\mathbb{R}P^n)^*$), real projective space of dimensions n (or its dual). However, note that in many contexts it is not considered as an *inner product* space, that is, we do not assume it is equipped with an inner product. This differentiation will become more clear in Chapter 3 where metrics are introduced.

2.1.1 Projectivities

We review some facts about projective transformations which will be important in Chapter 5 since they provide the basis of the theory of isometries for the metric spaces under consideration.

Definition 4. Given four points $\mathbf{a}, \mathbf{b}, \mathbf{c}, \mathbf{d} \in \mathbb{R}P^1$ with homogeneous coordinates $\mathbf{a} = (a_0, a_1)$, etc.. The *cross ratio* of the four points, written $(\mathbf{a}, \mathbf{b}; \mathbf{c}, \mathbf{d}) := \dfrac{|\mathbf{a}, \mathbf{c}||\mathbf{a}, \mathbf{d}|}{|\mathbf{b}, \mathbf{c}||\mathbf{b}, \mathbf{d}|}$, where $.|\mathbf{a}, \mathbf{c}|$ denotes the determinant $a_0 c_1 - a_1 c_0$, etc.

Definition 5. A *projectivity* of $\mathbb{R}P^1$ is a bijective map $\mathbb{R}P^1 \to \mathbb{R}P^1$ which preserves the cross ratio.

To obtain a similar notion for higher dimensions, we introduce an alternative definition:

Definition 6. For $n > 1$, a *projectivity* is a bijective map $\mathbb{R}P^n \to \mathbb{R}P^n$ or $\mathbb{R}P^n \to (\mathbb{R}P^n)^*$ which preserves linear dependence, and linear independence, of sets. The former is called a *collineation*, the latter, a *correlation*.

From this definition it is possible to deduce the following two theorems.

Theorem 7. *A projectivity is uniquely determined by its action on a linearly independent set of $n + 2$ points.*

Remark 8. Typically, these points are provided by $n+1$ basis vectors $\mathbf{e}_i$ and the so-called *unit* point $\mathbf{u}$. For our purposes, we choose the unit point to be $\mathbf{u} := \sum_i \mathbf{e}_i$.

Theorem 9. *A projectivity preserves the cross ratio of 4 collinear points.*

For a proof, see [Spe63], §21.

The collineations form a group. This group is generated by a set of involutions described as follows.

Definition 10. Let $\mathbf{Z}$ be a point and $\mathbf{m}$ be a hyperplane in $\mathbb{R}P^n$ such that $\mathbf{Z}$ is not incident with $\mathbf{m}$. Then the *harmonic homology* with center $\mathbf{Z}$ and axis $\mathbf{m}$ is the collineation $H_{Z,m}$ defined by:

$$H_{Z,m}(\mathbf{P}) = -\langle \mathbf{Z}, \mathbf{m} \rangle \mathbf{P} + 2\langle \mathbf{P}, \mathbf{m} \rangle \mathbf{Z} \tag{2.1}$$

A harmonic homology fixes the center (linewise) and the axis (pointwise), and its action on a point $\mathbf{P}$ is as follows: find the intersection $\mathbf{S}$ of the line $\mathbf{k}$ joining $\mathbf{Z}$ with $\mathbf{P}$, with the axis $\mathbf{m}$. Then $\mathbf{P}' := H_{Z,m}(\mathbf{P})$ is the unique point of $\mathbf{k}$ such that the point pairs $(\mathbf{Z}, \mathbf{S})$, $(\mathbf{P}, \mathbf{P}')$ separate each other harmonically. See Fig. 2.1. For a proof see the discussion below of centered collineations.

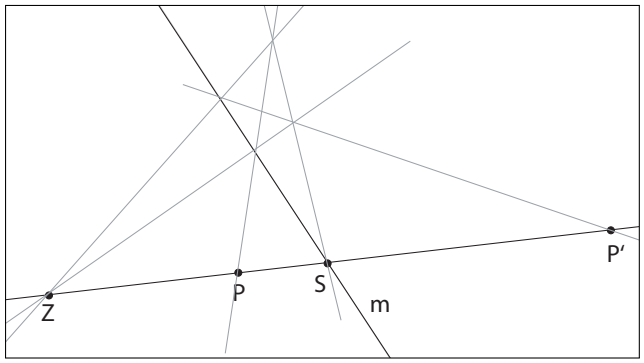

Fig. 2.1 A harmonic homology with center $\mathbf{Z}$ and axis $\mathbf{m}$ acting on a point $\mathbf{P}$. In gray, a harmonic quadrilateral determined by $\mathbf{P}, \mathbf{Z}$, and $\mathbf{S}$, which determines $\mathbf{P}'$ as "hamonic fourth point" to other three points. Other choices of this cross ratio λ lead a centered collineation with factor λ.

Remark 11. The harmonic homology is a special case of a *centered collineation*, a collineation of the form:

$$P_{Z,m,\lambda}(\mathbf{P}) = \lambda\langle \mathbf{Z}, \mathbf{m}\rangle \mathbf{P} + (1-\lambda)\langle \mathbf{P}, \mathbf{m}\rangle \mathbf{Z} \tag{2.2}$$

A centered collineation has center $\mathbf{Z}$ and axis $\mathbf{m}$ as in the harmonic homology. We say λ is the factor of the centered collineation. For $\lambda = -1$, one obtains the harmonic homology; $\lambda = 1$ yields the identity; $\lambda = 0$, the projection onto $\mathbf{Z}$; $\lambda = \infty$, projection onto $\mathbf{m}$. Notice that $P_{Z,m,0}$ is not defined for $\mathbf{P} \in \mathbf{m}$, and $P_{Z,m,\infty}$ is not defined for $\mathbf{P} = \mathbf{Z}$.

Theorem 12. *For* $\mathbf{P'} = P_{Z,m,\lambda}(\mathbf{P})$, $(\mathbf{S}, \mathbf{Z}; \mathbf{P}, \mathbf{P'}) = \lambda$.

Proof. WLOG we can assume $\mathbf{Z}$ is chosen so that $\langle \mathbf{Z}, \mathbf{m}\rangle = 1$. Define $x := \langle \mathbf{P}, \mathbf{m}\rangle$. Setting $\mathbf{S} = \alpha\mathbf{P} + \beta\mathbf{Z}$ and solving $\langle \mathbf{S}, \mathbf{m}\rangle = 0$ leads to $\mathbf{S} = \mathbf{P} - x\mathbf{Z}$. Assigning homogeneous coordinates $(0, 1)$ to $\mathbf{S}$ and $(1, 0)$ to $\mathbf{Z}$ leads then to coordinates $(x, 1)$ for $\mathbf{P}$ and (x, λ) for $\mathbf{P'}$. Evaluating the cross ratio $(\mathbf{S}, \mathbf{Z}; \mathbf{P}, \mathbf{P'})$ using Def. 4 yields the desired result. □

Remark 13. There are various ways to parametrize the family $P_{Z,m,\lambda}$; the one given above is chosen since it behaves nicely with respect to orientation of fixed points. For example, for positive λ, the point-pairs $(\mathbf{P}, \mathbf{P'})$ and $(\mathbf{Z}, \mathbf{S})$ do not separate each other, so the collineation preserves order along each invariant line. Correspondingly, fixed points $\mathbf{P} \in \mathbf{m}$ are mapped to positive multiples of themselves; the opposite is true for negative λ. For $\lambda = 0$, $\mathbf{P'}$ is not defined, and for $\lambda = \pm\infty$, the freedom to choose the sign shows that it is impossible to define an orientation in this case also.

Similar remarks apply for $\mathbb{R}P^{2n}$; in odd dimensions there is no way to consistently assign orientation to the fixed points using the formula, since all fixed points are reversed by the centered collineation. A similar analysis shows that $\mathbf{Z}$ is always mapped to a positive multiple of itself; this reflects the fact that for all λ, a small neighborhood of $\mathbf{Z}$ is mapped to a small neighborhood of itself with the same orientation.

Remark 14. Like any collineation, the harmonic homology has an induced action on the dual space of hyperplanes. Viewed as a collineation of the dual space, this is also a harmonic homology, with center $\mathbf{m}$ and axis $\mathbf{Z}$. Thus, the concept of harmonic homology is a *self-dual* one. One obtains the dual formula by dualizing (2.1):

$$H_{Z,m}(\mathbf{l}) = -\langle \mathbf{Z}, \mathbf{m}\rangle \mathbf{l} + 2\langle \mathbf{Z}, \mathbf{l}\rangle \mathbf{m} \tag{2.3}$$

This dual version will be important when we take up this theme again in Sect. 4.6.

2.2 Exterior algebra

Let V be a real vector space of dimension n. The exterior, or Grassmann, algebra $\bigwedge(\mathsf{V})$, is generated by the exterior product[1] $\wedge$ applied to the vectors of V. The exterior product

[1] Also called the outer or wedge product

is an alternating, bilinear operation. The algebra has a graded structure. The elements of grade-1 are defined to be the vectors of V; the exterior product of a k- and m-vector is a $(k+m)$-vector, when the operands are linearly independent subspaces. An element that can be represented as a wedge product of k 1-vectors is called a simple k-vector, or k-*blade*. The k-blades generate the vector subspace $\bigwedge^k(\mathsf{V})$, whose elements are said to have grade k. This subspace has dimension $\binom{n}{k}$, hence the total dimension of the exterior algebra is 2^n.

Simple and non-simple vectors. A k-blade represents the subspace of V spanned by the k vectors which define it. Hence, the exterior algebra contains within it a representation of the subspace lattice of V. For $n > 3$ there are also k-vectors which are not blades and do not represent a subspace of V. Such vectors occur as bivectors when $\mathsf{V} = \mathbb{R}^4$ and play an important role in the discussion of kinematics and dynamics in Chapter 8 and Chapter 9.

Dual Grassmann algebra. The same construction can be applied to construct $\bigwedge \mathsf{V}^*$, the exterior algebra of the dual vector space V^*. This is the algebra of alternating k-multilinear forms.

2.2.1 Determinant function

$\bigwedge^n(\mathsf{V})$ is a one-dimensional vector space. Let $\mathbf{I}$ be a basis element. Given a basis $\{\mathbf{v}_i\}$ for V, $\mathbf{v}_1 \wedge \mathbf{v}_2 ... \wedge \mathbf{v}_n \in \bigwedge^n(\mathsf{V})$, hence $\mathbf{v}_1 \wedge \mathbf{v}_2 ... \wedge \mathbf{v}_n = \alpha \mathbf{I}$ for some non-zero $\alpha \in \mathbb{R}$. Define a function

$$\triangle : \otimes^n \mathsf{V} \to \mathbb{R} \quad \text{by} \quad \triangle(\{\mathbf{v}_i\}) := \alpha$$

Then $\triangle$ is called the *determinant* function of $\bigwedge(\mathsf{V})$. It lets us define a canonical isomorphism between V and $\bigwedge^{n-1}(\mathsf{V}^*)$.

Theorem 15. $\mathsf{V} \cong \bigwedge^{n-1}(\mathsf{V}^*)$

Proof. Given $\mathbf{v} \in \mathsf{V}$, then define $\omega \in \bigwedge^{n-1}(\mathsf{V}^*)$ by

$$\omega(\mathbf{v}_1, \mathbf{v}_2, ...\mathbf{v}_{n-1}) := \triangle(\mathbf{v}, \mathbf{v}_1, \mathbf{v}_2, ..., \mathbf{v}_{n-1})$$

Conversely, given such an ω, there is a unique $\mathbf{v}$ such that the above equation is satisfied. Hence $\mathsf{V} \cong \bigwedge^{n-1}(\mathsf{V}^*)$. $\square$

Remark 16. By abstract nonsense, this implies $\mathsf{V}^* \cong \bigwedge^{n-1}(\mathsf{V})$.

2.2.2 Projectivized exterior algebra

The exterior algebra can be projectivized using the same process defined above for the construction of $P(\mathsf{V})$ from V, but applied to the vector spaces $\bigwedge^k(\mathsf{V})$. This yields the projectivized exterior algebra $W := \mathbf{P}(\bigwedge(\mathsf{V}))$. The operations of $\bigwedge(\mathsf{V})$ carry over to $\mathbf{P}(\bigwedge \mathsf{V})$, since, roughly speaking: "Projectivization commutes with outer product". That is, for two elements $X, Y \in \bigwedge(\mathsf{V})$:

$$\mathbf{P}(X) \wedge \mathbf{P}(Y) = \mathbf{P}(X \wedge Y)$$

The difference lies in how the elements and operations are projectively interpreted. The k-blades of $\mathbf{P}(\bigwedge \mathsf{V})$ correspond to $(k-1)$-dimensional subspaces of $\mathbf{P}(V)$. All multiples of the same k-blade represent the same projective subspace, and differ only by intensity ([Whi98], §16-17). 1-blades correspond to points; 2-blades to lines; 3-blades to planes, etc.

2.2.2.1 Dual exterior algebra The algebra $\mathbf{P}(\bigwedge \mathsf{V}^*)$ is formed by projectivizing the dual algebra $\bigwedge(\mathsf{V}^*)$. $\mathbf{P}(\bigwedge \mathsf{V}^*)$ is the alternating algebra of k-multilinear forms. By abstract nonsense, $\mathbf{P}(\bigwedge \mathsf{V}^*) = (\mathbf{P}(\bigwedge \mathsf{V}))^*$: projectivization commutes with dualization. $\mathbf{P}(\bigwedge \mathsf{V}^*)$ is naturally isomorphic to $\mathbf{P}(\bigwedge \mathsf{V})$; again, the difference lies in how the elements and operations are interpreted. Like $\mathbf{P}(\bigwedge \mathsf{V})$, $\mathbf{P}(\bigwedge \mathsf{V}^*)$ represents the subspace structure of $\mathbf{P}(\mathsf{V})$, but turned on its head: 1-vectors represent projective hyperplanes, while simple (n-1)-vectors represent projective points. The outer product $\mathbf{a} \wedge \mathbf{b}$ corresponds to the *meet* rather than *join* operator. See also Fig. 2.4.

2.2.2.2 Notation alert In order to distinguish the two outer products of $\mathbf{P}(\bigwedge \mathsf{V})$ and $\mathbf{P}(\bigwedge \mathsf{V}^*)$, we write the outer product in $\mathbf{P}(\bigwedge \mathsf{V})$ as $\vee$, and leave the outer product in $\mathbf{P}(\bigwedge \mathsf{V}^*)$ as $\wedge$. These symbols match closely the affiliated operations of join (union $\cup$) and meet (intersection $\cap$), resp. Note, however, they are reversed from some modern literature ([HZ91]).

2.2.3 Exterior power of a map

Given a linear map $f : \mathsf{V} \to \mathsf{V}$, there is an induced grade-preserving map $\bigwedge(f) : \bigwedge(\mathsf{V}) \to \bigwedge(\mathsf{V})$ called the *exterior power* of f. Its action on a simple k-vector $\mathbf{a} = \mathbf{e}_{i_1} \wedge ... \wedge \mathbf{e}_{i_k}$ is defined by

$$\wedge^k(f) = f(\mathbf{e}_{i_1}) \wedge ... \wedge f(\mathbf{e}_{i_k} \tag{2.4}$$

For $f : \mathsf{V} \to \mathsf{V}^*$, one defines a map $\bigwedge(f) : \bigwedge(\mathsf{V}) \to \bigwedge(\mathsf{V}^*)$ by using the wedge in the dual algebra in the RHS of (2.4).

Remark 17. $\wedge^n(f)$ gives the determinant of the matrix of f when f is expressed in terms of a basis $\{\mathbf{v}_i\}$ satisfying $\triangle(\{\mathbf{v}_i\}) = 1$.

2.2.3.1 The adjoint map Given $f : \mathsf{V} \to \mathsf{V}^*$, construct the exterior power $\bigwedge^{n-1}(f) : \bigwedge(\mathsf{V}) \to \bigwedge(\mathsf{V}^*)$. By Sect. 2.2.1, $\bigwedge^{n-1}(f)$ can be considered as a map $\mathsf{V}^* \to \mathsf{V}$. It is called the *adjoint* of f. We write $f^* := \bigwedge^{n-1}(f)$. With respect to a basis, the matrix of f^* is the "matrix of cofactors" of the matrix of f, which isn't surprising considering the role played in its definition by the $\triangle$ function. For invertible f, f^* is the unique linear map satisfying $\langle \mathbf{u}, \mathbf{x} \rangle = \langle f(\mathbf{x}), f^*(\mathbf{u}) \rangle$.

Remark 18. The adjoint is sometimes defined by identifying V and V^* using a metric. See for example [DFM07], Sec. 4.3.2. We prefer to avoid the use of metrics where they are not required. See related discussion in Sect. 5.10.

2.2.4 Equal rights for $\mathbf{P}(\bigwedge \mathsf{V})$ and $\mathbf{P}(\bigwedge \mathsf{V}^*)$

From the point of view of representing V, $\mathbf{P}(\bigwedge \mathsf{V})$ and $\mathbf{P}(\bigwedge \mathsf{V}^*)$ are equivalent. There is no *a priori* reason to prefer one to the other. Every geometric element in one algebra occurs in the other, and any configuration in one algebra has a dual configuration in the other obtained by applying the Principle of Duality [Cox87], to the configuration. We refer to $\mathbf{P}(\bigwedge \mathsf{V})$ as a *point-based*, and $\mathbf{P}(\bigwedge \mathsf{V}^*)$ as a *plane-based*, algebra.[2]

Depending on the context, one or the other of the two algebras may be more useful. Here are some examples:

1. **Joins and meets.** $\mathbf{P}(\bigwedge \mathsf{V})$ is the natural choice to calculate subspace joins, and $\mathbf{P}(\bigwedge \mathsf{V}^*)$, to calculate subspace meets. See Sect. 2.3.1.4.
2. **Spears and axes.** Lines appear in two aspects: as spears (bivectors in $\mathbf{P}(\bigwedge \mathsf{V})$) and axes (bivectors in $\mathbf{P}(\bigwedge \mathsf{V}^*)$). See Sect. 2.2.4.1.
3. **Euclidean geometry.** $\mathbf{P}(\bigwedge \mathsf{V}^*)$ is the correct choice to use for modeling euclidean geometry. See Sect. 5.3.
4. **Reflections in planes.** $\mathbf{P}(\bigwedge \mathsf{V}^*)$ has advantages for kinematics, since it naturally allows building up rotations as products of reflections in planes. See Sect. 5.6.1.

We turn now to item 2 above, highlighting the importance of maintaining $\mathbf{P}(\bigwedge \mathsf{V})$ and $\mathbf{P}(\bigwedge \mathsf{V}^*)$ as equal citizens.

2.2.4.1 There are no lines, only spears and axes! Most of this work is focused on the case $\mathsf{V} = \mathbb{R}^4$. In this case, bivectors are self-dual. This has interesting consequences for how they are interpreted.

Given two points $\mathbf{x}$ and $\mathbf{y} \in \mathbf{P}(\bigwedge \mathsf{V})$, the condition that a third point $\mathbf{z}$ lies in the subspace spanned by the 2-blade $\mathbf{l} := \mathbf{x} \vee \mathbf{y}$ is that $\mathbf{x} \vee \mathbf{y} \vee \mathbf{z} = 0$, which implies that $\mathbf{z} = \alpha\mathbf{x} + \beta\mathbf{y}$ for some α, β not both zero. In projective geometry, such a set is called a *point range*. We prefer the more colorful term *spear*. Dually, given two planes $\mathbf{x}$ and $\mathbf{y} \in W^*$, the condition that a third plane $\mathbf{z}$ passes through the subspace spanned by the 2-blade $\mathbf{l} := \mathbf{x} \wedge \mathbf{y}$ is that $\mathbf{z} = \alpha\mathbf{x} + \beta\mathbf{y}$. In projective geometry, such a set is called a *plane pencil*. We prefer the more colorful term *axis*.

Within the context of $\mathbf{P}(\bigwedge \mathsf{V})$ and $\mathbf{P}(\bigwedge \mathsf{V}^*)$, lines exist only in one of these two aspects: of spear – as bivector in $\mathbf{P}(\bigwedge \mathsf{V})$ – and axis – as bivector in $\mathbf{P}(\bigwedge \mathsf{V}^*)$. This naturally generalizes to non-simple bivectors: there are point-wise bivectors (in $\mathbf{P}(\bigwedge \mathsf{V})$), and plane-wise bivectors (in $\mathbf{P}(\bigwedge \mathsf{V}^*)$.) Many of the important operators of geometry and dynamics we will meet below, such as the polarity on the metric quadric (Sect. 4.4), and the inertia tensor of a rigid body (Sect. 9.3), map $\langle \mathbf{P}(\bigwedge \mathsf{V}) \rangle_2$ to $\langle \mathbf{P}(\bigwedge \mathsf{V}^*) \rangle_2$ and hence map spears to axes and vice-versa. Having both algebras on hand preserves the qualitative difference between these dual aspects of the generic term "line".

Remark 19. It is possible to build up projective geometry by beginning with the line as the primitive element and constructing points and planes from this primitive element.

[2] We prefer the dimension-dependent formulation *plane-based* to the more precise *hyperplane-based*. We also prefer not to refer to the plane-based algebra as the *dual* algebra, since this formulation depends on the accident that the original algebra is interpreted as point-based.

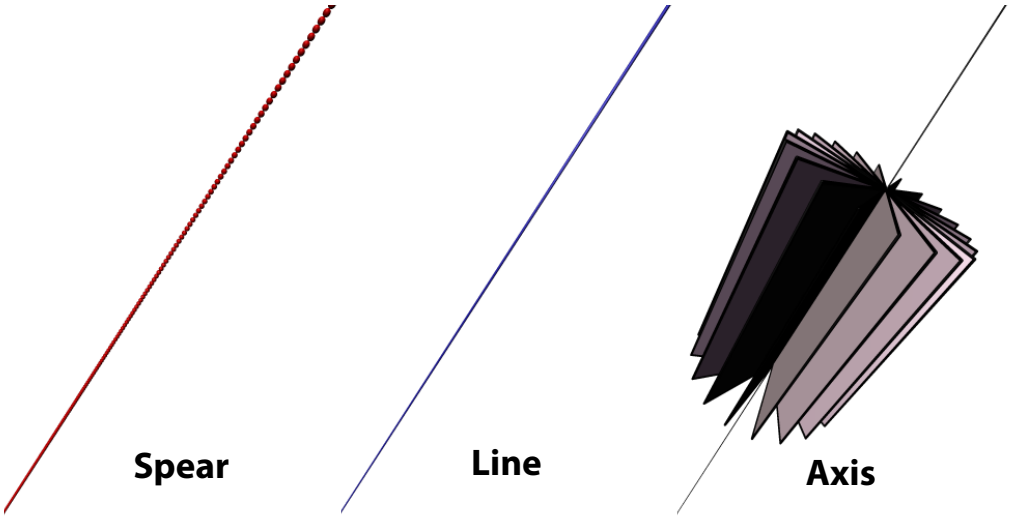

Fig. 2.2 Three aspects of line: spear (all incident points); line *qua* line; and axis (all incident planes).

This would then provide a third way to view a line, so to speak, in its own right rather than built out of points or planes. This approach for example can be found in [Sto09]. But this approach does not lend itself to representing the subspace structure of $\mathbb{R}P^3$ with Grassmann algebras.

2.3 Poincaré Duality

Our treatment differs from other approaches (for example, Grassmann-Cayley algebras) in explicitly maintaining both algebras on an equal footing rather than expressing the wedge product in one in terms of the wedge product of the other (as in the Grassman-Cayley *shuffle* product) ([Sel05], [Per09]). To switch back and forth between the two algebras, we construct an algebra isomorphism that, given an element of one algebra, produces the element of the second algebra which corresponds to the same geometric entity of V^*.

This algebra isomorphism can be stated and proved in a coordinate-free way using advanced techniques of modern multilinear algebra ([Gre67b], Ch. 6, §2). In this form the isomorphism is called the *Poincaré isomorphism*, and the resulting equivalence, *Poincaré duality*. We derive it here using a particular coordinate system which simplifies the exposition. We first show how this works for the case of interest $\mathsf{V} = \mathbb{R}^4$.

2.3.1 The isomorphism J

Each weighted subspace S of $\mathbb{R}P^3$ corresponds to a unique element S_W of $\mathbf{P}(\bigwedge \mathsf{V})$ and to a unique element S_{W^*} of $\mathbf{P}(\bigwedge \mathsf{V}^*)$. We seek a bijection $\mathbf{J} : \mathbf{P}(\bigwedge \mathsf{V}) \leftrightarrow \mathbf{P}(\bigwedge \mathsf{V}^*)$ such that $J(S_W) = S_{W^*}$. If we have found $\mathbf{J}$ for the basis k-blades, then it extends by linearity to multivectors. This will be the desired Poincaré isomorphism. To that end, we introduce a basis for $\mathbb{R}^4$ and extend it to a basis for $\mathbf{P}(\bigwedge \mathsf{V})$ and $\mathbf{P}(\bigwedge \mathsf{V}^*)$ so that $\mathbf{J}$ takes a particularly simple form. Refer to Fig. 2.3.

2.3.1.1 The canonical basis A basis $\{\mathbf{e}^0, \mathbf{e}^1, \mathbf{e}^2, \mathbf{e}^3\}$ of $\mathbb{R}^4$ corresponds to a coordinate tetrahedron for $\mathbb{R}P^3$, with corners occupied by the basis elements[3]. Use the same names to identify the elements of $P(\bigwedge^1(\mathbb{R}^4))$ which correspond to these projective points. Further, let $\mathbf{I}^0 := \mathbf{e}^0 \wedge \mathbf{e}^1 \wedge \mathbf{e}^2 \wedge \mathbf{e}^3$ be the basis element of $P(\bigwedge^4(\mathbb{R}^4))$, and $\mathbf{1}^0$ be the basis element for $P(\bigwedge^0(\mathbb{R}^4))$. Let the basis for $P(\bigwedge^2(\mathbb{R}^4))$ be given by the six edges of the tetrahedron:

$$\{\mathbf{e}^{01}, \mathbf{e}^{02}, \mathbf{e}^{03}, \mathbf{e}^{12}, \mathbf{e}^{31}, \mathbf{e}^{23}\}$$

where $\mathbf{e}^{ij} := \mathbf{e}^i \wedge \mathbf{e}^j$ represents the oriented line joining $\mathbf{e}^i$ and $\mathbf{e}^j$.[4] Finally, choose a basis $\{\mathbf{E}^0, \mathbf{E}^1, \mathbf{E}^2, \mathbf{E}^3\}$ for $P(\bigwedge^3(\mathbb{R}^4))$ satisfying the condition that $\mathbf{e}^i \vee \mathbf{E}^i = \mathbf{I}^0$. This corresponds to choosing the i^{th} basis 3-vector to be the plane opposite the i^{th} basis 1-vector in the fundamental tetrahedron, oriented in a consistent way.

We repeat the process for the algebra $\mathbf{P}(\bigwedge \mathsf{V}^*)$, writing indices as subscripts. Choose the basis 1-vector $\mathbf{e}_i$ of $\mathbf{P}(\bigwedge \mathsf{V}^*)$ to represent the same plane as $\mathbf{E}_i$. That is, $\mathbf{J}(\mathbf{E}_i) = \mathbf{e}_i$. Let $\mathbf{I}_0 := \mathbf{e}_0 \wedge \mathbf{e}_1 \wedge \mathbf{e}_2 \wedge \mathbf{e}_3$ be the pseudoscalar of the algebra. Construct bases for grade-0,

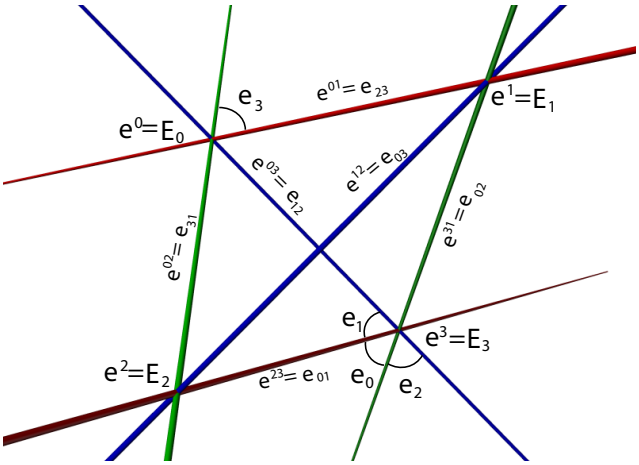

Fig. 2.3 Fundamental tetrahedron with dual labeling. Entities in W have superscripts; entities in W^* have subscripts. Planes are identified by labeled angles of two spanning lines. A representative sampling of equivalent elements is shown.

[3] We use superscripts for $\mathbf{P}(\bigwedge \mathsf{V})$ and subscripts for $\mathbf{P}(\bigwedge \mathsf{V}^*)$ since $\mathbf{P}(\bigwedge \mathsf{V}^*)$ will be the more important algebra for our purposes.

[4] Note that the orientation of $\mathbf{e}^{31}$ is reversed; this is traditional since Plücker introduced these line coordinates.

feature	$\mathbf{P}(\bigwedge \mathsf{V})$	$\mathbf{P}(\bigwedge \mathsf{V}^*)$
0-vector	scalar $\mathbf{1}^0$	scalar $\mathbf{1}_0$
vector	point $\{e^i\}$	plane $\{e_i\}$
bivector	"spear" $\{e^{ij}\}$	"axis" $\{e_{ij}\}$
trivector	plane $\{E^i\}$	point $\{E_i\}$
4-vector	$\mathbf{I}^0$	$\mathbf{I}_0$
outer product	join $\vee$	meet $\wedge$

Table 2.1 Comparison of $\mathbf{P}(\bigwedge \mathsf{V})$ and $\mathbf{P}(\bigwedge \mathsf{V}^*)$ for $\mathsf{V} = \mathbb{R}^4$.

grade-2, and grade-3 using the same rules as above for $\mathbf{P}(\bigwedge \mathsf{V})$ (i. e., replacing subscripts by superscripts). The results are represented in Table 2.1.

Given this choice of bases for $\mathbf{P}(\bigwedge \mathsf{V})$ and $\mathbf{P}(\bigwedge \mathsf{V}^*)$, examination of Fig. 2.3 makes clear that, on the basis elements, $\mathbf{J}$ takes the following simple form:

$$\mathbf{J}(e^i) := E_i, \qquad \mathbf{J}(E^i) := e_i, \qquad \mathbf{J}(e^{ij}) := e_{kl} \tag{2.5}$$

where in the last equation, $(ijkl)$ an even permutation of (0123).

Fig. 2.4 gives a graphical representation of Table 2.1, and the isomorphism $\mathbf{J}$.

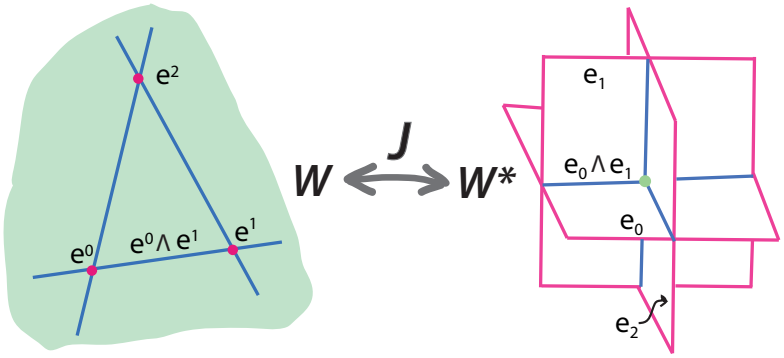

Fig. 2.4 The standard Grassmann $\mathbf{P}(\bigwedge \mathsf{V})$ and its dual $\mathbf{P}(\bigwedge \mathsf{V}^*)$ are related by the Poincare isomorphism $\mathbf{J}$.

2.3.1.2 Description of J Furthermore, $\mathbf{J}(\mathbf{1}^0) = \mathbf{I}_0$ and $\mathbf{J}(\mathbf{I}^0) = \mathbf{1}_0$ since these grades are one-dimensional. To sum up: the map $\mathbf{J}$ is grade-reversing and, considered as a map of coordinate-tuples, it is the identity map on all grades except for bivectors. What happens for bivectors? In $\mathbf{P}(\bigwedge \mathsf{V})$, consider $\mathbf{e}^{01}$, the joining line of points $\mathbf{e}^0$ and $\mathbf{e}^1$ (refer to Fig. 2.3). In $\mathbf{P}(\bigwedge \mathsf{V}^*)$, the same line is $\mathbf{e}_{23}$, the intersection of the only two planes which contain both of these points, $\mathbf{e}_2$ and $\mathbf{e}_3$. On a general bivector, $\mathbf{J}$ takes the form:

$$\mathbf{J}(a_{01}e^{01} + a_{02}e^{02} + a_{03}e^{03} + a_{12}e^{12} + a_{31}e^{31} + a_{23}e^{23}) = \\ a_{23}e_{01} + a_{31}e_{02} + a_{12}e_{03} + a_{03}e_{12} + a_{02}e_{31} + a_{01}e_{23}$$

The coordinate-tuple is reversed. See Fig. 2.2. Since $\mathbf{J}^{-1}$ is obtained from the definition of $\mathbf{J}$ by swapping superscripts and subscripts, we can consider $\mathbf{J} : W \leftrightarrow W^*$ as a defined on both algebras, with $\mathbf{J}^2$ the identity. The full significance of $\mathbf{J}$ will only become evident after metrics are introduced. See Sect. 5.10.

2.3.1.3 J in n-dimensions Here we generalize the construction above for $n = 4$ to arbitrary dimension, to show how to construct the algebra isomorphism $\mathbf{J}$ with the desired property, and connect it to the principle of *Poincaré duality*. We take up the issue of $\mathbf{J}$ again in Sect. 5.10 where we discuss it in relation to alternative formulations involving a metric.

A subset $S = \{i_1, i_2, ...i_k\}$ of $N = \{1, 2, ..., n\}$ is called a *canonical* k-*tuple* of N if $i_1 < i_2 < ... < i_k$. For each canonical k-tuple of N, define $S^\perp$ to be the canonical $(n-k)$-tuple consisting of the elements $N \setminus S$. For each unique pair $\{S, S^\perp\}$, swap a pair of elements of $S^\perp$ if necessary so that the concatenation $SS^\perp$, as a permutation P of N, is even. Call the collection of the resulting sets $\mathfrak{S}$. For each $S \in \mathfrak{S}$, define $\mathbf{e}^S = \mathbf{e}^{i_1}...\mathbf{e}^{i_k}$. We call the resulting set $\{\mathbf{e}^S\}$ the *canonical basis* for $\mathbf{P}(\bigwedge \mathsf{V})$ generated by $\{\mathbf{e}^i\}$.

Consider $\mathbf{P}(\bigwedge \mathsf{V}^*)$, the dual algebra to $\mathbf{P}(\bigwedge \mathsf{V})$. Choose a basis $\{\mathbf{e}_1, \mathbf{e}_2, ...\mathbf{e}_n\}$ for $\mathbf{P}(\bigwedge \mathsf{V}^*)1$ so that $\mathbf{e}_i$ represents the same oriented subspace represented by the basis *(n-1)*-vector $\mathbf{e}^{(i^\perp)}$ of $\mathbf{P}(\bigwedge \mathsf{V})$. Construct the canonical basis (as above) of $\mathbf{P}(\bigwedge \mathsf{V}^*)$ generated by the basis $\{\mathbf{e}_i\}$. Then define a map $\mathbf{J} : \mathbf{P}(\bigwedge \mathsf{V}) \to \mathbf{P}(\bigwedge \mathsf{V}^*)$ by $\mathbf{J}(\mathbf{e}^S) = \mathbf{e}_{S^\perp}$ and extend by linearity.

$\mathbf{J}$ is an "identity" map on the subspace structure of V: it maps a simple k-vector $B \in W$ to the simple $(n-k)$-vector $\in \mathbf{P}(\bigwedge \mathsf{V}^*)$ which represents the same geometric entity as B does in $\mathbb{R}P^n$. *Proof:* By construction, $\mathbf{e}^S$ represents the join of the 1-vectors $\mathbf{e}_{i_j}, (i_j \in S)$ in W. This is however the same subspace as the meet of the $n-k$ basis 1-vectors $\mathbf{e}_{i_j}, (i_j \in S^\perp)$ of $\mathbf{P}(\bigwedge \mathsf{V}^*)$, since $\mathbf{e}_i$ is incident with $\mathbf{e}^j \iff j \neq i$.

We now show how to use $\mathbf{J}$ to define meet and join operators valid for both $\mathbf{P}(\bigwedge \mathsf{V})$ and $\mathbf{P}(\bigwedge \mathsf{V}^*)$.

2.3.1.4 Projective join and meet Knowledge of $\mathbf{J}$ allows equal access to join and meet operations. We define a meet operation $\wedge$ for two blades $A, B \in \mathbf{P}(\bigwedge \mathsf{V})$:

$$A \wedge B = \mathbf{J}(\mathbf{J}(A) \wedge \mathbf{J}(B)) \tag{2.6}$$

and extend by linearity to the whole algebra. There is a similar expression for the join $\vee$ operation for two blades $A, B \in \mathbf{P}(\bigwedge \mathsf{V}^*)$:

$$A \vee B := \mathbf{J}(\mathbf{J}(A) \vee \mathbf{J}(B)) \tag{2.7}$$

2.4 Remarks on homogeneous coordinates

We use the terms *homogeneous* model and *projective* model interchangeably, to denote the projectivized version of Grassmann (and, later, Clifford) algebra.

The projective model allows a certain freedom in specifying results within the algebra. In particular, when the calculated quantity is a subspace, then the answer is only defined up to a non-zero scalar multiple. In some literature, this fact is represented by always surrounding an expression x in square brackets $[x]$ when one means "the projective element corresponding to the vector space element x". Similarly, $\mathbf{x}\mathbb{R}$ is used to represent "the 1-dimensional vector subspace corresponding to the projective point $\mathbf{x}$". We do not adhere to this level of rigor here, since in most cases the intention is clear.

Some of the formulas introduced below take on a simpler form which take advantage of this freedom, but they may appear unfamiliar to those used to working in the more strict vector-space environment. On the other hand, when the discussion later turns to kinematics and dynamics, then this projective equivalence is no longer strictly valid. Different representatives of the same subspace represent weaker or stronger instances of a velocity or momentum (to mention two possibilities). In such situations terms such as *weighted* point or "point with intensity" will be used. See [Whi98], Book III, Ch. 4. See also Sect. 9.2.3.1 below, which discusses the use of homogeneous coordinates with respect to the inertia tensor of a rigid body.

2.5 Guide to the literature

[PW01] (Chapter 1 and Section 2.2) provides a good overview of the background material on projective geometry and exterior algebra. For detailed background on exterior algebras, see [Wik], [Bou89], or [Gre67b]. For more on Poincaré duality, consult [Gre67b]., Sec. 6.8. [Kow09] provides a good introduction to projective geometry with a synthetic component.

Chapter 3
Metric foundations

Projective geometry was originally discovered as an extension of euclidean geometry, motivated by the experiences of perspective painters. The reverse path, to discover euclidean (and other metric spaces) within projective geometry, occurred in the second half of the 19^{th} century. This chapter is devoted to the prerequisites of this construction, which will be described in Chapter 4, and forms itself the basis for introducing Clifford algebras in Chapter 5.

The key ingredient in this construction is the concept of a *quadric surface* in $\mathbb{R}P^n$. A non-degenerate quadratic form yields a unique non-degenerate quadric surface, in a way we will make precise below. Such non-degenerate surfaces will serve to model non-euclidean geometry. Degenerate quadric surfaces, on the other hand, are not uniquely specified by a single quadratic form. We restrict attention to a subset of such degenerate quadric surfaces (which we term *admissable*), which will be used to model euclidean, and other related, geometries.

Most of the original results are synthetic ones; we present only the analytic version. For details of both approaches, see [Kow09], Chapter 4.

Remark 20. Since we work in the n-dimensional space $\mathbf{P}(\mathsf{V})$, we assume throughout this chapter that the dimension of V is $n+1$.

3.1 Symmetric bilinear maps and quadratic forms

We introduce the important concepts from linear algebra before turning to the application of these to construct quadric surfaces in $\mathbb{R}P^n$ in the next section.

Begin with a symmetric bilinear map B on a real vector space V, that is a bilinear mapping

$$B : \mathsf{V} \otimes \mathsf{V} \to \mathbb{R} \text{ such that } B(\mathbf{x}, \mathbf{y}) = B(\mathbf{y}, \mathbf{x}) \ \forall \ \mathbf{x}, \mathbf{y} \in \mathsf{V}$$

To each such B one defines the corresponding real quadratic form

$$Q : \mathsf{V} \to \mathbb{R} \text{ by } Q(\mathbf{x}) := B(\mathbf{x}, \mathbf{x})$$

Conversely, given such a Q, there is a unique symmetric bilinear form B (obtained by *polarizing* Q), which is related to the given Q in this way. Throughout this discussion, B and Q are assumed to be related in this way.

Let $\mathbf{x} \in \mathsf{V}$ and $\mathbf{u} \in \mathsf{V}^*$. Every bilinear map B determines a linear map $L_B : \mathsf{V} \to \mathsf{V}^*$ by the condition $B(\mathbf{x}, \mathbf{y}) = \langle L_B\mathbf{x}, \mathbf{y}\rangle$. When B is symmetric, $\langle L_B\mathbf{x}, \mathbf{y}\rangle = \langle L_B\mathbf{y}, \mathbf{x}\rangle$.

By the results of Sect. 2.2.3.1, the adjoint map ${L_B}^*$, defined as $\bigwedge^{n-1}(f)$, represents the induced quadratic form on V^*.

Definition 21. The *adjoint* bilinear form $B^* : \mathsf{V}^* \otimes \mathsf{V}^* \to \mathbb{R}$ is defined by

$$B^*(\mathbf{u}, \mathbf{v}) := \langle \mathbf{u}, {L_B}^*\mathbf{v}\rangle$$

The *adjoint* quadratic form Q^* satisfies $Q^*(\mathbf{u}) = B^*(\mathbf{u}, \mathbf{u})$.

Definition 22. $\mathbf{Q} := \{\mathbf{u} \mid \ Q(\mathbf{u}) = 0\}$ is called the *zero-set* of Q.

Remark 23. $\mathbf{Q}$ is well-defined in $\mathbf{P}(\mathsf{V})$, and $\mathbf{Q}^*$ is well-defined in $\mathbf{P}(\mathsf{V}^*)$.

Definition 24. The rank $r(Q)$ of a quadratic form Q is equal to the rank of any matrix representing it.

3.1.1 Normal form of a quadratic form

By standard results of linear algebra ([BM97], Ch. 9), it is possible to choose a basis for V for which the matrix of B is diagonal: $B(\mathbf{e}_i, \mathbf{e}_j) = \epsilon\delta_{i,j}$ where $\mathbf{e}_i$ is a basis vector, $\delta_{i,j}$ is the Kronecker delta function, and $\epsilon \in \{-1, 0, 1\}$. The number of 1's, 0's, and -1's along the diagonal is then an invariant (under action of $\mathsf{L}(\mathsf{V}, \mathsf{V})$) of Q, called the *signature*, a triple of integers $S_Q := (p, m, z)$ where $p+m+z$ is the dimension of the underlying vector space, and p, m, and z are the numbers of positive, negative, and zero entries along the diagonal of the matrix representing B.[1]

The signature (p, m, z) is not essentially different from the signature (m, p, z). Hence we can assume that $p \geq m$. We sometimes call this an *inner product* structure and write $Q(\mathbf{x}, \mathbf{y}) = \mathbf{x} \cdot \mathbf{y}$.

3.1.1.1 Sign vectors for signatures To simplify notation for this, we represent a specific instance of signature (p, m, z) with an $(n + 1)$-vector consisting of the symbols $\{+, -, 0\}$. For example, $(+0-)$ represents the quadratic form $x_0^2 - x_2^2$, one of six possible forms for $(1, 1, 1)$. We call $(+0-)$ a *sign vector* for the signature. We typically use an alphabetical ordering to choose a canonical representative of these six possibilities.

$r(Q^*)$ depends on $r(Q)$, and can be easily calculated by considering the canonical matrix given above and its adjoint:

[1] The signature is traditionally defined as the $p-m$. To fully determine Q, one needs also the rank $r(Q)$ and the dimension $n + 1$. The signature introduced here is an equivalent way of encoding these 3 numbers.

$$r(Q^*) = \begin{cases} n+1 & \text{if } r(Q) = n+1 \\ 1 & \text{if } r(Q) = n \\ 0 & \text{if } r(Q) < n \end{cases} \tag{3.1}$$

Theorem 25. *If $(p, m, 0)$ is the signature of Q, then the signature of Q^* is*

$$\begin{cases} (p, m, 0) & \textit{if } m \textit{ is even} \\ (m, p, 0) & \textit{otherwise} \end{cases} \tag{3.2}$$

Proof. Consider the standard form above and knowledge of cofactors.

Remark 26. This means that when $r(Q) = n + 1$, Q^* has equivalent signature to Q.

Definition 27. A point $\mathbf{x}$ such that $Q(\mathbf{x}, \mathbf{y}) = 0 \ \forall \ \mathbf{y}$ is called a *singular point* of Q. Q is said to be *degenerate* if it has a singular point; otherwise, *non-degenerate*. The set of all singular points is called the *vertex* of Q.

Remark 28. Q is non-degenerate $\iff$ $z = 0$. In this case there are $\lceil \frac{n+1}{2} \rceil$ distinct possibilities such that $p \geq m$.

Remark 29. The vertex of Q is a closed subspace of V of dimension $(n + 1 - r(Q))$.

3.1.2 Pole and Polar

Definition 30. For a point $\mathbf{x}$, the *polar* of $\mathbf{x}$, $\mathbf{x}^\perp := \{\mathbf{y} \mid B(\mathbf{x}, \mathbf{y}) = 0\}$. $\mathbf{x}$ is a *regular* point with respect to Q if $\mathbf{x}^\perp$ has dimension $n - 1$.

Remark 31. $\mathbf{y} \in \mathbf{x}^\perp \iff L_B(\mathbf{x})(\mathbf{y}) = 0$. Hence $\mathbf{x}^\perp = ker(L_B)$. $\mathbf{x}$ is regular is equivalent to $L_B(\mathbf{x}) \neq 0$, in which case $\mathbf{x}^\perp$ can be identified with $L_B \in \mathsf{V}^*$. If $\mathbf{x}$ is not regular, then it is singular, and $\mathbf{x}^\perp = \mathsf{V}$, which is equivalent to $L_B(\mathbf{x}) = 0$.

We state without proof the following important result ([Kow09], Section 4.2):

Theorem 32. *For non-degenerate Q, the map $L_B : \mathsf{V} \to \mathsf{V}^*$ is a polarity and every point is regular.*

Remark 33. This polarity is called the polarity *on the quadric* Q.

3.1.2.1 Restriction of Q to subspace

Definition 34. For a closed $\mathcal{X} \subset \mathsf{V}$, the *polar* of $\mathcal{X}$, $\mathcal{X}^\perp := \{\mathbf{y} \mid B(\mathbf{x}, \mathbf{y}) = 0 \ \forall \ \mathbf{x} \in \mathcal{X}\}$. $\mathcal{X}$ is a *regular* subspace with respect to Q if $\mathcal{X}^\perp$ has dimension $dim(n - 1 - dim(\mathcal{X})$.

If $\mathcal{X}$ is a k-dimensional subspace of V, the restriction of Q to $\mathcal{X}$ is a quadratic form $Q_\mathcal{X}$. When $\mathcal{X}$ is regular, $Q_\mathcal{X}$ is non-degenerate. We have the following decomposition of Q (for later reference):

Theorem 35. *Let $\mathcal{X}$ be a regular k-dimensional subspace of $\mathbb{R}P^n$. Then $Q = Q_\mathcal{X} + Q_{\mathcal{X}^\perp}$.*

3.2 Quadric surfaces

Definition 36. An *admissable quadric surface* is a pair of non-zero quadratic forms of the form (Q, Q^*). The quadric surface is called *standard* if Q is defined on V, and Q^* is defined on V^*; and it is called *dual* if Q is defined on V^* and Q^*, on V.

Remark 37. The full theory of quadric surfaces lies outside the scope of this work. It forms a part of classical projective geometry. There are a wide variety of degenerate possibilities which do not fulfill the above conditions and which do not lead to Cayley-Klein spaces. The above subset suffices to model the geometries which form the object of our investigations.

Remark 38. A quadric surface (Q, Q^*) is sometimes defined as the zero-sets $(\mathbf{Q}, \mathbf{Q}^*)$. We prefer to work with the quadratic forms themselves.

Remark 39. A quadric surface in $\mathsf{V} = \mathbb{R}P^2$ is called a *conic section.*

Theorem 40. *For an admissable quadric surface* $r(Q) = n + 1$ *or* $r(Q) = n$.

Proof. This follows directly from the definition of Q and Q^* by considering the three cases for $r(Q)$:

- $r(Q) = n + 1$: Then $Q^* \cong Q$ and both are non-zero.
- $r(Q) = n$: we can suppose the sign vector for Q is (0++...- - -) where there are p +'s and m -'s. Then Q^* can be calculated via the cofactor matrix; one obtains (x000...000) where $x = +$ if m is even, and otherwise $-$.
- $r(Q) < n$: then $Q^* = 0$ so the pair is not admissable.

Remark 41. Consider the example in the proof, when $r(Q) = n$. Interpreted as a standard quadric surface, $\mathcal{V}_Q$ is the point $\mathbf{E}_0 = (1, 0, ...0)$; $\mathcal{V}_{Q^*}$ consists of the plane bundle centered at this point. There is a similar incidence condition on $\mathcal{V}_Q$ and $\mathcal{V}_{\widehat{Q}}$ for a general quadric surface $(Q, \widehat{Q})$ which we have omitted since it is not relevant for our purposes.

Remark 42. The same example can be interpreted as a dual quadric surface (conic section). Then $\mathcal{V}_{Q_0}$ is the plane $\mathbf{e}_0$, and $\mathcal{V}_{Q_0{}^*}$, the point field contained in it. This dual conic section turns out to be the appropriate choice to arrive at a model of the euclidean plane. See Sect. 4.3. In general, $Q = (1, 0, n)$ and $Q^* = (n, 0, 1)$ yield the proper metric for n-dimensional euclidean space. See below, Sect. 4.3.

We collect the observations of the previous remarks regarding the singular elements of an quadric surfaces of the form (Q, Q^*):

Theorem 43. *Let* $\mathcal{Q}$ *be a quadric surface of the form* (Q, Q^*). *Then* $\mathbf{a} \in \mathcal{V}_{Q^*} \iff \langle \mathbf{a}, \mathbf{v} \rangle = 0$ *for some* $\mathbf{v} \in \mathcal{V}_Q$.

Proof. For rank-n Q, the previous remarks suffice to establish the result. For rank-k with $k < n$, $\mathcal{V}_Q$ has dimension $n + 1 - k > 1$. $\mathbf{a}$ has co-dimension 1 viewed as a subspace of the dual space. Hence the two subspaces have non-empty intersection, hence there exists $\mathbf{v} \in \mathcal{V}_Q$ with the desired property. □

Remark 44. To see that there are quadric surfaces which are not admissable: Let $Q = (+00)$ and $\widehat{Q} = (00+)$. Then Q, defined on V, is the point range $x_0^2 = 0$ (doubled) and $\widehat{Q}$, defined on V^*, is the line pencil $u_2^2 = 0$ (doubled). The line pencil is incident with the point range. This represents a valid conic section. On the other hand, both Q and $\widehat{Q}$ are rank-1 quadratic forms, so are not admissable. See Type VII in Sect. 3.2.2.2 below.

3.2.1 Rank-n quadric surfaces via limiting process

Because of their importance for the sequel, we also investigate how to derive the rank-n quadratic surfaces (standard and dual) from the rank-$(n+1)$ surfaces by a geometric limiting process.

For example, begin in $\mathbb{R}P^2$ with $Q = (\text{-}++)$ in standard form, represented in point coordinates as $Q(\mathbf{x}) = -x_0^2 + x_1^2 + x_2^2$. Define $Q_\epsilon := -\epsilon^2 x_0^2 + x_1^2 + x_2^2$. For $\epsilon \neq 0$, Q_ϵ is non-degenerate and by the definition of adjoint, ${Q_\epsilon}^* = u_0^2 - \epsilon^2 u_1^2 - \epsilon^2 u_2^2$. Then:

$$\lim_{\epsilon \to 0} Q_\epsilon = x_1^2 + x_2^2 \tag{3.3}$$

$$\lim_{\epsilon \to 0} {Q_\epsilon}^* = u_0^2 \tag{3.4}$$

The limiting values $Q_0 = (0++)$ and ${Q_0}^* = (+00)$, are in agreement with the result obtained in Thm. 40.

Remark 45. The limiting process can also be carried out in the direction of ∞. To evaluate this limit, one then uses projective invariance under multiplication by a non-zero factor to multiply through by $-\epsilon^{-2}$ and obtains:

$$\lim_{\epsilon \to \infty} Q_\epsilon = x_0^2 \tag{3.5}$$

$$\lim_{\epsilon \to \infty} {Q_\epsilon}^* = u_1^2 + u_2^2 \tag{3.6}$$

Remark 46. Here the limit is the dual conic section discussed in Remark 42; interpreting the original conic section dually leads to the original standard limit.

Remark 47. We include the limit as $\epsilon \to \infty$ since that is the method originally used by Klein ([Kle26]) to establish the euclidean metric. However one takes the limit, and whether one begins with a standard or dual conic section, one has two geometric limits: either one expands an oval conic section until it flattens out to a plane, or one contracts it until it collapses into a point. The former leads to euclidean geometry; the latter to dual euclidean geometry. One can also begin with the totally imaginary conic $(+++)$ but then the result is less geometrically meaningful.

Remark 48. Applied to a general non-degenerate signature $(p, m, 0)$, one can attach the ϵ^2 term to any of the $n+1$ positions; the resulting signatures will be $Q = (p, m-1, 1)$ or $Q = (p-1, m, 1)$, depending on whether the ϵ^2 term was attached to a negative or positive term; and $Q^* = (1, 0, p+m-1)$.

Remark 49. If one attaches ϵ to more than one term of the polynomial defining Q, one arrives at surfaces with rank less than n. More complicated non-admissable signatures can be generated by more complicated limiting process (see Type VII in Example 2 below). Such surfaces will not be of interest for our later investigations.

3.2.2 Enumeration of low-dimension quadric surfaces

We give here an enumeration of quadric surfaces in $\mathbb{R}P^n$ for $n = 2$ and $n = 3$ since all the important examples of interest to us are already present.

3.2.2.1 Example $\mathbb{R}P^1$ For $n = 1$, there are three possible quadratic forms. See Table 3.2.2.1. The possible choices of Q are listed in alphabetical order, where $(+, -, 0)$ is the alphabetical order of the basic symbols. For simplified book-keeping, we assign each possibility a roman numeral identifier which we call the *Type*.

Q	Q^*	Type	**Q**
(++)	(++)	I	2 conjugate imaginary points
(+-)	(+-)	II	2 real points
(+0)	(0+)	III	1 real double point

Table 3.1 The three possible signatures in $\mathbb{R}P^1$.

3.2.2.2 Example $\mathbb{R}P^2$ For $n = 2$ there are seven possible quadric surfaces (conic sections). All but one is admissable. See Table 3.2.2.2.

There are exactly two non-equivalent non-degenerate conic sections with signature $(3, 0, 0)$ and $(2, 1, 0)$. The first is completely imaginary, the second is a real oval.

Let homogeneous point coordinates be represented by (x, y, w) and homogeneous line coordinates by (u, v, t). There are also degenerate conic sections, such as two intersecting point ranges. This can be represented by the equation $(x + y)(x - y) = x^2 - y^2 = 0$. Hence, its signature is $(+ - 0)$. It has rank 2. By the above, the signature on the dual space is (00+). This corresponds to the line pencil in the intersection point $(0, 0, 1)$ of the two point ranges of **Q**, counted twice.

We can also find degenerate conic sections beginning with the dual space of lines. Then, the analogous equation $u^2 - v^2 = 0$ corresponds to a pair of real line pencils that share a common line $w = 0$.

We can also have the totally imaginary rank-2 conic $x^2 + y^2 = 0$ in point space. The sign vector (++0) in point space yields sign vector (00+) in line space. The latter is again a real line pencil at the origin $(0, 0, 1)$, the intersection of the two conjugate imaginary point ranges $(x + iy) = 0$ and $(x - iy) = 0$. If one begins in line space, this construction yields a totally imaginary pair of line pencils which share the real point range $z = 0$. This conic section, we will see, is the signature needed to model euclidean geometry.

Notice that two complex conjugate imaginary point ranges have a real point in common; and two complex conjugate imaginary line pencils have a real line pencil in common. The type identifiers have been assigned to agree with those in [Kow09]. Of the degenerate cases (III-VII), only Type VII does not satisfy $\widehat{Q} = Q^*$.

Q	$\widehat{Q}$	Type	$\mathbf{Q}$	$\mathbf{Q}^*$
(+++)	(+++)	II	pointwise imaginary conic	linewise imaginary conic
(++-)	(++-)	I	pointwise oval conic	linewise oval conic
(++0)	(00+)	IV	2 conjugate imaginary point ranges	real double line pencil
(+-0)	(00+)	III	2 real point ranges	real double line pencil
(+00)	(0++)	VI	real double point range	2 conjugate imaginary line pencils
(+00)	(0+-)	V	real double point range	2 real line pencils
(+00)	(00+)	VII	real double point range	real double line pencil

Table 3.2 The seven possible conic sections (quadric surfaces) in $\mathbb{R}P^2$.

3.3 Guide to the literature

For a standard treatment of symmetric bilinear forms and quadratic forms see [Gre67a], Ch. 9-10. For details in for $\mathbb{R}P^2$ and a listing of the 18 distinct quadric surfaces for $\mathbb{R}P^3$, see [Kow09], Section 4.4. For a detailed discussion of degenerate quadratic forms in arbitrary dimension, see [SS04], p. 157, or [Gie82].

Chapter 4
Cayley-Klein spaces

Equipped with the results on admissable quadric surfaces from Chapter 3, we now turn to the Cayley-Klein construction of metric spaces within $\mathbb{R}P^n$. We begin by describing in detail how the construction works for the three metric planes: elliptic, hyperbolic, and euclidean. Using these examples as a guide, we then define what a Cayley-Klein space is and list the spaces of interest for this study. We discuss the exceptional features of pseudo-euclidean spaces. Finally, we show that the isometry group of a Cayley-Klein space can be generated by the subset of harmonic homologies whose axes are proper.

All the examples are set in the projective plane $\mathbb{R}P^2$.

4.1 Example 1: the elliptic plane

Introduce the non-degenerate quadratic surface (Q, Q^*) with $Q = (3, 0, 0)$. Then $\mathbf{Q}$ is a completely imaginary conic, whose points satisfy $x_0^2 + x_1^2 + x_2^2 = 0$, and $\mathbf{Q}^*$ is the same conic in its dual, line-wise aspect.

Define a distance function on the points of $\mathbb{R}P^2$ as follows: for two points $\mathbf{x}$ and $\mathbf{y} \in \mathbb{R}P^2$, find the two complex conjugate points $\mathbf{f}_+$ and $\mathbf{f}_-$, where the line joining $\mathbf{x}$ and $\mathbf{y}$ intersects $\mathbf{Q}$. We choose subscripts $+$ and $-$ so that the points $(\mathbf{f}_+, \mathbf{x}, \mathbf{y}, \mathbf{f}_-)$ defines a cyclic order of the four points on the line. Define the distance:

$$d(\mathbf{x}, \mathbf{y}) = \frac{1}{2i} \ln(f_+, f_-; \mathbf{x}, \mathbf{y})$$

The resulting value is a real-valued function (Exercise), and for three collinear points, satisfies

$$d(\mathbf{x}, \mathbf{y}) + d(\mathbf{y}, \mathbf{z}) = d(\mathbf{x}, \mathbf{z})$$

and the other axioms which characterize a metric space.

Using basic functional identities, it is possible to show ([Wei35]):

$$d(\mathbf{x},\mathbf{y}) = \cos^{-1}\left(\frac{B(\mathbf{x},\mathbf{y})}{\sqrt{B(\mathbf{x},\mathbf{x})B(\mathbf{y},\mathbf{y}))}}\right)) \tag{4.1}$$

The right-hand side is the expression for the angle between two vectors in $\mathbb{R}^3$. If we assume $Q(\mathbf{x},\mathbf{x}) = Q(\mathbf{y},\mathbf{y}) = 1$, then this represents the angle between points on the unit sphere, and the distance function is the central angle between these two points. However, since in $\mathbb{R}P^2$ $\mathbf{x} \equiv -\mathbf{x}$, the unit sphere contains two copies of this space, which is called the *elliptic* plane. It satisfies all axioms of euclidean geometry except the Parallel Postulate, since in $\mathbb{R}P^2$ every two lines interesect.

4.1.1 Isometries

Projectivities which preserve $\mathbf{Q}$ are isometries of the elliptic plane. For, suppose A is such a projectivity and $\mathbf{x}$ and $\mathbf{y}$ are two points in $\mathbb{R}P^2$, with distance $d(\mathbf{x},\mathbf{y})$ as above. Then the distance of $A(\mathbf{x})$ and $A(\mathbf{y})$ is:

$$d(A(\mathbf{x}),A(\mathbf{y})) = \frac{1}{2i}\ln(\mathbf{g}_+,\mathbf{g}_-;A(\mathbf{x}),A(\mathbf{y}))$$

where $\mathbf{g}_+,\mathbf{g}_-$ are the intersections of the transformed line with $\mathbf{Q}$, with cyclic order $(\mathbf{g}_+,A(\mathbf{x}),A(\mathbf{y}),\mathbf{g}_-)$.

Lemma 50. $\mathbf{g}_+ = A(\mathbf{f}_+)$ *and* $\mathbf{g}_- = A(\mathbf{f}_-)$

Proof. Since A preserves $\mathbf{Q}$, $\{\mathbf{g}_+,\mathbf{g}_-\} = \{A(\mathbf{f}_+),A(\mathbf{f}_-)\}$. Since a projectivity preserves cyclic order on lines, $\mathbf{g}_+ = A(\mathbf{f}_+)$ and $\mathbf{g}_- = A(\mathbf{f}_-)$. □

Then the distance between two transformed points is unchanged:

$$\begin{aligned} d(A(\mathbf{x}),A(\mathbf{y})) &= \frac{1}{2i}\ln(A(\mathbf{f}_+),A(\mathbf{f}_-);A(\mathbf{x}),A(\mathbf{y})) \\ &= \frac{1}{2i}\ln(f_+,f_-;\mathbf{x},\mathbf{y}) \\ &= d(\mathbf{x},\mathbf{y}) \end{aligned}$$

where we have used the invariance of cross ratio under projectivities.

4.2 Example 2: the hyperbolic plane

Using instead the non-degenerate quadratic form Q with signature $(2,1,0)$ leads to important differences to the elliptic plane. Now $\mathbf{Q}$ is a real conic section, in affine coordinates the unit circle, which separates $\mathbb{R}P^2$ into two components. We call the points of $\mathbf{Q}$ the *ideal* points of the metric space.

We choose the interior $\mathbb{K}$, the unit disk, as the set of *proper* points $\mathcal{P}$ of the metric space. Similar remarks apply to $\mathbf{Q}^*$; as *proper* lines we choose the component $\widehat{\mathcal{P}}$ of $\mathbb{R}P^{2*}$

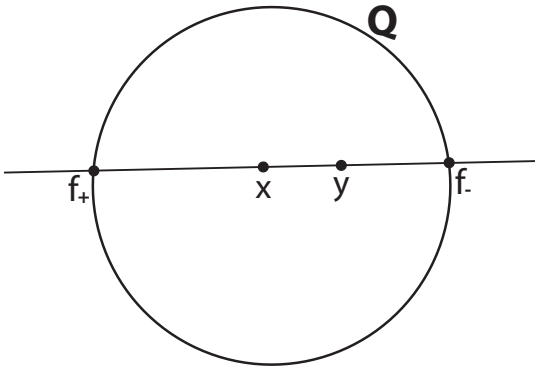

Fig. 4.1 Distance calculation for $Q = (2, 1, 0)$ involves the four marked points: $\mathbf{x}$ and $\mathbf{y}$ plus the intersections $\mathbf{f}_+$ and $\mathbf{f}_-$ of the line joining $\mathbf{x}$ and $\mathbf{y}$ with the quadric $\mathbf{Q}$.

consisting of lines which lie "outside" $\mathbf{Q}^*$; these are lines which cut $\mathbf{Q}$ in two real points. Then two proper points are joined by a proper line, although two proper lines do not always intersect in a proper point.

A *hyperbolic line* is a chord of the unit circle. Such a chord always belongs to a proper line. To simplify notation, we will not always carefully distinguish between proper lines and the proper chord of hyperbolic points lying inside the unit circle.

The distance function is defined similarly to above, but since the joining line of two points in $\mathbb{K}$ intersects $\mathbf{Q}$ in two *real* points, the distance function looks like:

$$d(\mathbf{x}, \mathbf{y}) = \frac{1}{2} \ln(f_+, f_-; \mathbf{x}, \mathbf{y})$$

which is equivalent to:

$$d(\mathbf{x}, \mathbf{y}) = \cosh^{-1}\left(\frac{B(\mathbf{x}, \mathbf{y})}{\sqrt{B(\mathbf{x}, \mathbf{x})B(\mathbf{y}, \mathbf{y})}}\right) \tag{4.2}$$

See Fig. 4.1.

Isometries, as in the previous example, consist of projectivities which preserve $\mathbf{Q}$. The resulting metric space consisting of proper points and proper lines, is a model for two-dimensional hyperbolic geometry, which also satisfies all the axioms of euclidean geometry except the parallel postulate. For details see [Kow09], Sec. 6.1.

4.3 Example 3: the euclidean plane

Here the conic section is given by the dual quadric surface (Q, Q^*) for $Q = (0{+}{+})$. The point-wise description of the surface is $x_0^2 = 0$ and the line-wise is $u_1^2 + u_2^2 = 0$. Hence $\mathbf{Q}$ is

the line $x_0 = 0$, doubled, and $\widehat{\mathbf{Q}}$ is a pair of conjugate imaginary line pencils $u_i + iu_2 = 0$ and $u_i - iu_2 = 0$. Note that these two pencils intersect in the real line $\mathbf{x}_0 = 0$.

As in the hyperbolic case, define the ideal points and lines of the metric space to be $\mathbf{Q}$ and $\mathbf{Q}^*$, resp. Define the proper points to be $\mathbb{R}P^2 \setminus \mathbf{Q}$, and the proper lines to be $\mathbb{R}P^{2*} \setminus \mathbf{Q}^*$. Proper elements are sometimes called *euclidean*, or *finite*. The euclidean plane is denoted as $\mathbf{E}^2$.

4.3.1 The euclidean distance function

Since $\mathbf{Q}$ is flat, it is no longer possible to define a distance function using the cross ratio as in the non-degenerate cases above, since every proper line intersects $\mathbf{Q}$ in a single real point. Instead, we use a limiting process of non-degenerate metrics to arrive at the desired distance function. To simplify the exposition, we derive the euclidean distance function for a euclidean line rather than plane; the argument for the plane (and higher dimensions) proceeds in the same way.

Introduce a family Q_ϵ of quadratic forms (with associated bilinear form B_ϵ) parametrized by the real parameter $\epsilon \to \infty$ as above, (3.5), but based on $Q = (3, 0, 0)$. Consider two proper points $\mathbf{x} = (x_0, x_1)$ and $\mathbf{y} = (y_0, y_1)$. Then $x_0 \neq 0$ and $y_0 \neq 0$. Choose the projective representative so that $x_0 = y_0 = 1$. Then:

$$B_\epsilon(\mathbf{x}, \mathbf{y}) := \epsilon x_0 y_0 + x_1 y_1 = \epsilon + x_1 y_1$$

By (4.1), the distance function d_ϵ associated to Q_ϵ is determined by:

$$\cos d_\epsilon(\mathbf{x}, \mathbf{x}) = \frac{B_\epsilon(\mathbf{x}, \mathbf{y})}{\sqrt{B_\epsilon(\mathbf{x}, \mathbf{x}) B_\epsilon(\mathbf{y}, \mathbf{y}))}} \tag{4.3}$$

Abbreviate $d_\epsilon(\mathbf{x}, \mathbf{y})$ as d_ϵ.

Rewrite (4.3) and manipulate:

$$\cos^2(d_\epsilon)\langle \mathbf{x}, \mathbf{x}\rangle_\epsilon \langle \mathbf{y}, \mathbf{y}\rangle_\epsilon = \langle \mathbf{x}, \mathbf{y}\rangle_\epsilon \tag{4.4}$$

$$\cos^2(d_\epsilon)(\epsilon + x_1^2)(\epsilon + y_1^2) = (\epsilon + (x_1 y_1))^2 \tag{4.5}$$

$$\cos^2(d_\epsilon)(\epsilon^2 + \epsilon((y_1)^2 + (x_1)^2) + (x_1 y_1)^2) = \epsilon^2 + 2\epsilon(x_1 y_1) + (x_1 y_1)^2 \tag{4.6}$$

Now consider the limit as $\epsilon \to \infty$. It's clear from (4.3) that $\lim_{\epsilon \to \infty} \cos d_\epsilon = 1$. So we can replace $\cos {d_\epsilon}^2$ by $(1 - d_\epsilon^2)$, and simplify the resulting expressions:

$$(1 - d_\epsilon^2)(\epsilon^2 + \epsilon(y_1^2 + x_1^2) + (x_1 y_1)^2) = \epsilon^2 + 2\epsilon(x_1 y_1) + (x_1 y_1)^2 \tag{4.7}$$

$$\epsilon(y_1^2 + x_1^2 - 2x_1 y_1) = d_\epsilon^2(\epsilon^2 + \epsilon(y_1^2 + x_1^2) + (x_1 y_1)^2) \tag{4.8}$$

$$(x_1 - y_1)^2 = d_\epsilon^2(\epsilon + (y_1^2 + x_1^2) + \frac{1}{\epsilon}(x_1 y_1)^2) \tag{4.9}$$

Notice that the LHS is the square of the desired euclidean distance function. In order to make the limit converge to this, define a new distance function $\hat{d}_\epsilon := \sqrt{\epsilon} d_\epsilon$. This is exactly the scaling needed to prevent the distance from going to zero in the limit. One

obtains:

$$\lim_{\epsilon\to\infty} \hat{d}_\epsilon^2 = \frac{(x_1-y_1)^2}{(1+\frac{1}{\epsilon}(y_1^2+x_1^2)+\frac{1}{\epsilon^2}(x_1y_1)^2} \tag{4.10}$$

$$= (x_1-y_1)^2 \tag{4.11}$$

Remark 51. The above process, applied to the plane, produces the familiar euclidean distance function

$$d(\mathbf{x},\mathbf{y}) = \sqrt{(x_1-y_1)^2+(x_2-y_2)^2} \tag{4.12}$$

Remark 52. A similar limiting process produces distance functions for any pseudo-euclidean metric.

Isometries. The group of projectivities preserving $\mathbf{Q}$ and $\mathbf{Q}^*$ includes isotropic scaling transformations. One obtains the euclidean group by further requiring that the projectivity preserves the distance function (4.12).

Remark 53. **Measuring angle between lines.** In all three metric planes above, the angle between two proper lines which intersect in a proper point is given by the formula:

$$d(\mathbf{u},\mathbf{v}) = \cos^{-1}\left(\frac{B^*(\mathbf{u},\mathbf{v})}{\sqrt{B^*(\mathbf{u},\mathbf{u})B^*(\mathbf{v},\mathbf{v}))}}\right) \tag{4.13}$$

When the lines intersect in the point $\mathbf{E}_0$, the result follows from the fact that Q^*, restricted to such lines, is identical for all three geometries. If the two lines intersect in another proper point $\mathbf{P}$, then find an isometry moving $\mathbf{P}$ to $\mathbf{E}_0$ and measure the angle of the transformed lines. That such isometries exist follows from the standard result that the isometry groups of these geometries are transitive on proper points [TL97].

4.4 The Cayley-Klein Construction

The examples above are all examples of *Cayley-Klein* spaces. Based on Cayley's 1859 paper ([Cay59], and later developed as part of his *Erlangen program* by Klein ([Kle26]), such spaces are metric spaces created in projective space $\mathbb{R}P^n$ based on quadratic forms. The examples above illustrate all the important features of this construction.

The general Cayley-Klein construction in its modern formulation is based on a nested sequence of subspaces X_i of $\mathbb{R}P^n$, and a non-degenerate quadratic form Q_i defined on each X_i. The admissable quadric surfaces correspond to the simplest of such sequences, of length 1 (rank-$(n+1)$ quadric surface) and length 2 (rank-n quadric surface). For simplicity we have chosen an exposition based on quadric surfaces (the original approach of Klein [Kle26]) instead of the more general modern approach. A second advantage of the formulation in terms of a pair $(Q,\widehat{Q})$ is that it lends itself to dualization, which meshes well with the projective approach used throughout this study. Interested readers are referred to [Gie82] to see how the modern definition is compatible with the one presented here.

4.4.1 Defining a metric space

We consider first a standard quadric surface $\mathcal{Q} = (Q, Q^*)$, so that Q is defined on $\mathbb{R}P^n$, and Q^*, on $(\mathbb{R}P^n)^*$. One defines a metric space M_Q as follows. Let $\mathcal{P}$ (the *proper* points of M_Q) be a connected component of $\mathbb{R}P^n \setminus \mathbf{Q}$, and $\widehat{\mathcal{P}}$ (the *proper* planes[1] of M_Q) be a connected component of $(\mathbb{R}P^{\setminus})^*\mathbf{Q}^*$.

The points of $\mathbf{Q}$ are called *ideal* points; the planes of $\mathbf{Q}^*$, ideal planes. Points and planes which are neither proper nor ideal are called *improper*. That is, an ideal point, although not proper, is also not improper. This partition into three categories is convenient for the ensuing discussions. The quadric surface (Q, Q^*) is called the *absolute figure* of M_Q.

Measurement in this metric space is discussed in Sect. 4.4.3.

Remark 54. When $\mathcal{Q}$ is dual, one defines a metric space M_Q in a similar way, except that the roles of Q and Q^* are reversed (the former determines the ideal planes, and the latter, the ideal points).

Remark 55. When $\mathbf{Q} \neq \emptyset$, there are two choices for $\mathcal{P}$: $\mathcal{P}^+ := \{P \in \mathbb{R}P^n \mid Q(P) > 0\}$ and $\mathcal{P}^- := \{P \in \mathbb{R}P^n \mid Q(P) < 0\}$. At least one of these sets is non-empty for admissable quadric surfaces. Similar remarks apply to $\widehat{\mathcal{P}}$. When all four of these sets are non-empty, there are four different combinations, each of which potentially yields a different metric space M_Q.

4.4.2 Cayley-Klein spaces of interest

We are now in a position to give names to the spaces of interest:

Definition 56. Let $\mathcal{C}$ be a Cayley-Klein space whose absolute figure is the admissable quadric surface $\mathcal{Q} := (Q, Q^*)$. Then $\mathcal{C}$ is an *admissable* Cayley-Klein space. It is called:

- *elliptic* n-space $\mathbf{Ell}^n$ if $Q = (n+1, 0, 0)$,
- *hyperbolic* n-space $\mathbf{H}^n$ if $Q = (n, 1, 0)$, $\mathcal{P} = \mathcal{P}^-$, $\widehat{\mathcal{P}} = \widehat{\mathcal{P}}^+$,
- *dual hyperbolic* n-space $\mathbf{H}^{n*}$ if $Q = (n, 1, 0)$, $\mathcal{P} = \mathcal{P}^+$, $\widehat{\mathcal{P}} = \widehat{\mathcal{P}}^-$,
- a *pseudo-euclidean* n-space if $\mathcal{Q}$ is dual rank-n, and
- a *dual pseudo-euclidean* n-space if $\mathcal{Q}$ is standard rank-n.
- The pseudo-euclidean space with $Q = (n, 0, 1)$ is called *euclidean* n-space $\mathbf{E}^n$.
- The dual pseudo-euclidean space with $Q = (n, 0, 1)$ is called *dual euclidean* n-space $\mathbf{E}^{n*}$.

Remark 57. Note that the definitions of elliptic and hyperbolic spaces do not depend on whether one uses a standard or dual quadric surface. There are two types of hyperbolic space, depending on how one chooses the proper points and planes. Hyperbolic space consists pointwise of the interior of the unit ball $\mathcal{P}^-$ and planewise of the planes which intersect the unit ball ($\widehat{\mathcal{P}}^+$). Dual hyperbolic space consists of points and planes which lie outside the unit ball ($\mathcal{P}^+$). Dual hyperbolic space is the image of hyperbolic space under the polarity of $\mathbb{R}P^n$ determined by $\mathcal{Q}$ (see Sect. 6.2.2.2).

[1] We use *plane* here instead of the more awkward but correct *hyperplane* to denote an element of $(\mathbb{R}P^n)^*$.

Remark 58. Elliptic space $\mathbf{Ell}^n$ is closely related to the n-dimensional sphere $\mathbf{S}^n$. The latter is the universal cover of the former; the covering is 2:1. Consult [Gun10], §2.2 and §3.3, for a detailed discussion of the relationship of these two spaces, including computational aspects. Almost any result established for $\mathbf{Ell}^n$ is either directly true also for $\mathbf{S}^n$, or can be easily amended to be true. We state our results here for $\mathbf{Ell}^n$ only.

Remark 59. So-called de Sitter space arises by using $\mathcal{P}^+$ along with $\widehat{\mathcal{P}}^+$: points exterior to the unit ball, and planes which intersect the unit ball. There are improper planes consisting of proper points! See [Kow09], §6.4, for more on de Sitter space; we don't discuss it further.

Remark 60. A euclidean space is also pseudo-euclidean; this is chosen to avoid the awkward construction "euclidean and pseudo-euclidean" to refer to dual rank-n quadrics. The reversal of the dual attribute in these spaces due to the fact that the euclidean metric requires that Q (the less degenerate quadratic form) be defined in V^*; hence the dual euclidean must be based on V.

Remark 61. We focus in the sequel on the euclidean (and occasionally on the dual euclidean) case; many of the results carry over naturally to the other pseudo-euclidean spaces.

4.4.2.1 Terminology alert. The euclidean vector space signature $(n+1, 0, 0)$ becomes, in the projective setting, the *elliptic* signature. And the euclidean signature in the projective setting, is the degenerate one introduced above.

4.4.3 Measurement

The nature of measurement of distances in a Cayley-Klein space depends qualitatively on whether the quadric surface is degenerate or not.

4.4.3.1 Non-degenerate measurement If Q is non-degenerate, one can define a distance function on pairs of proper points whose joining line is not tangent to Q, hence intersects $\mathbf{Q}$ in two distinct points, by using the natural logarithm of the cross ratio of the two points and these two intersection points. See Fig. 4.1. The method is fully described for $n = 2$ in Sect. 4.1 and Sect. 4.2; the generalization to arbitrary n is immediate. A dual formula exists for the angle between two proper hyperplanes as in Remark 53. The example of the hyperbolic plane makes clear that the situation can be complicated; two lines can intersect in an ideal or improper point, in which case the angle between the two lines is not defined.

4.4.3.2 Pseudo-euclidean measurement When Q is degenerate, as in the euclidean plane example, one uses an appropriate limiting process of non-degenerate Q to derive a distance function not based on the cross ratio approach. Since we are only interested in rank-n quadric surfaces, for which $\widehat{Q} = Q^*$, the limiting process is essentially the same as the one shown above for the euclidean case in Sect. 4.3.1. To be precise, suppose $Q = (p, m, 1) = (0{+}{+}{+}...{-}\ {-}\ {-}...)$ and $Q^* = (1, 0, p + m) = (+00...0)$. Then, using the

same technique as in Sect. 4.3.1, the distance function for normalized proper points (with $x_0 = 1$) is given by

$$d(\mathbf{x}, \mathbf{y}) = \sqrt{\sum_{i=1}^{p}(x_i - y_i)^2 - \sum_{i=p+1}^{p+m}(x_i - y_i)^2} \tag{4.14}$$

Remark 62. The above distance definition applies to points in pseudo-euclidean spaces, and to hyperplanes in dual pseudo-euclidean spaces.

4.4.4 Peculiarities of pseudo-euclidean metrics

The nature of measurement in the pseudo-euclidean spaces is not without subtleties. We take the opportunity to discuss them now since they play a crucial role in geometry of such spaces. (Everything we say here also applies to dual pseudo-euclidean spaces, when properly "translated".)

4.4.4.1 Ideal points are free vectors We can assume $\mathbf{Q}$ is the plane $\mathbf{e}_0$. We can also assume proper points are normalized to have the $\mathbf{E}_0$ coordinate 1. For two such proper points $\mathbf{x}$ and $\mathbf{y}$, define $\mathbf{v} := \mathbf{x} - \mathbf{y}$. Then $\mathbf{v} \in \mathbf{Q}$ (since $v_0 = 0$), that is, $\mathbf{v}$ is an ideal point. On the other hand, as the difference of two proper points, $\mathbf{v}$ is a *free vector*. Hence, free vectors can be identified with ideal points.

Remark 63. The proper points and the ideal points of the pseudo-euclidean space constitute the points and vectors of an *affine space* ([Gre67a], Ch. 10).

4.4.4.2 Transferring the rank-n metric to $\mathbf{e}_0$ (4.14) can be written in the form:

$$d(\mathbf{x}, \mathbf{y}) = \sqrt{B(\mathbf{x} - \mathbf{y}, \mathbf{x} - \mathbf{y})} = \sqrt{B(\mathbf{v}, \mathbf{v})}$$

We have, however, no right to write this, since B represents the symmetric bilinear form on V, while $\mathbf{v} \in \mathsf{V}^*$. In fact, $\mathbf{x}, \mathbf{y} \in \mathcal{V}_{Q^*} \Rightarrow B^*(\mathbf{x}, \mathbf{y}) = 0$. The two points should have inner product 0; however, the euclidean distance formula implies that their inner product is given by the rank-n quadratic form Q rather than the rank-1 quadratic form Q^*. This is a point whose importance for (pseudo-) euclidean geometry is difficult to overestimate: *The ideal hyperplane $\mathcal{V}_{Q^*} \subset \mathbb{R}P^n$ of a pseudo-euclidean space M_Q is naturally equipped with the non-degenerate quadratic form, given by the restriction to the non-degenerate part of the rank-n quadratic form Q.* We write this transferred quadratic form on the ideal plane field as Q_∞.

4.4.4.3 Possible perspectives for understanding How can this "overriding" of the normal inner product in the ideal plane $\mathbf{e}_0$ be understood? The following observations provide different perspectives:

1. The limiting process described above in Sect. 3.2.1 that led to the degenerate pseudo-euclidean signature can be restricted to the proper points $\mathcal{P} \subseteq \mathbb{R}P^n \setminus \mathbf{Q}^*$. This leaves

the signature on $\mathbf{Q}^*$ alone, hence it retains the restriction of the original signature to $\mathbf{Q}^*$, which is exactly Q_∞.
2. For $\mathbf{X}_1$, $\mathbf{X}_2 \in \mathcal{V}_Q$, consider any two planes $\mathbf{x}_1$ and $\mathbf{x}_2$ such that $\mathbf{x}_i^\perp = \mathbf{X}_i$. Define a symmetric bilinear form $B_\infty(\mathbf{X}_1, \mathbf{X}_2) := \widehat{B}(\mathbf{x}_1, \mathbf{x}_2)$. This is well-defined since parallel planes have the same polar point. This in effect transfers the quadratic form Q^* to $\mathcal{V}_{Q^*}$.
3. As noted above, it is the unique inner product consistent with the euclidean distance function (4.14).

Remark 64. Since the quadratic form Q^* is extremely degenerate (rank 1), it is perhaps not surprising that much of euclidean geometry is carried out via operations with free vectors (ideal points), for which the inner product is non-degenerate (rank n). The natural presence of the non-degenerate quadratic form with signature $(p, m, 0)$ on the ideal plane $\mathbf{e}_0$ of pseudo-euclidean spaces (and, naturally, for the ideal points of the dual spaces), is an essential feature of doing geometry in these spaces. We take repeated advantage of it in the sequel. To the best of our knowledge, it has remained unremarked in the literature. As we'll see in Sect. 6.1.1 and Sect. 7.3.1, the Clifford algebra model presented here is well-equipped to recognize this subtle fact: Q_∞ can be calculated using operations within the algebra.

4.5 Cayley-Klein spaces as differentiable manifolds

One can also handle Cayley-Klein space as differentiable manifold. Then one is led naturally to the question what is the tangle bundle of the manifold, or, locally, what is the tangent space T_P at a point P of the space? Here we take advantage of the freedom we have to choose a representative for our projective point, and we choose representatives such that $\|Q(P)\| = 1$. That is, for the proper points $\mathbf{X}$, $Q(P)$ is constant. Then for any curve $P(t) \in \mathbf{X}$, $B(P, \dot{P}) = 0$. The set of all such possible $\dot{P}$ is used to construct T_P. On the other hand, this is the same as the polar plane $P^\perp$. Hence, we have arrived at the important result:

Theorem 65. *The tangent space T_P at a proper point of a Cayley-Klein space can be identified with $P^\perp$.*

Cayley-Klein spaces as Riemannian manifolds. One can further require of a Cayley-Klein space that it is a *Riemannian* manifold, that is, the tangent space at every point has a euclidean vector space structure, or equivalently, the metric relations are given by a positive definite quadratic form. Then one is left with only three possibilities in every dimension n. This can be shown as follows: By Thm. 65, the tangent space at a point $\mathbf{x}$ is the polar $\mathbf{x}^\perp$. Since the signature of $\mathbf{x}^\perp$ should by assumption be $(n, 0, 0)$, the possibilities for Q are easily enumerated. These are given in Table 67.

Definition 66. A Cayley-Klein space of dimension n is called a *Cayley-Klein* geometry if for every proper point $\mathbf{x}$, $\mathbf{x}^\perp$ has signature $(n, 0, 0)$.

Remark 67. These are the 3 geometries which have the same axiomatic structure as euclidean geometry with the (possible) exception of the Parallel Postulate. See [Kow09] and [TL97].

Q	Q^*	type	name
(n+1,0,0)	(n+1,0,0)	SD	elliptic
(n,1,0)	(n,1,0)	SD	hyperbolic
(n,0,1)	(1,0,n)	D	euclidean

Table 4.1 The quadric surfaces for three classical Cayley-Klein geometries in $\mathbb{R}P^n$. S = standard, D = dual.

Remark 68. **Semi-riemannian Cayley-Klein spaces.** Other signatures result in spaces which are not Riemannian, since the signature of the tangent space is not positive definite. For example, for $Q = (2, 2, 0)$, the quadric surface is a 1-sheeted hyperboloid; the polar plane of points of $\mathbb{R}P^n \setminus \mathbf{Q}$, may have signature $(1, 2, 0)$ or $(2, 1, 0)$; in either case, there are directions in which one "sees" Q and directions in which one doesn't. Hence $(2, 2, 0)$ does not give rise to a Riemannian manifold.

4.6 Isometries of Cayley-Klein spaces.

Motions of a metric space which preserve the distance between points play an important role in studying the space. In this section we discuss such motions in Cayley-Klein spaces.

Definition 69. An *isometry* of a metric space F is a bijection of F such that for every pair of points $\mathbf{P}, \mathbf{Q}$, $d(\mathbf{P}, \mathbf{Q}) = d(F(\mathbf{P}), F(\mathbf{Q}))$.

Theorem 70. *An* isometry *of a Cayley-Klein space $\mathbb{C}$ with a non-degenerate metric quadric (Q, Q^*) is a collineation F of $\mathbb{R}P^n$ such that $F(Q) = Q$. For degenerate (Q, Q^*), F must additionally preserve the distance function on $\mathbb{C}$.*

Remark 71. The proof is essentially that given in Sect. 4.1.1.

Remark 72. In the euclidean case, isotropic scaling is a collineation that preserves the quadric (Q, Q^*), but does not preserve distance.

Definition 73. A *reflection* of a Cayley-Klein space is a harmonic homology with center $\mathbf{Z}$ and axis $\mathbf{m}$ such that $\mathbf{Z}$ and $\mathbf{m}$ are a polar pair. If $\mathbf{Z}$ is proper, then $\mathbf{m} = \mathbf{Z}^\perp$; if $\mathbf{m}$ is proper, then $\mathbf{Z} = \mathbf{m}^\perp$.

The conditions on the center and axis are necessitated by the asymmetry of the degenerate metric. Note that the definition implies that $\mathbf{Z} \notin \mathbf{Z}^\perp$.

Theorem 74. *A reflection R of a Cayley-Klein space is an isometry.*

Proof. We prove this for a non-degenerate metric by showing $R(Q) = Q$. Define $\langle \mathbf{X}, \mathbf{Y} \rangle := B(\mathbf{X}, \mathbf{Y})$. From the proof of Thm. 12, $\mathbf{P} = \mathbf{S} + x\mathbf{Z}$ and $R(\mathbf{P}) =: \mathbf{P}' = -\mathbf{S} + x\mathbf{Z}$ with $\langle \mathbf{S}, \mathbf{Z} \rangle = 0$. $\mathbf{P} \in Q \iff \langle \mathbf{P}, \mathbf{P} \rangle = 0$. Substitute to obtain

$$\begin{aligned} 0 = \langle \mathbf{P}, \mathbf{P} \rangle &= \langle \mathbf{S} + x\mathbf{Z}, \mathbf{S} + x\mathbf{Z} \rangle \\ &= \langle \mathbf{S}, \mathbf{S} \rangle + x^2 \langle \mathbf{Z}, \mathbf{Z} \rangle + 2x \langle \mathbf{S}, \mathbf{Z} \rangle \\ &= \langle -\mathbf{S}, -\mathbf{S} \rangle + x^2 \langle \mathbf{Z}, \mathbf{Z} \rangle \\ &= \langle -\mathbf{S}, -\mathbf{S} \rangle + x^2 \langle \mathbf{Z}, \mathbf{Z} \rangle - 2x \langle \mathbf{S}, \mathbf{Z} \rangle \\ &= \langle \mathbf{P}', \mathbf{P}' \rangle \end{aligned}$$

Hence $R(\mathbf{P}) \in Q$. Hence by Thm. 70, R is an isometry. For the euclidean case, one can choose coordinate system so that $\mathbf{m} = \mathbf{e}_1$. Then $\mathbf{Z} = \mathbf{E}_1$. Given proper points $\mathbf{P}$ and $\mathbf{Q}$, it is easy to verify that the distance function between these two points (4.12) is preserved. □

Definition 75. A reflection is called *proper* if its axis is proper.

Remark 76. The reflection in an improper hyperplane $\mathbf{a}$ is a point reflection in the proper point $\mathbf{a}^\perp$. The latter can be generated by reflections in n hyperplanes passing through the point. Hence, the isometry group can be generated using proper reflections.

We include a standard result on the important role of reflections. See [Bac59], §9 for a proof.

Theorem 77. *The isometry group of an admissable Cayley-Klein space is generated by proper reflections.*

Remark 78. The fact that the isometries are generated by *proper* reflections will play an important, simplifying role in the subsequent development. See in particular Sect. 5.6.2.

4.7 Guide to the literature

The best introduction to non-euclidean geometry via the Cayley-Klein construction remains the classic [Kle26]. See also [Kow09] for a modern treatment of the same material limited to the plane. See [Wei35], pp. 55-6, for detailed account of the elliptic plane. [TL97] includes a thorough treatment of the 3-dimensional case along with the theory of quotient spaces of these Cayley-Klein geometries. [Gie82] is a standard reference for modern Cayley-Klein theory. See also [SS04].

Chapter 5
Clifford algebra

In this chapter we merge the results on projectivized Grassmann algebras from Chapter 2 with the Cayley-Klein metric construction from Chapter 4 to obtain *real Clifford algebras*. We show that, given an admissable quadric surface (Q, Q^*), there is a Clifford algebra whose *geometric product* faithfully reproduces the inner product structure of (Q, Q^*). We establish some results in n dimensions. For example, we show that multiplication by the unit pseudoscalar $\mathbf{I}$ is equivalent to the polarity on the metric quadric of the Cayley-Klein space. We introduce a family of Clifford algebras Cl^n_κ corresponding to the Cayley-Klein *geometries* of euclidean, elliptic, and hyperbolic n-space. We discuss how the isometry group of the Cayley-Klein geometry appears in the Clifford algebra. This leads to a description of the most important sub-algebras of the Clifford algebra. This n-dimensional treatment provides the foundation for the detail consideration of the 2-dimensional and 3-dimensional cases in Chapter 6 and Chapter 7, resp.

The chapter closes with a pair of appendices devoted to clarification work. The first is devoted to a a widespread confusion in the literature regarding representation of reflections in planes vs. reflections in points. The second concerns another widespread confusion in the literature: between the non-metric isomorphism $\mathbf{J}$ introduced in Chapter 2 and the polarity on the elliptic metric quadric, which is often used (inappropriately, we claim) for the same purpose.

Throughout this discussion $\mathsf{V} = \mathbb{R}^{n+1}$ so that $\mathbf{P}(\mathsf{V}) = \mathbb{R}P^n$.

5.1 Clifford algebra = Cayley-Klein + Grassmann algebra

The discussion of the previous chapter shows how to construct Cayley-Klein metric spaces in $\mathbb{R}P^n$ by selecting an admissable (standard or dual) quadric surface $\mathcal{Q} = (Q, Q^*)$. We now turn to the question of how this construction can be integrated with the associated Grassmann algebras $\mathbf{P}(\bigwedge \mathsf{V})$ and $\mathbf{P}(\bigwedge \mathsf{V}^*)$. The resulting product structure should contain both the inner product (from $\mathcal{Q}$) and the outer product of the Grassmann algebra.

For standard (dual) $\mathcal{Q}$, define a *geometric product* on 1-vectors of $\mathbf{P}(\bigwedge \mathsf{V})$ ($\mathbf{P}(\bigwedge \mathsf{V}^*)$) by:

$$\mathbf{xy} := B(\mathbf{x},\mathbf{y}) + \mathbf{x}\wedge\mathbf{y} \tag{5.1}$$
$$= \mathbf{x}\cdot\mathbf{y} + \mathbf{x}\wedge\mathbf{y} \tag{5.2}$$

where $\mathbf{x}\cdot\mathbf{y} := B(\mathbf{x},\mathbf{y})$ is the inner product associated to the quadratic form Q. This definition can be meaningfully extended to the full exterior algebra. The resulting product is associative. The algebra is called a *real Clifford algebra*.

Remark 79. If Q has the signature (p,m,z), where $p+m+z = n+1$, denote the corresponding real Clifford algebra constructed on $\mathbf{P}(\bigwedge\mathsf{V})$ by $\mathbf{P}(\mathbb{R}_{p,m,z})$; that constructed on $\mathbf{P}(\bigwedge\mathsf{V}^*)$, as $\mathbf{P}(\mathbb{R}^*_{p,m,z})$. We assume a canonical basis of $\mathbf{P}(\bigwedge\mathsf{V})$ ($\mathbf{P}(\bigwedge\mathsf{V}^*)$) (see Sect. 2.3.1.3) generated by the basis 1-vectors with signature $(s+++...---...)$, where $s\in\{+,0,-\}$, as described in Sect. 3.2.

5.2 Clifford algebra fundamentals

We review some notation and facts of Clifford algebras which we'll need in the sequel. Let $\mathcal{C}$ be a Clifford algebra and $\mathbf{X}$ and $\mathbf{Y}$ arbitrary multivectors.

- $\overline{\mathbf{X}}$ represents the *conjugation* of $\mathbf{X}$. For a k-vector $\mathbf{X}$, $\overline{\mathbf{X}} = (-1)^k\mathbf{X}$, hence projectively $\overline{\mathbf{X}}\equiv\mathbf{X}$.
- $\widetilde{\mathbf{X}}$ represents the *reversal* of $\mathbf{X}$. For a k-vector $\mathbf{X}$, $\widetilde{\mathbf{X}} = (-1)^{\frac{k(k-1)}{2}}\mathbf{X}$, hence projectively $\widetilde{\mathbf{X}}\equiv\mathbf{X}$.
- $\langle\mathbf{X}\rangle_k$ represents the grade-k part of $\mathbf{X}$. $\mathbf{X}$ is a k-vector $\iff$ $\langle\mathbf{X}\rangle_j\neq 0$ exactly for $j=k$.
- For a k-vector $\mathbf{X}$ and an m-vector $\mathbf{Y}$,

$$\mathbf{XY} = \sum_i \langle\mathbf{XY}\rangle_i \quad \text{where } i\in\{|k-m|,|k-m|+2,...,k+m\}$$

- For a k-vector $\mathbf{X}$, $\mathbf{X}^2 = \langle\mathbf{X}^2\rangle_0$: the square of a k-vector is a scalar.
- The inner product $\mathbf{X}\cdot\mathbf{Y} := \langle\mathbf{X},\mathbf{Y}\rangle_{|k-m|}$.
- The outer product $\mathbf{X}\wedge\mathbf{Y} = \langle\mathbf{X},\mathbf{Y}\rangle_{k+m}$.
- The *commutator* product $\mathbf{X}\times\mathbf{Y} := \frac{1}{2}(\mathbf{XY}-\mathbf{YX})$.

Remark 80. We assume a basic familiarity with real Clifford algebras, as can be found in [DFM07], [HS87], or [Lou01], Ch. 14.

Remark 81. Almost without exception, the standard literature on Clifford algebras omits the degenerate signature case. For example, all the standard sources mentioned above do so. As a result, the discussion here adapts, wherever possible, existing results for non-degenerate signatures to be valid also for the degenerate signatures handled here, and develops alternative strategies when such adaptation is not possible. For example, out use of Poincaré duality to implement the join operator reflects the fact that for a degenerate metric the metric polarity cannot be used for this purpose – as is common practice ([HS87], [DFM07]).

5.3 Cayley-Klein compatibility check

The quadric surface associated to the Cayley-Klein spaces studied here consists of a pair (Q, Q^*), but the definition (5.1) refers only to Q. Our first step in verifying that the Cayley-Klein construction can be transferred to the Grassmann algebra is to verify that Q^* is compatible with the resulting geometric product. The inner product Q^* on dual vectors should be given in the Clifford algebra by the Clifford inner product (defined in the previous section) on n-vectors. To be precise:

Theorem 82. *For* $\mathbf{u} \in \bigwedge^n(\mathsf{V})$, $\mathbf{u} \cdot \mathbf{u} = Q^*(\mathbf{u})$.

Proof. We prove this first for canonical basis vectors $\mathbf{E}_i$ of $\bigwedge^n(\mathsf{V})$, which satisfy $\mathbf{E}_i = \pm\prod_{j\neq i} e_j$. Then

$$\begin{aligned}
\mathbf{E}_i \cdot \mathbf{E}_i &= \langle \mathbf{E}_i \mathbf{E}_i \rangle_0 && (5.3)\\
&= \mathbf{E}_i^2 && (5.4)\\
&= (\prod_{j\neq i} e_j)(\prod_{j\neq i} e_j) && (5.5)\\
&= -1^{\frac{n(n+1)}{2}} \prod_{j\neq i} e_j^2 && (5.6)
\end{aligned}$$

For a non-degenerate signature $Q = (p, m, 0)$, this leads to following:

$$\mathbf{E}_i^2 = \begin{cases} (-1)^{\frac{n(n+1)}{2}+m} & \text{if } 0 \leq j < p \\ (-1)^{\frac{n(n+1)}{2}+m-1} & \text{if } p \leq j \leq (p+m) = n+1 \end{cases} \tag{5.7}$$

Depending on the parity of $\frac{n(n+1)}{2}$ and m, one arrives at the signature $(p, m, 0)$ or $(m, p, 0)$. By Sect. 3.2, both are equivalent to the original signature $(p, m, 0)$, which is also Q^*. So, for the non-degenerate case, the claim is established.

This leaves the case of rank-n quadric surfaces (Q, Q^*). Evaluating (5.3) for this case yields:

$$\mathbf{E}_i^2 = \begin{cases} 0 & \text{if } 1 \leq j \leq n \\ (-1)^{\frac{n(n+1)}{2}+m} & \text{if } j = 0 \end{cases} \tag{5.8}$$

This agrees with the calculations for the pseudo-euclidean signatures in the proof of Thm. 40 and also here one has $\mathbf{E}_i \cdot \mathbf{E}_i = Q^*(\mathbf{E}_i)$. Since both sides of the desired result are bilinear in $\mathbf{u}$, the result can be extended to arbitrary elements $\mathbf{u} \in \bigwedge^n(\mathsf{V})$. □

Remark 83. By Sect. 3.2, the theorem can be uniquely extended to an inner product consistent with B^*.

Remark 84. Notice we have attached the quadratic form Q of a *standard* quadric surface to $\mathbf{P}(\bigwedge \mathsf{V})$ and that of a *dual* quadric surface, to $\mathbf{P}(\bigwedge \mathsf{V}^*)$. When Q is non-degenerate, one obtains an isomorphic algebra by attaching Q^* instead to $\mathbf{P}(\bigwedge \mathsf{V}^*)$ (standard), or to $\mathbf{P}(\bigwedge \mathsf{V})$ (dual). But when Q is rank-n (standard), attaching Q^* to $\mathbf{P}(\bigwedge \mathsf{V}^*)$ leads

to inconsistent results, since the induced metric on n-vectors is 0, whereas it should have rank-n. In particular, the pseudo-euclidean Cayley-Klein spaces must be based on $\mathbf{P}(\bigwedge \mathsf{V}^*)$, and the dual pseudo-euclidean spaces, on $\mathbf{P}(\bigwedge \mathsf{V})$.

We next show that the polarity on the metric quadric is available directly via the Clifford algebra product.

5.4 Metric polarity via pseudoscalar multiplication

It is standard result of Clifford algebras that multiplication by the pseudoscalara $\mathbf{I}$ is a grade-reversing algebra homomorphism, and an isomorphism when $\mathbf{I}^2 \neq 0$. Here we want to connect this multiplication to the polarity on the metric quadric introduced in Sect. 3.1.2.

Theorem 85. *Define* $\Theta : \mathbf{P}(\bigwedge \mathsf{V}) \to \mathbf{P}(\bigwedge \mathsf{V})$ *by* $\Theta(\mathbf{X}) = \mathbf{XI}$. *Then* $\Theta(\mathbf{X}) = \mathbf{J} \circ \bigwedge(L_B)$.

Proof. Let $\mathbf{e}_i$ be a basis 1-vector. Then since $\mathbf{e}_i\mathbf{E}_i = \mathbf{I}$,

$$\mathbf{e}_i\mathbf{I} = \mathbf{e}_i^2\mathbf{E}_i \tag{5.9}$$

On the other hand,

$$\mathbf{J}(\bigwedge(L_B)(\mathbf{e}_i)) = \mathbf{J}(L_B(\mathbf{e}_i)) = \mathbf{J}(\mathbf{e}_i^\perp) \tag{5.10}$$

The application of $\mathbf{J}$ in the last equation moves the element from $\bigwedge^1(\mathsf{V}^*)$ to the corresponding entity in $\bigwedge^n(\mathsf{V})$. A consideration of the admissable signatures for Q establishes the equality of the RHS of (5.9) and the RHS of (5.10).

Observe that $\Theta(\mathbf{a} \wedge \mathbf{b}) = \Theta(\mathbf{a}) \vee \Theta(\mathbf{b})$ for two 1-vectors $\mathbf{a}$ and $\mathbf{b}$. Hence, Θ can be written as an exterior power of a map. Since it agrees with the map $\mathbf{J} \circ \bigwedge(L_B)$ on 1-vectors, it must be the same map on the whole algebra. □

5.5 The Clifford algebras Cl^n_κ

The remainder of this study concentrates on the three Cayley-Klein geometries, leaving the pseudo-euclidean signatures to the side. We show how known results of these geometries can be expressed within the Clifford algebra setting, in many cases with surprising elegance and compactness.

As pointed out above, for non-degenerate metrics, there are no grounds to prefer beginning with $\mathbf{P}(\bigwedge \mathsf{V})$ or $\mathbf{P}(\bigwedge \mathsf{V}^*)$ to build up the Clifford algebra, since the induced metric on the dual algebra is identical to the original metric. Remark 84, however, shows the necessity of using $\mathbf{P}(\bigwedge \mathsf{V}^*)$ for the euclidean case, we build the non-euclidean algebras in the same way. For the elliptic case, that results in the algebra $\mathbf{P}(\mathbb{R}^*_{n+1,0,0})$; for the hyperbolic case, $\mathbf{P}(\mathbb{R}^*_{n,1,0})$. We refer to the approach based on these algebras as the *dual* approach, or the *dual* construction.

5.5.1 Notation

In order to handle these three cases in a metric-neutral way, we introduce some notation. For discussions which apply equally well to all three algebras, we use the notation Cl^n_κ, where $\mathbf{e}_0^2 = \kappa$, to denote the corresponding Clifford algebra; there are three cases corresponding to $\kappa \in \{-1, 0, 1\}$. For metric-specific remarks, we supply a specific value of κ. This value of κ also represents the constant Gaussian curvature of the space when considered as a Riemannian manifold ([TL97]).

Some other commonly used structures associated to these algebras:

- The even sub-algebra generated by vectors of even grade, will be denoted by Cl^{n+}_κ.
- The sub-algebra generated by scalars and pseudoscalars, will be denoted by $Cl^{n\dagger}_\kappa$.
- We use G^n_κ to refer to the associated n-dimensional geometries, and refer to these collectively as κ-geometries. We will have need to refer to the Lie matrix groups representing the isometries of G^n_κ. We refer to these groups generically as $\mathbf{G}^n_\kappa$ with Lie algebra $\mathfrak{g}^n_\kappa$. We do not derive these groups here, they can be found in the literature, for example, see [TL97].

The Lie groups for the three cases are shown in (5.11). We focus on the direct isometries since these will be important in the discussion of rigid body motion. The presence of the P in the name indicates that the groups are projectivized; since they are all subgroups of the projective group $PGL(n+1, \mathbb{R})$. $SE(n)$, the euclidean group, is the semi-direct product $PSO(n, 0) \rtimes \mathbb{R}(n)$. One important theme of the later chapters will be to show how to find finite coverings of these groups inside Cl^{n+}_κ for $n = 2$ and $n = 3$.

$$\Gamma^n_\kappa = \begin{cases} PSO(n, 1) & \kappa = -1 \\ SE(n) & \kappa = 0 \\ PSO(n + 1, 0) & \kappa = 1 \end{cases} \tag{5.11}$$

Remark 86. We retain the Grassmann algebra $\mathbf{P}(\bigwedge \mathsf{V})$ solely as an exterior algebra, primarily for calculating the join operator. Again, this decision is based on the fact that the metric relations in the euclidean case are poorly behaved. For the non-euclidean case, one could perhaps also carry out metric operations in $\mathbf{P}(\bigwedge \mathsf{V}^*)$; this is not done here. All metric operations are carried out in $\mathbf{P}(\bigwedge \mathsf{V}^*)$. Or equivalently, we attach the metric $(0, 0, n + 1)$ to W, forcing all inner products to zero.

Remark 87. **Notation alert.** Due to the more prominent role of $\mathbf{P}(\bigwedge \mathsf{V}^*)$, the basis element for scalar and pseudoscalar in $\mathbf{P}(\bigwedge \mathsf{V}^*)$ will be written without index as $\mathbf{1}$ and $\mathbf{I}$; we may even omit $\mathbf{1}$ when writing scalars, as is common in the literature.

5.6 Isometries via conjugation

One of the most powerful aspects of Clifford algebras for metric geometry is the ability to realize isometries as conjugation operators of the form:

$$\underline{\mathbf{g}}(\mathbf{X}) := \mathbf{g}\mathbf{X}\mathbf{g}^{-1} \tag{5.12}$$

where $\mathbf{X}$ is any geometric element of the algebra and $\mathbf{g}$ is a specific geometric element, unique to the isometry. We will prove below (Thm. 89) that when $\mathbf{g}$ is a *proper* 1-vector, then $\underline{\mathbf{g}}$ is a reflection in $\mathbf{g}$, hence by Thm. 77, the elements generated by such $\mathbf{g}$ generate the isometry group of the Cayley-Klein space.

Remark 88. Since *conjugation* is an overloaded mathematical term, we also use the less ambiguous term *sandwich* operator to refer to $\underline{\mathbf{g}}$.

5.6.1 Reflections

Let $\mathbf{a}$ be a normalized 1-vector representing a proper hyperplane in a κ-geometry. Then $\mathbf{a}^{-1} = \mathbf{a}$, and the sandwich (5.12) takes then the form $\underline{\mathbf{a}}(\mathbf{X}) := \mathbf{a}\mathbf{X}\mathbf{a}$. We show that $\underline{\mathbf{a}}$ represents a reflection in the hyperplane $\mathbf{a}$, in the sense of Def. 73: $\mathbf{a}$ is the axis of the reflection, and $\mathbf{a}^\perp$ is the center. Fig. 5.1 shows the situation for $n = 2$.

Let $\mathbf{b}$ be another hyperplane. Then, applying Def. 73, the reflection R of $\mathbf{b}$ in $\mathbf{a}$ is given by:

$$\begin{aligned} R(\mathbf{b}) &= -\langle \mathbf{a}^\perp, \mathbf{a}\rangle \mathbf{b} + 2\langle \mathbf{a}^\perp, \mathbf{b}\rangle \mathbf{a} \\ &= -\mathbf{S}(\mathbf{a}^\perp \wedge \mathbf{a})\mathbf{b} + 2\mathbf{S}(\mathbf{a}^\perp \wedge \mathbf{b})\mathbf{a} \\ &= -(\mathbf{a}\cdot\mathbf{a})\mathbf{b} + 2(\mathbf{a}\cdot\mathbf{b})\mathbf{a} \end{aligned}$$

Here we have converted the evaluation map $\langle , \rangle$ to the wedge product, then applied Ex. 6.1.1.1-5 to convert to inner product.

Theorem 89. $R(\mathbf{b}) = \underline{\mathbf{a}}(\mathbf{b})$.

Proof.

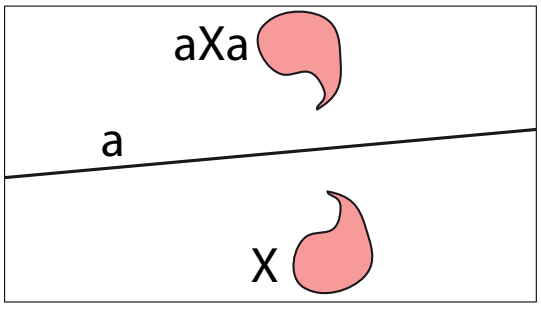

Fig. 5.1 The sandwich of an arbitrary object $\mathbf{X}$ in the algebra with a 1-vector is a reflection of the object in the hyperplane represented by the 1-vector.

$$\begin{aligned}
\mathbf{aba} &= \mathbf{a}(\mathbf{b}\cdot\mathbf{a} + \mathbf{b}\wedge\mathbf{a}) \\
&= (\mathbf{a}\cdot\mathbf{b})\mathbf{a} + \mathbf{a}(\mathbf{b}\wedge\mathbf{a}) \\
(\mathbf{a}\cdot\mathbf{a})\mathbf{b} &= (\mathbf{aa})\mathbf{b} = \mathbf{a}(\mathbf{ab}) \\
&= \mathbf{a}(\mathbf{a}\cdot\mathbf{b} + \mathbf{a}\wedge\mathbf{b}) \\
&= (\mathbf{a}\cdot\mathbf{b})\mathbf{a} - \mathbf{a}(\mathbf{b}\wedge\mathbf{a}) \\
\mathbf{aba} + (\mathbf{a}\cdot\mathbf{a})\mathbf{b} &= 2(\mathbf{a}\cdot\mathbf{b})\mathbf{a} \\
\mathbf{aba} &= -(\mathbf{a}\cdot\mathbf{a})\mathbf{b} + 2(\mathbf{a}\cdot\mathbf{b})\mathbf{a}
\end{aligned}$$

5.6.2 Spin group

Multiplication of 1-vectors corresponds to composition of reflections. It's useful to introduce some definitions to describe the situation.

Definition 90. A *versor* is an element that can be written as the product of 1-vectors. A versor is called *even* if it can be written as the product of an even number of 1-vectors. A versor is called *proper* if it is the product of proper 1-vectors.

Remark 91. When $\mathbf{g}$ is a proper versor, the above proof also shows that $\underline{\mathbf{g}}$ is an isometry, since it is by definition a product of proper reflections. An even proper versor then corresponds to a direct isometry, an odd versor to an indirect one. By Thm. 77, the proper versors generate the isometry group.

Definition 92.
- The *pin group* $\mathbf{Pin}^n_{+\kappa}$ of the Clifford algebra Cl^n_κ is the group generated by 1-vectors $\mathbf{a}$ satisfying $\mathbf{a}^2 = 1$.
- The *spin group* $\mathbf{Spin}^n_{+\kappa}$ of the Clifford algebra Cl^n_κ is the subgroup of $\mathbf{Pin}^n_{+\kappa}$ consisting of even proper versors.
- An element of $\mathbf{Spin}^n_{+\kappa}$ is called a *rotor*.

Remark 93. When $\mathbf{a}$ is improper but not ideal, $\mathbf{a}^\perp = \mathbf{aI}$ is a proper point, and the reflection in $\mathbf{a}$ is a point reflection in $\mathbf{a}^\perp$. The latter is not a reflection in the Cayley-Klein geometry. This is the reason we restrict $\mathbf{Pin}^n_{+\kappa}$ to proper 1-vectors. The point reflection can be written in this restricted group as the n-versor $\mathbf{a}^\perp$, which is the product of n proper 1-vectors.

Remark 94. The condition $\mathbf{a}^2 = 1$ for the pin group is equivalent to the condition that $\mathbf{a}$ is normalized proper. It follows from the definition of $\mathbf{Spin}^n_{+\kappa}$ that group elements satisfy $\mathbf{a}^{-1} = \widetilde{\mathbf{a}}$ so $\mathbf{a}\widetilde{\mathbf{a}} = 1$. The latter condition is commonly used to define the group. Then it may happen that some elements are not versors ([HS87], Ch. 3). But since the isometry groups we study are generated by reflections in *proper* 1-vectors, our groups in fact consist of proper versors. Additionally, some treatments also include the larger group $\mathbf{Spin}^n_\kappa := \{\mathbf{g} \in Cl^{n+}_\kappa \mid \mathbf{g}\widetilde{\mathbf{g}} = \pm 1\}$. Due to our use of proper versors, we do not have to consider this group.

Remark 95. Some authors ([HS87], [Per09]) refer to an element of the spin group as a *spinor* but this assumes familiarity with an non-trivial program carried out by Hestenes

to justify the use of this term ([Lou01], p. 327). Since our interest here is not in spinors *per se*, we use the term *rotor* instead. [HS87] defines a rotor as an even versor. For reasons given above, we restrict this to even proper versors. Note that the discussion of the spin group in [HS87] is overly complicated by the presence of a power of -1 which the dual approach avoids (for a discussion of this problem see Sect. 5.9 below).

Remark 96. We will discuss $\mathbf{Spin}^n_{+\kappa}$ (for $n = 2$ and $n = 3$) in more detail in the following chapters, and show that they satisfy the properties listed in the "wish-list" of Chapter 1. The group $\mathbf{Pin}^n_{+\kappa}$ will occupy less of our attention because it does not satisfy these properties.

Definition 97. The *logarithm* of a rotor $\mathbf{g}$ is a bivector $\mathbf{L}$ such that $\mathbf{g} = e^{\mathbf{L}}$.

Remark 98. We will show that for Cl^2_κ (Chapter 6) and Cl^3_κ (Chapter 7), every rotor has a logarithm.

5.7 The structure of Cl^n_κ

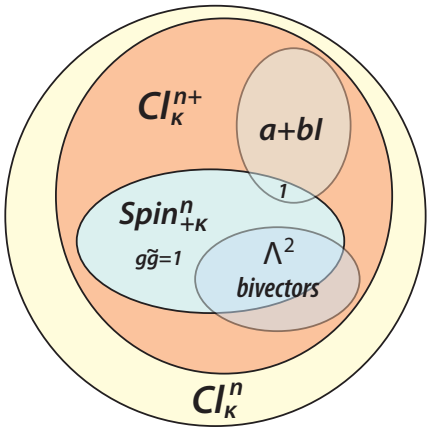

Fig. 5.2 The important sub-algebras and sub-spaces of Cl^n_κ.

Fig. 5.2 gives a simplified overview of the structural entities in Cl^n_κ introduced above. We have omitted $\mathbf{Pin}^n_{+\kappa}$ since we are mostly concerned here with the direct isometry group. The even sub-algebra Cl^{n+}_κ contains the sub-algebra $Cl^{n\dagger}_\kappa$, consisting of scalars and pseudoscalars.

Cl^{n+}_κ also contains the spin group $\mathbf{Spin}^n_{+\kappa}$. As we have seen, these are the elements of Cl^3_κ which have been normalized to satisfy $\mathbf{g}\tilde{\mathbf{g}} = 1$; in general, they form a finite cover of the direct isometry group $\mathbf{G}$ of the Cayley-Klein space.

Finally, the bivectors $\bigwedge^2 \subset Cl^n_\kappa$ can be identified with the Lie algebra. It's straightforward to verify that $\mathbf{\Sigma} \in (\bigwedge^2 \cap \mathbf{Spin}^n_{+\kappa}) \iff \mathbf{\Sigma}$ is simple. Such a bivector is a rotor, representing an order-2 rotation around its line.

Chapter 6 and Chapter 7 provide a detailed account of these sub-algebras and subspaces for dimension 2 and 3, resp.

5.8 Guide to the (Lack of) Literature

[Lou01] gives a good introduction to real Clifford algebras with a wealth of examples. [HS87] has a rich collection of formulas and themes. Neither provides any significant treatment of degenerate metrics as present in the euclidean algebra Cl^n_0. [Abl86] is concerned with spin groups in such degenerate Clifford algebras. However, our pin and spin groups are simpler than his (and than the general non-degenerate spin groups also) due to the fact mentioned above our groups are generated by *proper* reflections, so we are above to provide a self-contained treatment of them here.

Many results in the standard literature are stated for vector spaces rather than Cayley-Klein spaces in projective space. This leads to slight differences in how the groups are defined, since some isometries which are distinct in the vector space setting are equivalent in the projective space setting. Finally, the dual construction based on W^* is not worked out in detail in the literature, as we are forced to do here by the euclidean metric. For all these reasons, the following chapters prove a series of results that are similar but not identical to standard results.

5.9 Appendix: Reflections in points and in hyperplanes

This is an appropriate point to discuss a matter of practical concern regarding how reflections are represented in Clifford algebra, and which much of the standard literature handles rather sloppily. We saw above that when $\mathbf{a}$ is a 1-vector, then $\underline{\mathbf{a}}$ is the reflection in $\mathbf{a}$. In the dual algebra W^*, $\mathbf{a}$ represents a hyperplane (for $n = 2$, a line); in the standard algebra W, it represents a point. (We leave aside for the moment the question of whether $\mathbf{a}$ is proper or not, since this distinction is not relevant for the issue at hand.)

A consequence of these observations is that reflections in hyperplanes are not given naturally in point-based algebras by sandwich operators with 1-vectors, but with codimension-1 vectors. It is however common practice in the literature to represent such a reflection using a sandwich with a 1-vector (see for example [DFM07], p. 168, or [HS87], Ch. 3). In the vector space model of $\mathbb{R}^n$, one writes for the reflection of a point $\mathbf{X}$ in a hyperplane whose normal vector is $\mathbf{P}$:

$$\mathbf{X} \to -\mathbf{PXP} \tag{5.13}$$

Without the minus sign, the expression $\mathbf{PXP}$ represents a *reflection* in the *vector* $\mathbf{P}$. In 3 dimensions, this is a rotation of π radians around the line $\mathbf{P}\mathbb{R}$. See Fig. 5.3. To obtain the reflection in the plane $\mathbf{p}$ orthogonal to $\mathbf{P}$, one must compose this vector reflection with the point reflection in the origin, which is achieved by multiplying by -1.This undoes

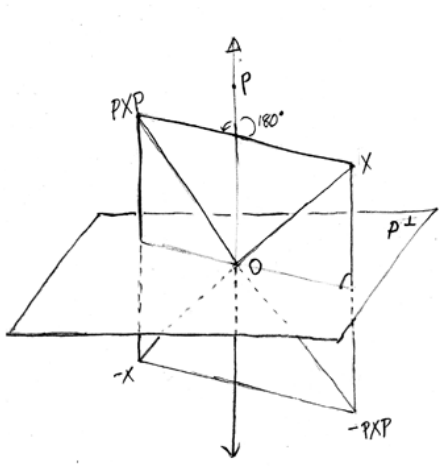

Fig. 5.3 In the vector space Clifford algebra $\mathbb{R}_3$, reflection in the line $\mathbf{P}\mathbb{R}$ is given by $\mathbf{PXP}$. Reflection in the hyperplane $\mathbf{P}^\perp$, on the other hand, is given by $-\mathbf{PXP}$.

the rotation around the line $\mathbf{P}\mathbb{R}$ and introduces a reflection in the orthogonal plane. This yields the expression $-\mathbf{PXP}$ as the form for a reflection in the plane orthogonal to $\mathbf{P}$. See also [Lou01], pp. 57-8.

This illustrates another advantage to the dual homogeneous model presented here, since reflections in points and in planes are represented without any extra minus signs.

5.10 Appendix: Poincaré duality and the elliptic metric polarity

We can now appreciate better the significance of the Poincaré isomorphism: $\mathbf{J} : \mathbf{P}(\bigwedge \mathsf{V}) \leftrightarrow \mathbf{P}(\bigwedge \mathsf{V}^*)$. Consider the map $\mathbf{\Pi} : \mathbf{P}(\bigwedge \mathsf{V}) \to \mathbf{P}(\bigwedge \mathsf{V})$ defined analogously to $\mathbf{J}$ in (2.5) for the case $\mathsf{V} = \mathbb{R}^4$:

$$\mathbf{\Pi}(e^i) := E^i, \quad \mathbf{\Pi}(E^i) := e^i, \quad \mathbf{\Pi}(e^{ij}) := e^{kl} \tag{5.14}$$

$\mathbf{\Pi}$ is the same as $\mathbf{J}$, but interpreted as a map to $\mathbf{P}(\bigwedge \mathsf{V})$ instead of $\mathbf{P}(\bigwedge \mathsf{V}^*)$. It's trivial to verify that $\mathbf{\Pi}$ is the polarity on the elliptic metric quadric with signature $(4, 0, 0)$.

For general dimension n, recall the definition of $\mathbf{J}$ using a canonical basis in Sect. 2.3.1.3. Instead, equip $\mathbf{P}(\bigwedge \mathsf{V})$ with signature $(n, 0, 0)$ to form the Clifford algebra $\mathbf{P}(\mathbb{R}_{n,0,0})$ with pseudoscalar $I = \mathbf{e}^N$. Then, by Thm. 85, the polarity on the metric quadric is given by $\mathbf{e}^S\mathbf{I} = \mathbf{e}^{(S^\perp)}$, where equality follows from the fact that for the canonical basis, $(\mathbf{e}^S)^{-1} = \mathbf{e}^S$.This is the polarity $\mathbf{\Pi} : \mathbf{P}(\bigwedge \mathsf{V}) \to \mathbf{P}(\bigwedge \mathsf{V})$ on the elliptic metric quadric (see Sect. 4.4).

Conclusion: Both $\mathbf{J}$ and $\mathit{\Pi}$ represent valid grade-reversing involutive algebra isomorphisms. The **only** difference is the target space: $\mathit{\Pi} : \mathbf{P}(\bigwedge \mathsf{V}) \to \mathbf{P}(\bigwedge \mathsf{V})$, while $\mathbf{J} : \mathbf{P}(\bigwedge \mathsf{V}) \to \mathbf{P}(\bigwedge \mathsf{V}^*)$.

5.10.1 The regressive product via a metric

Given the point-based exterior algebra W, the outer product $A \wedge B$ represents the join of subspaces A and B.[1] The *meet* operator $A \vee B$ (also known as the *regressive* product) is often defined as

$$\Pi(\Pi(A) \wedge \Pi(B))$$

([HS87], [DFM07]). That is, the elliptic metric (any nondegenerate metric suffices) is introduced in order to provide a solution to a projective (incidence) problem. By Sect. 2.3.1.4, the same result is also given via $\mathbf{J}(\mathbf{J}(A) \wedge \mathbf{J}(B)$. (Here, the $\wedge$ denotes the outer product in $\mathbf{P}(\bigwedge \mathsf{V}^*)$).

5.10.1.1 The Hodge $\star$ operator A map very similar in spirit to $\mathbf{J}$ is described in [PW01], p. 150. The $\star$ operator is presented there as a way of generating *dual* coordinates, which is an apt description of the $\mathbf{J}$ operator also. One can then define the regressive product by $\star(\star A \wedge \star B)$. Formally, however, $\star$ is a map from W to W, so is identical to the metric polarity Π.

5.10.2 Comparison

The two methods to calculate the regressive product yield the same result, but they have very different conceptual foundations. As pointed out in Sect. 2.2.4, the meet and join operators live the exterior algebra $\mathbf{P}(\bigwedge \mathsf{V})$ and its dual. $\mathbf{J}$ provides the bridge between these two projective algebras, hence provides a projective *explanation* for what is a projective operation. A related advantage of $\mathbf{J}$ is that it also is useful when used "alone" – whereas Π (and also $\star$) – when imported to realize the regressive product – is only valid when it appears in the second power, and hence disappears. For these reasons, we propose a differentiation of the terminology to reflect this mathematical differentiation. Instead of referring to multiplication by $\mathbf{I}$ (or $\mathbf{I}^{-1}$) as the *duality* operator, we propose it should be called the *metric polarity* operator This is consistent with the mathematical literature. The purely projective term *duality* would be reserved for the $\mathbf{J}$ operator. To be precise, $\mathbf{J}(\mathbf{X})$ gives the *dual coordinates* of $\mathbf{X}$.

[1] In this paragraph we depart from the notation adopted for this thesis which represents the outer product in $\mathbf{P}(\bigwedge \mathsf{V})$ with the symbol $\vee$.

Chapter 6
Metric planes via Cl^2_κ

This chapter is devoted to the exploration of the two-dimensional members Cl^2_κ of the family of Clifford algebras introduced in the previous chapter. We demonstrate that the algebraic structures provide compact, elegant representation of the classical metric planes: euclidean, hyperbolic, and elliptic.

We undertake this study of the 2D case first, due to the unfamiliar concepts involved – notably the dual construction and the degenerate euclidean metric. Then, when we turn to the 3D case in Chapter 7, we can focus on the special challenges which it presents, notably the existence of non-simple bivectors.

This chapter begins by discussing metric-neutral properties of Cl^2_κ, before turning to metric-specific discussions. It then analyses the structure of the isometry groups, demonstrates the existence of logarithms for every rotor. This leads to a classification of the flow generated by exponentiating a general bivector. The chapter closes with a discussion of how the results can be related to known results of Lie groups and algebras.

6.1 Description of the algebras

Notation. For denoting general vectors in the algebra: we denote 1-vectors with small bold Roman letters, and 2-vectors with capital bold Roman letters.

A basis for the algebra Cl^2_κ is given by

$$\{\mathbf{1} := \mathbf{1}_0, \mathbf{e}_0, \mathbf{e}_1, \mathbf{e}_2, \mathbf{E}_0 := \mathbf{e_1 e_2}, \mathbf{E}_1 := \mathbf{e_2 e_0}, \mathbf{E}_2 := \mathbf{e_0 e_1}, \mathbf{I} := \mathbf{e}_0\mathbf{e}_1\mathbf{e}_2\}$$

with the relations

$$\{\mathbf{e}_0^2 = \kappa; \quad \mathbf{e}_1^2 = \mathbf{e}_2^2 = 1\}$$

This induces on the higher grades the following metric relations:

$$\{\mathbf{E}_0^2 = -1; \quad \mathbf{e}_1^2 = \mathbf{e}_2^2 = \mathbf{I}^2 = -\kappa\} \tag{6.1}$$

	$\mathbf{1}$	$\mathbf{e}_0$	$\mathbf{e}_1$	$\mathbf{e}_2$	$\mathbf{E}_0$	$\mathbf{E}_1$	$\mathbf{E}_2$	$\mathbf{I}$
$\mathbf{1}$	$\mathbf{1}$	$\mathbf{e}_0$	$\mathbf{e}_1$	$\mathbf{e}_2$	$\mathbf{E}_0$	$\mathbf{E}_1$	$\mathbf{E}_2$	$\mathbf{I}$
$\mathbf{e}_0$	$\mathbf{e}_0$	κ	$\mathbf{E}_2$	$-\mathbf{E}_1$	$\mathbf{I}$	$-\kappa\mathbf{e}_2$	$\kappa\mathbf{e}_1$	$\kappa\mathbf{E}_0$
$\mathbf{e}_1$	$\mathbf{e}_1$	$-\mathbf{E}_2$	$\mathbf{1}$	$\mathbf{E}_0$	$\mathbf{e}_2$	$\mathbf{I}$	$-\mathbf{e}_0$	$\mathbf{E}_1$
$\mathbf{e}_2$	$\mathbf{e}_2$	$\mathbf{E}_1$	$-\mathbf{E}_0$	$\mathbf{1}$	$-\mathbf{e}_1$	$\mathbf{e}_0$	$\mathbf{I}$	$\mathbf{E}_2$
$\mathbf{E}_0$	$\mathbf{E}_0$	$\mathbf{I}$	$-\mathbf{e}_2$	$\mathbf{e}_1$	$-\mathbf{1}$	$-\mathbf{E}_2$	$\mathbf{E}_1$	$-\mathbf{e}_0$
$\mathbf{E}_1$	$\mathbf{E}_1$	$\kappa\mathbf{e}_2$	$\mathbf{I}$	$-\mathbf{e}_0$	$\mathbf{E}_2$	$-\kappa$	$-\kappa\mathbf{E}_0$	$-\kappa\mathbf{e}_1$
$\mathbf{E}_2$	$\mathbf{E}_2$	$-\kappa\mathbf{e}_1$	$\mathbf{e}_0$	$\mathbf{I}$	$-\mathbf{E}_1$	$\kappa\mathbf{E}_0$	$-\kappa$	$-\kappa\mathbf{e}_2$
$\mathbf{I}$	$\mathbf{I}$	$\kappa\mathbf{E}_0$	$\mathbf{E}_1$	$\mathbf{E}_2$	$-\mathbf{e}_0$	$-\kappa\mathbf{e}_1$	$-\kappa\mathbf{e}_2$	$-\kappa$

Table 6.1 Geometric product in Cl^2_κ.

Inspection of the multiplication table Table 6.1 reveals that the geometric product of a k- and l-vector yields a product that involves at most two grades. When these two grades are $|k-l|$ and $k+l$, we can write the geometric product for 2 arbitrary blades $\mathbf{A}$ and $\mathbf{B}$ as

$$\mathbf{AB} = \mathbf{A} \cdot \mathbf{B} + \mathbf{A} \wedge \mathbf{B}$$

The only exception is $(l, k) = (2, 2)$ where the grades $|k-l| = 0$ and $|k-l|+2 = 2$ occur. Then using the commutator product (Sect. 5.2):

$$\langle \mathbf{AB} \rangle_2 = \mathbf{A} \times \mathbf{B}$$

where $\mathbf{A}$ and $\mathbf{B}$ are bivectors. Hence, every product of k- and l- vectors can be decomposed into *pure grade* parts using the inner, outer, and commutator products. We'll find this is also true for $n = 3$ (see Chapter 7). Since all vectors in Cl^2_κ are blades, the above decompositions are valid for the product of any two vectors in this algebra.

6.1.1 The geometric product

The geometric product can be understood by studying its restriction to *pure grade* elements, that is, products of k- and m-vectors for all possible k and m. For this purpose, define two arbitrary 1-vectors $\mathbf{a}$ and $\mathbf{b}$ and two arbitrary bivectors $\mathbf{P}$ and $\mathbf{Q}$ with

$$\mathbf{a} = a_0\mathbf{e}_0 + a_1\mathbf{e}_1 + a_2\mathbf{e}_2, \quad \text{etc.}$$

These coordinates are of course not instrinsic but they can be useful in understanding how the metric is working in the various products, especially with regard to the distinguished role of $\mathbf{e}_0$. For the following *metric-neutral* discussion we assume, unless otherwise noted, that these vectors are proper elements of the κ-geometry. We sometimes use the special symbol $\mathbf{X}$ to denote a k-vector of arbitrary grade.

1. **Norms.** It is often useful to normalize vectors to have a particular intensity. In general, define the norm of a proper k-vector $\mathbf{X}$ as $\|\mathbf{X}\| := \sqrt{|\mathbf{X} \cdot \mathbf{X}|}$. When the norm

is non-zero, we can apply linearity to show that $\frac{\mathbf{X}}{\|\mathbf{X}\|}$ has norm ± 1. It is often convenient to work with normalized vectors, for example, in evaluating homogeneous distance and angle formulas such as (4.1) and (4.2). Proper elements, since they do not belong to $\mathbf{Q}$ or $\mathbf{Q}^*$, have non-zero norm, hence can be normalized. It is even sometimes possible to introduce a meaningful norm for ideal elements. See the separate discussions of the euclidean plane (Sect. 6.2.3) and hyperbolic plane (Sect. 6.2.2) below.

2. **Pseudoscalar magnitudes.** Define $\mathbf{S} : \mathbf{P}(\bigwedge^2 \mathbb{R}^{2*}) \to \mathbf{P}(\bigwedge^0 \mathbb{R}^{2*})$ by $\mathbf{S}(\alpha\mathbf{I}) = \frac{1}{\mathbf{I}}(\alpha\mathbf{I}) = \alpha$. This gives the scalar magnitude of a pseudoscalar in relation to the basis pseudoscalar $\mathbf{I}$. It is well-defined since $\mathbf{P}(\bigwedge^2 \mathbb{R}^{2*})$ is one-dimensional with basis element $\mathbf{I}$. Note that this expression does **not** depend on the existence of $\mathbf{I}^{-1}$. We sometimes use $(\mathbf{a} \vee \mathbf{P}) = \mathbf{S}(\mathbf{a} \wedge \mathbf{P})$ for the same purpose.
3. **Inverses.** k-vectors with non-zero norm also have unique inverses. $\mathbf{X}^{-1} = \frac{\mathbf{X}}{\mathbf{X} \cdot \mathbf{X}}$. Hence, proper points and planes in the model have unique inverses.
4. $\mathbf{a} \wedge \mathbf{P} = (a_0 p_0 + a_1 p_2 + a_2 p_2)\mathbf{I} = (\mathbf{a} \vee \mathbf{P})\mathbf{I} = \langle \mathbf{a}, \mathbf{P} \rangle$ vanishes only if $\mathbf{a}$ and $\mathbf{P}$ are incident. Otherwise, when $\mathbf{a}$ and $\mathbf{P}$ are normalized, it is related to the distance of the point to the line. Details follow in the discussions of specific metrics.
5. $\mathbf{P} \cdot \mathbf{a} = (p_2 a_1 - p_1 a_2)\mathbf{e}_0 + (p_0 a_2 - \kappa p_2 a_0)\mathbf{e}_1 + (\kappa p_1 a_0 - p_0 a_1)\mathbf{e}_2$ is a line which passes through $\mathbf{P}$ and is perpendicular to $\mathbf{a}$. Reversing the order changes the orientation of the line.
6. $\mathbf{P} \vee \mathbf{Q}$ is the joining line of $\mathbf{P}$ and $\mathbf{Q}$. $\|\mathbf{P} \vee \mathbf{Q}\|$ has a metric-specific significance; see metric-specific discussions below.
7. $\mathbf{a} \wedge \mathbf{b} =: \mathbf{T}$ is the intersection point of the lines $\mathbf{a}$ and $\mathbf{b}$. Reversing the order reverses the orientation of the resulting point.
8. $\mathbf{a} \cdot \mathbf{b}$ has different interpretations, depending on whether the two lines intersect in a proper, ideal, or improper point. For normalized lines $\mathbf{a}$ and $\mathbf{b}$ that intersect in a proper point with angle α, $\mathbf{a} \cdot \mathbf{b} = \cos(\alpha)$. Which of the two possible angles is being measured here depends on the orientation of the lines. The other cases will be discussed in the metric-specific treatment below.
9. $\mathbf{P} \times \mathbf{Q}$ is the polar point of the line $\mathbf{P} \vee \mathbf{Q}$, since a direct calculation confirms that $\mathbf{P} \times \mathbf{Q} = -(\mathbf{P} \vee \mathbf{Q})\mathbf{I}$.
10. $\mathbf{a}^\perp := \mathbf{a}\mathbf{I} = \kappa a_0 \mathbf{E}_0 + a_1 \mathbf{E}_1 + a_2 \mathbf{E}_2$ is the polar point of the line $\mathbf{a}$.
11. $\mathbf{P}^\perp := \mathbf{P}\mathbf{I} = p_0 \mathbf{e}_0 + \kappa(p_1 \mathbf{e}_1 + p_2 \mathbf{e}_2)$ is the polar line of the point $\mathbf{P}$.

6.1.1.1 Examples We provide examples throughout the exposition which derive results of interest. Many details of these examples are left to the reader to fill in.

1. All the results obtained above in Sect. 6.1.1 can also be framed in the n-dimensional context, where 1-vectors representing $(n-1)$-dimensional hyperplanes, and n-vectors represent points. Then $\mathbf{a} \wedge \mathbf{b}$ is an $(n-2)$-dimensional subspace common to $\mathbf{a}$ and $\mathbf{b}$, etc. The reader is encouraged to work out some examples to familiarize himself with the n-dimensional analogs.
2. When the arguments to the formulas in Sect. 6.1.1 are not normalized, one can incorporate the norms in the fomulas in a straightforward way. For example, the

formula for the angle between non-normalized proper lines is:

$$\cos d = \frac{\mathbf{a} \cdot \mathbf{b}}{\|\mathbf{a}\|\|\mathbf{b}\|}$$

Similar expressions appear in all the other formulas.

3. **Projection onto a line, and onto a point.** For a proper normalized line $\mathbf{a}$ and proper point $\mathbf{P}$, $(\mathbf{P} \cdot \mathbf{a})\mathbf{a}^{-1}$ is the orthogonal projection of the point $\mathbf{P}$ onto $\mathbf{a}$. $(\mathbf{a} \cdot \mathbf{P})\mathbf{P}^{-1}$ is the line through $\mathbf{P}$ perpendicular to $(\mathbf{a} \cdot \mathbf{P})$.
4. **Orthogonal decomposition.**
   - **Of a line with respect to a second line.** Notice that $(\mathbf{aa})\mathbf{b} = \mathbf{a}(\mathbf{ab})$. Then, for proper normalized lines $\mathbf{a}$ and $\mathbf{b}$, $\mathbf{b} = \mathbf{b}_\parallel + \mathbf{b}_\perp := (\mathbf{a} \cdot \mathbf{b})\mathbf{a} + \mathbf{a} \cdot (\mathbf{a} \wedge \mathbf{b})$. $\mathbf{b}_\perp$ is perpendicular to $\mathbf{a}$.
   - **Of a point with respect to a line.** Using the same approach, for a proper normalized line $\mathbf{a}$ and proper normalized point $\mathbf{P}$, $\mathbf{P} = \mathbf{P}_\parallel + \mathbf{P}_\perp := \mathbf{a}(\mathbf{a} \cdot \mathbf{P}) + \mathbf{a}(\mathbf{a} \wedge \mathbf{P})$. $\mathbf{P}_\parallel$ lies on $\mathbf{a}$ and $\mathbf{P}_\perp$ is a multiple of $\mathbf{a}^\perp$.
5. The following identities involving the geometric product are useful:

   a. $\mathbf{a} \cdot \mathbf{b} = \mathbf{S}(\mathbf{a} \wedge \mathbf{bI}) = \mathbf{a} \vee \mathbf{bI}$.
   b. $\mathbf{P} \times \mathbf{Q} = -(\mathbf{P} \vee \mathbf{Q})\mathbf{I}$.

6.2 Metric-specific discussion

The foregoing discussion has handled the algebras Cl^n_κ from a metric-neutral standpoint. We now turn to a discussion of metric-specific features.

6.2.1 Elliptic plane via Cl^2_1

The elliptic plane is characterized by the nature of its absolute as a totally imaginary non-degenerate conic section (Sect. 4.1). Most of the metric-specific aspects of this geometry can be explained via reference to this feature.

(6.1) shows that the induced signature on 2-vectors is $(0, 3, 0)$, equivalent to the original metric $(3, 0, 0)$.

The polarity on the metric quadric, implemented in the Clifford algebra by multiplication by $\mathbf{I}$, is a self-map of the plane, hence introduces no new qualitative phenomena. It essentially flips angles and lengths, and corresponds to the well-known polarity of a triangle and its polar triangle. Compare to the hyperbolic plane discussion below Sect. 6.2.2.

The elliptic plane is the least complicated of the metric planes. There are neither ideal nor improper points or lines, so every vector (2-vector) can be normalized to have norm 1 (-1).

A check of the multiplication table Table 6.1 reveals that $Cl^{2+}_1 \backsimeq \mathbb{H}$. We will return to this isomorphism below in Remark 101 after a discussion of isometries.

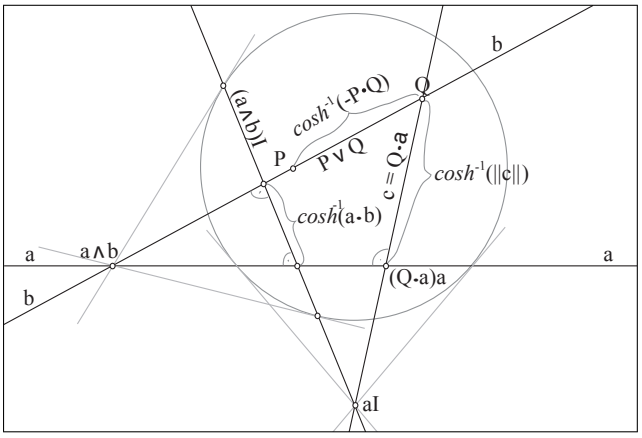

Fig. 6.1 A selection of the geometric products between various k-blades in the the hyperbolic plane via $\mathbb{R}_{2,1,0}$. Points and lines are assumed to be normalized.

6.2.2 Hyperbolic plane via Cl^2_{-1}

The hyperbolic plane is characterized by the nature of its absolute as a totally real non-degenerate conic section (Sect. 4.2). Most of the metric-specific aspects of this geometry can be explained via reference to this feature. We sometimes refer to proper elements as *hyperbolic* elements.

The induced metric on 2-vectors (points) is $(2, 1, 0)$, exactly equal to the original signature (compare to elliptic case).

Following the discussion in Sect. 4.3, ideal points and lines satisfy $\|\mathbf{X}\| = 0$; hyperbolic points and properly improper lines satisfy $\|\mathbf{X}\| < 0$; properly improper points and hyperbolic lines satisfy $\|\mathbf{X}\| > 0$. Hence, normalized hyperbolic points satisfy $\mathbf{P} \cdot \mathbf{P} = -1$ and normalized hyperbolic lines satisfy $\mathbf{m} \cdot \mathbf{m} = 1$.

6.2.2.1 Enumeration of various products We now carry out an investigation analogous to Sect. 6.1.1. See the companion diagram in Fig. 6.1. Due to the large number of possible combinations of proper, ideal, and improper points and lines, only a sampling of the many possibilities are given here; the remaining are left as an exercise for the reader.

1. **Ideal norm of ideal points.** Ideal elements satisfy by definition $\mathbf{X} \cdot \mathbf{X} = 0$. Define the *ideal norm* $\|\mathbf{a}\|_\infty$ of an ideal line $\mathbf{a}$ by $\|\mathbf{a}\|_\infty := \|\mathbf{a} \vee \mathbf{e}_0\|$, where the latter is the point norm defined in Sect. 6.1.1. $\|\mathbf{a}\|_\infty = \sqrt{a_1^2 + a_2^2}$ is the euclidean norm of the direction vector of $\mathbf{a}$.
   Similar remarks apply to ideal points. For such a point $\mathbf{P}$, one defines $\|\mathbf{P}\|_\infty := \|\mathbf{P} \vee \mathbf{E}_0\|$; the result is the euclidean norm of the direction vector of the line joining $\mathbf{P}$ with the origin $\mathbf{E}_0$.
   Note that the norms $\|\mathbf{X}\|_\infty$ defined here are non-zero for non-zero $\mathbf{X}$. These norms are applied in Sect. 6.3.2 to provide canonical forms for isometries associated to ideal elements.
2. **Hyperbolic distance.**

- **Between lines.** For normalized hyperbolic $\mathbf{a}$ and $\mathbf{b}$, such that $\mathbf{a}\wedge\mathbf{b}$ is hyperbolic, the angle between the lines satisfies $\cos\alpha = \mathbf{a}\cdot\mathbf{b}$. When $\mathbf{a}\wedge\mathbf{b}$ is improper, the hyperbolic distance d between them (measured along the common normal $(\mathbf{a}\wedge\mathbf{b})\mathbf{I}$) satisfies $\cosh d = \mathbf{a}\cdot\mathbf{b}$.
- **Between points.** For normalized hyperbolic $\mathbf{P}$ and $\mathbf{Q}$, the hyperbolic distance d between $\mathbf{P}$ and $\mathbf{Q}$ satisfies $\cosh d = -\mathbf{P}\cdot\mathbf{Q}$.

3. $\mathbf{a}\wedge\mathbf{P}$ vanishes only if $\mathbf{a}$ and $\mathbf{P}$ are incident. Otherwise, when both are hyperbolic and normalized, $\cosh^{-1}(\mathbf{a}\wedge\mathbf{P})\mathbf{I}$ is the hyperbolic distance between $\mathbf{a}$ and $\mathbf{P}$. The other cases are left as exercises.
4. $\mathbf{a}\cdot\mathbf{b} = \cosh^{-1} d$ for normalized hyperbolic lines $\mathbf{a}$ and $\mathbf{b}$ that meet in an improper point. Here d is the hyperbolic distance between the two lines measured along the common perpendicular. See Fig. 6.1.
5. $\mathbf{aI}$ is the polar point of the line $\mathbf{a}$: the intersection of the tangent lines at the intersections points of $\mathbf{a}$ with the ideal circle. The polar point of a hyperbolic line is an improper point; the polar point of an improper line is a hyperbolic point. The polar point of an ideal line is the ideal point where the ideal line touches the ideal circle.
6. $\mathbf{PI}$ is the polar line of the point $\mathbf{P}$. The polar line of a hyperbolic point is improper; the polar line of an improper point is hyperbolic; the polar line of an ideal point is ideal: the tangent line to the ideal circle at the ideal point.

6.2.2.2 Dual hyperbolic plane As explained in Sect. 5.4, the metric polarity $\mathbf{I}$ is an algebra isomorphism. Thus, polar to the model of the hyperbolic plane H consisting of the points of the open unit disk, there is a model of the hyperbolic plane $\hat{H} := \mathbf{I}(H)$, whose "points" are the improper lines of H, the lines "outside" the unit disk. Such a line we call a *dual hyperbolic* line. And an improper point of H is a *dual hyperbolic* point of $\hat{H}$. All the metric relations that are true for points within H carry over and are true for such lines in $\hat{H}$. The distance between two such lines is the hyperbolic distance between the polar points in H, etc. Contemplating Fig. 6.1 is recommended to familiarize oneself with the nature of this polarity. Note that both $\mathbf{P}(\mathbb{R}^*_{2,1,0})$ and the dual Clifford algebra $\mathbf{P}(\mathbb{R}_{2,1,0})$ contain H **and** $\hat{H}$. As explained in Sect. 4.4.2, the dual hyperbolic plane arises by choosing different sets of proper points and lines when constructing the Cayley-Klein space.

6.2.3 Euclidean plane via Cl^2_0

The euclidean plane has the most complicated behavior due to the degenerate and asymmetric nature of Q and Q^*. Since it also of the most interest for applications, we investigate the Clifford algebra $\mathbf{P}(\mathbb{R}^*_{2,0,1})$ in detail.

6.2.3.1 Consequences of degeneracy The pseudoscalar $\mathbf{I}$ satisfies $\mathbf{I}^2 = 0$. Hence, $\mathbf{I}^{-1}$ is not defined. Many standard formulas of geometric algebra are, however, typically stated using $\mathbf{I}^{-1}$ ([DFM07, HS87]), since that can simplify things for nondegenerate metrics. As explained in Sect. 2.4, many formulas remain projectively valid when $\mathbf{I}^{-1}$ is replaced by $\mathbf{I}$; in such cases this is the solution we adopt.

6.2.3.2 Notation $\mathbf{e}_0$ is the *ideal* line of the plane, $\mathbf{e}_1$ is the line $x = 0$ and $\mathbf{e}_2$, the line $y = 0$. $\mathbf{E}_0$ is the origin $(1, 0, 0)$ while $\mathbf{E}_1$ and $\mathbf{E}_2$ are the *ideal* points in the $x-$ and $y-$ direction, resp. Points and lines which are not ideal, are called *finite*, or *euclidean*.

6.2.3.3 Converting to and from traditional notation The natural embedding of a euclidean *position* $\mathbf{x} = (x, y)$ we write as $\mathbf{i}(\mathbf{x}) = \mathbf{E}_0 + x\mathbf{E}_1 + y\mathbf{E}_2$. A euclidean *vector* $\mathbf{v} = (x, y)$ corresponds to an ideal point (see Sect. 4.4.4); we denote its embedding with the same symbol $\mathbf{i}(\mathbf{v}) = x\mathbf{E}_1 + y\mathbf{E}_2$. We sometimes refer to such an element as a *free* vector. Conversely, a bivector $w\mathbf{E}_0 + x\mathbf{E}_1 + y\mathbf{E}_2$ with $w \neq 0$ corresponds to the euclidean point $(\frac{x}{w}, \frac{y}{w})$. We refer to w as the *intensity* or *weight* of the bivector. And, we write $\underline{\mathbf{A}}$ to refer to $\mathbf{i}^{-1}(\mathbf{A})$. The line $ax + by + c = 0$ maps to the 1-vector $c\mathbf{e}_0 + a\mathbf{e}_1 + b\mathbf{e}_2$. A line is euclidean if and only if $a^2 + b^2 \neq 0$.

6.2.3.4 Enumeration of various products Here we extend the results of Sect. 6.1.1 to include metric-specific euclidean features.

1. **Norms.**
   - **1-vectors.** $\mathbf{a}^2 = \mathbf{a} \cdot \mathbf{a} = a_1^2 + a_2^2$. Then $\dfrac{\mathbf{a}}{\|\mathbf{a}\|}$ is a vector with norm 1, defined for all vectors except $\mathbf{e}_0$ and its multiples. In particular, all euclidean lines can be normalized to have norm 1. Note that when $\mathbf{a}$ is normalized, then so is $-\mathbf{a}$. These two lines represents opposite *orientations* of the line.
   - **2-vectors.** $\mathbf{P}^2 = \mathbf{P} \cdot \mathbf{P} = p_0^2\mathbf{E}_0^2 = -p_0^2$. Define the *norm* of $\mathbf{P}$ to be p_0 and write it $\|\mathbf{P}\|$. Note that this can take positive or negative values, in contrast to $\sqrt{\mathbf{P} \cdot \mathbf{P}}$. Then $\dfrac{\mathbf{P}}{\|\mathbf{P}\|}$ is a bivector with norm 1, defined for all bivectors except where $p_0 = 0$, that is, ideal points. In particular, all euclidean points can be normalized to have norm 1. This is also known as *dehomogenizing*.
2. **Euclidean distance.** For normalized proper $\mathbf{P}$ and $\mathbf{Q}$, $\|\mathbf{P} \vee \mathbf{Q}\|$ is the euclidean distance between $\mathbf{P}$ and $\mathbf{Q}$.
3. **Ideal norm on ideal points.** Recall the discussion in Sect. 4.4.4.2, where the existence of a almost non-degenerate metric on ideal euclidean points was highlighted. How this can be implemented in the Clifford algebra is described in this and the following point. First define a norm on ideal points. Let $\mathbf{V}$ be ideal (that is, a free vector) and $\mathbf{P}$ *any* normalized euclidean point. $\|\mathbf{V}\|_\infty := \|\mathbf{V} \vee \mathbf{P}\| = \sqrt{v_1^2 + v_2^2}$ is the length of $\mathbf{V}$ as element of the vector space $\mathbb{R}^2$. $\|\mathbf{V}\|_\infty$ is called the ideal norm of $\mathbf{V}$. $\dfrac{\mathbf{V}}{\|\mathbf{V}\|_\infty}$ is normalized to have length 1.
4. **Angles between free vectors.** For normalized ideal points $\mathbf{U}$ and $\mathbf{V}$ ($\|\mathbf{V}\|_\infty = 1$, etc): ,
$$\langle \mathbf{U}, \mathbf{V} \rangle_\infty := (\mathbf{U} \vee \mathbf{P}) \cdot (\mathbf{V} \vee \mathbf{P}) = \cos\alpha$$
where $\mathbf{P}$ is **any** normalized proper point and α is the angle between the vectors. In effect, one converts the points to lines with the desired direction, and then calculates the angle between these lines.

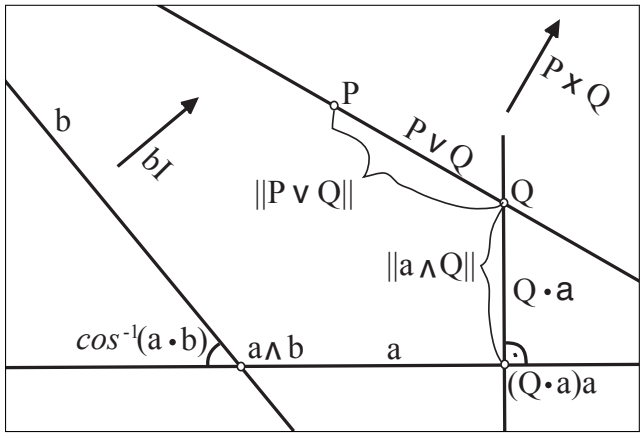

Fig. 6.2 A graphical representation of selected geometric products between various k-blades in the euclidean algebra Cl^2_0. Points and lines are assumed to be normalized. Ideal points are drawn as vectors, distances indicated by norms.

5. $\mathbf{S}(\mathbf{a} \wedge \mathbf{P}) = \mathbf{a} \vee \mathbf{P}$, when $\mathbf{a}$ and $\mathbf{P}$ are normalized, equals the signed distance of the point to the line.
6. $\mathbf{PI} = p_0\mathbf{e}_0$ is the polar line of the point $\mathbf{P}$: for finite points, the ideal line, weighted by the intensity of $\mathbf{P}$. Ideal points have no polar line.

6.2.3.5 Examples The following examples illustrate features of the euclidean plane.

1. **Parallel lines.** $\mathbf{a}$ and $\mathbf{b}$ are parallel when they intersect in an ideal point: $(\mathbf{a} \wedge \mathbf{b}) \neq 0$ but $\|(\mathbf{a} \wedge \mathbf{b})\| = 0$. When the lines are normalized, the distance between the two lines is then
$$\|\mathbf{a} \wedge \mathbf{b}\|_\infty$$
2. **Ideal elements.** It is instructive to consider what changes have to be made to the above formulas in the case one or more of the parameters are ideal. We have in fact considered such cases in the discussion above of how to calculate the angle between ideal points.
3. For normalized $\mathbf{A}, \mathbf{B}$, and $\mathbf{C}$, the area of $\Delta\mathbf{ABC}$ is given by $(\mathbf{A} \vee \mathbf{B}) \wedge \mathbf{C}$. This reduces to the determinant rule for calculating the area of a triangle.
4. **Triangle centers.** Given a euclidean triangle $\mathbf{ABC}$, this exercise shows how to use $\mathbf{P}(\mathbb{R}^*_{2,0,1})$ to calculate the four classical triangle centers, and prove three lie on the Euler line. Consult Fig. 6.3.
   a. $\Delta\mathbf{ABC}$ can be assumed to have normalized corners $A = \mathbf{E}_0$, $B = \mathbf{E}_0 + b_1\mathbf{E}_1$, and $C = \mathbf{E}_0 + c_1\mathbf{E}_1 + c_2\mathbf{E}_2$.
   b. Define the edge-lines $\mathbf{a} := \mathbf{B} \vee \mathbf{C}$, $\mathbf{b} := \mathbf{C} \vee \mathbf{A}$, and $\mathbf{c} := \mathbf{A} \vee \mathbf{B}$.
   c. The median $\mathbf{m_A}$, perpendicular bisector $\mathbf{p}_a$, altitude $\mathbf{t}_a$ and angle bisector $\mathbf{n}_a$ associated to the pair $\mathbf{a}$ and $\mathbf{A}$ are given by the following formulas:
   - $\mathbf{m}_a = (\mathbf{B} + \mathbf{C}) \vee \mathbf{A}$
   - $\mathbf{p}_a = (\mathbf{B} + \mathbf{C}) \cdot \mathbf{a}$
   - $\mathbf{t}_a = \mathbf{A} \cdot \mathbf{a}$
   - $\mathbf{n}_a = \|\mathbf{c}\|\mathbf{b} + \|\mathbf{b}\|\mathbf{c}$

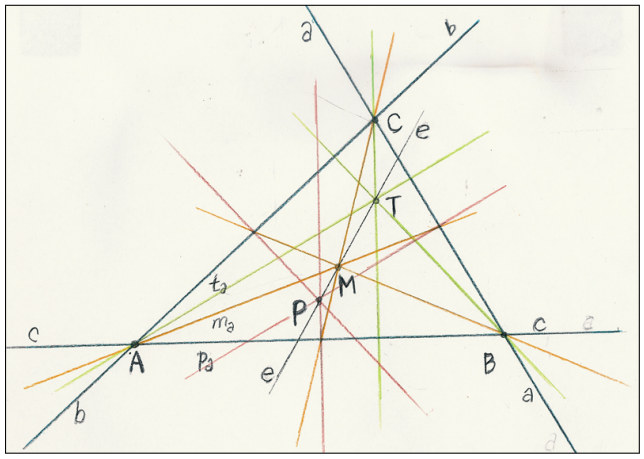

Fig. 6.3 The three triangle centers **M** (centroid), **T** (orthocenter), and **P** (circumcenter) lying on the Euler line **e** of the triangle **ABC**.

d. Analogous formulas for the lines associated to **b** and **c** are obtained by permuting the symbols.
e. $\mathbf{m}_a$, $\mathbf{m}_b$, and $\mathbf{m}_c$ are co-punctual; their common point is the *centroid* **M** of the triangle. [Hint: to show that the three lines go through the same point you can show the outer product of all three is 0. If you work with the fully general forms for **A**, **B**, and **C** (don't use 4a), you can alternatively show that the expression for the intersection of two of the lines is symmetric in {**a**,**b**,**c**} and {**A**, **B**,**C**}.]
f. One can also show each of the following triple of lines are co-punctual:
   - ($\mathbf{p}_a$, $\mathbf{p}_b$, $\mathbf{p}_c$), to obtain the *circumcenter* **P**,
   - ($\mathbf{t}_a$, $\mathbf{t}_b$, $\mathbf{t}_c$), to obtain the *orthocenter* **T**, and
   - ($\mathbf{n}_a$, $\mathbf{n}_b$, $\mathbf{n}_c$), to obtain the *incenter* **N**.
g. **M**, **P**, and **T** lie on a line **e** (the *Euler line* of the triangle). [Hint: to show three points lie on a line, show that the join ($\vee$) of two of the points has vanishing outer product with the third.
h. **M** lies between **P** and **T** on the Euler line, and is twice as far from **T** as from **P**. This can be shown by establishing that $\mathbf{M}\wedge(\mathbf{P}\vee\mathbf{T}) = 0$, and that $2\mathbf{M}\vee\mathbf{P} = \mathbf{M}\vee\mathbf{T}$.

6.3 Isometries

The discussion of Sect. 5.6 implies that in Cl^2_κ, a proper 1-vector **a** gives rise to the conjugation operator $\underline{\mathbf{a}}$ which is a reflection in the normalized line **a** ($\mathbf{a}^2 = 1$). The restriction to proper **a** is necessary, since for improper **a** (which only arise in the hyperbolic plane), $\underline{\mathbf{a}}$ is a rotation of π radians around the proper point $\mathbf{a}^\perp$.

6.3.1 Rotations

Adapting a well-known result in plane geometry to be metric-neutral yields:

> When two proper lines intersect in a proper point $\mathbf{R}$, the composition of the reflections in the two lines is a rotation around $\mathbf{R}$, through an angle equal to twice the angle between the two lines.

Translating this into the language of the Clifford algebra, the composition of reflections in lines $\mathbf{a}$ and $\mathbf{b}$ will look like:

$$\begin{aligned}\mathbf{P}' &= \mathbf{b}(\mathbf{aPa})\mathbf{b}\\ &= \mathbf{TP}\widetilde{\mathbf{T}}\end{aligned}$$

where we write $\mathbf{T} := \mathbf{ba}$, and $\widetilde{\mathbf{T}}$ is the reversal of $\mathbf{T}$.

Remark 99. The intersection $\mathbf{R}$ of the two lines will be fixed by the resulting isometry. The nature of the isometry depends on the value of $\mathbf{R}^2$, which determines whether it is a proper, ideal, or properly improper point. In any case $\mathbf{T}\widetilde{\mathbf{T}} = \mathbf{abba} = 1$, so $\mathbf{T} \in \mathbf{Spin}^2_{+\kappa}$.

Remark 100. The above discussion can be made valid for arbitrary dimension n, by taking into account that $\mathbf{a} \wedge \mathbf{b}$ is not a point but a simple $(n-2)$-dimensional subspace invariant under the rotation.

For now, we consider only the case where $\mathbf{R}$ is proper. Then $\langle \mathbf{R} \rangle_0 = \mathbf{a} \cdot \mathbf{b} = \cos\alpha$ where α is the angle between the two lines (Sect. 6.1.1). If we write $\mathbf{T}$ with normalized $\mathbf{R}$ we obtain:

$$\mathbf{T} = \cos(\alpha) + \sin(\alpha)\mathbf{R}$$

If one substitutes this into (6.2) and multiplies out, one arrives at the result quoted above, that a point $\mathbf{P}$ undergoes a rotation of 2α around the point $\mathbf{R}$. (Simple check: let $\mathbf{a} = \mathbf{e}_1$ and $\mathbf{b} = \mathbf{e}_2$).

Given a proper point $\mathbf{R}$ and an angle θ, one could construct a rotor producing the rotation of θ degrees around $\mathbf{R}$ by finding two lines $\mathbf{l}_1$ and $\mathbf{l}_2$ through $\mathbf{R}$ which meet at an angle of $\dfrac{\theta}{2}$. But this is not necessary. In Sect. 5.6.2 below, a direct way is shown to create this rotor by applying the exponential function to the 2-vector representing its invariant point.

Remark 101. **An extension of quaternions.** Note that $Cl^{2+}_1 \backsimeq \mathbb{H}$ under the mapping $(\mathbf{1}, \mathbf{i}, \mathbf{j}, \mathbf{k}) \to (\mathbf{1}, \mathbf{E}_0, \mathbf{E}_1, \mathbf{E}_2)$. The former algebra is projectivized, so acts on the elliptic plane; while the latter is traditionally associated to $\mathbb{R}^3$. For the moment we consider Cl^2_1 as non-projectivized. Then for a 1-vector $\mathbf{a}$ of $Cl^2_\kappa 1$, $\underline{\mathbf{a}}$ represents a reflection in the plane $\mathbf{a}$. Hence, we have found an algebraic structure which extends the quaternions in an important respect, allowing not just rotations around lines in $\mathbb{R}^3$ but also reflections in planes. We will return to this question in Chapter 12 and give a cumulative account of further discoveries related to the questions posed in Chapter 1.

Remark 102. **Rotation versus translation.** A rotation around a point $\mathbf{P}$ in the elliptic plane is equivalent to a translation by the same angle along its polar line $\mathbf{PI} = \mathbf{P}^\perp$. We

obtain a representation via the latter if we use the point-based model $\mathbf{P}(\mathbb{R}_{3,0,0})$; then 2-vectors are lines, and a sandwich of the form in this algebra

$$(\cos\alpha + \mathbf{m}\sin\alpha)\mathbf{X}(\cos\alpha - \mathbf{m}\sin\alpha)$$

represents the translation of angle α along the 2-vector (line) m. This is another way of seeing that the elliptic plane can be built just as well using $\mathbf{P}(\bigwedge \mathsf{V})$ as $\mathbf{P}(\bigwedge \mathsf{V}^*)$. Similar remarks apply to the hyperbolic plane, replacing trig functions with hyperbolic trig functions. However, note that in contrast to the elliptic case, the axis of translation will be an *improper* line.

In both cases, the result of using $\mathbf{P}(\bigwedge \mathsf{V})$ as the basis of the Clifford algebra is that rotations around a proper point are represented by bivectors, that is, by lines. Since we generally prefer to characterize a rotation by its center point rather than its invariant line, this illustrates another advantage of the dual construction based on $\mathbf{P}(\bigwedge \mathsf{V}^*)$. And, furthermore, if we want to include the euclidean case we are forced to use $\mathbf{P}(\bigwedge \mathsf{V}^*)$, since the polar line of every euclidean point is the ideal line.

6.3.1.1 Examples

1. **Point reflection.** A point reflection in a proper point $\mathbf{P}$ is an isometry that sends each point $\mathbf{Q}$ to its reflected image on the "other side" of $\mathbf{P}$. In particular, the image of $\mathbf{Q}$ lies on the line $\mathbf{P} \vee \mathbf{Q}$ on the other side of $\mathbf{P}$ an equal distance to $\mathbf{P}$. $\mathbf{Q} \to \mathbf{P}\mathbf{Q}\widetilde{\mathbf{P}}$ realizes this point reflection. On the other hand, this is a rotation since $\mathbf{P} \in \mathbf{Spin}^2_{+\kappa}$. The apparent contradiction can be resolved by observing that $\cos(\pi/2) = 0$.
2. **Glide reflection.** The composition of a reflection in a line $\mathbf{m}$ with a rotor that leaves $\mathbf{m}$ invariant is called a glide-reflection (for example, a rotation around the point $\mathbf{m}^\perp$). A glide reflection is uniquely characterized by its axis and the distance which points on the axis are moved. Clearly every glide reflection is the product of three reflections. And, generically, the product of three reflections is a glide reflection. We leave it as an exercise for the reader to find the axis and distance of this glide reflection given the three reflections.

6.3.2 Logarithms for 2D rotors

The following discussion shows how to find the logarithm of a rotor $\mathbf{g} \in \mathbf{Spin}^2_{+\kappa}$.

Definition 103. Given a rotor $\mathbf{g}$, let $\mathbf{B} := \langle \mathbf{g} \rangle_2$, and $s = \mathbf{B}^2$. Then the rotor is:

- *elliptic*, if $s < 0$,
- *parabolic* if $s = 0$, and
- *hyperbolic*, if $s > 0$.

The associated isometries $\underline{\mathbf{g}}$ are called *elliptic* rotations, *parabolic* rotations, and *hyperbolic* rotations.

6.3.2.1 Norm of simple rotor

We need a metric-neutral way to refer to the magnitude of an simple rotor. First we use the ideal norms introduced in the metric-specific discussions to define a non-zero norm for a bivector.

Definition 104. Given a simple bivector $\mathbf{B}$.

- The norm $N(\mathbf{B})$ is:
$$N(\mathbf{B}) = \begin{cases} \|\mathbf{B}\| & \text{if } \mathbf{B}^2 \neq 0 \\ \|\mathbf{B}\|_\infty & \text{otherwise} \end{cases} \tag{6.2}$$
- $\mathbf{B}$ is *normalized* if $N(\mathbf{B}) = 1$.
- A logarithm $t\mathbf{B}$ of a rotor is called *normalized* if $\mathbf{B}$ is normalized,
- If $t\mathbf{B}$ is a normalized logarithm of a rotor $\mathbf{g}$, t is the *measure* of $\mathbf{g}$.

Remark 105. We include the adjective *simple* in the definition so the definition can be used in other dimensions as well.

Remark 106. For an elliptic rotor, the measure is just the ordinary angle; for a hyperbolic rotor it is a "hyperbolic" distance it moves points on its proper axis; and for parabolic rotor it is either a euclidean distance (when $\mathbf{I}^2 = 0$) or related (when $\mathbf{I}^2 = -1$).

Theorem 107. *Every rotor in $\mathbf{g} \in \mathbf{Spin}^2_{+\kappa}$ has a normalized logarithm.*

Proof. Write $\mathbf{g} = a + \mathbf{B}$ where $\mathbf{B} = \langle \mathbf{g} \rangle_2$. Then by assumption

$$\mathbf{g}\widetilde{\mathbf{g}} = a^2 - \mathbf{B}^2 = 1$$

There are three cases depending on the type of $\mathbf{B}$.

- **Elliptic.** Then there exists $\theta \neq 0$ such that $s = \cos(\theta)$ and $\|\mathbf{B}\| = \sin(\theta)$. Define $\mathbf{B}_N := \dfrac{\mathbf{B}}{\sin\theta}$, with $\mathbf{B}_N^2 = -1$. Then $\mathbf{g} = \cos(\theta) + \sin(\theta)\mathbf{B}_N$. On the other hand, the formal exponential $e^{\theta \mathbf{B}_N}$ can be evaluated to yield:
$$\begin{aligned} e^{\theta \mathbf{B}_N} &= \sum_{i=0}^{\infty} \frac{(\theta \mathbf{B}_N)^i}{i!} \\ &= \cos(\theta) + \sin(\theta)\mathbf{B}_N \end{aligned}$$
$\mathbf{g} = e^{\theta \mathbf{B}_N} \Longrightarrow \theta \mathbf{B}_N$ is a normalized logarithm of $\mathbf{g}$.
- **Parabolic.** $\mathbf{B}$ is an ideal point. Then we can assume that $s = 1$ (if $s = -1$, the element $-\mathbf{g}$ with $s = 1$ has the same sandwich behavior as $\mathbf{g}$). Suppose $\|\mathbf{B}\|_\infty = t$, then find $\mathbf{B}_N$ such that $\mathbf{B} = t\mathbf{B}_N$ with $\|\mathbf{B}_N\|_\infty = 1$. Again, the formal exponential $e^{t\mathbf{B}}$ can be evaluated to yield:
$$\begin{aligned} e^{t\mathbf{B}} &= \sum_{i=0}^{\infty} \frac{(t\mathbf{B}_N)^i}{i!} \\ &= 1 + t\mathbf{B}_N \end{aligned}$$
$\mathbf{g} = e^{\mathbf{B}} \Longrightarrow t\mathbf{B}_N (= \mathbf{B})$ is a normalized logarithm of $\mathbf{g}$.
- **Hyperbolic.** Then there exists $t \neq 0$ such that $s = \cosh(t)$ and $\|\mathbf{B}\| = \sinh(t)$. Define $\mathbf{B}_N := \dfrac{\mathbf{B}}{\sinh t}$, with $\mathbf{B}_N^2 = 1$. Then $\mathbf{g} = \cosh(t) + \sinh(t)\mathbf{B}_N$. As above, the formal exponential $e^{t\mathbf{B}_N}$ can be evaluated to yield:

$$e^{t\mathbf{B}_N} = \sum_{i=0}^{\infty} \frac{(t\mathbf{B}_N)^i}{i!}$$
$$= \cosh(t) + \sinh(t)\mathbf{B}_N$$

$\mathbf{g} = e^{t\mathbf{B}_N} \Longrightarrow t\mathbf{B}_N$ is a normalized logarithm of $\mathbf{g}$.
□

6.3.2.2 Classification of metric bivectors The proof of Thm. 107 shows that the nature of an isometry is determined by the value of $\mathbf{I}^2$ and $\mathbf{B}^2$, as enumerated in Def. 103. Only 6 of the $3 \times 3 = 9$ possibilities can occur. Table 6.2 shows the allowed combinations.

	-1	0	1
-1	✓	✓	✓
0	✓	✓	X
1	✓	X	X

Table 6.2 Allowed combinations of $\mathbf{I}^2$ (horizontal) and $\mathbf{B}^2$ (vertical).

6.3.3 The flow generated by a bivector

We can explore the differences among these 6 types of rotors by investigating a 1-parameter family of curves generated by the respective logarithms. We obtain these curves by parametrizing the exponential forms obtained above for $\underline{\mathbf{g}}$. If $\langle \mathbf{g} \rangle_2 = \mathbf{B}$ is the bivector part of the rotor, then there is a one-parameter family of isometries given by

$$\underline{\mathbf{g}}_t(\mathbf{X}) = e^{t\mathbf{B}} \mathbf{X} e^{-t\mathbf{B}}$$

Each point $\mathbf{X}$ in $\mathbb{R}P^2$ (not just the proper points of the model) determines one such curve, for $t \in (-\infty, \infty)$. We will return to this theme later in Chapter 8, where we will explore the constant vector field which underlies this system and justify the term *integral* curves applied to these curves. The characteristic pictures of the foliation of the projective plane by these six types of curves is shown in Fig. 6.4.

6.3.3.1 Elliptic rotors These are the *elliptic* rotors of Def. 103. The three cases $\mathbf{B}^2 = -1$ all exhibit a similar picture: nested conic sections enclosing the proper fixed point $\mathbf{B}$, the *center* of the motion. The polar line $\mathbf{B}^\perp$ is called the *axis* of the isometry. We can characterize the family of conic sections using the familiar terminology based in euclidean geometry. When $\mathbf{I}^2 = 0$, they remain euclidean circles; in the non-euclidean case, they become parabolic by touching $\mathbf{e}_0$, then expand further and become hyperbolas, which

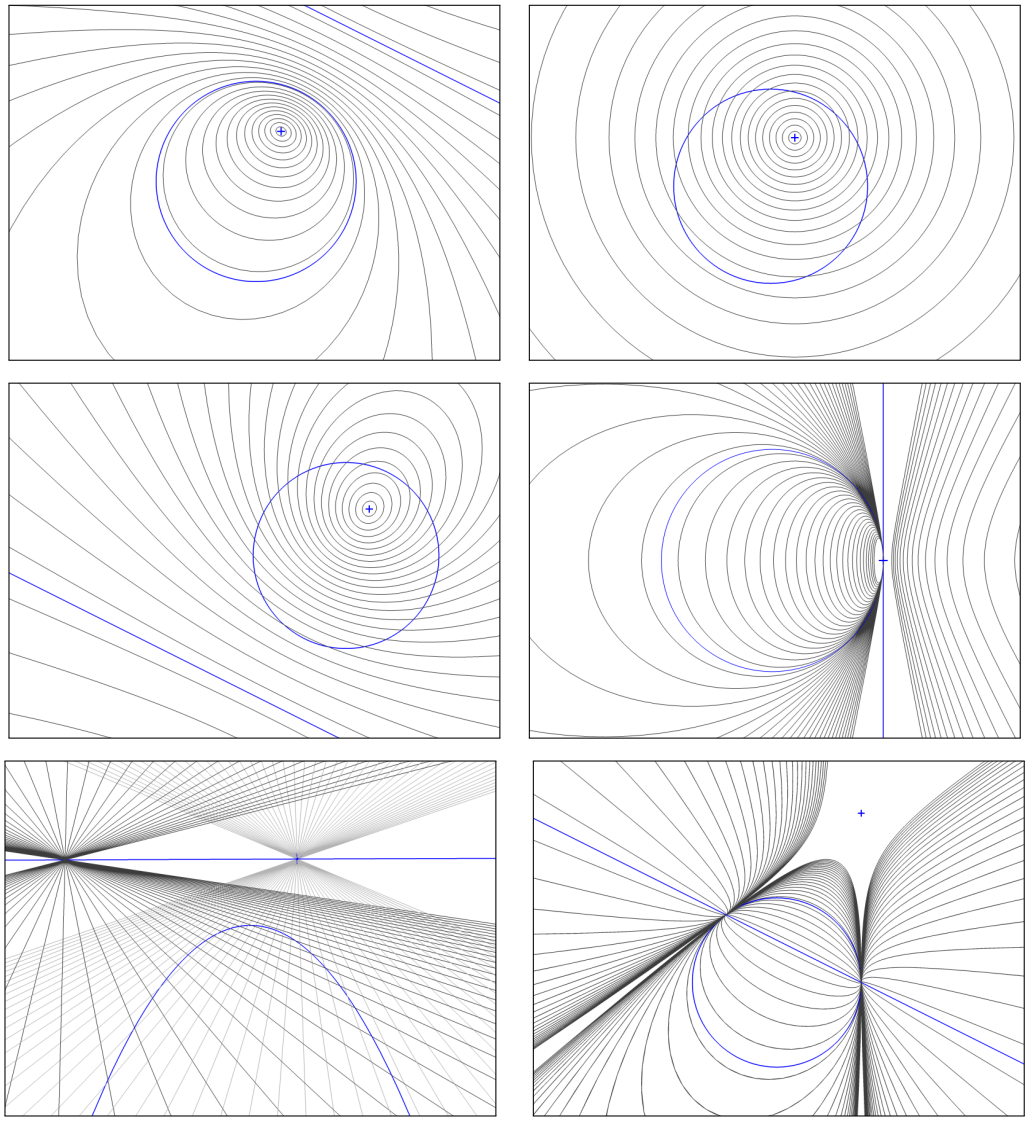

Fig. 6.4 Integral curve patterns for the six possibilities of $(\mathbf{I}^2, \mathbf{B}^2)$: (-1,-1),(0,-1),(1,-1),(-1,0),(0,0),(-1,1). The case (0,0), euclidean translation, is shown in perspective.

then approach $\mathbf{B}^\perp$ from both sides. Of course in the non-euclidean geometry itself the line $\mathbf{e}_0$ has no special significance; it is only a useful aid to the euclidean-trained imagination.

6.3.3.2 Parabolic rotors In order to provide a canonical form for these curves we assume $\mathbf{B}$ normalized so that $\|\mathbf{B}\|_\infty = 1$.

The case of $\mathbf{B}^2 = 0$, when $\mathbf{I}^2 = 0$, yields euclidean translations; the integral curves consist of parallel lines in direction of translation. In this case $\mathbf{B}$ is an ideal point. In Fig. 6.4 this case is shown in perspective. The ideal line $\mathbf{e}_0$ is shown in blue although it is not the polar line of $\mathbf{B}$ as in the other figures. The darker lines are the integral curves; the lighter lines meet in $\mathbf{B}$. The meeting point of the darker lines is the polar point of $\mathbf{B}$ with respect to the elliptic metric on the ideal ine $\mathbf{e}_0$.

When $\mathbf{I}^2 = -1$, one calls the integral curves *horocycles*; to understand them better, it is useful to consider the projectivity M which maps the unit circle to the parabola $\mathcal{P}$ whose axis is the x-axis, which passes through the $\mathbf{E}_0$ and $\mathbf{E}_1$. Consider the family of parabolas given by $\mathcal{P}$, translated in the positive direction along the x-axis. In can be shown that the horocycles, are the images of this family of parabolas under the inverse mapping M^{-1}. When one considers **all** parabolas (also those along the negative x-axis), one obtains a complete set of integral curves for this type of rotor.

6.3.3.3 Hyperbolic rotors Finally, the case $\mathbf{B}^2 = 1$ occurs only when $\mathbf{I}^2 = -1$. Then $\mathbf{B}$ is an improper fixed point, and $\mathbf{B}^\perp$ is a proper fixed line, the *axis* of the hyperbolic translation. Points move along conic sections which all pass through the two intersections points of this axis with the ideal circle. The unit circle itself is one such conic section. As in the previous cases, these conic sections outside of the unit circle contact $\mathbf{e}_0$ and wrap around to approach $\mathbf{B}^\perp$ from the other side.

6.3.4 Lie groups and Lie algebras

The above remarks provide a realization of the direct isometry group $\mathbf{G}^2_\kappa$ of the geometry G^2_κ and of its Lie algebra $\mathfrak{g}^2_\kappa$ within Cl^2_κ. The spin group $\mathbf{Spin}^2_{+\kappa}$ forms a double cover of $\mathbf{G}^2_\kappa$ since the rotors $\mathbf{g}$ and $-\mathbf{g}$ represent the same isometry. Within Cl^{2+}_κ, the spin group consists of elements of unit norm; the Lie algebra consists of the pure bivectors as a vector space, so includes the zero element. The exponential map $\mathbf{X} \to e^{\mathbf{X}}$ is a covering map: locally bijective with a finite fiber. This structure is completely analogous to the way the unit quaternions sit inside $\mathbf{P}(\mathbb{R}^{*+}_{3,0,0})$ and form a double cover of $SO(3)$. The full group – including indirect isometries – is also naturally represented in Cl^2_κ as the group $\mathbf{Pin}^2_{+\kappa}$ generated by reflections in proper lines. This exponential map is depicted in Fig. 6.5.

6.4 Guide to the literature

6.4.0.1 The euclidean case There is a substantial literature on the four-dimensional even subalgebra $\mathbf{P}(\mathbb{R}^{*+}_{2,0,1})$ with basis $\{\mathbf{1}, \mathbf{E}_0, \mathbf{E}_1, \mathbf{E}_2\}$. In an ungraded setting, this structure is known as the *planar quaternions*. The original work appears to have been done by Study ([Stu91], [Stu03]); this was subsequently expanded and refined by Blaschke in his elegant monograph [Bla38]. Study's parametrization of the full planar euclidean group

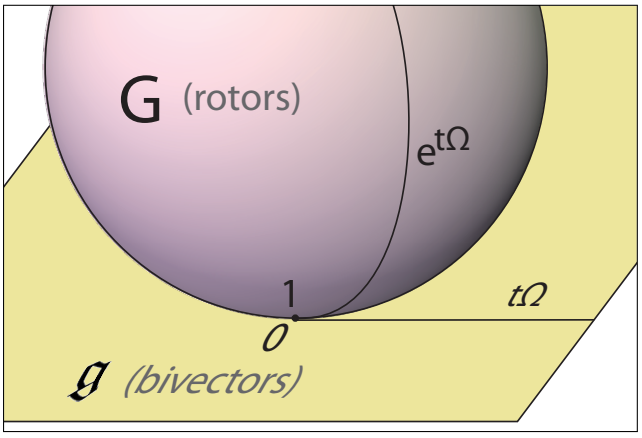

Fig. 6.5 The exponential map of the Lie algebra (bivectors) to the Lie group ($\mathbf{Spin}^2_{+\kappa}$).

as "quasi-elliptic" space is worthy of more attention. Modern accounts include [PW01], Ch. 8, and [McC90].[1]

6.4.0.2 The non-euclidean case Existing literature on the algebras $\mathbb{R}_{3,0,0}$ and $\mathbb{R}_{2,1,0}$ can be adapted by dualization and projectivization to yield the results described here. However, we are not aware of other efforts to describe the elliptic and hyperbolic plane directly using these dual homogeneous Clifford algebras, nor of any metric-neutral treatment which combines this with the euclidean case as here.

[1] which however confuses the euclidean inner product on vectors with the inner product on points.

Chapter 7
Metric spaces via Cl^3_κ

The extension of the results in the previous chapter to the three-dimensional case Cl^3_κ is mostly straightforward. Many of the results can be carried over virtually unchanged. For a two-dimensional configuration $\mathcal{C}_2$ in Cl^2_κ, the analogous configuration $\mathcal{C}_3$ in Cl^3_κ is obtained by replacing 1-vectors (lines) by 1-vectors (planes), and 2-vectors (points) by 3-vectors (points). A more precise discussion is given below in Sect. 7.3.1.

The main challenge in three dimensions is due to the existence of non-simple bivectors; in fact, most bivectors are **not** simple! This means that the geometric interpretation of a bivector is usually **not** a simple geometric entity, such as a spear or an axis, but a more general object known in the classical literature as a *linear line complex*, or *null system*. Such entities are crucial in kinematics and dynamics. Because of their importance, we provide a review of their essential non-metric properties in Sect. 7.2.

The main result of this chapter shows that a given non-simple bivector $\mathbf{\Omega}$ can always be factored into the form $\mathbf{\Omega} = (\alpha + \beta\mathbf{I})\mathbf{\Phi}$ where $\alpha, \beta \in \mathbb{R}$ and $\mathbf{\Phi}$ is simple. $\mathbf{\Phi}$ is called an *axis* of $\mathbf{\Omega}$. This factorization is key to finding the logarithm of a rotor. It also makes it possible to interpret non-simple bivectors geometrically within the Cayley-Klein 3-space. To arrive at this factorization, the sub-algebra consisting of scalars and pseudoscalars (known as Study numbers) plays a crucial role.

7.1 Introduction

As a basis for the full algebra we adopt the terminology for the exterior algebra $\mathbf{P}(\bigwedge \mathbb{R}^{4*})$ in Sect. 2.3. Consult Fig. 2.3 for an overview of the basis vectors.

Notation. We continue to denote 1-vectors (planes) with bold small Roman letters $\mathbf{a}$; trivectors (points) will be denoted with bold capital Roman letters $\mathbf{P}$; and bivectors will be represented with bold capital Greek letters $\mathbf{\Xi}$.[1]

We begin with a non-metric discussion of bivectors. We work in $\mathbf{P}(\bigwedge \mathsf{V}^*)$, since that is the foundation of the metric. As a result, even readers familiar with bivectors from

[1] A convention apparently introduced by Klein, see [Kle72].

a *point-based* perspective will probably benefit from going through the following *plane-based* development. We begin with an overview of projective properties of bivectors, that is, properties that can be derived from the outer product alone.

7.2 Projective properties of bivectors.

We begin with a simple bivector $\mathbf{\Sigma} := \mathbf{a} \wedge \mathbf{b}$ where $\mathbf{a}$ and $\mathbf{b}$ are two planes with coordinates $\{a_i\}$ and $\{b_i\}$. The resulting bivector has coordinates

$$p_{ij} := a_i b_j - a_j b_i \quad (ij \in \{01, 02, 03, 12, 31, 23\}) \tag{7.1}$$

in $\mathbf{P}(\bigwedge^2 \mathbb{R}^{4*})$. These are the plane-based Plücker coordinates for the intersection line (*axis*) of $\mathbf{a}$ and $\mathbf{b}$. If q^{km} are the point-based coordinates for the same line, then by a well-known result in line geometry (already touched on by our discussion of $\mathbf{J}$ in Sect. 2.3.1.2), there is some non-zero λ such that $q^{km} = \lambda p_{ij}$, for $(ijkm)$ an even permutation of (0123).

A simple calculation yields:

$$\mathbf{\Sigma} \wedge \mathbf{\Sigma} = 2(p_{01}p_{23} + p_{02}p_{31} + p_{03}p_{12})\mathbf{I}$$

By the anti-symmetry of $\wedge$,

$$\mathbf{\Sigma} \wedge \mathbf{\Sigma} = (\mathbf{a} \wedge \mathbf{b}) \wedge (\mathbf{a} \wedge \mathbf{b}) = 0.$$

Conversely, if $\mathbf{\Sigma} \wedge \mathbf{\Sigma} = 0$, the bivector is simple ([Hit03]).

It is sometimes useful to have $\mathbf{\Sigma} \wedge \mathbf{\Phi}$ as a scalar; this is facilitated by the identity:

$$\mathbf{\Sigma} \wedge \mathbf{\Phi} = (\mathbf{\Sigma} \vee \mathbf{\Phi})\mathbf{I} \tag{7.2}$$

Given a second axis $\mathbf{\Phi} = \mathbf{c} \wedge \mathbf{d}$, the condition $\mathbf{\Sigma} \wedge \mathbf{\Phi} = 0$ implies the two lines have a plane in common. (7.2) also implies $\mathbf{\Sigma} \vee \mathbf{\Phi} = 0$, so they also have a point in common. For general bivectors,

$$\mathbf{\Sigma} \wedge \mathbf{\Phi} = (p_{01}q_{23} + p_{02}q_{31} + p_{03}q_{12} + p_{12}q_{03} + p_{31}q_{02} + p_{23}q_{01})\mathbf{I} \tag{7.3}$$

The parenthesized expression is called the Plücker inner product of the two bivectors, and is written $\langle \mathbf{\Sigma}, \mathbf{\Phi} \rangle_P$. With this inner product, the space of bivectors $P(\bigwedge^2(\mathbb{R}^4)^*)$ is the Cayley-Klein space

$$\mathfrak{B} := \mathbf{P}(\mathbb{R}^{3,3}),$$

and the space of lines is the quadric surface

$$\mathcal{L} := \{\mathbf{\Sigma} \mid \mathbf{\Sigma} \wedge \mathbf{\Sigma} = 0\} \subset \mathfrak{B}.$$

$\mathcal{L}$ is sometimes called the *Klein* quadric, or the *Plücker* quadric. It is also the *Grassmann variety* $G_{4,2}$. Note that the natural coordinates for $\mathfrak{B}$ do not yield a diagonal form for

the absolute quadric. They are however generally retained since they are closely tied to the coordinate system of the underlying $\mathbb{R}P^3$. For a discussion of a diagonal basis see Remark 117.

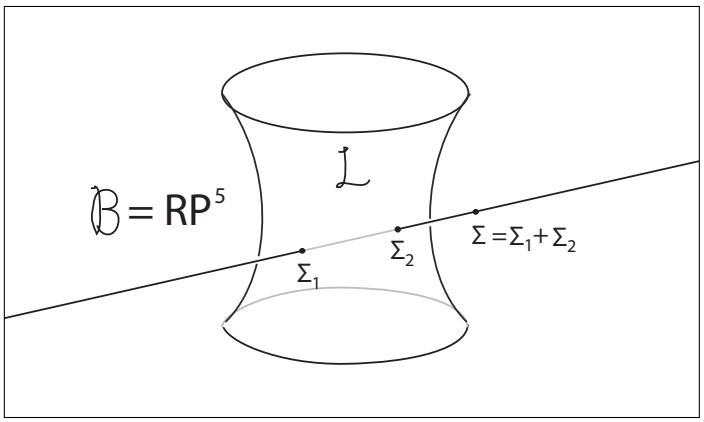

Fig. 7.1 $\mathcal{L}$ is a quadric surface in $\mathfrak{B}$ defined by the quadratic form $\langle , \rangle_P$, the Plücker inner product. A general line in $\mathfrak{B}$ which intersects $\mathcal{L}$ in two points $\mathbf{\Sigma}_1$ and $\mathbf{\Sigma}_2$ has in general no other points in common with the quadric.

Definition 108. Two bivectors $\mathbf{\Sigma}$ and $\mathbf{\Phi}$ are *in involution* when $\mathbf{\Sigma} \wedge \mathbf{\Phi} = 0$, .

For a fixed $\mathbf{\Sigma}$, the orthogonal complement $\{\mathbf{\Phi} \mid \mathbf{\Sigma} \wedge \mathbf{\Phi} = 0\}$ is a 4-dimensional hyperplane of $\mathfrak{B}$ consisting of all bivectors in involution to $\mathbf{\Sigma}$. To prevent confusion later with the orthogonal complement with respect to the metric quadric coming from the Cayley-Klein space in $\mathbb{R}P^3$, we denote the orthogonal complement with respect to the Plücker metric as $\mathbf{\Sigma}^{\vdash}$.

7.2.1 Linear line complexes

The intersection of $\mathbf{\Sigma}^{\vdash}$ with $\mathcal{L}$ is a 3-dimensional quadric submanifold $\mathbf{M}_2^3$ called a *linear line complex*. When $\mathbf{\Sigma}$ is simple, it is called a *special* line complex, and consists of all lines which intersect $\mathbf{\Sigma}$.

7.2.1.1 Pencils of line complexes Two bivectors $\mathbf{\Sigma}$ and $\mathbf{\Phi}$ span a line in $\mathfrak{B}$, called a line complex pencil, or bivector pencil. Points on this line are of the form $\alpha\mathbf{\Sigma} + \beta\mathbf{\Phi}$ for $\alpha, \beta \in \mathbb{R}$, both not 0. Finding the simple bivectors on this line involves solving the following equation in the homogeneous coordinate $\lambda = \alpha : \beta$:

$$0 = (\alpha\mathbf{\Sigma} + \beta\mathbf{\Phi}) \vee (\alpha\mathbf{\Sigma} + \beta\mathbf{\Phi}) \tag{7.4}$$

$$= \alpha^2(\mathbf{\Sigma} \vee \mathbf{\Sigma}) + 2\alpha\beta(\mathbf{\Phi} \vee \mathbf{\Sigma}) + \beta^2(\mathbf{\Phi} \vee \mathbf{\Phi}) \tag{7.5}$$

This equation can be undetermined (when $\mathbf{\Sigma}$ and $\mathbf{\Phi}$ are intersecting lines), or have 0, 1, or 2 real homogeneous roots. See [PW01] for details. Finding the intersection of a bivector pencil with $\mathcal{L}$ is a common procedure in line geometry. It's used below in the discussion of the null polarity, and later to calculate the axes of a non-simple bivector.

7.2.1.2 Null polarity associated to a non-simple bivector Assume that $\mathbf{\Sigma}$ is not simple. Then $\mathbf{\Sigma}$ determines a collineation of $\mathfrak{B}$, the *harmonic homology*:

$$\mathbf{H_\Sigma} : \mathfrak{B} \to \mathfrak{B}$$

with center $\mathbf{\Sigma}$ and axis $\mathbf{\Sigma}^\vdash$ (see Def. 10). It is a reflection of the Cayley-Klein space $\mathfrak{B}$. An element $\mathbf{\Phi}$ of $\mathcal{L}$ is mapped to another element of $\mathcal{L}$ which lies on the line in $\mathfrak{B}$ determined by $\mathbf{\Sigma}$ and $\mathbf{\Phi}$. This is generically a second intersection, distinct from $\mathbf{\Phi}$.

To proceed, we need a theorem relating projectivities of $\mathbb{R}P^3$ and projectivities of $\mathfrak{B}$ preserving $\mathcal{L}$. See [PW01], p. 144, for a proof.

Theorem 109. *The group of projectivities of $\mathbb{R}P^3$ and the group of collineations of $\mathfrak{B}$ preserving $\mathcal{L}$ are isomorphic.*

This result confirms that the harmonic homology $\mathbf{H_\Sigma}$ has an associated projectivity on $\mathbb{R}P^3$, the *null polarity* associated to $\mathbf{\Sigma}$. We use the same symbol to refer to this projectivity. The image $\mathbf{H_\Sigma}(\mathbf{\Phi})$ of a line $\mathbf{\Phi}$ is called the *conjugate* line of $\mathbf{\Phi}$ with respect to the null polarity. By definition of the harmonic homology, this is given by:

$$\mathbf{H_\Sigma}(\mathbf{\Phi}) = -(\mathbf{\Sigma} \vee \mathbf{\Sigma})\mathbf{\Phi} + 2(\mathbf{\Phi} \vee \mathbf{\Sigma})\mathbf{\Sigma}$$

On the other hand, a line complex pencil which includes $\mathbf{\Sigma}$, includes at most two elements of $\mathcal{L}$. These two elements are then conjugate lines with respect to the null polarity of $\mathbf{\Sigma}$. Lines which are equal to their conjugate are called *null* lines. Geometrically, this means the bivector pencil is tangent to the Plücker quadric. These are the members of the linear line complex associated to $\mathbf{\Sigma}$.

How can one identify the null lines in $\mathbb{R}P^3$? For example, which null lines pass through a given point $\mathbf{P}$? Recall $\mathbf{\Sigma}$ is non-simple. Define the null plane of $\mathbf{P}$ as $N_\mathbf{\Sigma}(\mathbf{P}) := \mathbf{\Sigma} \vee \mathbf{P}$. Then $N_\mathbf{\Sigma}(\mathbf{P}) \vee \mathbf{P} = 0$, so $\mathbf{P}$ lies in its own null plane. Also, let $\mathbf{Q}$ be another point of $N_\mathbf{\Sigma}(\mathbf{P})$. Then apply the associativity of the $\vee$ product to obtain:

$$\begin{aligned} 0 = N_\mathbf{\Sigma}(\mathbf{P}) \vee \mathbf{Q} &= (\mathbf{\Sigma} \vee \mathbf{P}) \vee \mathbf{Q} \\ &= \mathbf{\Sigma} \vee (\mathbf{P} \vee \mathbf{Q}) \end{aligned}$$

This shows that the line $\mathbf{P} \vee \mathbf{Q}$ is in involution to $\mathbf{\Sigma}$, hence a null line. Conversely, any null line of $\mathbf{\Sigma}$ passing through $\mathbf{P}$ can be written in the form $\mathbf{P} \vee \mathbf{Q}$, and one can reverse the reasoning to conclude it must lie in $N_\mathbf{\Sigma}(\mathbf{P})$. So the null lines passing through $\mathbf{P}$ are the line pencil determined by $\mathbf{P}$ and its null plane.

When $\mathbf{\Sigma}$ is simple, null plane and points are only defined for points and planes not incident with $\mathbf{\Sigma}$, and $N_\mathbf{\Sigma}$ is not a projectivity.

One can also dualize the discussion to define the *null point* of a plane $N_\mathbf{\Sigma}(\mathbf{a}) := \mathbf{\Sigma} \wedge \mathbf{a}$. See Fig. 7.2. Then $N_\mathbf{\Sigma}(N_\mathbf{\Sigma}(\mathbf{a})) = \mathbf{a}$ by (7.12) , showing that $N_\mathbf{\Sigma}$ is an involution, hence in fact deserves the name null *polarity*. For details see [PW01]. We will encounter the null polarity later in Chapter 8, where it plays a crucial role in kinematics.

7.2.1.3 Subspaces of $\mathfrak{B}$ As remarked above, the Plücker polar of a point $\mathbf{\Sigma}$ in $\mathfrak{B}$ intersects $\mathcal{L}$ in a 3-dimensional quadric submanifold called the linear line complex associ-

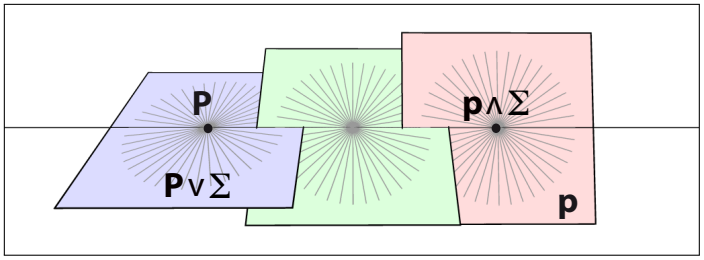

Fig. 7.2 Three null point/plane pairs belonging to a single null line. For a null point/plane pair, $\mathbf{P} = \mathbf{\Sigma} \wedge \mathbf{p}$ and $\mathbf{p} = \mathbf{\Sigma} \vee \mathbf{P}$.

ated to $\mathbf{\Sigma}$. Occasionally $\mathbf{\Sigma}$ itself is referred to as the line complex, but this is technically inprecise.

The Plücker polar of a line $\mathcal{L} \in \mathfrak{B}$ intersects $\mathcal{L}$ in a 2-dimensional quadric submanifold called a line congruence, or congruence for short. This congruence comes in four varieties, depending on the nature of the intersections of $\mathcal{L}$ with $\mathcal{L}$ in (7.5): hyperbolic, parabolic, and elliptic have $(2, 1, 0)$ intersections, resp., with the Plücker quadric. The Plücker polar of a 2-plane is another 2-plane which, generically, intersects $\mathcal{L}$ in a non-degenerate conic section, whose image is $\mathbb{R}P^3$ is a regulus. The degenerate cases are important for a full understanding of line space but exceed the scope of this study.

7.2.1.4 Isotropic subspaces of $\mathfrak{B}$ It is useful to have an understanding of subspaces of $\mathfrak{B}$ lying entirely in $\mathcal{L}$. The simplest example, an isotropic line, corresponds to a line pencil in $\mathbb{R}P^3$. There are two types of isotropic planes, arising from line bundles (all the lines through a point) and line fields (all the lines in a plane) in $\mathbb{R}P^3$. These are usually referred to as α-planes and β-planes, resp. Two planes of the same type intersect in a point; two such planes of differing types intersect in a line, when they are incident in $\mathbb{R}P^3$, or not at all.

With these remarks we close our discussion of the projective properties of bivectors and the associated null polarities.

7.3 Description of the algebras Cl^3_κ

We now proceed to a description of the metric-related features of these 3D algebras, focusing on the new features related to bivectors. We intersperse metric-specific discussions more frequently than in Chapter 6.

We leave the construction of a multiplication table analogous to Table 6.1 as an exercise. As in the two-dimensional case, most of the geometric products of a basis k- and m-vector obey the pattern $AB = A \cdot B + A \wedge B$. Two new exceptions involve the product of a bivector with another bivector, and with a trivector:

$$\mathbf{\Xi\Phi} = \mathbf{\Xi} \cdot \mathbf{\Phi} + \mathbf{\Xi} \times \mathbf{\Phi} + \mathbf{\Xi} \wedge \mathbf{\Phi} \tag{7.6}$$

$$\mathbf{\Xi P} = \mathbf{\Xi} \cdot \mathbf{P} + \mathbf{\Xi} \times \mathbf{P} \tag{7.7}$$

Here, as before, the commutator product $A \times B := \frac{1}{2}(AB - BA)$.

7.3.1 Metric-neutral enumeration of geometric product

All the products described in 6.1.1 have counter-parts here, obtained by leaving points alone and replacing lines by planes. For example, the statement from Sect. 6.1.1:

> $\mathbf{a} \cdot \mathbf{b}$ has different interpretations, depending on whether the two lines intersect in a proper, ideal, or improper point. For normalized lines $\mathbf{a}$ and $\mathbf{b}$ that intersect in a proper point with angle α, $\mathbf{a} \cdot \mathbf{b} = \cos(\alpha)$.

remains true for $n = 3$ when "line" is replaced by "plane", and "point" is replaced by "line":

> $\mathbf{a} \cdot \mathbf{b}$ has different interpretations, depending on whether the two planes intersect in a proper, ideal, or improper line. For normalized planes $\mathbf{a}$ and $\mathbf{b}$ that intersect in a proper line with angle α, $\mathbf{a} \cdot \mathbf{b} = \cos(\alpha)$.

Here we focus on the task of enumerating the products that involve bivectors. For that purpose, we extend the definition of $\mathbf{a}$,$\mathbf{b}$, $\mathbf{P}$, and $\mathbf{Q}$ to have an extra coordinate, and introduce two arbitrary bivectors, which may or may not be simple:

$$\begin{aligned}\boldsymbol{\Xi} &:= p_{01}\mathbf{e}_{01} + p_{02}\mathbf{e}_{02} + p_{03}\mathbf{e}_{03} + p_{12}\mathbf{e}_{12} + p_{31}\mathbf{e}_{31} + p_{23}\mathbf{e}_{23} \\ \boldsymbol{\Phi} &:= g_{01}\mathbf{e}_{01} + g_{02}\mathbf{e}_{02} + g_{03}\mathbf{e}_{03} + g_{12}\mathbf{e}_{12} + g_{31}\mathbf{e}_{31} + g_{23}\mathbf{e}_{23}\end{aligned}$$

See metric-specific discussions which follow for details of the following properties.

1. **Inner product.**

$$\boldsymbol{\Xi} \cdot \boldsymbol{\Phi} = -(p_{12}g_{12} + p_{31}g_{13} + p_{23}g_{23} + \kappa(p_{01}g_{01} + p_{02}g_{02} + p_{03}g_{03})) \tag{7.8}$$

   $\boldsymbol{\Xi}\cdot\boldsymbol{\Phi}$ is a symmetric bilinear form on bivectors, called the *Killing* form.[2] We sometimes write $\boldsymbol{\Xi} \cdot \boldsymbol{\Phi} = \langle \boldsymbol{\Xi}, \boldsymbol{\Phi} \rangle_K$. We call a bivector *ideal* if $\boldsymbol{\Xi} \cdot \boldsymbol{\Xi} = 0$, and *proper* if $\boldsymbol{\Xi}^2 < 0$, and *improper* if $\boldsymbol{\Xi}^2 > 0$. The latter occurs only for $\kappa = -1$.

2. **Norm.** Define the norm as before $\|\boldsymbol{\Xi}\| = \sqrt{|\boldsymbol{\Xi} \cdot \boldsymbol{\Xi}|}$. Then for non-ideal $\boldsymbol{\Xi}$, $\dfrac{\boldsymbol{\Xi}}{\|\boldsymbol{\Xi}\|}$ has norm 1; we call it a normalized bivector.

3. **Inverses.** For non-ideal $\boldsymbol{\Xi}$, define $\boldsymbol{\Xi}^{-1} = \dfrac{\boldsymbol{\Xi}}{\boldsymbol{\Xi} \cdot \boldsymbol{\Xi}}$. Inverses are unique.

4. The square of a bivector consists of a scalar and a pseudoscalar:

$$\begin{aligned}\boldsymbol{\Xi}^2 &= \langle \boldsymbol{\Xi}^2 \rangle_0 + \langle \boldsymbol{\Xi}^2 \rangle_4 \\ &= \boldsymbol{\Xi} \cdot \boldsymbol{\Xi} + \boldsymbol{\Xi} \wedge \boldsymbol{\Xi}\end{aligned}$$

   Sect. 7.6 studies the sub-algebra $Cl^{3\dagger}_\kappa$ of such elements, which play a key role in handling non-simple bivectors.

[2] This inner product is well-known for its role in the classification of Lie algebras. The connection to its appearance here will become clear once we establish that the bivectors form the Lie algebra of the isometry group of the Cayley-Klein space below.

5. $\boldsymbol{\Xi} \wedge \boldsymbol{\Phi} = (\boldsymbol{\Xi} \vee \boldsymbol{\Phi})\mathbf{I} = \langle \boldsymbol{\Xi}, \boldsymbol{\Phi} \rangle_P \mathbf{I}$ is the Plücker inner product times $\mathbf{I}$. When $\boldsymbol{\Xi}$ and $\boldsymbol{\Phi}$ are simple, the magnitude of this product is proportional to the distance of the two lines. See metric-specific discussions below.
6. **Commutator.** $\boldsymbol{\Xi} \times \boldsymbol{\Phi}$ is a bivector which is in involution to both $\boldsymbol{\Xi}$ and $\boldsymbol{\Phi}$ (Exercise). We'll meet this later in the discussion of kinematics (Chapter 8) as the Lie bracket.
7. **Null point.** $\mathbf{a} \wedge \boldsymbol{\Xi}$, for simple $\boldsymbol{\Xi}$, is the intersection point of $\boldsymbol{\Xi}$ with the plane $\mathbf{a}$, or 0 if they are incident; in general it's the *null point* of the plane with respect to $\boldsymbol{\Xi}$.
8. **Null plane.** $\mathbf{P} \vee \boldsymbol{\Xi}$, for simple $\boldsymbol{\Xi}$, is the joining plane of $\mathbf{P}$ and $\boldsymbol{\Xi}$, or 0 if they are incident; in general it's the *null plane* of the point with respect to $\boldsymbol{\Xi}$.
9. $\mathbf{P} \cdot \boldsymbol{\Xi}$, for simple $\boldsymbol{\Xi}$, is a plane passing through $\mathbf{P}$ perpendicular to $\boldsymbol{\Xi}$.
10. $\mathbf{P} \times \boldsymbol{\Xi}$, for simple $\boldsymbol{\Xi}$, is a point orthogonal to the plane through $\mathbf{P}$ and $\boldsymbol{\Xi}$. For the euclidean metric, this is naturally an ideal point.
11. $\mathbf{a} \cdot \boldsymbol{\Xi}$, for simple $\boldsymbol{\Xi}$, is a plane containing $\boldsymbol{\Xi}$ whose intersection with $\mathbf{a}$ is perpendicular to $\boldsymbol{\Xi}$.
12. Applying the metric polarity to a bivector $\boldsymbol{\Xi}$ yields:

$$\boldsymbol{\Xi}^\perp = \boldsymbol{\Xi}\mathbf{I} = p_{23}\mathbf{e}_{01} + p_{31}\mathbf{e}_{02} + p_{12}\mathbf{e}_{03} + \kappa(p_{03}\mathbf{e}_{12} + p_{02}\mathbf{e}_{31} + p_{01}\mathbf{e}_{23}) \tag{7.9}$$

This is the polar bivector of $\boldsymbol{\Xi}$ with respect to the metric quadric. Note that here we **do** use the standard notation $\boldsymbol{\Xi}^\perp$ to denote the polar line. The bivector pencil spanned by $\boldsymbol{\Xi}$ and $\boldsymbol{\Xi}^\perp$ plays an important role in Sect. 7.7 below.

7.3.1.1 Examples

1. The products $\mathbf{a} \cdot \mathbf{b}, \mathbf{P} \cdot \mathbf{Q}, \mathbf{a} \wedge \mathbf{P}, \mathbf{a} \cdot \mathbf{P}, \mathbf{P} \vee \mathbf{Q}, \mathbf{P} \times \mathbf{Q}, \mathbf{aI}, \mathbf{PI}$ from Sect. 6.1.1 can be translated to 3D using the method described at the beginning of Sect. 7.3.1. The definition of norm to points and planes can also be easily translated into 3D.
2. Many of the products in Sect. 7.3.1 are described only for simple $\boldsymbol{\Xi}$. It is a non-trivial question, what the analogous statements are for non-simple $\boldsymbol{\Xi}$.
3. The inner and outer products are both symmetric bilinear forms in their arguments. They are related via the metric polarity: $\boldsymbol{\Xi} \cdot \boldsymbol{\Phi} = \boldsymbol{\Xi} \vee \boldsymbol{\Phi}\mathbf{I} = \boldsymbol{\Xi}\mathbf{I} \vee \boldsymbol{\Phi}$.
4. In a Cayley-Klein geometry, the intersection of two proper planes is a proper line, and every proper line arises in this way. One can use the fact that $\mathbf{a}^2 > 0$ for a proper plane, and that $\mathbf{e}_i\mathbf{e}_j = -\mathbf{e}_j\mathbf{e}_i$ to show that the definition of a proper line above is consistent with this behavior.
5. **Orthogonal projection.** Here we investigate orthogonal projections involving lines. Not only can one project points onto lines, but lines can also be projected onto points. To be more precise: One can project points onto spears, and axes onto bundles. For simplicity we have replaced $\mathbf{X}^{-1}$ by $\mathbf{X}$ without effecting the validity of the result, *qua* subspace.

   a. **Projecting a point onto a line, and *vice-versa*.** For proper $\mathbf{P}$ and proper simple $\boldsymbol{\Pi}$, $\mathbf{p} := \mathbf{P} \cdot \boldsymbol{\Pi}$ is the unique plane of $\mathbf{P}$ perpendicular to $\boldsymbol{\Pi}$, and $\mathbf{p}\boldsymbol{\Pi}$ is the intersection of this plane with $\boldsymbol{\Pi}$: the orthogonal projection of $\mathbf{P}$ on $\boldsymbol{\Pi}$. Furthermore, $\mathbf{p}\boldsymbol{\Pi} \vee \mathbf{P}$ is the unique line through $\mathbf{P}$ intersecting $\boldsymbol{\Pi}$ at right angles.[3]

[3] Compare the brevity of this expression with Section 11.9 of [DFM07].

See Fig. 7.3. **pP**, on the other hand, is the unique line of **P** perpendicular to **p**. It meets **Π** at $\mathbf{p}^\perp$.

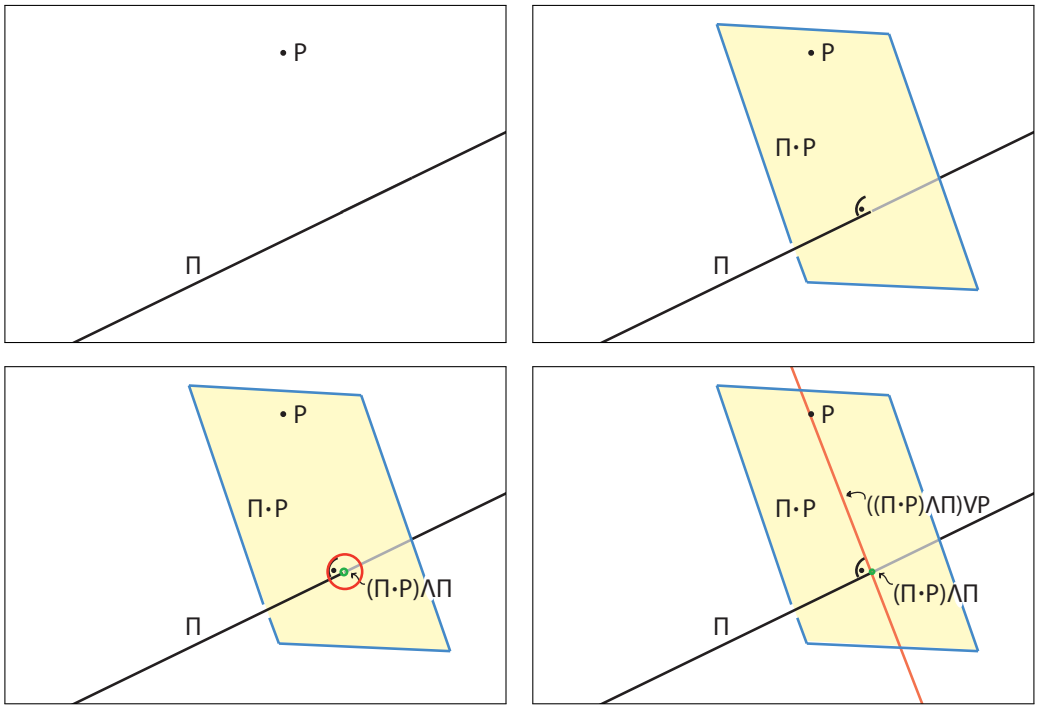

Fig. 7.3 Step-by-step construction of the unique perpendicular through the point **P** to the line **Π**. First (upper right) $\mathbf{\Pi}\cdot\mathbf{P}$ is the perpendicular plane to **Π** passing through **P**. Then (lower left) wedging this plane with **Π** gives the intersection point with **Π**, and finally (lower right) joining this to **P** gives the desired line.

b. **Projecting a line onto a plane, and *vice-versa*** For proper **a** and simple **Π**, $\mathbf{p} := \mathbf{\Pi}\cdot\mathbf{a}$ is the unique plane of **Π** perpendicular to **a**. **pa** is the orthogonal projection of **Π** onto **a**. **pΠ** is the plane of **Π** perpendicular to **p**. $\mathbf{p\Pi}\wedge\mathbf{a}$ is the unique line of **a** perpendicular to **Π**.

6. **Intersection and join of two lines.** Assume $\mathbf{\Xi}\wedge\mathbf{\Phi}=0$ for simple bivectors **Ξ** and **Φ**, with $\mathbf{\Xi}\neq\mathbf{\Phi}$. For a point **P** not in the plane spanned by **Ξ** and **Φ**, $\mathbf{\Xi}\wedge(\mathbf{\Phi}\vee\mathbf{P})$ is the common point. For a plane **a** not passing through the common point, $\mathbf{\Xi}\vee(\mathbf{\Phi}\wedge\mathbf{a})$ is the common plane of the two lines. With probability 1, one can obtain such a **P** (**a**) by choosing a random point (plane). Can you find a reliable way to obtain such a **P** and such a **a**?
7. **Incidence of point and line.** A point **P** lies on the simple bivector **Ξ** $\iff$ $\mathbf{P}\vee\mathbf{\Xi}=0$. One can use (7.13) above to show this is equivalent to $\mathbf{P}\times\mathbf{\Xi}=0$. In both cases the formulas are valid also for non-simple **Ξ**, since, for non-simple **Ξ**, neither expression can vanish.

8. The following identities involving involving general bivectors, and a 3-vector $\mathbf{P}$ are useful for what follows, and can be verified by direct calculation (in the next-to-last one, $\mathbf{P}$ is proper normalized):

$$(\mathbf{\Xi} \times \mathbf{\Phi}) \wedge \mathbf{\Xi} = 0 \tag{7.10}$$
$$\mathbf{\Xi I} \vee \mathbf{\Phi} = \mathbf{\Xi} \vee (\mathbf{\Phi I}) = \mathbf{\Xi} \cdot \mathbf{\Phi} \tag{7.11}$$
$$-2\mathbf{\Xi} \wedge (\mathbf{\Xi} \vee \mathbf{P}) = (\mathbf{\Xi} \vee \mathbf{\Xi})\mathbf{P} \tag{7.12}$$
$$\mathbf{\Xi} \times \mathbf{P} = (\mathbf{\Xi} \vee \mathbf{P})\mathbf{I} \tag{7.13}$$
$$2\mathbf{P} \times (\mathbf{\Xi} \times \mathbf{P}) = \mathbf{P\Xi P} - \mathbf{P}^2\mathbf{\Xi} \tag{7.14}$$
$$\mathbf{P} \cdot (\mathbf{\Xi} \times \mathbf{P}) = 0 \tag{7.15}$$

7.4 Metric-specific remarks

7.4.1 Elliptic

All planes, lines, and points of $\mathbb{R}P^3$ are proper elements of elliptic space. As a result, elliptic space exhibits a simplicity and symmetry unmatched by the other spaces under consideration. In particular, elliptic 3-space contains interesting geometric structures which have fascinated mathematicians since they were first reported by Clifford [Cli82c]. We discuss them here since they appear below in Sect. 7.7.2, and the theme is intimately connected to the genesis of Clifford algebras.

7.4.1.1 Clifford parallels In analogy to euclidean parallels, Clifford parallels are elliptic lines which have infinitely many common normals, one through each point, and the distance between the two parallels measured along these normals is constant. However, in contrast to euclidean parallels, which meet in an ideal point, Clifford parallels don't meet, in fact, they have linking number one as topological circles. In contrast to the euclidean case, through a given point not on a line, there are exactly two Clifford parallels to the given line. One is a *left* Clifford parallel, the other, a *right* Clifford parallel. The set of left (right) Clifford parallels to a given line form an *elliptic line congruence*, see above, Sect. 7.2.1.3. The set of Clifford left parallels at a given distance to a given line form a regulus; the set of right parallels at the same distance forms the complementary regulus. Such a regulus is called a *Clifford torus* and is interesting since it has gaussian curvature 0: it is a euclidean torus embedded in elliptic space.

Each set of Clifford parallels determines a 1-parameter family of isometries of elliptic space which map each such parallel line to itself. In this respect they are like euclidean translations. Such a translation of elliptic space is called a (left or right) *Clifford translation*. Representing the points of elliptic space as unit quaternions, already Cayley showed such a translation along a set of left (right) parallels can be implemented by left (right) multiplication by a unit quaternion. We take up this theme again in Sect. 7.11.1 below, where we show how these translations appear in $\mathbf{Spin}^3_{+1}$.

7.4.2 Hyperbolic

The proper points of hyperbolic space form the interior of the unit ball. The ideal points are the unit sphere, sometimes called the ideal sphere. Lines and planes are ideal if they are tangent to the ideal sphere. Improper points, lines, and planes lie outside the ideal sphere. The polar of a proper element is improper. In particular, the polar of a proper bivector $\mathbf{\Xi}$ is improper. The polar of an ideal element is again ideal. Table 7.1 shows how to identify the type of a hyperbolic element from the sign of its square:

X	proper	ideal	improper
plane	+	0	-
line	-	0	+
point	-	0	+

Table 7.1 Sign of $\mathbf{X}^2$ for hyperbolic space.

7.4.2.1 Ideal norm of ideal elements One can also introduce a normalization for ideal elements in the hyperbolic case. For example, for an ideal point $\mathbf{V}$, define

$$\|\mathbf{V}\|_\infty := \|\mathbf{V} \vee \mathbf{E}_0\|$$

This effectively yields the euclidean vector norm of the direction vector represented by $\mathbf{V}$ (ignoring the w-coordinate). Similarly for an ideal plane $\|\mathbf{a}\|_\infty := \|\mathbf{a} \wedge \mathbf{e}_0\|$. For an ideal line $\mathbf{\Xi}$,

$$\|\mathbf{\Xi}\|_\infty := \|\mathbf{\Xi} \wedge \mathbf{e}_0\| = \sqrt{q_{12}^2 + q_{31}^2 + q_{23}^2} \quad (= \sqrt{q_{01}^2 + q_{02}^2 + q_{03}^2})$$

The term in parentheses follows from the condition that it is an ideal line. Such norms are useful in order to normalize ideal elements to be "the same size". We use them below in defining logarithms of rotors involving ideal bivectors in Sect. 6.3.2.1.

7.4.3 Euclidean

$\mathbf{e}_0$ now represents the ideal *plane* of space, the other basis vectors represent the coordinate planes. $\mathbf{E}_0$ is the origin of space while $\mathbf{E}_1 = \mathbf{e}_0\mathbf{e}_3\mathbf{e}_2$ is the ideal point in the x-direction, similarly for $\mathbf{E}_2$ and $\mathbf{E}_3$. The bivector $\mathbf{e}_{01}$ is the ideal line in the $x = 0$ plane, and similarly for $\mathbf{e}_{02}$ and $\mathbf{e}_{03}$. $\mathbf{e}_{23}, \mathbf{e}_{31}$, and $\mathbf{e}_{12}$ are the x-, y-, and z-axis, resp. We use $\mathbf{i}$ again to denote the embedding of euclidean points, lines, and planes, from $\mathbb{R}P^3$ into the Clifford algebra.

7.4.3.1 Ideal norm of Ideal elements. The ideal points of euclidean space consist of points lying in $\mathbf{e}_0$, points of the form $x\mathbf{e}_1 + y\mathbf{e}_2 + z\mathbf{e}_3$. As in the 2D case, we can obtain the familiar euclidean vector norm for an ideal point by the expression $\|\mathbf{V}\|_\infty := \|\mathbf{V} \vee \mathbf{P}\|$, where $\mathbf{P}$ is **any** normalized euclidean point. We also obtain a similar norm on an ideal

line $\boldsymbol{\Xi}$ by joining the line with *any* normalized euclidean point $\mathbf{P}$, and taking the norm of the plane: $\|\boldsymbol{\Xi}\|_\infty = \|\boldsymbol{\Xi} \vee \mathbf{P}\|$. We normalize ideal bivectors with respect to this norm. We call this the *secondary* norm on these elements.

7.4.3.2 A euclidean decomposition of bivectors There is a convenient decomposition of bivectors based on the ideal plane of euclidean space. Write the bivector $\boldsymbol{\Xi}$ as the sum of two simple bivectors $\boldsymbol{\Xi} = \boldsymbol{\Xi}_\infty + \boldsymbol{\Xi}_o$:

$$\begin{aligned}\boldsymbol{\Xi}_\infty &:= p_{01}\mathbf{e}_{01} + p_{02}\mathbf{e}_{02} + p_{03}\mathbf{e}_{03}\\ \boldsymbol{\Xi}_o &:= p_{12}\mathbf{e}_{12} + p_{31}\mathbf{e}_{31} + p_{23}\mathbf{e}_{23}\end{aligned}$$

This is the unique decomposition of $\boldsymbol{\Xi}$ as the sum of a line lying in the ideal plane ($\boldsymbol{\Xi}_\infty$) and a euclidean part ($\boldsymbol{\Xi}_o$). It is sometimes useful to write $\boldsymbol{\Xi} = (\boldsymbol{\Xi}_\infty; \boldsymbol{\Xi}_o)$. This decomposition is useful in characterizing the simple bivectors:

$$\boldsymbol{\Xi}_o \wedge \boldsymbol{\Xi}_\infty = 0 \iff \boldsymbol{\Xi}_o \vee \boldsymbol{\Xi}_\infty = 0 \iff \boldsymbol{\Xi} \text{ is simple.}$$

We say a bivector is *ideal* if $\boldsymbol{\Xi}_o = 0$, otherwise it is *euclidean*. $\boldsymbol{\Xi}_o$ is a line through the origin, whose direction is given by the ideal point $\mathbf{N}_{\boldsymbol{\Xi}} := -\mathbf{e}_0\boldsymbol{\Xi}_o = p_{23}\mathbf{E}_1 + p_{31}\mathbf{E}_2 + p_{12}\mathbf{E}_3$. We call $\mathbf{N}_{\boldsymbol{\Xi}}$ the *direction vector* of the bivector. For simple $\boldsymbol{\Xi}$, $\boldsymbol{\Xi} \wedge \mathbf{N}_{\boldsymbol{\Xi}} = 0$: the direction vector lies on the line. The following identities can be easily verified:

1. $\boldsymbol{\Xi} \wedge \boldsymbol{\Phi} = \boldsymbol{\Xi}_\infty \wedge \boldsymbol{\Phi}_o + \boldsymbol{\Xi}_o \wedge \boldsymbol{\Phi}_\infty$.
2. $\boldsymbol{\Xi} \times \boldsymbol{\Phi} = (\boldsymbol{\Xi}_\infty \times \boldsymbol{\Phi}_o + \boldsymbol{\Xi}_o \times \boldsymbol{\Phi}_\infty; \boldsymbol{\Xi}_o \times \boldsymbol{\Phi}_o)$.
3. $\boldsymbol{\Xi} \cdot \boldsymbol{\Phi} = \boldsymbol{\Xi}_o \cdot \boldsymbol{\Phi}_o$.
4. $\boldsymbol{\Xi}$ is simple $\iff \boldsymbol{\Xi}_\infty \wedge \boldsymbol{\Xi}_o = 0$.
5. $\mathbf{N}_{\boldsymbol{\Xi}} = -\mathbf{e}_0\boldsymbol{\Xi}$.
6. $\mathbf{e}_0\boldsymbol{\Xi}_o \vee \mathbf{E}_0 = \boldsymbol{\Xi}_o$.

Remark 110. This decomposition is widely used in the literature on euclidean line geometry, where the Plücker line coordinates are arranged as a pair of ordinary 3-vectors $(\mathbf{l}, \mathbf{l}')$. Due to our dual construction, $\mathbf{l}$ corresponds to our $\boldsymbol{\Xi}_o$ and $\mathbf{l}'$, traditionally called the *moment* of the line with respect to the origin, corresponds to $\boldsymbol{\Xi}_\infty$. The geometric product of two lines is then pieced together via ordinary inner and cross products operations these 3-vectors, as indicated in the list above.

Invariance properties. This decomposition is interesting due to its invariance properties with respect to euclidean translations. First, consider the case of a line passing through the origin $\mathbf{E}_0$. Then $\boldsymbol{\Xi} = \mathbf{E}_0 \vee \mathbf{N}$ where $\mathbf{N}$ can be assumed to be ideal. Note that $\boldsymbol{\Xi} = \boldsymbol{\Xi}_o$ in this case. Let $\mathbf{T}$ be the ideal point representing a translation vector. Then the image of $\boldsymbol{\Xi}$ under this translation is:

$$\begin{aligned}\boldsymbol{\Xi}_T &= (\mathbf{E}_0 + \mathbf{T}) \vee \mathbf{N} && (7.16)\\ &= \boldsymbol{\Xi} + \mathbf{T} \vee \mathbf{N} && (7.17)\\ &= (\mathbf{T} \vee \mathbf{N}\ ;\ \boldsymbol{\Xi}_o) && (7.18)\end{aligned}$$

where we have used the fact that ideal points are invariant under translations, and that the join of two ideal points is an ideal line ($\mathbf{T} \vee \mathbf{N}$). Since any line is the translation of a

line through the origin, this shows that $\mathbf{\Xi}_o$ is invariant under translations, while $\mathbf{\Xi}_\infty$ is not.

We can be more precise.

Theorem 111. *Two simple bivectors $\mathbf{\Xi}$ and $\mathbf{\Phi}$ are parallel when $\mathbf{\Xi}_o \equiv \mathbf{\Phi}_o$. In this case, let $\mathbf{P}_{\mathbf{\Xi}}$ and $\mathbf{P}_{\mathbf{\Phi}}$ be two normalized euclidean points on $\mathbf{\Xi}$ and $\mathbf{\Phi}$, resp. Then $\mathbf{\Xi} - \mathbf{\Phi} = \mathbf{N}_{\mathbf{\Xi}} \vee (\mathbf{P}_{\mathbf{\Xi}} - \mathbf{P}_{\mathbf{\Phi}})$ and is, moreover, an ideal line.*

Proof. The two lines intersect in $\mathbf{N}_{\mathbf{\Xi}}$, an ideal point, hence are parallel. Then $\mathbf{\Xi} = \mathbf{N}_{\mathbf{\Xi}} \vee \mathbf{P}_{\mathbf{\Xi}}$ and $\mathbf{\Phi} = \mathbf{N}_{\mathbf{\Xi}} \vee \mathbf{P}_{\mathbf{\Phi}}$. The desired equality follows directly. $\mathbf{\Xi} - \mathbf{\Phi}$ is ideal since both factors of the $\vee$ are ideal.

7.4.3.3 Examples

1. **Relationships of lines.** In this exercise, both $\mathbf{\Xi}$ and $\mathbf{\Phi}$ are normed euclidean simple bivectors.

   a. **Distance between lines.** For normalized $\mathbf{\Xi}$ and $\mathbf{\Phi}$, $\mathbf{\Xi} \wedge \mathbf{\Phi} = \sin(\alpha) d_{\mathbf{\Xi}\mathbf{\Phi}}$, where $d_{\mathbf{\Xi}\mathbf{\Phi}}$ is the euclidean distance between the two lines, and α is the angle between their two direction vectors. This can be seen by considering the tetrahedron spanned by unit vectors on $\mathbf{\Xi}$ and $\mathbf{\Phi}$.]

   b. **Dual norm and dual angle.** Define the *dual norm* $\|\mathbf{\Xi}\|_d := \langle \mathbf{\Xi} \rangle_0 + \langle \mathbf{\Xi} \rangle_4$. Then $\|\mathbf{\Xi}\mathbf{\Phi}\|_d = 0 \iff \mathbf{\Xi}$ and $\mathbf{\Phi}$ intersect at right angles. In general,

   $$\|\mathbf{\Xi}\mathbf{\Phi}\|_d = \pm(\cos(\alpha) - \sin(\alpha) d_{\mathbf{\Xi}\mathbf{\Phi}} \mathbf{I}$$

   where α is the angle between the direction vectors of $\mathbf{\Xi}$ and $\mathbf{\Phi}$. This is called the *dual angle* of $\mathbf{\Xi}$ and $\mathbf{\Phi}$ and measures both the angle between the directions **and** the distance between the lines.

7.5 The structure of Cl^3_κ

The remainder of the chapter focuses on the representation of isometries in Cl^3_κ. The presentation is roughly similar to that of Cl^2_κ, but is complicated by the presence of non-simple bivectors. In order to develop tools to overcome these complications, one must take advantage of the more differentiated structure of the Clifford algebra.

Fig. 7.4 repeats with Fig. 5.2 with the addition of historical labels specific to dimension 3. The even subalgebra Cl^{3+}_κ is isomorphic to the *biquaternions* introduced by Clifford and studied exhaustively by Study in [Stu03]. As we will also see below, the key for this analysis is provided by the sub-algebra $Cl^{3\dagger}_\kappa$, which are studied in Sect. 7.6, and whose elements are known as *Study numbers*.

The key result of the following discussion can be stated as: *Every bivector can be factored as the product of a Study number and a simple bivector.* (See Corollary 121 below.) This result forms the basis for a series of geometrical insights into the structure of the individual isometries.

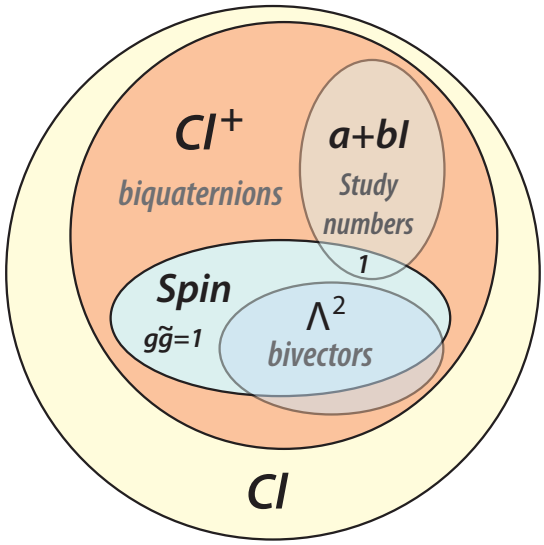

Fig. 7.4 The important sub-algebras and sub-spaces of Cl^3_κ.

7.6 Study numbers

The scalars and pseudoscalars of a Clifford algebra always form a sub-algebra $Cl^{n\dagger}_\kappa$. This sub-algebra plays an important role in calculations in the Clifford algebra. For example, the square of a bivector $\boldsymbol{\Xi}$ in Cl^3_κ is of this form: $\boldsymbol{\Xi}^2 = \boldsymbol{\Xi}\cdot\boldsymbol{\Xi} + \boldsymbol{\Xi}\wedge\boldsymbol{\Xi}$. An element of $Cl^{3\dagger}_\kappa$ we call a *Study number* .

Study introduced Study numbers in ([Stu03]). Instead of $\mathbf{I}$, he used ϵ to specify the extra unit. His biquaternion algebra $\mathbb{B}$ consisted of the 8 units:

$$1, \mathbf{i}, \mathbf{j}, \mathbf{k}, \epsilon, \epsilon\mathbf{i}, \epsilon\mathbf{j}, \epsilon\mathbf{k}$$

Define a map $\phi : \mathbb{B} \to Cl^{3+}_\kappa$ by:

$$\phi(1) := 1;\ \phi(\mathbf{i}) := \mathbf{e}_{12};\ \phi(\mathbf{j}) := \mathbf{e}_{31};\ \phi(\mathbf{k}) := \mathbf{e}_{23};$$
$$\phi(\epsilon) := \mathbf{I};\ \phi(\epsilon\mathbf{i}) := \mathbf{e}_{03};\ \phi(\epsilon\mathbf{j}) := \mathbf{e}_{02};\ \phi(\epsilon\mathbf{k}) := \mathbf{e}_{01};$$

and extend by linearity. Then it is straightforward to verify that ϕ is an isomorphism of $\mathbb{B}$ with Cl^{3+}_κ. Further examination of the connection between ϵ and $\mathbf{I}$ would lead beyond the scope of this work.

Remark 112. **Terminology alert..** Study originally used the term *dual* numbers to describe numbers of the form $a + b\epsilon$, without specializing a specific value for ϵ^2. Blaschke ([Bla42]), following Study, confirms this; he refers to numbers for the elliptic case satisfying $\epsilon^2 = 1$ as dual numbers. Only relatively recently in the modern literature (see for example [PW01]) has the definition of dual number begun to be restricted to the case

$\epsilon^2 = 0$. In order to avoid conflicts with this modern usage, we have chosen to introduce the term Study numbers to refer to the metric-neutral form, in honor of their inventor.

When $\mathbf{I}^2 = -1$, the Study numbers are isomorphic to the *complex* numbers; when $\mathbf{I}^2 = 1$, to the *Clifford* numbers; and when $\mathbf{I}^2 = 0$, to the *dual* numbers. There is a certain amount of terminology common to all three cases which we introduce now; metric-specific features will be discussed below. Use of the term *Study number* in the following list is always assumes a particular choice of $\mathbf{I}^2$. It turns out that many calculations in Cl^3_κ can be effectively solved with the aid of Study numbers. We proceed to derive the necessary facts.

- **Center** Elements of $Cl^{3\dagger}_\kappa$ commute with other elements of Cl^{3+}_κ: they form the *center* of Cl^{3+}_κ.
- **Conjugate.** Define the *conjugate* $\overline{\mathbf{z}} = a - b\mathbf{I}$. $\mathbf{z}\overline{\mathbf{z}} = a^2 - \mathbf{I}^2 b^2 \in \mathbb{R}$.
- **Norm.** Define the *norm* $\|\mathbf{z}\| := \sqrt{|\mathbf{z}\overline{\mathbf{z}}|}$. A Study number $\mathbf{z}$ is said to be *ideal* if $\|\mathbf{z}\| = 0$.
- **Normed.** For non-ideal $\mathbf{z}$, define the $\mathbf{z}_N = \dfrac{\mathbf{z}}{\|\mathbf{z}\|}$. $\mathbf{z}_N$ is a real multiple of $\mathbf{Z}$ that has norm ± 1.
- **Inverse.** For non-ideal $\mathbf{z}$, define the *inverse* $\mathbf{z}^{-1} = \dfrac{\overline{\mathbf{z}}}{\mathbf{z}\overline{\mathbf{z}}}$. The inverse is the unique Study number $\mathbf{w}$ such that $\mathbf{z}\mathbf{w} = 1$.
- **Square root.** Almost always, square roots of Study numbers exist. Let $\mathbf{z} = a + b\mathbf{I}$ be a Study number. Then $\sqrt{\mathbf{z}} = x + y\mathbf{I}$:
  1. $\mathbf{I}^2 = 0$**.** We require $a \neq 0$. Then $x := \sqrt{a}$ and $y := \dfrac{b}{2\sqrt{a}}$.
  2. $\mathbf{I}^2 = 1$**.** We require $a^2 - b^2 \neq 0$. For $a^2 > b^2$, let $r := \sqrt{a^2 - b^2}$. Find θ so that $\mathbf{z} = r(\cosh\theta + \mathbf{I}\sinh\theta)$. Then $x := \sqrt{r}\cosh\frac{\theta}{2}$ and $y := \sqrt{r}\cosh\frac{\theta}{2}$. For $a^2 < b^2$, reverse roles of sinh and cosh.
  3. $\mathbf{I}^2 = -1$**.** Let $r := \sqrt{a^2 + b^2}$. Find θ so that $\mathbf{z} = r(\cos\theta + \mathbf{I}\sin\theta)$. Then $x := \sqrt{r}\cos\frac{\theta}{2}$ and $y := \sqrt{r}\cos\frac{\theta}{2}$.

7.7 The axes of a bivector

Given $\mathbf{g} \in Cl^{3+}_\kappa$. It is easy to show that

$$\mathbf{z} := \mathbf{g}\widetilde{\mathbf{g}}$$

is a Study number $a + b\mathbf{I}$. Define the *Study norm* of $\mathbf{g}$ as

$$\|\mathbf{g}\|_S := c + d\mathbf{I} = \sqrt{\mathbf{z}},$$

when this exists. When, furthermore, the norm is non-zero, it has an inverse, and we can normalize $\mathbf{g}$ with respect to this norm, as follows.

Define

$$\mathbf{g}_N := {\|\mathbf{g}\|_S}^{-1}\mathbf{g}. \tag{7.19}$$

Then $\mathbf{g}_N\widetilde{\mathbf{g}_N} = 1$, since $\|\widetilde{\mathbf{g}}\|_S = \|\mathbf{g}\|_S$.

Now we want to specialize to the case that $\mathbf{g} = \boldsymbol{\Xi}$ is a bivector, with normalized form $\boldsymbol{\Xi}_N$. Then $\boldsymbol{\Xi}_N$ is simple, since $\boldsymbol{\Xi}_N \wedge \boldsymbol{\Xi}_N = 0$. We can rewrite $\boldsymbol{\Xi}_N$ from its definition as:

$$(c + d\mathbf{I})\boldsymbol{\Xi}_N = c\boldsymbol{\Xi}_N + d\boldsymbol{\Xi}_N^{\perp} = \boldsymbol{\Xi} \tag{7.20}$$

(7.20) expresses $\boldsymbol{\Xi}$ as a linear combination of $\boldsymbol{\Xi}_N$ and its polar line $\boldsymbol{\Xi}_N^{\perp}$. This motivates the following definition, whose significance will only become apparent in our study of isometries in Sect. 7.9.

Definition 113. A simple bivector $\boldsymbol{\Phi}$ is called an *axis* of a bivector $\boldsymbol{\Xi}$ if there exists a Study number $\mathbf{z}$ such that $\mathbf{z}\boldsymbol{\Phi} = \boldsymbol{\Xi}$.

If $\boldsymbol{\Xi}$ is simple, then $\boldsymbol{\Xi}$ is an axis of itself.

7.7.1 Euclidean axes

For $\mathbf{I}^2 = 0$, there are two cases. If $\boldsymbol{\Xi}$ is ideal, then it is also simple, hence an axis. Then $\boldsymbol{\Xi} = (\boldsymbol{\Xi}_\infty; 0)$. Let $\boldsymbol{\Theta} = (\boldsymbol{\Theta}_\infty; \boldsymbol{\Theta}_o)$ be a simple euclidean bivector such that $\boldsymbol{\Theta}_o = \boldsymbol{\Xi}_\infty$. Then $\boldsymbol{\Theta}$ is an axis of $\boldsymbol{\Xi}$ since $\boldsymbol{\Theta}\mathbf{I} = \boldsymbol{\Xi}$. So ideal euclidean bivectors have, in addition to themselves, ∞^2 other axes, which constitute a line bundle centered at the ideal point polar to $\boldsymbol{\Xi}$ in the elliptic metric of the ideal plane.

Otherwise, $\boldsymbol{\Xi}$ is proper and $\boldsymbol{\Xi}\mathbf{I}$ is an ideal line called the *secondary axis* of $\boldsymbol{\Xi}$. The secondary axis is not an axis of $\boldsymbol{\Xi}$ since it doesn't satisfy Def. 113. ($\mathbf{z}\boldsymbol{\Phi}\mathbf{I}$ is ideal, but $\boldsymbol{\Xi}$ is not.)

7.7.2 Noneuclidean axes

For $\mathbf{I}^2 \neq 0$: if $\boldsymbol{\Phi}$ is an axis of $\boldsymbol{\Xi}$, then so is its polar line $\boldsymbol{\Phi}\mathbf{I}$, since

$$(\mathbf{z}\mathbf{I}^{-1})(\boldsymbol{\Phi}\mathbf{I}) = \boldsymbol{\Xi}$$

7.7.2.1 Non self-polar bivectors Furthermore, if $\boldsymbol{\Xi}$ satisfies $\boldsymbol{\Xi} \not\equiv \boldsymbol{\Xi}^{\perp}$, we can describe the axes in more detail, since any axis lies in the pencil $\mathcal{L}_{\boldsymbol{\Xi}}$ in $\mathfrak{B}$ determined by $\boldsymbol{\Xi}$ and $\boldsymbol{\Xi}^{\perp}$. For non-simple $\boldsymbol{\Xi}$, $\mathcal{L}_{\boldsymbol{\Xi}}$ contains at most two real intersections with $\mathcal{L}$. If $\boldsymbol{\Xi}$ is simple but proper, it and its polar $\boldsymbol{\Xi}^{\perp}$ are distinct and non-intersecting (as a straightforward evaluation of $(\alpha\boldsymbol{\Xi} + \beta\boldsymbol{\Xi}^{\perp}) \cdot (\gamma\boldsymbol{\Xi} + \delta\boldsymbol{\Xi}^{\perp})$ shows), and the same holds. Otherwise, $\boldsymbol{\Xi}$ is ideal simple, and $\mathcal{L}$ is a line pencil tangent to $\mathbf{Q}$; all its elements are axes of $\boldsymbol{\Xi}$.

In any case, when $\mathcal{L}_{\boldsymbol{\Xi}}$ is well-defined, all bivectors in $\mathcal{L}_{\boldsymbol{\Xi}}$ share the same axes.

7.7.2.2 Self-polar bivectors: Clifford bivectors This leaves the case that $\boldsymbol{\Xi} \equiv \boldsymbol{\Xi}^{\perp}$. Examination of the possibilities for $\mathbf{I}$ show that this can only happen if $\mathbf{I}^2 = 1$. Then any bivector of the form

$$\boldsymbol{\Xi} = (x\mathbf{e}_{01} + y\mathbf{e}_{02} + z\mathbf{e}_{03}) \pm (z\mathbf{e}_{12} + y\mathbf{e}_{31} + x\mathbf{e}_{23})$$

satisfies $\boldsymbol{\Xi} \equiv \boldsymbol{\Xi}^\perp$. Hence $\boldsymbol{\Xi}$ and $\boldsymbol{\Xi}^\perp$ do not determine a line in $\mathfrak{B}$. In fact, such bivectors have many axes. For, let $\boldsymbol{\Phi}$ be any bivector of the form

$$\boldsymbol{\Phi} = (a\mathbf{e}_{01} + b\mathbf{e}_{02} + c\mathbf{e}_{03}) \pm ((z-c)\mathbf{e}_{12} + (y-b)\mathbf{e}_{31} + (x-a)\mathbf{e}_{23})$$

Clearly, $\boldsymbol{\Phi}$ belongs to a 3-dimensional linear subspace of $\mathfrak{B}$ parametrized by the 3 values (a, b, c), and its intersection with $\mathcal{L}$ is a 2-dimensional manifold. Assume then that $\boldsymbol{\Phi}$ lies in this submanifold, hence is simple. Since by construction

$$(1 \pm \mathbf{I})\boldsymbol{\Phi} = \boldsymbol{\Xi}$$

$\boldsymbol{\Phi}$ fulfils the condition of Def. 113. This motivates the following definition:

Definition 114. A *left Clifford bivector* $\boldsymbol{\Xi}$ is an elliptic bivector satisfying $\boldsymbol{\Xi}\mathbf{I} = -\boldsymbol{\Xi}$; a *right Clifford bivector* is one satisfying $\boldsymbol{\Xi}\mathbf{I} = \boldsymbol{\Xi}$.

By considering what this implies for the Plücker coordinates for the bivector, one obtains as an immediate consequence: A left [right] Clifford bivector $\boldsymbol{\Xi}$ has the form

$$\boldsymbol{\Xi} = (x\mathbf{e}_{01} + y\mathbf{e}_{02} + z\mathbf{e}_{03}) + [-](z\mathbf{e}_{12} + y\mathbf{e}_{31} + x\mathbf{e}_{23})$$

The set of right Clifford bivectors $\mathcal{C}_r$ span a 2-plane in $\mathfrak{B}$, of signature $(---)$. In fact, for two bivectors in this plane, $\boldsymbol{\Xi} \vee \boldsymbol{\Phi} = \boldsymbol{\Xi} \cdot \boldsymbol{\Phi} = -2(x^2 + y^2 + z^2)$. The left Clifford bivectors $\mathcal{C}_l$ span a similar 2-plane with signature $(+++)$; these two planes have empty intersection and span $\mathfrak{B}$, hence any bivector can be written uniquely as the sum of a right and left Clifford bivector. We next state a lemma which we will need later in Sect. 7.11.1.

Lemma 115. *For $\boldsymbol{\Xi} \in \mathcal{C}_r$ and $\boldsymbol{\Phi} \in \mathcal{C}_l$, $\boldsymbol{\Xi}\boldsymbol{\Phi} = 0$.*

Proof. Then by Def. 114, $\boldsymbol{\Xi} = \frac{1-\mathbf{I}}{2}\boldsymbol{\Xi}$ and $\boldsymbol{\Phi} = \frac{1+\mathbf{I}}{2}\boldsymbol{\Phi}$. Hence

$$\boldsymbol{\Xi}\boldsymbol{\Phi} = \frac{1-\mathbf{I}}{2}\boldsymbol{\Xi}\frac{1+\mathbf{I}}{2}\boldsymbol{\Phi} = \frac{(1-\mathbf{I})(1+\mathbf{I})}{4}\boldsymbol{\Xi}\boldsymbol{\Phi} = \frac{1^2 - \mathbf{I}^2}{4}\boldsymbol{\Xi}\boldsymbol{\Phi} = 0$$

□

Remark 116. The name derives from the fact that all the axes of a Clifford bivector $\boldsymbol{\Xi}$ are *Clifford parallel* to each other. See Sect. 7.4.1 for more on Clifford parallels. We'll see below in Sect. 7.9 that exponentiating a Clifford bivector $\boldsymbol{\Xi}$ produces elliptic isometries (so-called Clifford translations) which leave $\boldsymbol{\Xi}$ and all its axes invariant; the motion is a flow along these axes. This is the only isometry besides euclidean translations in which all points move along straight lines. Sect. 7.11.1 analyzes Clifford translations in more detail.

Remark 117. **A diagonal Plücker basis.** The use of left and right Clifford bivectors as a basis for $\mathfrak{B}$ was first proposed by Klein, who suggested using the basis $\{\mathbf{e}_{01} \pm \mathbf{e}_{23}, \mathbf{e}_{02} \pm \mathbf{e}_{31}, \mathbf{e}_{03} \pm \mathbf{e}_{12}\}$ instead of the standard Plücker basis. The choice of $+$ yields the right Clifford bivectors; $-$ yields the left Clifford bivectors. Obviously in this basis the Plücker inner product is diagonal $(+++--)$.

7.7.2.3 Axis pairs Clearly, the foregoing discussion implies that if there are exactly two axes, then they are polar partners with respect to the metric quadric. On the other hand, Sect. 7.2.1.2 shows that they are conjugate with respect to the null polarity determined by $\boldsymbol{\Xi}$. Hence, another characterization, in the non-degenerate case, of the axes of a non-Clifford bivector is that they are the unique pair of lines which are conjugate both with respect to the null polarity of $\boldsymbol{\Xi}$ and with respect to the metric quadric. In the Clifford case, $\boldsymbol{\Xi}$ is a fixed point of the metric polarity and there are infinitely many lines through $\boldsymbol{\Xi}$, each of which yields an axis pair of $\boldsymbol{\Xi}$.

Remark 118. Axes, in particular axis pairs, are key to understanding of applications of this material to kinematics and dynamics. For example, a rotor can, generically, be uniquely decomposed as a pair of commuting rotations around an axis pair of its grade-2 component. See Thm. 134.

7.7.3 Calculating an axis

(7.19) yields an axis for $\boldsymbol{\Xi}$ except when

$$\mathbf{s} := \sqrt{\boldsymbol{\Xi}\widetilde{\boldsymbol{\Xi}}} = \sqrt{-\boldsymbol{\Xi}\cdot\boldsymbol{\Xi} - \boldsymbol{\Xi}\wedge\boldsymbol{\Xi}}$$

doesn't exist, or is zero. We consider these two cases in turn.

I. $\mathbf{s}$ isn't defined in two cases (see Sect. 7.6 above):

   a. **Ideal euclidean.** $\mathbf{I}^2 = 0$ and $\boldsymbol{\Xi}\cdot\boldsymbol{\Xi} = 0$. But then $\boldsymbol{\Xi}\wedge\boldsymbol{\Xi} = 0$, so $\boldsymbol{\Xi}$ is simple, and we are in the case that $\mathbf{s} = 0$, treated below.
   b. **Clifford bivector (elliptic).** $\mathbf{I}^2 = 1$ and $\boldsymbol{\Xi}\cdot\boldsymbol{\Xi} = \pm\boldsymbol{\Xi}\vee\boldsymbol{\Xi}$. By inspection, this is the case when $\boldsymbol{\Xi}$ is a Clifford bivector. We have described above how to calculate the axes of Clifford bivectors. And, conversely, if $\boldsymbol{\Xi}\cdot\boldsymbol{\Xi} = \pm\boldsymbol{\Xi}\vee\boldsymbol{\Xi}$, $\boldsymbol{\Xi}$ is a Clifford bivector. To see this, recall the fact that $a^2 + b^2 \geqslant 2ab$ with equality $\iff a = b$. Apply this to the three pairs $(p_{01}, p_{23}), (p_{02}, p_{31})$, and (p_{03}, p_{12}) of the coordinates of an arbitrary bivector

$$\boldsymbol{\Xi} := p_{01}\mathbf{e}_{01} + p_{02}\mathbf{e}_{02} + p_{03}\mathbf{e}_{03} + p_{12}\mathbf{e}_{12} + p_{31}\mathbf{e}_{31} + p_{23}\mathbf{e}_{23}$$

   to show that $\boldsymbol{\Xi}\cdot\boldsymbol{\Xi} = \pm\boldsymbol{\Xi}\vee\boldsymbol{\Xi}$ only for Clifford bivectors.

II. $\mathbf{s} = 0$. Then it has no inverse. This can happen only if $\boldsymbol{\Xi}$ is ideal and simple. Then $\boldsymbol{\Xi}$ is its own axis, but there are also other axes. There are two cases:

   a. **Ideal euclidean.** $\mathbf{I}^2 = 0$. There are additionally ∞^2 other axes, proper lines $\boldsymbol{\Theta}$ such that $\boldsymbol{\Theta}\mathbf{I} = \boldsymbol{\Xi}$, described in Sect. 7.7.1.
   b. **Ideal hyperbolic.** $\mathbf{I}^2 = -1$. There are additionally ∞^1 other axes, the elements of the line pencil spanned by $\mathbf{I}$ and $\mathbf{I}^\perp$.

Remark 119. The exceptional cases discussed above correspond to cases where $\boldsymbol{\Xi}$ and $\boldsymbol{\Xi}^\perp$ do not determine a regular bivector pencil in $\mathfrak{B}$. In the elliptic case, since $\boldsymbol{\Xi} = \boldsymbol{\Xi}^\perp$; in the euclidean case, since $\boldsymbol{\Xi}^\perp = 0$; and in the hyperbolic case since the bivector pencil is

isotropic, and consists of simple bivectors, all of which are axes of every other element of the pencil.

We state for future reference the result of our investigation:

Theorem 120. *Let n be the number of axes of a bivector $\boldsymbol{\Xi}$. Then*

$$n = \begin{cases} 1 & \text{if } \mathbf{I}^2 = 0 \text{ and } \boldsymbol{\Xi}^2 \neq 0; \\ \infty^2 & \text{if } \mathbf{I}^2 = 0 \text{ and } \boldsymbol{\Xi}^2 = 0; \\ \infty^1 & \text{if } \mathbf{I}^2 = -1 \text{ and } \boldsymbol{\Xi}^2 = 0; \\ 2 & \text{if } \mathbf{I}^2 \neq 0,\ \boldsymbol{\Xi}^2 \neq 0, \text{ and } \boldsymbol{\Xi} \neq \boldsymbol{\Xi}^\perp; \\ \infty^2 & \text{if } \mathbf{I}^2 = 1,\ \boldsymbol{\Xi}^2 \neq 0, \text{ and } \boldsymbol{\Xi} = \boldsymbol{\Xi}^\perp. \end{cases} \tag{7.21}$$

One consequence of this theorem is that every bivector has an axis. We rephrase this slightly to a more precise form:

Corollary 121. *For every bivector $\boldsymbol{\Xi}$, there exists a Study number $\mathbf{z}$ and a simple bivector $\boldsymbol{\Phi}$ such that $\boldsymbol{\Xi} = \mathbf{z}\boldsymbol{\Phi}$.*

Remark 122. By the theorem, such a factorization is not in general unique.

The existence and structure of axes for bivectors is an important ingredient in the discussion of logarithms in Sect. 126 below. Another important ingredient is Study analysis as described in the next section.

7.7.3.1 Examples

1. **The common normal of two lines.** Let $\boldsymbol{\Xi}$ and $\boldsymbol{\Phi}$ be two skew simple proper bivectors in elliptic 3-space.
   a. $\boldsymbol{\Theta} := \boldsymbol{\Xi} \times \boldsymbol{\Phi}$ is a bivector which is in involution to both $\boldsymbol{\Xi}$ and $\boldsymbol{\Phi}$.
   b. When $\boldsymbol{\Theta}$ has exactly two axes, $\boldsymbol{\Theta}_1$ and $\boldsymbol{\Theta}_2$, each is a line perpendicular to both $\boldsymbol{\Xi}$ and $\boldsymbol{\Phi}$.
   c. Let $\mathbf{a}$ be a plane not containing $\boldsymbol{\Theta}_1$. Then the intersections of $\boldsymbol{\Theta}_1$ with $\boldsymbol{\Xi}$ and $\boldsymbol{\Phi}$ are $((\mathbf{a} \wedge \boldsymbol{\Theta}_1) \vee \boldsymbol{\Phi}) \wedge \boldsymbol{\Xi}$ and $((\mathbf{a} \wedge \boldsymbol{\Theta}_1) \vee \boldsymbol{\Xi}) \wedge \boldsymbol{\Phi}$, resp. Similarly for $\boldsymbol{\Theta}_2$.
   d. The shortest distance between the two lines is given by the shorter of the distances between the two pairs of points found.
   e. Similar treatments can be given for euclidean and hyperbolic space but only one axis is proper.

2. **The cylindroid** Given a regular bivector pencil (i. e., one that has two points common with $\mathcal{L}$), one can ask: how does the set of axes for this pencil appear in $\mathbb{R}P^3$? By continuity, these axes should sweep out a developable surface which contains the lines corresponding to these two points. It is a well-known result of classical euclidean line geometry that this surface, when expressed in point coordinates in $\mathbb{R}P^3$, is a cubic surface in the variables (x, y, z, w). For the non-euclidean case, one has to be more careful in stating the question, since in general each bivector in the pencil has two axes, and one must choose one of this pair in a continuous fashion. One can then follow through analogous reasoning as in the euclidean case and arrive at a quartic surface. See [Hea84] for a treatment of the elliptic cylindroid.

7.8 Study analysis.

Analysis in these Clifford algebras proceeds analogously to analysis over complex numbers. We use the fact that the important elements of the algebra can be normalized to have square -1, 1, or 0. These elements then can be substituted into formal power series such as exponentials and trigonometric functions, and known results of convergence follow in the same way for complex numbers when one uses the fact that $i^2 = -1$.

Let $\mathbf{\Phi}$ be some entity such that $\mathbf{\Phi}^2 \in \{-1, 0, 1\}$ which commutes with scalars and pseudoscalars. For our purposes this will be a simple normalized bivector, but much of what follows is formally true for such a more general unit. Such an element satisfies $\mathbf{\Phi}^2 \in \{-1, 0, 1\}$. Note that for $\mathbf{I}^2 = 1$, only the case $\mathbf{\Xi}^2 = -1$ occurs; for $\mathbf{I}^2 = 0$, $\mathbf{\Xi}^2 = 0$ is also possible; while for $\mathbf{I}^2 = -1$, all three possibilities occur.

$\mathbf{\Phi}^2$	$f_1(t)$	$f_2(t)$	$\mathbf{I}^2\mathbf{\Phi}^2$	$f_3(u)$	$f_4(u)$
1	$\cosh(t)$	$\sinh(t)$	1	$\cosh(u)$	$\sinh(u)$
0	1	t	0	1	u
-1	$\cos(t)$	$\sin(t)$	-1	$\cos(u)$	$\sin(u)$

Table 7.2 f_1, f_2, f_3, and f_4.

We begin with a formal evaluation of $e^{(t+u\mathbf{I})\mathbf{\Phi}}$. We define implicitly four real-valued functions f_1, f_2, f_3, and f_4 as follows:

$$e^{(t+u\mathbf{I})\mathbf{\Phi}} = e^{t\mathbf{\Phi}} e^{(u\mathbf{I}\mathbf{\Phi})} \tag{7.22a}$$

$$= (f_1(t) + f_2(t)\mathbf{\Phi})(f_3(u) + f_4(u)\mathbf{I}\mathbf{\Phi}) \tag{7.22b}$$

$$= (f_1(t)f_3(u) + f_2(t)f_4(u)\mathbf{\Phi}^2\mathbf{I}) + (f_2(t)f_3(u) + f_1(t)f_4(u)\mathbf{I})\mathbf{\Phi} \tag{7.22c}$$

f_1 and f_2 depend only on the value of $\mathbf{\Phi}^2$; while $f_3(u)$ and $f_4(u)$ depend on $\mathbf{I}^2\mathbf{\Phi}^2$. See Table 7.2.

$\mathbf{I}^2$	$\mathbf{\Phi}^2$	$e^{(t+u\mathbf{I})\mathbf{\Phi}}$
1	-1	$\cos(t)\cos(u) - \sin(t)\sin(u)\mathbf{I} + (\sin(t)\cos(u) + \cos(t)\sin(u)\mathbf{I})\mathbf{\Phi}$
0	-1	$\cos(t) - \sin(t)u\mathbf{I} + (\sin(t) + \cos(t)u\mathbf{I})\mathbf{\Phi}$
0	0	$1 + (t + u\mathbf{I})\mathbf{\Phi}$
-1	-1	$\cos(t)\cosh(u) - \sin(t)\sinh(u)\mathbf{I} + (\sin(t)\cosh(u) + \cos(t)\sinh(u)\mathbf{I})\mathbf{\Phi}$
-1	0	$1 + (t + u\mathbf{I})\mathbf{\Phi}$
-1	1	$\cosh(t)\cos(u) - \sinh(t)\sin(u)\mathbf{I} + (\sinh(t)\cos(u) + \cosh(t)\sin(u)\mathbf{I})\mathbf{\Phi}$

Table 7.3 $e^{(t+u\mathbf{I})\mathbf{\Phi}}$ based on possible values of $\mathbf{I}^2$ and $\mathbf{\Phi}^2$.

We will make heavy use of (7.22c) below when we calculate logarithms of rotors. Table 7.3 gives an overview of the six specific forms which (7.22c) takes in reality.

7.9 Isometries

The results of Sect. 6.3 can be carried over without significant change to 3D. For a proper 1-vector $\mathbf{a}$, the sandwich operation $\underline{\mathbf{a}}(\mathbf{P}) = \mathbf{aPa}$ is a reflection in the plane represented by $\mathbf{a}$. For a pair of proper 1-vectors $\mathbf{a}$ and $\mathbf{b}$ with $\mathbf{g} := \mathbf{ab}$, $\underline{\mathbf{g}}(\mathbf{P}) = \mathbf{gP}\widetilde{\mathbf{g}}$ is a rotor fixing the line $\mathbf{a} \wedge \mathbf{b} = \langle \mathbf{g} \rangle_2$ point-wise.

Definition 123. A rotor which fixes a line point-wise is called a *rotator*.

We will see below that this is equivalent to the condition that the bivector part of the rotor is simple. We can also carry over to such rotators, the terminology of Def. 103 (*elliptic rotator, parabolic rotator*, and *hyperbolic rotator*) based on the nature of the simple bivector $\mathbf{a} \wedge \mathbf{b}$.

It's not hard to see that the set of rotators is not closed under composition. First, note that the composition of two rotators is an isometry. Let $\mathbf{h} := \mathbf{cd}$ be another rotator. Then $\mathbf{k} = \mathbf{\Xi\Phi} = \mathbf{abcd}$. When the two lines $\mathbf{a} \wedge \mathbf{b}$ and $\mathbf{c} \wedge \mathbf{d}$ do not intersect. $\langle \mathbf{gh} \rangle_4 \neq 0$. Only when the axes of $\mathbf{g}$ and $\mathbf{h}$ intersect, $\langle \mathbf{gh} \rangle_4 = 0$ and the product is a rotator.

Remark 124. **Polar rotators.** In the case that the bivectors satisfy $\mathbf{h} = \mathbf{gI}$, it is straightforward to describe the motion. First observe that the bivectors $\langle \mathbf{g} \rangle_2$ and $\langle \mathbf{h} \rangle_2$ are simple, and are invariant under both rotations: fixed pointwise by the "own" rotation, and translated along itself by the other. It is also an easy calculation that the two rotations commute: $\mathbf{gh} = \mathbf{hg}$. So, to follow a point $\mathbf{P}$, rotate it around the line $\langle \mathbf{g} \rangle_2$ and around the line $\langle \mathbf{h} \rangle_2$, in either order. This motivates the following definition, which we'll spend the rest of the chapter investigating.

Definition 125. A *screw motion* is an isometry that can be factored as two commuting rotations around simple, non-intersecting bivectors of the form $\mathbf{\Xi}$ and $\mathbf{\Xi I}$.

Remark 126. **Terminology alert.** In order to have a mutually-exclusive notation, in this definition we do not consider the identity mapping a rotation, so the rotations on each of $\mathbf{\Xi}$ and $\mathbf{\Xi I}$ are non-trivial.

Like the linear line complex, a screw motion has no counterpart in 2D. In fact, $\langle \mathbf{k} \rangle_2$ is a non-simple bivector $\iff$ $\mathbf{k}$ is the rotor of a screw motion. We will prove this in Corollary 141; to do so, we need to extend 2D results on rotors.

7.10 Rotor logarithms

The analysis of the logarithms of isometries $\underline{\mathbf{g}}$ for $\mathbf{g} \in \mathbf{Spin}^3_{+\kappa}$ is more difficult than for $\mathbf{Spin}^2_{+\kappa}$ due to the presence of non-simple bivectors. Nevertheless, a full theory of

logarithms and exponentials for 3D is possible; we present it below. The general plan: to first establish results for rotators, then to show how non-rotator rotors can be decomposed as the product of two commuting rotators. The axis of the bivector part of the rotor plays a distinguished role in these proceedings.

We begin with two technical lemmas which we will need for calculating logarithms in Sect. 7.10.2.

Write

$$\mathbf{g} = \langle \mathbf{g} \rangle_0 + \langle \mathbf{g} \rangle_2 + \langle \mathbf{g} \rangle_4 = s_1 + \mathbf{\Xi} + p_1 \mathbf{I} \tag{7.23}$$

Then the condition that $\mathbf{g} \in \mathbf{Spin}^3_{+\kappa}$ can be written as:

$$1 = \mathbf{g}\widetilde{\mathbf{g}} = s_1^2 + p_1^2 \mathbf{I}^2 + 2 s_1 p_1 \mathbf{I} - \mathbf{\Xi} \cdot \mathbf{\Xi} - (\mathbf{\Xi} \vee \mathbf{\Xi})\mathbf{I} \tag{7.24}$$

Lemma 127. *If* $\mathbf{g} \in \mathbf{Spin}^3_{+\kappa}$ *as above, then* $\mathbf{\Xi}$ *is simple* $\iff$ $p_1 = 0$ *or* $s_1 = 0$.

Proof. The coefficient of $\mathbf{I}$ on the RHS of (7.24) is zero. □

We will need the following lemma regarding elliptic rotors.

Lemma 128. *Assume* n *is odd,* $\mathbf{I}^2 = 1$, $\mathbf{g}$ *a rotor. Then* $\mathbf{gI}$ *is a rotor and* $\underline{\mathbf{g}} \equiv \underline{\mathbf{gI}}$.

Proof. The condition that n is odd is necessary so that $\mathbf{gI} \in Cl^{n+}_{\kappa}$. We establish that $\mathbf{gI} \in \mathbf{Spin}^n_{+\kappa}$:

$$\begin{aligned}(\mathbf{gI})(\widetilde{\mathbf{gI}}) &= \mathbf{gI}\widetilde{\mathbf{I}}\widetilde{\mathbf{g}} \\ &= \mathbf{gI}^2\widetilde{\mathbf{g}} \\ &= \mathbf{g}\widetilde{\mathbf{g}} = 1\end{aligned}$$

Let $\mathbf{X}$ represent a k-vector.

$$\begin{aligned}\underline{\mathbf{gI}}(\mathbf{X}) &= \mathbf{gIX}\widetilde{\mathbf{I}}\widetilde{g} \\ &= (-1)^k \mathbf{gXI}\widetilde{\mathbf{I}}\widetilde{g} \\ &= (-1)^k \mathbf{gX}\widetilde{g} \\ &= (-1)^k \underline{\mathbf{g}}(\mathbf{X}) \\ &= \overline{\underline{\mathbf{g}}(\mathbf{X})} \equiv \underline{\mathbf{g}}(\mathbf{X})\end{aligned}$$

where we have used $\mathbf{XI} = (-1)^k \mathbf{IX}$ and $\widetilde{\mathbf{I}}\widetilde{\mathbf{I}} = 1$. The conjugation operation on the last line does not effect the result since each k-vector is mapped to a non-zero multiple of itself. □

Remark 129. The lemma implies that $\mathbf{Spin}^3_{+1}$ is generallly a $4:1$ cover of $SO(4)$, since $\mathbf{g} \neq \mathbf{gI}$ except when $\mathbf{g}$ is a Clifford bivector. Hence, with this exception, $\mathbf{g}, -\mathbf{g}, \mathbf{gI}$, and $-\mathbf{gI}$, all distinct, correspond to the same isometry; otherwise only $\mathbf{g}$ and $-\mathbf{g}$ are distinct. ?

Remark 130. Note that for a normalized axis $\mathbf{\Phi}$, $\mathbf{\Phi}^2 \in \{-1, 0, 1\}$.

7.10.1 The logarithms of a simple rotor

We begin our detailed study of logarithms with a simple case that can be analyzed using the same techniques used in 2D.

Definition 131. For a rotor $\mathbf{g}$, $\langle \mathbf{g} \rangle_2$ is the *bivector part* of $\mathbf{g}$. A rotor is *simple* if its bivector part is simple. An *axis* of a rotor is an axis of its bivector part.

Theorem 132. *A simple rotor in* $\mathbf{Spin}^3_{+\kappa}$ *has a normalized logarithm.*

Proof. Suppose, in (7.23), that $\mathbf{\Xi}$ is simple. Then by Lemma 127 either $s_1 = 0$ or $p_1 = 0$. We can assume $p_1 = 0$. Indeed, assume $p_1 \neq 0$. Then, when $\mathbf{I}^2 = 1$, $\mathbf{gI}$ is also a rotor which by Lemma 128 is equivalent to $\mathbf{g}$ and has $p_1 = 0$; if $\mathbf{I}^2 = -1$ or $\mathbf{I}^2 = 0$, then the assumption $p_1 \neq 0$ leads to a contradiction: $p_1^2\mathbf{I}^2 - \mathbf{\Xi}^2 = -p_1^2 - \mathbf{\Xi}^2 = 1$ or $-\mathbf{\Xi}^2 = 1$. The rest of the proof is identical to that of Thm. 107 if one replaces $\mathbf{B}$ by $\mathbf{\Xi}$ and the parameter a by s_1. The resulting logarithms represent lines of fixed points rather than a single fixed point. □

7.10.1.1 Examples These results combined with those of Sect. 7.8 can be used directly to calculate the form of simple rotors.

1. How can one find the rotor corresponding to a rotation of $\dfrac{2\pi}{3}$ radians around the line through the origin and the point $(1, 1, 1)$? First, let the unknown rotor be $\mathbf{g}$. The axis of $\mathbf{g}$ will be

$$\begin{aligned}\mathbf{\Xi} :&= \mathbf{E}_0 \vee (\mathbf{E}_1 + \mathbf{E}_2 + \mathbf{E}_3) \\ &= \mathbf{E}_0 \wedge \mathbf{E}_1 + \mathbf{E}_0 \wedge \mathbf{E}_2 + \mathbf{E}_0 \wedge \mathbf{E}_3 \\ &= \mathbf{e}_{23} + \mathbf{e}_{31} + \mathbf{e}_{12} = \mathbf{e}_{12} + \mathbf{e}_{31} + \mathbf{e}_{23}\end{aligned}$$

   $\mathbf{\Xi} \cdot \mathbf{\Xi} = 3$, so we normalize $\mathbf{\Xi}_N = \dfrac{1}{\sqrt{3}}(\mathbf{e}_{12} + \mathbf{e}_{31} + \mathbf{e}_{23})$. Then by the above, to obtain a rotation of $\dfrac{2\pi}{3}$, one uses $\theta = \dfrac{\pi}{3}$ and calculates

$$\begin{aligned}e^{\theta \mathbf{\Xi}_N} &= \cos(\theta) + \sin(\theta)\mathbf{\Xi}_N \\ &= .5(1 + \mathbf{e}_{12} + \mathbf{e}_{31} + \mathbf{e}_{23})\end{aligned}$$

   Notice that the result is metric-neutral, since the line goes throught the origin $\mathbf{E}_0$, where all metrics agree.

2. In hyperbolic space, let $\mathbf{\Sigma}$ be the line of intersection of the planes $z = \frac{\sqrt{2}}{2}$ and $x = y$. Determine the rotator around the line $\mathbf{\Sigma}$ through an angle $\frac{\pi}{4}$.

   Solution. Represent the first plane as $\mathbf{a}_1 = \mathbf{e}_3 - \frac{\sqrt{2}}{2}\mathbf{e}_0$ and the second as $\mathbf{a}_2 = \mathbf{e}_1 - \mathbf{e}_2$. Then $\mathbf{\Sigma} = \mathbf{a}_1 \wedge \mathbf{a}_2 = \frac{\sqrt{2}}{2}(\mathbf{e}_{01} - \mathbf{e}_{02}) - \mathbf{e}_{31} - \mathbf{e}_{23}$. Verify that $\mathbf{\Sigma}^2 = -1$, hence is normalized proper. Then by the above results on simple rotors, the logarithm of the desired rotor $\mathbf{g}$ is $\frac{\pi}{8}\mathbf{\Sigma}$, and $e^{\frac{\pi}{8}\mathbf{\Sigma}} = \cos(\frac{\pi}{8}) + \sin(\frac{\pi}{8})\mathbf{\Sigma}$. One can obtain the same result from Table 7.3.

7.10.2 The logarithm of a general rotor

Let $\mathbf{\Phi}$ be an axis of $\mathbf{\Xi}$ (Thm. 120). Then there exists a Study number $s_2 + p_2\mathbf{I}$ satisfying:

$$(s_2 + p_2\mathbf{I})\mathbf{\Phi} = \mathbf{\Xi} \tag{7.25}$$

Substituting into (7.23) yields

$$\mathbf{g} = s_1 + p_1\mathbf{I} + (s_2 + p_2\mathbf{I})\mathbf{\Phi}$$

Finding the logarithm of $\mathbf{\Xi}$ is equivalent to finding a solution to:

$$e^{(t+u\mathbf{I})\mathbf{\Theta}} = \mathbf{g} \tag{7.26}$$

The left-hand side of (7.26) should be familiar from (7.22) above. Substituting for both sides we arrive at:

$$(f_1(t)f_3(u)+f_2(t)f_4(u)\mathbf{X}^2\mathbf{I})+(f_2(t)f_3(u)+f_1(t)f_4(u)\mathbf{I})\mathbf{\Theta} = s_1+p_1\mathbf{I}+(s_2+p_2\mathbf{I})\mathbf{\Phi} \tag{7.27}$$

We consider the right-hand side elements as given, and seek to solve for t and u. Examination of (7.27) reveals that the only hope for a solution is given by setting $\mathbf{\Theta} = \mathbf{\Phi}$, the axis of $\mathbf{\Xi}$. Furthermore, equating corresponding coefficients of both sides yields:

$$f_1(t)f_3(u) = \lambda s_1 \tag{7.28a}$$
$$f_2(t)f_4(u)\mathbf{\Phi}^2 = \lambda p_1 \tag{7.28b}$$
$$f_2(t)f_3(u) = \lambda s_2 \tag{7.28c}$$
$$f_1(t)f_4(u) = \lambda p_2 \tag{7.28d}$$

This appears to be overconstrained since there are four equations for two unknowns, but remember that $\mathbf{g}$ is normalized, so the entries of $\mathbf{g}$ cannot be arbitrary.

The following set of four equations suggests itself as a starting point for further investigations. We use the notation $a : b$ instead of $\frac{a}{b}$ to include the case that $b = 0$.

$$f_1(t) : f_2(t) = s_1 : s_2 = p_2 : \mathbf{\Phi}^2 p_1 \tag{7.29a}$$
$$f_3(u) : f_4(u) = s_1 : p_2 = s_2 : \mathbf{\Phi}^2 p_1 \tag{7.29b}$$

These equations provide, in general, two alternatives for each of the left-hand side unknowns.

7.10.2.1 Example: logarithm in the elliptic case For example, consider the elliptic case. Then every bivector satisfies $\mathbf{\Phi}^2 = -1$, and $\mathbf{I}^2\mathbf{X}^2 = -1$. Using Table 7.2 to find out the values of f_i leads to the equation:

$$\exp(t + u\mathbf{I})\mathbf{\Phi} = \cos(t)\cos(u) - \sin(t)\sin(u)\mathbf{I} + (\sin(t)\cos(u) + \cos(t)\sin(u)\mathbf{I})\mathbf{\Phi} \tag{7.30}$$

Then (7.29) looks like (substituting also $\mathbf{\Phi}^2 = -1$):

$$\cos(t) : \sin(t) = s_1 : s_2 = p_2 : -p_1 \tag{7.31a}$$
$$\cos(u) : \sin(u) = s_1 : p_2 = s_2 : -p_1 \tag{7.31b}$$

This leads to the solutions

$$t = \tan^{-1}(s_2, s_1) = \tan^{-1}(-p_1, p_2) \tag{7.32a}$$
$$u = \tan^{-1}(p_2, s_1) = \tan^{-1}(-p_1, s_2) \tag{7.32b}$$

Note that not all elements of $\mathcal{C} := \{s_1, p_1, s_2, p_2\}$ can be zero, since otherwise so is $\mathbf{g}$. So at least one of the two RHS alternatives on each line is valid. When both are valid, which should be used? We choose the alternative in which the largest absolute value among the elements of $\mathcal{C}$ occurs. This guarantees that $\tan^{-1}$ is defined, and also that the least chance for numerical errors occurs. The resulting solutions (t, u) satisfy (7.26), hence the conditions of Def. 97: $(t + u\mathbf{I})\mathbf{\Phi}$ is the logarithm of $\mathbf{g}$. Notice this logarithm is unique except up to multiplies of 2π in both t and u.

7.10.2.2 The general case The general case proceeds in exactly the same way, with other values for f_i. Depending on the values of $\mathbf{\Phi}^2$ and of $\mathbf{I}^2\mathbf{\Phi}^2$ (see Table 7.2), there are a total of 3 x 3 = 9 possible combinations of the function pairs $(f_1(t), f_2(t))$ and $(f_3(u), f_4(u))$, of which only 6 occur in reality (see Table 6.2). To simplify the notation of the desired logarithm, we introduce Table 7.4, similar to Table 7.2 but containing the possible solutions for the various cases. Notice that the solutions are unique, except for solutions involving $\tan^{-1}$, where integer multiplies of 2π can be added (last row of table).

Also, note there are no entries for t_2 or u_2 when $\mathbf{\Phi}^2 = 0$. In this case $e^{(t+u\mathbf{I})\mathbf{\Phi}}$ degenerates to $1 + (t + u\mathbf{I})\mathbf{\Phi}$ (see Table 7.3), and there are no alternatives to t_1 and u_1 for calculating t and u.

$\mathbf{\Phi}^2$	$t_1(\mathbf{\Phi}^2)$	$t_2(\mathbf{\Phi}^2)$	$\mathbf{I}^2\mathbf{\Phi}^2$	$u_1(\mathbf{I}^2\mathbf{\Phi}^2)$	$u_2(\mathbf{I}^2\mathbf{\Phi}^2)$
1	$\tanh^{-1}(s_2, s_1)$	$\tanh^{-1}(p_1, p_2)$	1	$\tanh^{-1}(p_2, s_1)$	$\tanh^{-1}(\mathbf{\Phi}^2 p_1, s_2)$
0	$\frac{s_2}{s_1}$	-	0	$\frac{p_2}{s_1}$	-
-1	$\tan^{-1}(s_2, s_1)$	$\tan^{-1} -p_1, p_2)$	-1	$\tan^{-1}(p_2, s_1)$	$\tan^{-1}(\mathbf{\Phi}^2 p_1, s_2)$

Table 7.4 Possible (t, u) solutions to $\exp(t + u\mathbf{I})\mathbf{\Phi} = \mathbf{g}$.

We collect the above results in a theorem:

Theorem 133. *Given a rotor* $\mathbf{g} \in \mathbf{Spin}^3_{+\kappa}$*, with normalized axis* $\mathbf{\Phi}$*, write*

$$\mathbf{g} = s_1 + p_1\mathbf{I} + (s_2 + p_2\mathbf{I})\mathbf{\Phi}$$

Let $\mathcal{C} := \{s_1, p_1, s_2, p_2\}$. *Choose* $t \in (t_1(\mathbf{\Phi}^2), t_2(\mathbf{\Phi}^2))$ *and* $u \in (u_1(\mathbf{I}^2\mathbf{\Phi}^2), u_2(\mathbf{I}^2\mathbf{\Phi}^2))$ *(from Table 7.4), such that* t *and* u *derive from the formula involving the element of largest absolute value in* $\mathcal{C}$. *Then* $(t + u\mathbf{I})\mathbf{\Phi}$ *is a normalized logarithm of* $\mathbf{g}$.

7.10.3 Decomposing a rotor as two commuting rotators

We can also characterize the effect of $\underline{\mathbf{g}}$.

Theorem 134. *Given a rotor* $\mathbf{g} \in \mathbf{Spin}^3_{+\kappa}$ *with normalized axis* $\mathbf{\Phi}$ *and logarithm* $\mathbf{\Omega} = (t + u\mathbf{I})\mathbf{\Phi}$. *Then:*

1. $\underline{\mathbf{g}}$ *can be decomposed as the concatenation of two simple commuting rotors (at most one of which is the identity map)*

$$\mathbf{g} = \mathbf{g}_t\mathbf{g}_u = \mathbf{g}_t\mathbf{g}_u$$

   where $\mathbf{g}_t := e^{t\mathbf{\Phi}}$ *and* $\mathbf{g}_u := e^{u\mathbf{I}\mathbf{\Phi}}$,
2. $\mathbf{g}_t$ *is a rotation around the axis* $\mathbf{\Phi}$ *of measure* $2t$ *and* $\mathbf{g}_u$ *is a rotation around* $\mathbf{\Phi}\mathbf{I}$ *of measure* $2u$.

Proof. 1. Clearly $\mathbf{g}_t$ and $\mathbf{g}_u$ are simple rotors. If $t = 0$ then $\mathbf{g}_t = \mathbf{1}$, similarly for $u = 0$. But $t = 0$ and $u = 0$ cannot occur. Since $\mathbf{\Phi}$ and $\mathbf{I}\mathbf{\Phi}$ commute, the basic identity of the exponential function can be applied to prove commutativity:

$$\mathbf{g}_t\mathbf{g}_u = e^{t\mathbf{\Phi}}e^{u\mathbf{I}\mathbf{\Phi}} = e^{(t+u\mathbf{I})\mathbf{\Phi}} =$$
$$e^{(u\mathbf{I}+t)\mathbf{\Phi}} = e^{u\mathbf{I}\mathbf{\Phi}}e^{t\mathbf{\Phi}} = \mathbf{g}_u\mathbf{g}_t$$

2. One just confirms that Def. 104 is satisfied.
□

Remark 135. Note that the theorem does not assert that $\mathbf{\Phi}\mathbf{I}$ is also an axis. From the preceding discussion of axes, we know that $\mathbf{\Phi}\mathbf{I}$ will be an axis, except when $\mathbf{I}^2 = 0$, then it is a secondary axis.

Remark 136. One can also apply Thm. 120 to describe in how many different ways a given rotor can be decomposed in this way, since each distinct axis pair $(\mathbf{\Phi}, \mathbf{\Phi}^\perp)$ gives rise to a distinct decomposition. In the generic noneuclidean case (setting $\mathbf{\Xi} := \langle\mathbf{g}\rangle_2$), $\mathbf{I}^2 \neq 0$, $\mathbf{\Xi}^2 \neq 0$, and $\mathbf{\Xi} \neq \mathbf{\Xi}^\perp$, the decomposition is unique. For a discussion of two classes of isometries which have non-unique decomposition, see below, Sect. 7.11.

7.10.4 Pitch of a rotor

It's natural to ask whether there are invariants of rotor logarithms under group actions.

Definition 137. For a normalized logarithm $(t + u\mathbf{I})\mathbf{\Phi}$ of a rotor $\mathbf{h}$, the factor $t + u\mathbf{I}$ is called the *homogeneous pitch* of $\mathbf{h}$, and the ratio $u : t$ is called the *affine pitch*, or simply *pitch*, of the rotor.

Recall that the inner automorphism of a group determined by the group element $\mathbf{g}$ is defined by $\mathbf{h} \to \mathbf{ghg}^{-1}$. For $\mathbf{Spin}^3_{+\kappa}$ this is clearly just the isometry $\underline{\mathbf{g}}$ restricted to $\mathbf{Spin}^3_{+\kappa}$.

Lemma 138. *Let $\mathbf{\Xi} = (t + u\mathbf{I})\mathbf{\Phi}$ be a normalized logarithm of the rotor $\mathbf{h}$. The exponential curve $\mathbf{h}(s) := e^{s\mathbf{\Xi}}$, for $s \in \mathbb{R}$ satisfies $\mathbf{h}(s) \subset \mathbf{Spin}^3_{+\kappa}$.*

Proof. $\mathbf{h}(s) \in Cl^{3+}_\kappa$ by examination; furthermore, $\mathbf{h}(s)\widetilde{\mathbf{h}}(s) = e^{s\mathbf{\Xi}}e^{-s\mathbf{\Xi}} = 1$, so $\mathbf{h}(s) \in \mathbf{Spin}^3_{+\kappa}$. □

Theorem 139. *1. Homogeneous pitch is preserved under inner automorphisms of $\mathbf{Spin}^3_{+\kappa}$.*
2. Affine pitch is constant along $\mathbf{h}(s)$.

Proof. 1. Let $(t + u\mathbf{I})\mathbf{\Phi}$ be a normalized logarithm of $\mathbf{h}$. Then

$$\begin{aligned}\underline{\mathbf{g}}(\mathbf{h}) &= \mathbf{g}e^{(t+u\mathbf{I})\mathbf{\Phi}}\widetilde{\mathbf{g}} \\ &= e^{(t+u\mathbf{I})(\mathbf{g}\mathbf{\Phi}\widetilde{\mathbf{g}})} \\ &= e^{(t+u\mathbf{I})\underline{\mathbf{g}}(\mathbf{\Phi})}\end{aligned}$$

Here we have used the definition of the exponential function and the fact the scalars and pseudoscalars commute with bivectors. This shows that $(t + u\mathbf{I})\underline{\mathbf{g}}(\mathbf{\Phi})$ is a normalized logarithm of $\underline{\mathbf{g}}(\mathbf{h})$.The homogeneous pitch is clearly preserved.

2. By the lemma, $\mathbf{h}(s)$ is a rotor with normalized logarithm $(st + su\mathbf{I})\mathbf{\Phi}$. Clearly the affine pitch $su : st = u : t$ is constant along the curve. □

Remark 140. This definition of affine pitch agrees with the traditional one for pitch in euclidean line geometry (e.g., [PW01], §3.1). It is intuitively obvious that when a rotor undergoes an isometric motion, the amount of rotation and translation experienced by the transformed axis $\mathbf{\Phi}$ must equal that of the untransformed one. Furthermore, two rotors which result from the exponentiation of the same bivector (but for different values of time) will also preserve the proportion of rotation to translation.

7.10.5 Screw motions

We can now characterize screw motions as we anticipated at the beginning of this discussion:

Corollary 141. *A rotor $\mathbf{g}$ is a screw motion $\iff$ $\langle\mathbf{g}\rangle_2$ is non-simple.*

Proof. Let $\mathbf{\Xi} = \langle\mathbf{g}\rangle_2$. By the theorem, $\mathbf{g}$ has logarithm $(t + u\mathbf{I})\mathbf{\Phi}$. It's clear from Def. 125 that $\mathbf{g}$ is a screw motion $\iff$ $t \neq 0$ and $u \neq 0$. On the other hand, (7.27) shows that $\mathbf{\Xi}$ lies in the line complex pencil spanned by the axis pair $\mathbf{\Phi}$ and $\mathbf{\Phi}^\perp$. By the previous remark, $\mathbf{\Phi} \wedge \mathbf{\Phi}^\perp = 0$ only if $\mathbf{I}^2 = -1$ and $\mathbf{\Phi}$ is ideal. In all other cases $\mathbf{\Phi}$ and $\mathbf{\Phi}^\perp$ span a regular bivector pencil, so $\mathbf{\Xi}$ is different from either of $\mathbf{\Phi}$ and $\mathbf{\Phi}^\perp$, hence non-simple, exactly when $t \neq 0$ and $u \neq 0$. □

7.10.5.1 Classification of 3D Isometries The factorization given by Thm. 134 into two commuting rotations allows us to apply the classification of isometries from Sect. 6.3.2.2 also in the 3D case. Each 3D rotator naturally corresponds to some 2D type (obtained by slicing its axis by any orthogonal plane). One obtains thereby two 2D types for a given 3D isometry. For $\mathbf{I}^2 = 1$, both are elliptic rotations. For $\mathbf{I}^2 = 0$, one is elliptic and one is parabolic; and for $\mathbf{I}^2 = -1$, either one is elliptic and one is hyperbolic, or both are parabolic. Since the latter two axes intersect, their sum is also a line, hence the rotor is a rotator. Thus, there are three types of non-intersecting axis pairs, one for each metric, each of which represents the generic screw motion in that metric. The other types of isometries are related to cases in which one or the other of t or u in the logarithm are zero, and yield a pure rotator, which can be classified according to the 2D classification.

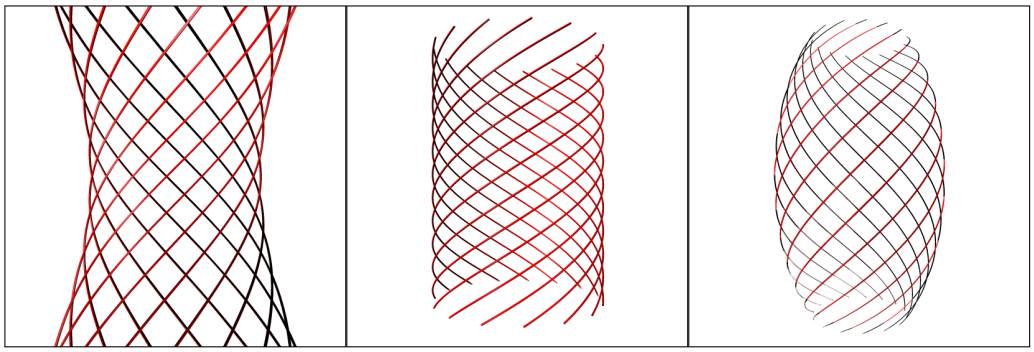

Fig. 7.5 Screw motions in the three classical geometries: elliptic, euclidean, hyperbolic.

7.10.5.2 Comparison of screw motions in different metrics Fig. 7.5 illustrates the difference between the screw motions in the three metrics. The screw motions are all of the form $\mathbf{g} = e^t\mathbf{\Phi}$ where $\mathbf{\Phi} = \mathbf{e}_{01} + .5\mathbf{e}_{23}$. This is a bivector which has as axis $\mathbf{e}_{23}$, the vertical z-axis. $\mathbf{e}_{01}$ is an axis in the non-euclidean cases and a secondary axis in the euclidean case (in this case it is the ideal horizon line, and represents a vertical translation). By the above discussion, the pitch of these screw motions is in every case .5. The figure shows the orbit of 15 points on a circle $\mathcal{C}$ of radius .5 lying in the $(x = y = 0)$ plane centered on $\mathbf{E}_0$. The orbit of a point $\mathbf{P} \in \mathcal{C}$ consists of points of the form $\underline{g(t)}(\mathbf{P})$ for t-values in $t \in [-1.5, 1.5]$. Finally, all three images are viewed from approximately the same distance with a field of view of 90 degrees. It is typical that in the elliptic case one cannot see the full extent of the curves.

These curves, in every metric, lie on a surface equidistant from the axis $\mathbf{e}_{23}$. In the elliptic case this is a hyperboloid; in the euclidean case, a cylinder; and in the hyperbolic case, an ellipsoid. In the elliptic case, the surface is also equidistant from the axis $\mathbf{e}_{01}$. Such an equidistant surface is called a *Clifford torus* and, as a submanifold of $\mathbf{Ell}^3$, has curvature 0, that is, is a euclidean torus in elliptic space ([Kle26]).

7.11 Clifford translations and euclidean translations

We have already mentioned in Sect. 7.4.1 that in elliptic space there are an exceptional set of isometries, the Clifford translations. We touched again on the same topic in Sect. 7.7.2 where we introduced Clifford bivectors. Here we want to discuss this topic in more detail and to connect Clifford translations to the the earlier representation, also mentioned in Sect. 7.4.1, involving left- and right-quaternion multiplication only. We show how the Clifford translations can be represented in $\mathbf{Spin}^3_{+1}$, work out an example involving Clifford parallels, and then close with a discussion of euclidean translations.

7.11.1 Clifford translations

The original representation of elliptic space via quaternions implemented isometries via left and right multiplication by quaternions (Sect. 7.4.1.1). Let

$$\mathbf{h} = \cos\theta + \sin\theta(x_0\mathbf{i} + y_0\mathbf{j} + z_0\mathbf{k})$$

be a unit quaternion (so $x_0^2 + y_0^2 + z_0^2 = 1$), and $\mathbf{P} = w + x\mathbf{i} + y\mathbf{j} + z\mathbf{k}$ be a second unit quaternion (so $x^2 + y^2 + z^2 + w^2 = 1$. Then, identifying the unit quaternions with a double covering of $\mathbf{Ell}^3$, $\mathbf{P} \to \mathbf{hP}$ is an isometry of elliptic space, a left Clifford translation; $\mathbf{P} \to \mathbf{Ph}$ is a distinct isometry, a right Clifford translation.

How are the same isometries be represented in Cl^3_1 as a sandwich $\underline{\mathbf{g}}$? Define the following elements:

$$\mathbf{\Phi} := \qquad x_0\mathbf{e}_{23} + y_0\mathbf{e}_{31} + z_0\mathbf{e}_{12} \tag{7.33a}$$

$$\mathbf{\Phi}^\perp := \mathbf{\Phi I} = x_0\mathbf{e}_{01} + y_0\mathbf{e}_{02} + z_0\mathbf{e}_{03} \tag{7.33b}$$

$$\mathbf{g}_o := e^{\frac{\theta}{2}\mathbf{\Phi}} = \cos\frac{\theta}{2} + \sin\frac{\theta}{2}\mathbf{\Phi} \tag{7.33c}$$

$$\mathbf{g}^-_\infty := e^{-\frac{\theta}{2}\mathbf{\Phi}^\perp} = \cos\frac{\theta}{2} - \sin\frac{\theta}{2}\mathbf{\Phi}^\perp \tag{7.33d}$$

$$\mathbf{g}^+_\infty := e^{\frac{\theta}{2}\mathbf{\Phi}^\perp} = \cos\frac{\theta}{2} + \sin\frac{\theta}{2}\mathbf{\Phi}^\perp \tag{7.33e}$$

$$\mathbf{g}_l := e^{\frac{\theta(1-\mathbf{I})}{2}\mathbf{\Phi}} = \mathbf{g}^-_\infty\mathbf{g}_o = \mathbf{g}_o\mathbf{g}^-_\infty \tag{7.33f}$$

$$\mathbf{g}_r := e^{\frac{\theta(1+\mathbf{I})}{2}\mathbf{\Phi}} = \mathbf{g}^+_\infty\mathbf{g}_o = \mathbf{g}_o\mathbf{g}^+_\infty \tag{7.33g}$$

Here $\mathbf{\Phi}$ is any line; we choose the coordinate system so it passes through the origin, with direction vector (x_0, y_0, z_0). $\mathbf{g}_o$ is a rotator around $\mathbf{\Phi}$. $\mathbf{g}^-_\infty$ and $\mathbf{g}^+_\infty$ are rotators of the same angle, around the polar line, through opposite and equal angles. $\mathbf{g}_l$ and $\mathbf{g}_r$, the product of $\mathbf{g}_o$ with $\mathbf{g}^-_\infty$ and $\mathbf{g}^+_\infty$, resp., have bivector parts which are left (resp., right) Clifford bivectors:

$$\langle \mathbf{g}_l \rangle_2 = -\sin(\theta)\frac{1-\mathbf{I}}{2}\mathbf{\Phi} = -\frac{\sin(\theta)}{2}(x_0\mathbf{e}_{01} + y_0\mathbf{e}_{02} + z_0\mathbf{e}_{03} + z_0\mathbf{e}_{12} + y_0\mathbf{e}_{31} + x_0\mathbf{e}_{23})$$
$$\langle \mathbf{g}_r \rangle_2 = -\sin(\theta)\frac{1+\mathbf{I}}{2}\mathbf{\Phi} = -\frac{\sin(\theta)}{2}(x_0\mathbf{e}_{01} + y_0\mathbf{e}_{02} + z_0\mathbf{e}_{03} - z_0\mathbf{e}_{12} - y_0\mathbf{e}_{31} - x_0\mathbf{e}_{23})$$

A straightforward calculation confirms that $\underline{\mathbf{g}_l}$ is the sandwich corresponding to the left Clifford translation, and $\underline{\mathbf{g}_r}$, the sandwich operator corresponding to the right Clifford translation. We call $\frac{1-\mathbf{I}}{2}\mathbf{\Phi}$ the left Clifford bivector associated to $\mathbf{\Phi}$ and write $\mathbf{\Phi}_l$; $\mathbf{\Phi}_r$ is similarly defined.

Using this representation of Clifford translations, we can carry out an analysis of the classical problems associated to such translations. We first define the Clifford parallels associated to a Clifford bivector, and prove that they have the desired invariance properties.

Definition 142. Given a right [left] Clifford bivector $\mathbf{\Xi}$, a *right [left] Clifford parallel belonging to* $\mathbf{\Xi}$ is a simple bivector $\mathbf{\Phi}$ such that $(1+\mathbf{I})\mathbf{\Phi} = \mathbf{\Xi}$ $[(1-\mathbf{I})\mathbf{\Phi} = \mathbf{\Xi}]$. Denote the set of all such parallels with $\mathcal{R}_{\mathbf{\Xi}}$ $[\mathcal{L}_{\mathbf{\Xi}}]$.

Remark 143. A Clifford parallel for $\mathbf{\Xi}$ is an axis for $\mathbf{\Xi}$.

We show that Clifford parallels of a Clifford bivector $\mathbf{\Xi}$ are invariant under the Clifford translations generated by $\mathbf{\Xi}$.

Theorem 144. *For $\mathbf{\Phi}$ a Clifford parallel belonging to a Clifford bivector $\mathbf{\Xi}$, $\underline{e^{t\mathbf{\Xi}}}(\mathbf{\Phi}) = \mathbf{\Phi}$.*

Proof. $\mathbf{\Xi\Phi} = (1+\mathbf{I})\mathbf{\Phi\Phi} = \mathbf{\Phi}(1+\mathbf{I})\mathbf{\Phi} = \mathbf{\Phi\Xi}$ since pseudoscalars commute with bivectors. Hence $\underline{e^{t\mathbf{\Xi}}}(\mathbf{\Phi}) = e^{t\mathbf{\Xi}}\mathbf{\Phi}e^{-t\mathbf{\Xi}} = e^{t\mathbf{\Xi}}e^{-t\mathbf{\Xi}}\mathbf{\Phi} = \mathbf{\Phi}$. □

Theorem 145. *Every left Clifford translation commutes with every right Clifford translation.*

Proof. A left Clifford translation $\mathbf{g}_l$ is of the form $e^{t\mathbf{\Xi}}$ for a left Clifford bivector $\mathbf{\Xi}$; a right Clifford translation $\mathbf{g}_r$ is of the form $e^{u\mathbf{\Phi}}$ for a right Clifford bivector $\mathbf{\Phi}$. By Lemma 115, $\mathbf{\Xi\Phi} = 0 = \mathbf{\Phi\Xi}$, so

$$\mathbf{g}_l\mathbf{g}_r = e^{t\mathbf{\Xi}}e^{u\mathbf{\Phi}} = e^{t\mathbf{\Xi}+u\mathbf{\Phi}} = e^{u\mathbf{\Phi}+t\mathbf{\Xi}} = e^{u\mathbf{\Phi}}e^{t\mathbf{\Xi}} = \mathbf{g}_r\mathbf{g}_l$$

Here we have used the commutativity of $\mathbf{\Xi}$ and $\mathbf{\Phi}$ to apply the exponential rule $e^a e^b = e^{a+b}$. □

Next we turn to showing that the set of Clifford parallels belonging to a Clifford bivector form an elliptic line congruence. We restrict attention to a right Clifford bivector; analogous results hold for a left Clifford bivector.

Lemma 146. *For a right Clifford bivector $\mathbf{\Xi}$ and another bivector $\mathbf{\Phi}$, $\mathbf{\Xi}\cdot\mathbf{\Phi} = \mathbf{\Xi}\vee\mathbf{\Phi}$.*

Proof. From (7.12), $\mathbf{\Xi I}\vee\mathbf{\Phi} = \mathbf{\Xi}\cdot\mathbf{\Phi}$. By Def. 114, $\mathbf{\Xi I} = \mathbf{\Xi}$. □

Lemma 147. *If $\mathbf{\Xi}$ and $\mathbf{\Phi}$ are right Clifford bivectors such that $\mathbf{\Xi}\wedge\mathbf{\Phi} = 0$, and $\mathbf{\Theta}$ is a Clifford parallel belonging to $\mathbf{\Phi}$, then $\mathbf{\Xi}\wedge\mathbf{\Theta} = 0$.*

Proof. Substituting $\mathbf{\Phi} = (1+\mathbf{I})\mathbf{\Theta}$ yields $0 = \mathbf{\Xi} \wedge (1+\mathbf{I})\mathbf{\Theta} = \mathbf{\Xi} \wedge \mathbf{\Theta} + \mathbf{\Xi} \wedge (\mathbf{\Theta}\mathbf{I}) = \mathbf{\Xi} \wedge \mathbf{\Theta} + (\mathbf{\Xi} \cdot \mathbf{\Theta})\mathbf{I} = 2\mathbf{\Xi} \wedge \mathbf{\Theta}$, where we have applied the previous lemma to get the final equality. □

We are now prepared to show that $\mathcal{R}_{\mathbf{\Xi}}$ is an elliptic line congruence. For, the 2-plane $\mathcal{C}_l$ with Plücker signature $(---)$ has an elliptic metric; the polar line of $\mathbf{\Xi}$ with respect to this metric is a line $\mathfrak{B}$ of right Clifford bivectors. The Plücker polar of this elliptic bivector pencil is, by definition, an elliptic congruence. The following theorem describes this congruence more exactly:

Theorem 148. $\mathfrak{B}^{\vdash} = \mathcal{R}_{\mathbf{\Xi}}$.

Proof. By definition, each point of $\mathfrak{B}$ is in involution to $\mathbf{\Xi}$, hence, by the lemma, to each Clifford parallel of $\mathbf{\Xi}$. Thus, $\mathcal{R}_{\mathbf{\Xi}} \subset \mathfrak{B}^{\vdash}$. We now show $\mathfrak{B}^{\vdash} \subset \mathcal{R}_{\mathbf{\Xi}}$. If $\mathbf{\Phi} \in \mathfrak{B}^{\vdash}$ is simple, we need to show that $\mathbf{\Phi}$ is a Clifford parallel, i.e., $(1+\mathbf{I})\mathbf{\Phi} \equiv \mathbf{\Xi}$. By assumption, $\mathbf{\Psi} \wedge \mathbf{\Phi} = 0$ for $\mathbf{\Psi} \in \mathfrak{B}$. By the first lemma, $\mathbf{\Psi} \cdot \mathbf{\Phi} = 0$ also. But then $0 = (\mathbf{\Psi} \cdot \mathbf{\Phi}) = \mathbf{\Psi} \vee (\mathbf{\Phi}\mathbf{I})$, which implies $\mathbf{\Phi}\mathbf{I} \in \mathfrak{B}^{\vdash}$. Then so is $(1+\mathbf{I})\mathbf{\Phi}$. But this is a right Clifford bivector, and there is only one such element in $\mathcal{C}_r$, namely, $\mathbf{\Xi}$. □

We conclude with a pair of simple corollaries.

Corollary 149. *Let $\mathbf{\Xi}$ be a Clifford bivector, and $\underline{e^{t\mathbf{\Xi}}}$ the one-parameter family of associated Clifford translations. Then the orbit of a point $\mathbf{P} \in \mathbf{Ell}^3$ under this family lies on a line.*

Proof. By Thm. 148, there is a unique Clifford parallel to $\mathbf{\Xi}$ passing through $\mathbf{P}$. By Thm. 144, such a Clifford parallel is invariant under the associated Clifford translations. Hence, the image of $\mathbf{P}$ is constrained to lie on this line. □

Corollary 150. *A right [left] Clifford translation is an elliptic screw motion with homogeneous pitch 1 [-1].*

Proof. Apply Def. 142 and Def. 137 to the logarithm of $\mathbf{\Xi}$ provided by Thm. 133. □

The above discussion of Clifford translations is intended to give a flavor of how one can establish classical results such as contained in [Bla42], Part I, and [PW01], §8.2, within the framework of bivectors and rotors in Cl^3_1. A more detailed analysis however exceeds the scope of this study.

Remark 151. **Comparison.** In the older representation of elliptic isometries via left- and right-quaternion multiplication, the simplest isometry is a Clifford translation. In Cl^3_1, on the other hand, the simplest isometry is a rotation. Consequently, we built a Clifford translation above out of two rotators in two polar lines. In the quaternion approach, one builds rotations out of Clifford translations: **gPh** is a rotation when the translation distances of **g** and **h** are the same. At a first glance, it would appear that the traditional approach using left- and right-quaternion multiplication provides a simpler, elegant representation for elliptic isometries, since it gives priority to Clifford translations, which do seem more essential than rotations for elliptic space. On the other hand, the bivectors and rotors which represent Clifford parallels and translations in Cl^3_1 have an immediate geometric interpretation which the pure quaternion approach lacks.

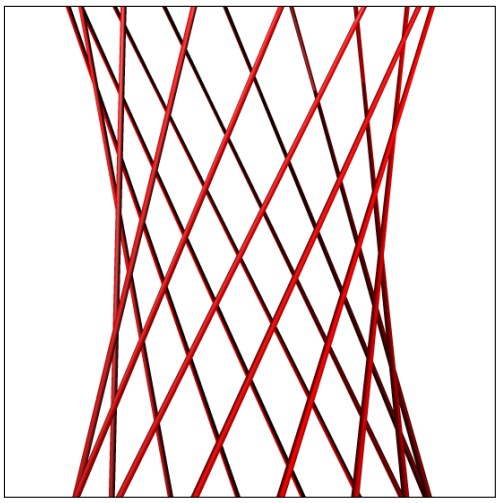

Fig. 7.6 An elliptic screw motion with unit homogeneous pitch is a Clifford translation. The one shown here has homogeneous pitch 1, otherwise it is identical to that shown in Fig. 7.5. One sees that the orbits of points are lines, arranged on a hyperboloid (a so-called Clifford torus).

7.11.2 Euclidean translations

Sect. 7.4.1 observed similarities between Clifford parallels and euclidean parallels, and Clifford translations and euclidean translations. As Klein pointed out in [Kle26], §8.5, this is not accidental, since under the limiting process that yields euclidean geometry beginning with elliptic geometry, the Clifford parallels (translations) degenerate into euclidean parallels (translations) in the limit. The Clifford parallels corresponding to a Clifford bivector $(1 \pm \mathbf{I})\mathbf{\Xi}$ become euclidean parallels passing through the euclidean ideal point $-\mathbf{e}_0 \wedge \mathbf{\Xi} = x\mathbf{E}_1 + y\mathbf{E}_2 + z\mathbf{E}_3$, and the translations become euclidean translations around the ideal line $x\mathbf{e}_{01} + y\mathbf{e}_{02} + z\mathbf{e}_{03}$, conjugate to this point in the elliptic metric of the ideal plane.

Euclidean translations exhibit several distinctive features which we discuss in the following sections.

7.11.2.1 The analysis of a euclidean translation Let $(t+u\mathbf{I})\mathbf{\Phi}$ be the logarithm of a euclidean translation. It is always possible to choose $\mathbf{\Phi}$ so that $\mathbf{I}\mathbf{\Phi} = 0$, that is $\mathbf{\Phi}$ is an ideal line. Then $\mathbf{\Phi}$ is its own axis. In this case, the value of u in the logarithm can be arbitrary: $(t + u\mathbf{I})\mathbf{\Phi} = t\mathbf{\Phi}$. $\mathbf{\Phi} = x_1\mathbf{e}_{01} + y_1\mathbf{e}_{02} + z_1\mathbf{e}_{03}$ is normalized, so $\|\mathbf{\Phi}\|_\infty^2 = x_1^2 + y_1^2 + z_1^2 = 1$. Then $\mathbf{g}_t = e^{t\mathbf{\Phi}} = 1+t\mathbf{\Phi}$. Let $\mathbf{P}$ be an arbitrary euclidean point $\mathbf{P} := \mathbf{E}_0+x\mathbf{E}_1+y\mathbf{E}_2+z\mathbf{E}_3$. Calculate the sandwich:

$$e^{t\mathbf{\Phi}}\mathbf{P}e^{-t\mathbf{\Phi}} = \mathbf{E}_0 + (x - 2tx_1)\mathbf{E}_1 + (y - 2ty_1)\mathbf{E}_2 + (z - 2tz_1)\mathbf{E}_3$$

This is a euclidean translation of distance $2t$ with direction vector $(-x_1, -y_1, -z_1)$. One of the peculiarities of euclidean translation rotor $\mathbf{g}$ is that left- and right-multiplication by $\mathbf{g}$ gives half the translation:

$$2\mathbf{g}\mathbf{P} = 2\mathbf{P}\widetilde{\mathbf{g}} = \mathbf{g}\mathbf{P}\widetilde{\mathbf{g}}$$

Remark 152. When one constructs the logarithm of a euclidean translation using a proper axis, then $t = 0$ and $\mathbf{\Phi I}$ is the ideal axis. Since the ideal axis is the simplest representative of the translation, it is preferable to work directly with the ideal axis instead of a proper axis. This is always possible, that is, one can require that $t \neq 0$ in the logarithm. This effectively forces euclidean translations to be handled as in the preceding paragraph, and avoids the illusory multiplicity provided by the proper axes.

7.11.2.2 Invariant line $\neq$ axis If $\mathbf{\Xi}$ is the bivector part of a rotor $\mathbf{g}$, the theorems above show that any axis of $\mathbf{\Xi}$ is invariant under the isometry $\underline{\mathbf{g}}$. Is the converse true? By the above discussion, a euclidean translation has rotor $\mathbf{g} = 1 + t(x_1\mathbf{e}_{01} + y_1\mathbf{e}_{02} + z_1\mathbf{e}_{03})$. Let $\mathbf{\Theta} = a\mathbf{e}_{01} + b\mathbf{e}_{02} + c\mathbf{e}_{03}$ be a euclidean ideal line. A quick calculation confirms that $\underline{\mathbf{g}}(\mathbf{\Theta}) = \mathbf{\Theta}$. Hence, all ideal lines are invariant under a euclidean translation, but none are axes of the rotor.

7.12 The continuous interpolation of the metric polarity

We close our discussion of three-dimensional geometry with an intriguing metric-related motion, which also illustrates the power of the Clifford algebra approach to represent heterogeneous concepts within a unified framework. It will also shed light on the significance of elements of $Cl^{n+}_\kappa \setminus \mathbf{Spin}^n_{+\kappa}$.

The polarity on the metric quadric (Thm. 32) is a correlation, that is, it maps points to planes and vice-versa. At first glance it would not appear possible to define a continuous transformation of Cl^n_κ which interpolates between a geometric configuration and its image under the metric polarity. The first step is to restrict the allowable configurations to a set which is mapped to itself under a correlation.

7.12.1 Surface elements

Definition 153. A *surface element* is a pair $\mathfrak{A} := \mathbf{a} + \mathbf{A}$ where $\mathbf{a}$ is a proper 1-vector, $\mathbf{A}$ is a proper n-vector, $\mathbf{a} \wedge \mathbf{A} = 0$. Denote the set of all surface elements by $\mathcal{S}$.

Note that $\mathcal{S}\mathbf{I} \subset \mathcal{S}$ with equality exactly when $\mathbf{I}^2 \neq 0$. We assume for the following discussion that $\mathbf{I}^2 = -1$ and $n = 3$. The construction generalizes directly to arbitrary n. $\mathbf{I}^2 = 1$ exhibits imaginary behavior which make it less suitable for an introductory treatment.

For a given surface element $\mathfrak{A} = \mathbf{a} + \mathbf{A}$, $\mathfrak{A}\mathbf{I} = \mathbf{a}\mathbf{I} + \mathbf{A}\mathbf{I} =: \widehat{\mathbf{A}} + \widehat{\mathbf{a}} = \widehat{\mathfrak{A}}$ is another surface element. We further assume that $\mathfrak{A}$ is normalized so that $\mathbf{a}^2 = -\mathbf{A}^2$. This is possible since both vectors are proper.

7.12.2 Definition of the interpolation

Define a one-parameter family of maps $\Theta_t : \mathfrak{S} \to \mathfrak{S}$ by $\Theta_t(\mathbf{X}) := \mathbf{X}(\cos t + \sin(t)\mathbf{I})$ for $t \in [0, \pi]$. Then for a surface element $\mathfrak{A}$:

$$\begin{aligned}\Theta_t(\mathfrak{A}) &= \cos t\mathfrak{A} + \sin(t)\widehat{\mathfrak{A}} \\ &= (\cos(t)\mathbf{a} + \sin(t)\mathbf{AI}) + (\cos(t)\mathbf{A} + \sin(t)\mathbf{aI}) \\ &=: \mathbf{a}_t + \mathbf{A}_t\end{aligned}$$

$\Theta_t(\mathfrak{A})$ is, as claimed, a surface element:

$$\begin{aligned}(\mathbf{a}_t + \mathbf{A}_t) \wedge (\mathbf{a}_t + \mathbf{A}_t) &= \cos^2(t)(\mathbf{a} \wedge \mathbf{A}) + \sin^2(t)(\mathbf{AI} \wedge \mathbf{aI}) + \cos(t)\sin(t)(\mathbf{a} \wedge \mathbf{aI} + \mathbf{AI} \wedge \mathbf{a}) \\ &= \cos(t)\sin(t)(\mathbf{a} \wedge \mathbf{aI} + \mathbf{AI} \wedge \mathbf{a}) \\ &= \cos(t)\sin(t)(\mathbf{a}^2 - \mathbf{A}^2) = 0\end{aligned}$$

Then Θ_t, as claimed, maps $\mathcal{S}$ to itself. At $t = 0$ and $t = \pi$, it is the identity map on a surface element, while at $t = \frac{\pi}{2}$, its value is the polar surface element. Hence, it represents the promised continuous interpolation of the polarity.

To understand the intermediate path better, define the axis $\mathbf{\Lambda} := \mathbf{a} \wedge \widehat{\mathbf{A}}$ and the spear $\mathbf{\Psi} = \mathbf{A} \vee \widehat{\mathbf{a}}$. Then a direct calculation shows that $\mathbf{a}_t \wedge \mathbf{\Lambda} = 0$ and $\mathbf{A}_t \vee \mathbf{\Psi} = 0$. In words: the surface element $\mathbf{a}_t + \mathbf{A}_t$ moves so that the plane $\mathbf{a}_t$ rotates around the axis $\mathbf{\Lambda}$ while the point $\mathbf{A}$ moves along the spear $\mathbf{\Psi}$. Thus, the motion is a linear one.

Through a direct calculation one can verify that at $t = \frac{\pi}{4}$ and $t = \frac{3\pi}{2}$, $\mathbf{a}_t^2 = \mathbf{A}_t^2 = 0$: the surface element becomes ideal. The points lie on the ideal sphere, the planes are tangent to it. This is singular position of the interpolation since $\Theta_t(\mathcal{S})$ collapses onto a 2-dimensional surface at these values.

The original configuration lies in hyperbolic space, while the polar configuration lies in polar hyperbolic space. The time values $t = \frac{\pi}{4}$ and $t = \frac{3\pi}{2}$ represent the transitions between these two spaces.

7.12.2.1 Examples

1. **Action on a plane bundle.** Consider a plane bundle in the proper point $\mathbf{P}$. This is a family of ∞^2 surface elements all sharing the same point. The polar of this bundle is the improper plane field $\mathbf{P}^\perp$, ∞^2 surface elements all lying in the same plane. At any time t, these surface elements determine a surface. One can show with an easy calculation that this is a hyperbolic sphere centered at $\mathbf{P}$. See Fig. 7.7.
2. **Action on lines.** The map Θ_t is well-defined not just on $\mathfrak{S}$ but on the full algebra Cl^3_{-1}. The subalgebra $Cl^{3\dagger}_{-1}$ is mapped to itself, as is $\mathbf{P}(\bigwedge^2)$. A bivector $\mathbf{\Xi}$ is mapped to an element of the pencil spanned by $\mathbf{\Xi}$ and $\mathbf{\Xi}^\perp$. This will be a non-simple bivector except for $t = 0$ and $t = \pi$. The ∞^3 surface elements centered on points of $\mathbf{\Xi}$ (lying in planes of $\mathbf{\Xi}$) are mapped at $t = \pi$ to the surface elements of $\mathbf{\Xi}^\perp$. Those lying in a plane $\mathbf{a}$ and centered on a point $\mathbf{P}$ of $\mathbf{\Xi}$ move under Θ_t to surface elements centered on the polar point $\mathbf{a}^\perp$ and lying in the plane $\mathbf{P}^\perp$, of $\mathbf{\Xi}^\perp$. One can show that all the surface elements of $\mathbf{\Xi}$ at time t envelop an *equi-distant* surface around $\mathbf{\Xi}$, all of whose points lie the same distance from $\mathbf{\Xi}$.

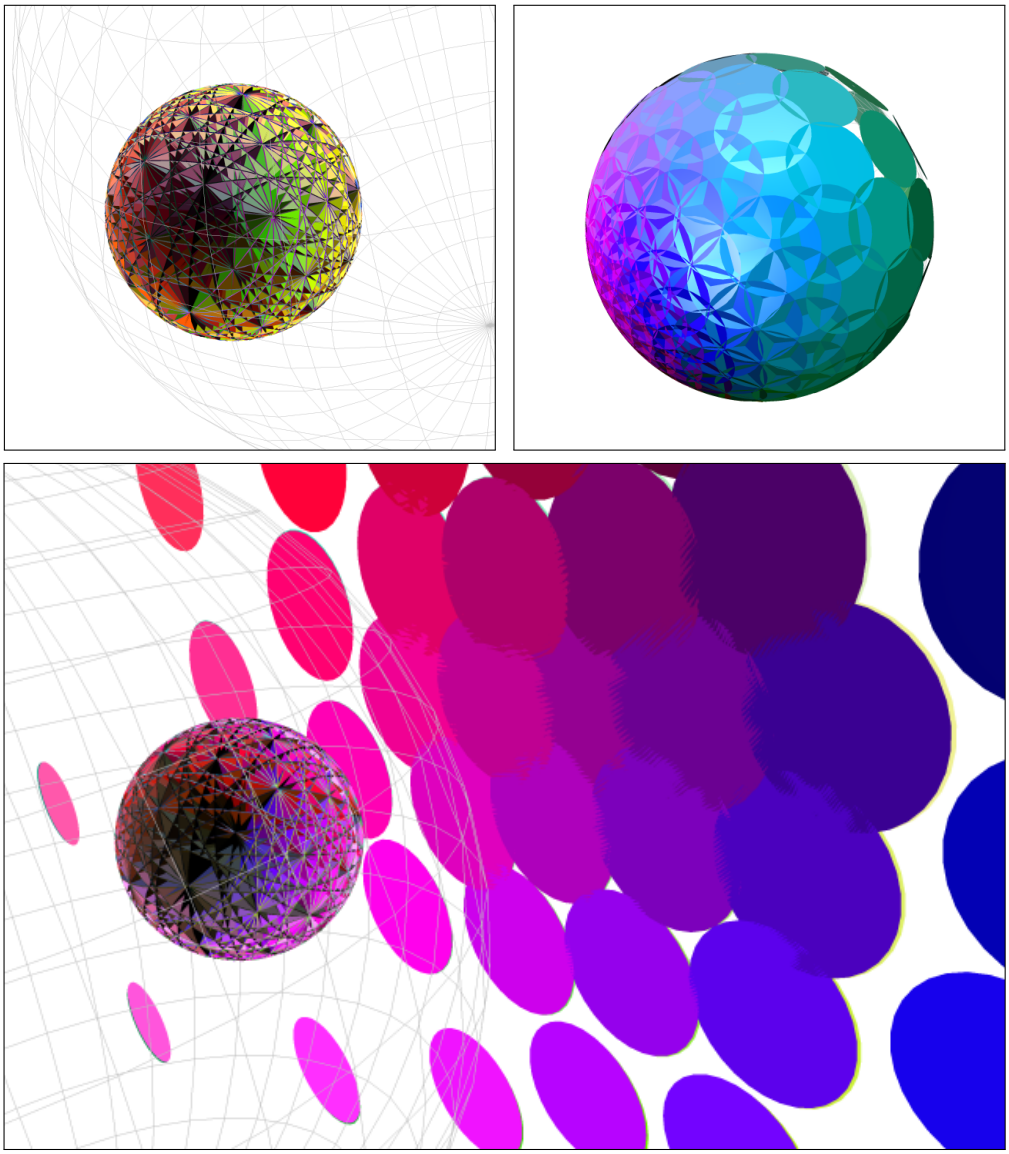

Fig. 7.7 Three views of the action of Θ_t on a plane bundle, for $t = 0$, $t = .5$, $t = 1$. At $t = 0$ and $t = 1$ each surface element is double covered, with two different oriented surface elements. The right-most figures shows both $t = 0$ and $t = 1$.

7.12.3 Relation to $\mathbf{Spin}^n_{+\kappa}$

Suppose $\mathbf{q} \in Cl^{3+}_\kappa$. Then $\mathbf{q}\widetilde{\mathbf{q}} = a + b\mathbf{I} =: \mathbf{z} \in Cl^{3\dagger}_\kappa$. If $\mathbf{z}$ has a non-zero square root $\mathbf{w}$, then $\mathbf{q}\mathbf{w}^{-1} = \mathbf{g} \in \mathbf{Spin}^3_{+\kappa}$. Consider the sandwich operator defined by $\mathbf{q}$, acting on a k-vector $\mathbf{X}$:

$$\begin{aligned}\underline{\mathbf{q}}\mathbf{X} &= \mathbf{q}\mathbf{X}\widetilde{\mathbf{q}} \\ &= \mathbf{g}\mathbf{w}\mathbf{X}\mathbf{w}\widetilde{\mathbf{q}} \\ &= (-1)^k\underline{\mathbf{g}}(\mathbf{X})\mathbf{z} \equiv \underline{\mathbf{g}}(\mathbf{X})\mathbf{z}\end{aligned}$$

We see that a sandwich by an arbitrary element of Cl^{3+}_κ can be factored as multiplication by an element of $Cl^{3\dagger}_\kappa$ (that has a square root) times a rotor isometry. For $\kappa = -1$, all elements of $Cl^{3\dagger}_\kappa$ have square roots. Due to this decomposition, we can study multiplication by an arbitrary $\mathbf{z} \in Cl^{2\dagger}_\kappa$ separately from the rotor isometry.

We can furthermore assume $\|\mathbf{z}\| = 1$ since we are working projectively. Then there exists $t \in [0, \pi]$ such that $\mathbf{z} = \cos t + \sin t\mathbf{I}$, and we see $\mathbf{X}\mathbf{z} = \Theta_t(\mathbf{X})$. Hence there is a one-dimensional family of sandwich operators in Cl^{3+}_κ which preserve the metric quadric while mapping an element $\mathbf{X}$ to a linear combination of $\mathbf{X}$ and $\mathbf{X}^\perp$. This makes clear why the condition $\mathbf{g}\widetilde{\mathbf{g}} = 1$ is required in order that $\underline{\mathbf{g}}$ is an isometry.

Remark 154. The continuous interpolation on the metric quadric can be applied to the integral curves shown in Fig. 6.4. Recall that the latter represent orbits of points under the rotor curves $e^{t\mathbf{P}} \subset \mathbf{Spin}^2_{+\kappa}$. If one imagines the curves also equipped with all their tangent vectors, then they are curves of surface elements, and Θ_t (more precisely: its 2D analog) permutes these curves among themselves. Furthermore, the two flows commute (since elements of $Cl^{n\dagger}_\kappa$ commute (up to projective equivalence) with other algebra elements.

7.13 Guide to the Literature

For background material on Sect. 7.2, the review of projective line geometry, see[PW01]. Chapters 2 and 3 contain a modern, more detailed treatment of the subject (intermixed with some euclidean material we handle later). Here we have restricted attention to results necessary for the sequel.

Much of the content of this chapter can be traced back to the theory of biquaternions, whose primary inventor was Clifford ([Cli82c]). Clifford's early death prevented a detailed development; this was achieved most prominently by Eduard Study in [Stu91] and [Stu03]. In these works Study worked out in rich detail the structure which in modern form appears as the even subalgebra Cl^{3+}_κ, with focus on the case $\kappa = 0$.

Study avoided using the term quaternion; the structure he described has nonetheless become known as the *dual quaternions*. As noted above in Sect. 7.6, his original use of "dual" included all three metric possibilities. His dual parameter ϵ maps to the pseudoscalar $\mathbf{I}$. A full description of the correspondence between the two systems lies outside the scope of this work, nor is the full scope of [Stu03] reflected in material presented here.

[Zie85] gives an excellent, differentiated survey of the historical development that led up to Study's work. Möbius, Plücker, Hamilton, Klein, and Clifford were Study's most important predecessors; he and Ball ([Bal00]) had a relationship based on mutual appreciation. Weiss, a student of Study's, wrote a concise introduction [Wei35] to Study's investigations which can be recommended. For beginners, [Bla54] provides a simpler introduction to Study's approach.

The main ingredient that Study's approach lacked was the graded structure of the exterior algebra. Study was familiar with and admiring of Grassmann's work ([Gra44]) but Study did not bring his biquaternions into direct connection with the exterior algebra. However, Study himself appears to be aware of the possibility of extending his work within a more comprehensive algebraic structure. He remarked at the end of [Stu03] (p. 595, translated by the author):

> The elementary geometric theory, that hovers thus before us, will surpass the construction possibilities of the quaternions, to the same degree that the geometry of dynamen surpasses the addition of vectors. The accessory analytic machinery will consist of a system of compound quantities, with eight, or better yet, with *sixteen* units. {Study's italics!}

It seems likely that Cl^3_κ is in fact the 16-dimensional algebraic realizations of Study's prophetic inkling.

The modern legacy of biquaternions is varied. Focusing just on euclidean applications, the adaption rate of Cl^3_0 among practitioners is low. Jon Selig, a robotics researcher, presented it in [Sel00] and [Sel05]. He, in turn, discovered the existence of this degenerate Clifford algebra as an exercise in the textbook [Por81], §13.86 ([Sel]), whose motivation can be traced back to [Stu03]. Most modern references that go beyond the use of linear algebra or quaternions, use dual quaternions in more or less original form ([McC90]). For non-euclidean Cayley-Klein spaces, it appears there has been little activity since [Bla42].

Another direction in which the biquaternions have been extended to a 16-dimensional algebra is via the so-called *quadriquaternions* ([Gsc91], which introduce another pair of quaternions to represent points and planes, at the cost of an extra operator to correct commutation relations provided for free by the graded structure of Cl^3_κ.

Blaschke ([Bla42], Part I), and Pottmann and Wallner ([PW01], §8.2), contain related discussions of Clifford translations and Clifford parallels based on left- and right-quaternion multiplication. The former shows clearly the step from quaternion to biquaternion representation. The latter has an abundance of related material.

The continuous interpolation of the metric polarity (Sect. 7.12) was first explored by Locher-Ernst in two articles which are reprinted in [LE70], pp. 55-75. He connects it to a non-euclidean Huygens principle of wave propagation. The same theme was handled in [Gsc91] using quadriquaternions.

Chapter 8
Kinematics

In this chapter we build on the rotor-related results of Chapter 7 to do kinematics: represent isometric motions and their derivatives. The bivectors, as the Lie algebra of the group, naturally play a crucial role, as the first theorem (Thm. 157) shows. We then turn in Sect. 8.2 to a discussion of the use of two coordinate systems, one based in the body and one in space. Thm. 161 describes a transformation rule for derivatives from one coordinate system to another. This yields, when applied to a bivector, the Lie bracket. Applied to the orbit of a point under an isometric motion, this yields a formula for the vector field associated to the motion. We give a novel factorization of this vector field as the composition of two polarities. Finally, we discuss the dual formulation of kinematics based on the projective foundations of our approach.

8.1 Isometric motions

Definition 155. An *isometric motion* is a C^1 path $g : [0,1] \to \mathbf{Spin}^3_{+\kappa}$ with $g(0) = \mathbf{1}$.

Remark 156. The terminology is a bit awkward due to the generality of the treatment; in specific cases one uses naturally the specific terms *euclidean motion*, etc.

Theorem 157. *For an isometric motion* $\mathbf{g}$*,* $\widetilde{\mathbf{g}}\dot{\mathbf{g}}$ *is a bivector.*

Proof. $\widetilde{\mathbf{g}}\dot{\mathbf{g}}$ is in the even subalgebra. For a bivector X, $\tilde{X} = -X$; for scalars and pseudoscalars, $\tilde{X} = X$. Hence it suffices to show $\widetilde{\widetilde{\mathbf{g}}\dot{\mathbf{g}}} = -\widetilde{\mathbf{g}}\dot{\mathbf{g}}$.

$$\begin{aligned} \widetilde{\mathbf{g}}\mathbf{g} &= 1 \\ \dot{(\widetilde{\mathbf{g}}\mathbf{g})} &= 0 \\ \dot{\widetilde{\mathbf{g}}}\mathbf{g} + \widetilde{\mathbf{g}}\dot{\mathbf{g}} &= 0 \\ \widetilde{\dot{\mathbf{g}}}\mathbf{g} + \widetilde{\mathbf{g}}\dot{\mathbf{g}} &= 0 \\ \widetilde{\widetilde{\mathbf{g}}\dot{\mathbf{g}}} &= -\widetilde{\mathbf{g}}\dot{\mathbf{g}} \end{aligned}$$

□

8.2 Coordinate systems

Up til now, we have been considering the behavior of the system at a single, arbitrary moment of time. But if we want to follow a motion over time, then there will be two natural coordinate systems. One, the *body* coordinate system, is fixed to the body and moves with it as the body moves through space. The other, usually called the *space* coordinate system, is the coordinate system of an unmoving observer. Once the motion starts, these two coordinate systems diverge. The following discussion assumes we observe a system as it evolves in time. All quantities are then potentially time dependent; instead of writing $\mathbf{g}(t)$, we continue to write $\mathbf{g}$ and trust the reader to bear in mind the time-dependence.

We use the subscripts X_s and X_c[1] to distinguish whether the quantity X belongs to the space or the body coordinate system. When we consider a isometric motion $\mathbf{g}$ as being applied to the body, then Sect. 5.6 established that the relation between body and space coordinate systems for *any* element $\mathbf{X} \in Cl^3_\kappa$, with respect to a motion $\mathbf{g}$, is given by the sandwich operator:

$$\mathbf{X}_s := \underline{\mathbf{g}}(\mathbf{X}_c) = \mathbf{g}\mathbf{X}_c\widetilde{\mathbf{g}}$$

Definition 158. The *velocity in the body* $\boldsymbol{\Omega}_c := \widetilde{\mathbf{g}}\dot{\mathbf{g}}$, and the *velocity in space* $\boldsymbol{\Omega}_s := \mathbf{g}\boldsymbol{\Omega}_c\widetilde{\mathbf{g}}$.

Remark 159. The situation is graphically depicted in Fig. 8.1. The derivative $\dot{\mathbf{g}}$ is an element of the tangent space $T_{\mathbf{g}}$. In order to produce an element of the Lie algebra this tangent vector has to pulled back to the tangent space of the identity element of the spin group by multiplication by $\mathbf{g}^{-1} = \widetilde{\mathbf{g}}$. Left multiplication produces $\boldsymbol{\Omega}_c$, right multiplication produces $\boldsymbol{\Omega}_s$.

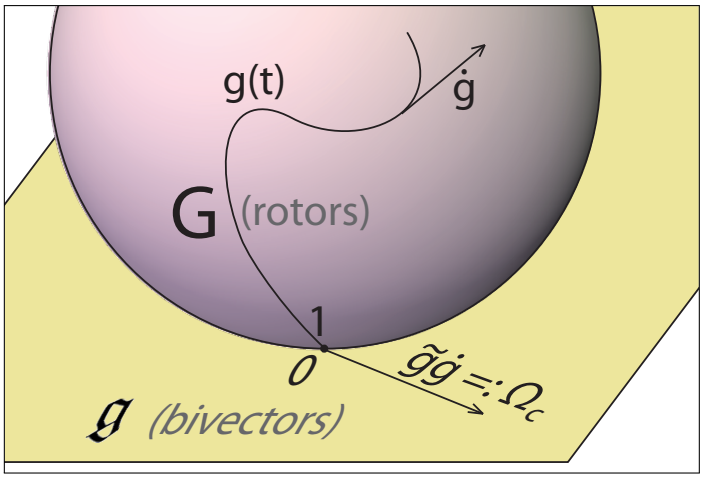

Fig. 8.1 The velocity in the body $\boldsymbol{\Omega}_c$ is $\dot{\mathbf{g}}$ pulled back to the identity via left multiplication by $\widetilde{\mathbf{g}}$.

[1] From *corpus*, Latin for body.

Remark 160. It is sometimes useful to evaluate expression at time $t = 0$. In that case, the two coordinate systems agree and we can omit the subscripts. Or, in expressions in which only the space coordinate system appears, it is also conventional to omit the subscripts.

8.3 Derivatives

We derive a general result for a time-dependent element (of arbitrary grade) in these two coordinate systems.

Theorem 161. *For time-varying* $\mathbf{X} \in Cl^3_\kappa$ *subject to the motion* $\mathbf{g}$ *with velocity in the body* $\mathbf{\Omega}_c$*,*

$$\dot{\mathbf{X}}_s = \mathbf{g}(\dot{\mathbf{X}}_c + 2(\mathbf{\Omega}_c \times \mathbf{X}_c))\tilde{\mathbf{g}} = \mathbf{g}\dot{\mathbf{X}}_c\tilde{\mathbf{g}} + 2(\mathbf{\Omega}_s \times \mathbf{X}_s)$$

Proof. Apply Leibniz rule to the sandwich product and rearrange terms:

$$\begin{aligned}
\dot{\mathbf{X}}_s &= \dot{\mathbf{g}}\mathbf{X}_c\tilde{\mathbf{g}} + \mathbf{g}\dot{\mathbf{X}}_c\tilde{\mathbf{g}} + \mathbf{g}\mathbf{X}_c\dot{\tilde{\mathbf{g}}} \\
&= \mathbf{g}(\tilde{\mathbf{g}}\dot{\mathbf{g}}\mathbf{X}_c + \dot{\mathbf{X}}_c + \mathbf{X}_c\dot{\tilde{\mathbf{g}}}\mathbf{g})\tilde{\mathbf{g}} \\
&= \mathbf{g}(\mathbf{\Omega}_c\mathbf{X}_c + \dot{\mathbf{X}}_c + \mathbf{X}_c\widetilde{\mathbf{\Omega}}_c)\tilde{\mathbf{g}} \\
&= \mathbf{g}(\dot{\mathbf{X}}_c + \mathbf{\Omega}_c\mathbf{X}_c - \mathbf{X}_c\mathbf{\Omega}_c)\tilde{\mathbf{g}} \\
&= \mathbf{g}(\dot{\mathbf{X}}_c + 2(\mathbf{\Omega}_c \times \mathbf{X}_c))\tilde{\mathbf{g}}
\end{aligned}$$

The next-to-last equality follows from the fact that for bivectors, $\widetilde{\mathbf{\Omega}} = -\mathbf{\Omega}$; the last equality is the definition of the commutator product. On the other hand,

$$\begin{aligned}
\dot{\mathbf{X}}_s &= \dot{\mathbf{g}}\mathbf{X}_c\tilde{\mathbf{g}} + \mathbf{g}\dot{\mathbf{X}}_c\tilde{\mathbf{g}} + \mathbf{g}\mathbf{X}_c\dot{\tilde{\mathbf{g}}} \\
&= \dot{\mathbf{g}}\tilde{\mathbf{g}}\mathbf{g}\mathbf{X}_c\tilde{\mathbf{g}} + \mathbf{g}\dot{\mathbf{X}}_c\tilde{\mathbf{g}} + \mathbf{g}\mathbf{X}_c\tilde{\mathbf{g}}\mathbf{g}\dot{\tilde{\mathbf{g}}} \\
&= \mathbf{g}\dot{\mathbf{X}}_c\tilde{\mathbf{g}} + 2(\mathbf{\Omega}_s \times \mathbf{X}_s)
\end{aligned}$$

□

Remark 162. We'll be interested in the case $\mathbf{X}_c = \mathbf{\Phi}_c$ is a bivector. In this case, $\mathbf{\Phi}_c$ and $\mathbf{\Omega}_c$ can be considered as Lie algebra elements, and $2(\mathbf{\Omega}_c \times \mathbf{\Phi}_c) = \mathbf{\Omega}_c\mathbf{\Phi}_c - \mathbf{\Phi}_c\mathbf{\Omega}_c$ is called the *Lie bracket*, sometimes written $[\mathbf{\Omega}_c, \mathbf{\Phi}_c]$. It expresses the change in one ($\mathbf{\Phi}_c$) due to an instantaneous motion represented by the other ($\mathbf{\Omega}$).

As an application of Thm. 161, we consider the orbit of a point $\mathbf{R}$ under a motion $\mathbf{g}$.

8.4 The orbit of a point under a motion

For a point $\mathbf{R}_0$, the motion $\mathbf{g}$ induces a path $\mathbf{R}(t)$, the *orbit* of the point $\mathbf{R}$, given by $\mathbf{R}(t) = \mathbf{g}(t)\mathbf{R}_0\widetilde{\mathbf{g}}(t)$. Applying the theorem yields

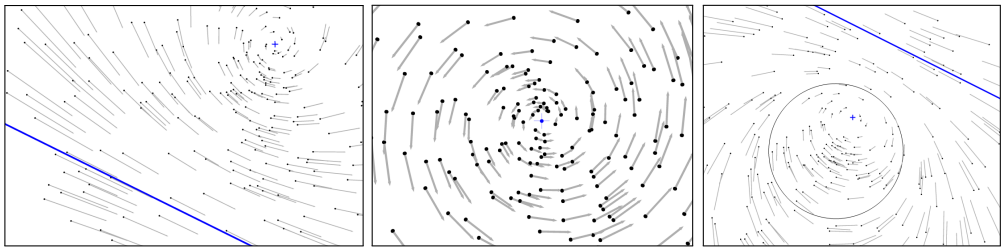

Fig. 8.2 In the metric plane, the velocity state $\mathbf{V}$ can be identified with the null point (small blue cross) of the vector field $2\mathbf{V} \times \mathbf{R}$, shown here in the neighborhood of $\mathbf{V} = \mathbf{E}_0 + .25\mathbf{E}_1 + .5\mathbf{E}_2$. From left to right: elliptic, euclidean, hyperbolic. The polar line of $\mathbf{V}$ is shown in blue. Notice it is invariant under the flow. In the hyperbolic plane, the ideal circle is also shown.

$$\dot{\mathbf{R}}(t) = 2(\boldsymbol{\Omega}(t) \times \mathbf{R}(t)) \tag{8.1}$$

where we have omitted the subscripts since everything is in the space coordinate system. We also omit the function notation $\dot{\mathbf{R}} = 2(\boldsymbol{\Omega} \times \mathbf{R})$ since everything is parametrized by t.

Remark 163. **Metric-neutral vector field.** In the euclidean case, from Sect. 7.3.1 we seen that $\boldsymbol{\Omega} \times \mathbf{R}$ is an ideal point, a free vector. In the general setting, (by the general form of (7.15)) $\boldsymbol{\Omega} \times \mathbf{R}$ is orthogonal to $\mathbf{R}$, hence lies in the polar plane of $\mathbf{R}$. In light of the identity of the polar plane of a point and the tangent space at the point (Thm. 65), we continue to use the term *vector field* to describe the assignment $\dot{\mathbf{R}} = 2(\boldsymbol{\Omega} \times \mathbf{R})$. The vector field for $t = 0$ (for a random selection of points $\mathbf{R}$) is pictured in Fig. 8.2 for the case of an elliptic rotor in the 3 metric planes. We next establish a connection to Fig. 6.4.

Remark 164. **Integral curve confirmation.** Let the rotor $\mathbf{g}$ have logarithm $\boldsymbol{\Omega}$. Define $\mathbf{g}(t) := e^{t\boldsymbol{\Omega}}$. Calculate:

$$\begin{aligned} \dot{\mathbf{g}}(t) &= \boldsymbol{\Omega} e^{t\boldsymbol{\Omega}} \\ &= \boldsymbol{\Omega}\mathbf{g}(t) \\ \dot{\mathbf{g}}(t)\widetilde{\mathbf{g}}(t) &= \boldsymbol{\Omega} \end{aligned}$$

Hence the velocity in space for this isometric motion is the constant bivector $\boldsymbol{\Omega}$, and at any time t, the vector field $\dot{\mathbf{R}}(t)$ is given by (8.1). Thus the curves $\mathbf{R}(t) = e^{t\boldsymbol{\Omega}}\mathbf{R}_0 e^{-t\boldsymbol{\Omega}}$ (shown in Fig. 6.4 in the 2D case) are in fact integral curves of the constant vector field $\boldsymbol{\Omega} \times \mathbf{R}$.

8.5 Null plane interpretation

By (7.13), $\boldsymbol{\Xi} \times \mathbf{P} = (\boldsymbol{\Xi} \vee \mathbf{P})\mathbf{I}$. Substituting this into (8.1) yields $\dot{\mathbf{R}} = 2(\boldsymbol{\Omega} \vee \mathbf{R})\mathbf{I}$. We recognize the result as the polar point (with respect to the metric) of the null plane of $\mathbf{R}$ (with respect to $\boldsymbol{\Omega}$). See Fig. 8.4. Thus, the vector field can be considered as the

composition of two simple polarities: first, the null polarity on $\mathbf{\Omega}$, then the polarity $\mathit{\Pi}$ on the metric quadric:

$$\mathbf{R} \xrightarrow{N_{\mathbf{\Omega}}} \mathbf{\Omega} \vee \mathbf{R} \xrightarrow{\mathit{\Pi}} (\mathbf{\Omega} \vee \mathbf{R})\mathbf{I} \xrightarrow{2} 2((\mathbf{\Omega} \vee \mathbf{R})\mathbf{I}) = \dot{\mathbf{R}}$$

(See Sect. 7.2.1.2). This leads to the somewhat surprising result that regardless of the metric used, the underlying null polarity remains the same. One could say, for a given point, its null plane provide a projective *ground* for kinematics, shared by all metrics; the individual metrics determine a different *perpendicular* direction to the plane, giving the direction which the point moves. See Fig. 8.3.

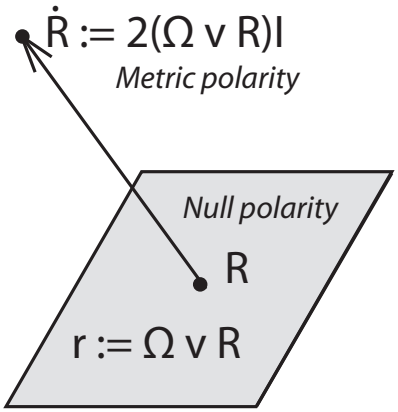

Fig. 8.3 The vector field induced by a bivector on a point $\mathbf{R}$ can be decomposed as the product of two polarities.

Remark 165. This decomposition only makes itself felt in the 3D case. In 2D, the null polarity is degenerate: $\mathbf{V} \vee \mathbf{R}$ is the joining line of $\mathbf{V}$ and $\mathbf{R}$, and $(\mathbf{V} \vee \mathbf{R})\mathbf{I}$ is the polar point of this line. Hence, all the vectors in the vector field lie in the polar line of $\mathbf{V}$.

A similar degeneracy occurs in 3D when $\mathbf{\Omega}$ is simple. One sees that the vector field vanishes wherever $\mathbf{\Omega} \vee \mathbf{R} = 0$. This only occurs if $\mathbf{\Omega}$ is a simple bivector and $\mathbf{R}$ is incident with it (Ex. 7.3.1.1-7). The picture is consistent with the knowledge, gained above, that in this case $e^{t\mathbf{\Omega}}$ generates a rotation (or translation) with axis $\mathbf{\Omega}$. All the vectors in the vector field determined by $\mathbf{\Omega}$ lie in the polar line of $\mathbf{\Omega}$.

Otherwise, when $\mathbf{\Omega}$ is non-simple, $\mathbf{\Omega} \vee \mathbf{R}$ is a plane $\mathbf{p}$ containing $\mathbf{R}$; when $\mathbf{R}$ is proper, so is $\mathbf{r}$ and $\mathbf{rI} \neq 0$. Hence, the vector field at any proper point $\mathbf{R}$ is non-null, and so no proper points remain fixed. In fact, when $\mathbf{I}^2 \neq 0$, $\mathbf{\Omega} \times \mathbf{R}$ is a bijection of $\langle Cl^3_\kappa \rangle_3$, and the inverse is given by the polar bivector:

$$(\mathbf{\Omega I}) \times (\mathbf{\Omega} \times \mathbf{R}) = \mathbf{R} \tag{8.2}$$

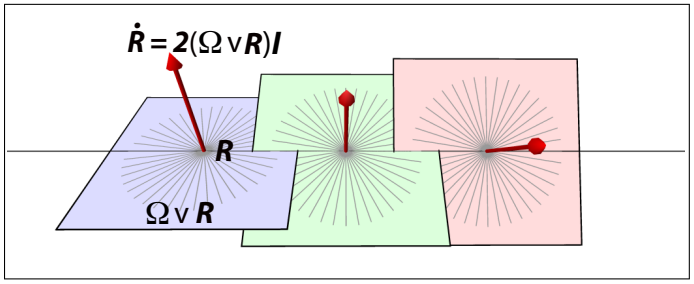

Fig. 8.4 A point $\mathbf{R}$, its null plane $(\boldsymbol{\Omega} \vee \mathbf{R})$, and the velocity vector $\dot{\mathbf{R}} = 2(\boldsymbol{\Omega} \vee \mathbf{R})\mathbf{I}$. Compare Fig. 7.2.

8.6 Dual formulation of kinematics

It is possible to dualize the basic kinematic formulation to be plane-based. Replace $\mathbf{R}$ with an arbitrary plane $\mathbf{r}$ in (8.1). Dual to $\dot{\mathbf{R}}$, the instantaneous direction of motion of the point, is

$$\dot{\mathbf{r}} = 2(\boldsymbol{\Omega} \times \mathbf{r}) = 2(\boldsymbol{\Omega} \vee \mathbf{r}\mathbf{I})$$

the instantaneous axis of rotation of the plane, where the second equality can be confirmed by a direct calculation.

Fig. 8.5 shows the configuration. $\mathbf{r}$ and $\mathbf{R}$ are any null plane/point pair with respect to the velocity state $\boldsymbol{\Omega}$. $\mathbf{p}$ and $\mathbf{P}$ are another null plane/point pair determined by $\mathbf{P} = \mathbf{r}\mathbf{I}$. The instantaneous velocity of $\mathbf{R}$ is along the line $\boldsymbol{\Lambda}_R := (\boldsymbol{\Omega} \vee \mathbf{R})\mathbf{I} \vee \mathbf{R}$. The instantaneous velocity of $\mathbf{r}$ is around the line $\boldsymbol{\Lambda}_r := (\boldsymbol{\Omega} \vee \mathbf{r}\mathbf{I}) \wedge \mathbf{r}$. The two lines are clearly conjugate lines of the null polarity of $\boldsymbol{\Omega}$:

$$\begin{aligned} N_{\boldsymbol{\Omega}}(\mathbf{p} \wedge \mathbf{r}) &= (\boldsymbol{\Omega} \wedge \mathbf{p}) \vee (\boldsymbol{\Omega} \wedge \mathbf{r}) \\ &= \mathbf{P} \vee \mathbf{R} \end{aligned}$$

There are infinitely many pairs of such conjugate lines, and each such pair determines a decomposition of $\boldsymbol{\Omega}$ as the sum of two lines.

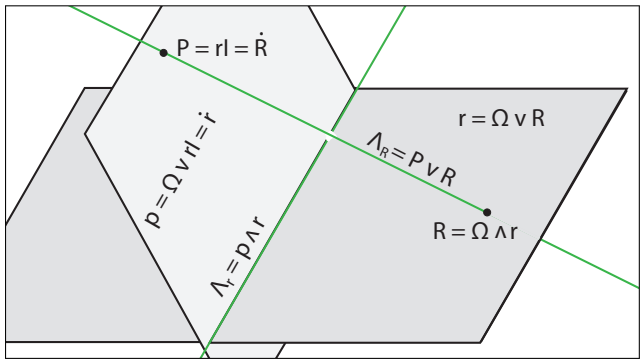

Fig. 8.5 A null plane/point pair $(\mathbf{r}, \mathbf{R})$, and a second pair $(\mathbf{p} = \boldsymbol{\Omega} \vee \mathbf{r}\mathbf{I}, \mathbf{P} = \mathbf{r}\mathbf{I})$. The meet of the planes and the join of the points give the instantaneous motion of the pair $(\mathbf{r}, \mathbf{R})$.

We call the assignment $\dot{\mathbf{r}} = 2(\boldsymbol{\Omega} \times \mathbf{r})$ a *co-vector* field. The co-vector field is the composition of the polarity $\mathit{\Pi}$ on the metric quadric followed by the null polarity $N_{\boldsymbol{\Omega}}$ with respect to $\boldsymbol{\Omega}$. The latter formulation is the same as the vector field, but the polarities are applied in opposite order:

$$\mathbf{r} \xrightarrow{\mathit{\Pi}} \mathbf{rI} \xrightarrow{N_{\boldsymbol{\Omega}}} \boldsymbol{\Omega} \vee \mathbf{rI} \xrightarrow{2} 2(\boldsymbol{\Omega} \vee \mathbf{rI}) = \dot{\mathbf{r}}$$

In the case of a non-degenerate metric, one can show a further equivalent form:

$$\dot{\mathbf{r}} = -2(\boldsymbol{\Omega}\mathbf{I} \wedge \mathbf{r})\mathbf{I}$$

This has the same form as $\dot{\mathbf{R}}$ except one uses the polar velocity $\boldsymbol{\Omega}\mathbf{I}$.

Remark 166. **Historical note.** The dual formulation of kinematics can be traced back to Lindemann ([Lin73]). He worked with non-euclidean metrics. He referred to the velocity state $\boldsymbol{\Omega}$ as the *rotational linear complex* associated to the motion, and $\boldsymbol{\Omega}\mathbf{I}$ as the *translational linear complex*. He observed that under the metric polarity, the infinitesimal picture involving $\boldsymbol{\Omega}$ is matched by another, isomorphic one involving $\boldsymbol{\Omega}\mathbf{I}$. In particular the decomposition of $\boldsymbol{\Omega}$ into two infinitesimal rotations around two conjugate axes corresponds to two infinitesimal translations around the polar spears, which are necessarily conjugate wrt $\boldsymbol{\Omega}\mathbf{I}$. The axes of $\boldsymbol{\Omega}$, in this formulation, are the common null lines of $\boldsymbol{\Omega}$ and $\boldsymbol{\Omega}\mathbf{I}$, underlining the fact that the dual formulation changes none of the kinematic events, only offers an alternative model for them.

Remark 167. **The role of $\boldsymbol{\Omega}\mathbf{I}$.** We have already seen in (8.2) that $\boldsymbol{\Omega}\mathbf{I}$ functions as a kind of "kinematic inverse" of $\boldsymbol{\Omega}$: applying $\boldsymbol{\Omega}\mathbf{I}$ to the vector field of $\boldsymbol{\Omega}$ gives the identity map. Furthermore, if $\boldsymbol{\Omega}$ is used as a generator for a motion via an exponential of the form $e^{(t+u\mathbf{I})\boldsymbol{\Phi}}$, where $\boldsymbol{\Phi}$ is an axis of $\boldsymbol{\Omega}$ (as described in Sect. 126), then in the generic case, $\boldsymbol{\Phi}$ is also an axis of $\boldsymbol{\Omega}\mathbf{I}$ and the same exponential can be used.

Remark 168. The lines $\boldsymbol{\Lambda}_R$ are called the *point characteristics* of the motion; the lines $\boldsymbol{\Lambda}_r$, the *plane characteristics* of the motion. The set of all point (plane) characteristics forms a quadratic line complex, that is, a 3-dimensional subset of $\mathcal{L}$ determined by a quadratic equation in Plücker coordinates. In particular, they form a so-called tetrahedral line complex: for every line of the complex, the cross ratio of its four intersections with the four planes of the fundamental tetrahedra is constant. See [Lin73] for details.

8.7 Guide to the Literature

See Sect. 9.11.

Chapter 9
Rigid body mechanics

This chapter shows how to model rigid body motion using the Clifford algebras Cl^3_κ described in the previous chapters. We handle all three cases simultaneously, specializing to one or the other algebra whenever exceptional situations require.

This chapter picks up where Chapter 8 left off. We will apply the concepts obtained there to explore the motion of mass particles and bodies built out of such particles. In Sect. 9.1, we give a homogeneous formulation of statics based on bivectors. We introduce dynamics with a new approach to newtonian particles (Sect. 9.2), formulated via duality in bivector space, such that the velocity and momentum state of the particle are "almost" an axis pair of the global velocity state. Collecting such particles yields rigid bodies (Sect. 9.3). The inertia tensor of a rigid body is derived as a positive definite quadratic form on the space of bivectors; a separate Clifford algebra is introduced to model this. In Sect. 9.5, equations of motion in the force-free case are derived, followed by the treatment of the presence of external forces. The dual formulation of dynamics is briefly sketched.

Along the way a variety of topics – such as a canonical 4-particle representation of a rigid body – are handled, and connections – such as the isomorphism of dynamics in $\mathbf{Ell}^n$ and $\mathbb{R}^{n+1}$ – are established, which reflect the geometric power of the metric-neutral, Clifford algebra approach.

The chapter closes with an appendix devoted to comparing the Clifford algebras presented here to those arising from the so-called *conformal* model.

Remark 169. In the following, we represent velocity states by $\mathbf{\Omega}$, momentum states by $\mathbf{\Pi}$, and forces by $\mathbf{\Delta}$.

9.1 Statics

Traditional euclidean statics addresses the behavior of rigid bodies near to equilibrium. It is only concerned with the question, whether a system of forces acting on a body is in equilibrium or not. Dynamics proper begins once one attempts to follow the motion in the case the system of forces is not in equilibrium.

Traditional formulation.A single force F acting along a line is represented traditionally as a pair of 3-vectors (V, M), where $V = (v_x, v_y, v_z)$ is the direction vector of the force, and $M = (m_x, m_y, m_z)$ is the moment with respect to the origin (see [Fea07], Ch. 2). The resultant of a system of forces $\{F_i\}$ is defined to be

$$\sum_i F_i = (\sum_i V_i, \sum_i M_i) =: (V, M)$$

From V and M one can describe the system of forces:

- The forces are in equilibrium $\iff V = M = 0$.
- $V = 0$ and $M \neq 0 \iff$ the resultant force is a *force couple*.
- $\langle V, M\rangle = 0 \iff$ the system represents a single force. (Here $\langle , \rangle$ is ordinary euclidean inner product.)

Homogeneous formulation. If P is a point on the line carrying the force, define $\mathbf{\Phi} := \mathbf{i}(P) \vee \mathbf{i}(V)$. $\mathbf{\Phi}$ is the weighted bivector representing this line. We call $\mathbf{\Phi}$ the *homogeneous form* of the force. Comparison with the definition of V and M above shows that:

$$\mathbf{\Phi} = m_x\mathbf{E}_{01} + m_y\mathbf{E}_{02} + m_z\mathbf{E}_{03} + v_z\mathbf{E}_{12} + v_y\mathbf{E}_{31} + v_x\mathbf{E}_{23}$$

That is, the six Plücker coordinates of the line carrying F are a rearrangement of the 2×3 coordinates of V and M. The mysterious "moment with respect to the origin" M is nothing else than the *ideal* part of the line, which reflects how the line with direction V is translated away from the origin (see Thm. 111). The resultant of a system of forces F_i is then $\sum_i \mathbf{\Phi}_i =: \mathbf{\Xi}$ a bivector, possibly non-simple.

Translated into the language of bivectors, the above list becomes:

- The forces are in equilibrium $\iff \mathbf{\Xi} = 0$.
- $\mathbf{\Xi}_o = 0 \iff$ the resultant force is a *force couple*.
- $\mathbf{\Xi} \wedge \mathbf{\Xi} = 0 \iff$ the system represents a single force.

Remark 170. The observant reader has perhaps observed that the above description of euclidean statics is purely projective. If one removes the euclidean metric, then the force-couple is just another simple force, and one obtains results on force systems that apply in any metric. See [Whi98], Book V, Chapter 1, "Systems of Forces". We return to the fact that the resultant of a set of simple forces is defined projectively rather than metrically in Chapter 12.

Remark 171. Given a line $\mathbf{\Phi}$, the conjugate line $\mathbf{\Theta}$ of $\mathbf{\Phi}$ with respect to a non-simple $\mathbf{\Xi}$ is characterized by the property that it is simple, and $\mathbf{\Xi} = \alpha\mathbf{\Phi} + \beta\mathbf{\Theta}$. A null line of the polarity associated to $\mathbf{\Xi}$ is a line for which this is impossible. A force system $\mathbf{\Xi}$ can be decomposed as the sum of a given simple bivector $\mathbf{\Phi}$ and its conjugate with respect to the null polarity of $\mathbf{\Xi}$, except when $\mathbf{\Phi}$ is a null line of $\mathbf{\Xi}$.

Remark 172. Note that the intensity of the bivectors representing the force system play a role. Hence, we are no longer working purely in the projective space $\mathfrak{B}$. However, the

intensity of the bivectors can be taken into account without giving up the projective representation. One must simply be careful to work with the correct representative of the projective points.

9.2 Newtonian particles

The basic object of Newtonian mechanics is a particle P with mass m located at the point $R \in \mathbb{R}^3$. Newton's law asserts that the force F acting on P is: $F = m\ddot{R}$. By Sect. 4.5, all the tangents spaces for our Cayley-Klein geometries are euclidean. Since derivatives are vectors in the tangent space of the point R, this definition of a newtonian force is metric-neutral, and so is the concept of a newtonian particle.

As far as possible we carry out the following discussion in a metric-neutral way. Occasionally we include remarks to connect the discussion to traditional euclidean formulations. We remind the reader of the identity $\mathbf{S}(\mathbf{\Xi} \wedge \mathbf{\Phi}) = \mathbf{\Xi} \vee \mathbf{\Phi}$, which we apply frequently to simplify the notation.

Define $\mathbf{R} := \mathbf{i}(R)$ as the 3-vector representing R in Cl^3_κ. We will assume throughout this discussion that $\mathbf{R}$ is normalized to $\|\mathbf{R}\| = 1$. This is possible since we are only interested in newtonian particles at proper points.

To obtain Newtoniam particles we define further:

Definition 173. The *spear* of the particle is $\mathbf{\Lambda} := \mathbf{R} \vee \dot{\mathbf{R}}$.

Definition 174. The *momentum state* of the particle is $\mathbf{\Pi} := m\mathbf{\Lambda}$.

Definition 175. The *velocity state* of the particle is $\mathbf{\Gamma} := \mathbf{\Lambda}\mathbf{I}$.

Definition 176. The *kinetic energy* E of the particle is

$$E := \frac{m}{2} N(\dot{\mathbf{R}})^2 = -\frac{m}{2} \mathbf{\Lambda} \cdot \mathbf{\Lambda} = -\frac{1}{2} \mathbf{\Gamma} \vee \mathbf{\Pi} \tag{9.1}$$

Remark 177. $N(\mathbf{P})$ is the norm on points introduced in Def. 104, which takes into account the possibility that $\mathbf{P}$ is ideal.

Remark 178. Fig. 9.1 shows the configuration of the particle's spear, momentum, and velocity. $\mathbf{\Pi}$ is a weighted bivector whose weight is proportional to the mass and the velocity of the particle. $\mathbf{\Gamma}$ is designed so that rotation around $\mathbf{\Gamma}$ results in the particle moving (translationally) along the spear $\mathbf{\Lambda}$, in the direction $\dot{\mathbf{R}}$. Up to the factor m, $\mathbf{\Gamma}$ is the polar line of $\mathbf{\Pi}$ with respect to the metric quadric. The definition of kinetic energy agrees with the traditional one. The second and third equalities for the kinetic energy can be verified by direct calculations.

Remark 179. **The euclidean case.** Since we can assume $\mathbf{R}$ is normalized, $\dot{\mathbf{R}}$ is an ideal point. $\mathbf{\Gamma}$ is also ideal, corresponding to the fact that the particle's motion is *translatory*. It is straightforward to verify that the linear and angular momentum of the particle

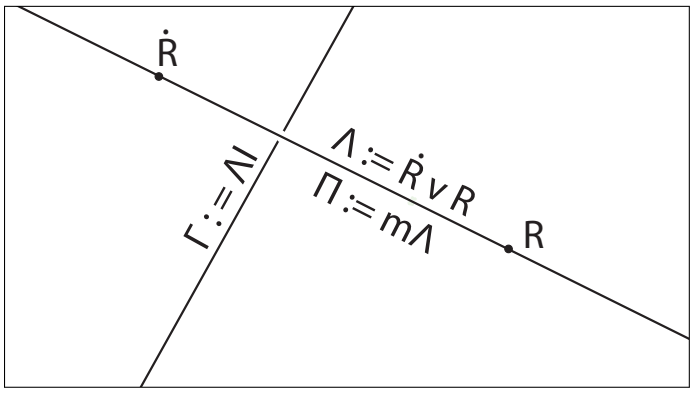

Fig. 9.1 The spear $\mathbf{\Lambda}$, momentum $\mathbf{\Pi}$ and velocity $\mathbf{\Omega}$ of a newtonian particle of mass m located at $\mathbf{R}$.

appear as $\mathbf{\Pi}_o$ and $\mathbf{\Pi}_\infty$, resp. Furthermore, a simple calculation shows that Def. 176 can be expressed in the more familiar form:

$$E = \frac{m}{2}\|\dot{\mathbf{R}}\|^2$$

9.2.1 Force-free system

For now, we consider only force-free systems. See Sect. 9.7 for extension to external forces.

Theorem 180. *If $F = 0$ then $\mathbf{\Lambda}$, $\mathbf{\Pi}$, $\mathbf{\Gamma}$, and E are conserved quantities.*

Proof. $F = 0$ implies $\ddot{\mathbf{R}} = 0$. Then:

- $\dot{\mathbf{\Lambda}} = (\dot{\mathbf{R}} \vee \dot{\mathbf{R}} + \mathbf{R} \vee \ddot{\mathbf{R}}) = 0$
- $\dot{\mathbf{\Pi}} = m\dot{\mathbf{\Lambda}} = 0$
- $\dot{\mathbf{\Gamma}} = (\dot{\mathbf{\Lambda}})\mathbf{I} = 0$
- $\dot{E} = \frac{1}{2}(\dot{\mathbf{\Gamma}} \vee \mathbf{\Pi} + \mathbf{\Gamma} \vee \dot{\mathbf{\Pi}}) = 0.$

□

9.2.2 Particles under the influence of a global velocity state

The key to analyzing rigid body motion is the observation that the constituent particles making up the body no longer follow their own natural motions, but instead are "governed by" an isometric motion $\mathbf{g}$ with associated global velocity state $\mathbf{\Omega} := \dot{\mathbf{g}}(0)$. $\mathbf{\Omega}$, in turn, determines $\dot{\mathbf{R}}$ as as described in Sect. 8.4. Fig. 9.2 shows the configuration of the newtonian particle in this case.

Then $\mathbf{\Pi}$, $\mathbf{\Gamma}$, and E depend on $\mathbf{\Omega}$ as follows:

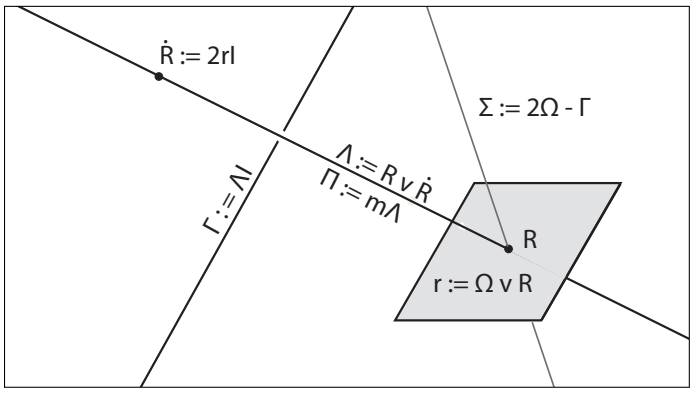

Fig. 9.2 For a newtonian particle located at $\mathbf{R}$ under the influence of a global velocity state $\mathbf{\Omega}$: the null plane $\mathbf{r} := \mathbf{\Omega} \vee \mathbf{R}$ of $\mathbf{R}$, the derivative $\dot{\mathbf{R}} := 2\mathbf{rI}$, the spear $\mathbf{\Lambda} := \mathbf{R} \vee \dot{\mathbf{R}}$ and particle velocity state $\mathbf{\Gamma} := \mathbf{\Lambda I}$. Finally, the difference $\mathbf{\Xi} = 2\mathbf{\Omega} - \mathbf{\Pi}$ is a line passing through $\mathbf{R}$.

$$\dot{\mathbf{R}} = 2(\mathbf{\Omega} \times \mathbf{R}) \tag{9.2}$$
$$\mathbf{\Pi} = 2m(\mathbf{R} \vee (\mathbf{\Omega} \times \mathbf{R})) \tag{9.3}$$
$$\mathbf{\Gamma} = 2(\mathbf{R} \vee (\mathbf{\Omega} \times \mathbf{R}))\mathbf{I} \tag{9.4}$$
$$= 2(\mathbf{R} \times (\mathbf{\Omega} \times \mathbf{R})) \tag{9.5}$$
$$E = -\frac{1}{2}\mathbf{\Gamma} \vee \mathbf{\Pi} \tag{9.6}$$
$$(= -2m(\mathbf{R} \times (\mathbf{\Omega} \times \mathbf{R})) \vee (\mathbf{R} \vee (\mathbf{\Omega} \times \mathbf{R}))) \tag{9.7}$$
$$= -\mathbf{\Omega} \vee \mathbf{\Pi} \tag{9.8}$$

The step from (9.4) to (9.5) follows from (7.14). The step from (9.6) to (9.8) is equivalent to the assertion that $2(\mathbf{\Omega} \vee \mathbf{\Pi}) = \mathbf{\Gamma} \vee \mathbf{\Pi}$. From $\mathbf{\Pi} = m\mathbf{R} \vee \dot{\mathbf{R}}$ it is enough to show $2(\mathbf{\Omega} \vee \mathbf{R}) = \mathbf{\Gamma} \vee \mathbf{R}$. Since both sides of the equation are planes passing through $\mathbf{R}$, it only remains to show that the planes have the same polar points. (This approach is designed to be also valid in the euclidean case.) This is equivalent to

Theorem 181. $2(\mathbf{\Omega} \times \mathbf{R}) = \mathbf{\Gamma} \times \mathbf{R}$.

Proof.

$$\mathbf{\Gamma} \times \mathbf{R} = 2(\mathbf{R} \times (\mathbf{\Omega} \times \mathbf{R}) \times \mathbf{R}) \tag{9.9}$$
$$= 2(\mathbf{R}(\mathbf{\Omega} \times \mathbf{R})\mathbf{R}) \tag{9.10}$$
$$= (\mathbf{R}(\mathbf{\Omega R} - \mathbf{R\Omega})\mathbf{R}) \tag{9.11}$$
$$= (\mathbf{R\Omega R}^2 - \mathbf{R}^2\mathbf{\Omega R}) \tag{9.12}$$
$$= (-\mathbf{R\Omega} + \mathbf{\Omega R}) \tag{9.13}$$
$$= 2(\mathbf{\Omega} \times \mathbf{R}) \tag{9.14}$$

Here we have used the fact that $\mathbf{R} \cdot (\mathbf{\Omega} \times \mathbf{R}) = 0$, the definition of $\times$, the fact that for proper points $\mathbf{R}^2 = -1$, and finally the definition of $\times$ a second time. □

Then the theorem yields immediately two corollaries:

Corollary 182. *The difference* $\mathbf{\Xi} := 2\mathbf{\Omega} - \mathbf{\Gamma}$ *is a simple bivector incident with* $\mathbf{R}$*.*

Proof. The theorem implies $\mathbf{\Xi} \times \mathbf{R} = 0$. But $\mathbf{\Xi} \times \mathbf{R} = (\mathbf{\Xi} \vee \mathbf{R})\mathbf{I}$ is the polar point of the plane $\mathbf{\Xi} \vee \mathbf{R}$. Hence $\mathbf{\Xi} \times \mathbf{R} = 0$ implies either

1. $\mathbf{\Xi} \vee \mathbf{R}$ is euclidean ideal, hence $(\mathbf{\Xi} \vee \mathbf{R})\mathbf{I} = 0$. But $\mathbf{\Xi} \vee \mathbf{R}$ is a plane through $\mathbf{R}$, hence it cannot be ideal. This leaves the second possibility
2. $\mathbf{\Xi} \vee \mathbf{R} = 0$, which can only happen if $\mathbf{\Xi}$ is simple and $\mathbf{R}$ is incident with it.

□

Corollary 183. *For non-simple* $\mathbf{\Omega}$*,* $\mathbf{\Xi}$ *is the conjugate line of* $\mathbf{\Gamma}$ *with respect to the null polarity* $\mathbf{\Omega}$*.*

Proof. This follows from the observation that the conjugate of a line $\mathbf{\Phi}$ with respect to a non-simple bivector $\mathbf{\Omega}$ is a line lying in the pencil spanned by $\mathbf{\Phi}$ and $\mathbf{\Omega}$. This condition is clearly satisfied by both $\mathbf{\Xi}$ and $\mathbf{\Gamma}$. Since there are at most two such lines in the pencil ($\mathbf{\Omega}$ is non-simple), the proof is complete. □

Remark 184. The significance of $\mathbf{\Xi}$ is not entirely clear. It can be used to argue that $(\mathbf{\Gamma}, \mathbf{\Pi})$ are "almost" an axis pair for $\mathbf{\Omega}$. $\mathbf{\Gamma}$ is the metric polar of $\mathbf{\Pi}$, while $\mathbf{\Gamma}$ is the conjugate of $\mathbf{\Xi}$ with respect to $\mathbf{\Omega}$. $\mathbf{\Pi}$ and $\mathbf{\Xi}$, however, are "close": they belong to the same line pencil in $\mathbf{R}$. It would be interesting to understand better the geometric significance, if any, of the difference $\mathbf{\Pi} - \mathbf{\Xi}$.

Remark 185. After completely our treatment of rigid body motion, we return for some further reflections on Newtonian particles in Sect. 9.3.

9.2.3 Inertia tensor of a particle

Define a real-valued bilinear operator $\mathbf{A}$ on pairs of bivectors:

$$\mathbf{A}(\mathbf{\Omega}, \mathbf{\Xi}) := -\frac{m}{2}((\mathbf{R} \vee 2(\mathbf{\Omega} \times \mathbf{R}))\mathbf{I}) \vee (\mathbf{R} \vee 2(\mathbf{\Xi} \times \mathbf{R})) \tag{9.15}$$

$$= \frac{m}{2}(\mathbf{R} \vee 2(\mathbf{\Omega} \times \mathbf{R})) \cdot (\mathbf{R} \vee 2(\mathbf{\Xi} \times \mathbf{R})) \tag{9.16}$$

where the step from (9.15) to (9.16) can be deduced from Sect. 7.3.1. (9.16) shows that $\mathbf{A}$ is symmetric since $\cdot$ on bivectors is symmetric: $\mathbf{\Lambda} \cdot \mathbf{\Delta} = \mathbf{\Delta} \cdot \mathbf{\Lambda}$. We call $\mathbf{A}$ the *inertia tensor* of the particle, since $E = \mathbf{A}(\mathbf{\Omega}, \mathbf{\Omega}) = -\mathbf{\Omega} \vee \mathbf{\Pi}$. We'll construct the inertia tensor of a rigid body out of the inertia tensors of its particles below. We overload the operator and write $\mathbf{\Pi} = \mathbf{A}(\mathbf{\Omega})$ to indicate the polar relationship between $\mathbf{\Pi}$ and $\mathbf{\Omega}$.

9.2.3.1 Homogeneous coordinates and the inertia tensor We assume throughout this discussion that all particles have positions $\mathbf{R}$ normalized so that $\|\mathbf{R}\| = 1$. On the other hand, the expression (9.16) for the inertia tensor clearly depends on $\|\mathbf{R}\|$: if one uses $\lambda\mathbf{R}$ instead of $\mathbf{R}$ throughout, then one obtains $\lambda^4\mathbf{A}(\mathbf{\Omega}, \mathbf{\Xi})$ instead of $\mathbf{A}(\mathbf{\Omega}, \mathbf{\Xi})$. The question naturally arises, are there possible inertia tensors which are only obtainable by using non-normalized particle positions $\mathbf{R}$? The answer is provided by the following theorem.

Theorem 186. *The inertia tensor for a particle with mass m and non-normalized position $\mathbf{R}$ is the same as that of the particle with mass $\|\mathbf{R}\|^4 m$ at normalized position $\dfrac{\mathbf{R}}{\|\mathbf{R}\|}$.*

Proof. Directly verify the claim by subsituting into (9.15). □

9.3 Rigid bodies

Begin with a finite set of mass points P_i; for each derive the velocity state $\mathbf{\Gamma}_i$, the momentum state $\mathbf{\Pi}_i$, and the inertia tensor $\mathbf{A}_i$.[1] Such a collection of mass points is called a *rigid body* when the distance between each pair of points remains constant under an isometric motion.

Extend the momenta and energy to the collection of particles by summation. Also define the mass of the rigid body as the sum of the masses.

$$\mathbf{\Pi} := \sum \mathbf{\Pi}_i = \sum \mathbf{A}_i(\mathbf{\Omega}) \tag{9.17a}$$

$$E := \sum E_i = \sum \mathbf{A}_i(\mathbf{\Omega}, \mathbf{\Omega}) \tag{9.17b}$$

$$m := \sum m_i \tag{9.17c}$$

Note that we can avoid referring to the individual velocity states by virtue of (9.8). Since for each single particle these quantities are conserved when $F = 0$, we have:

Theorem 187. $\mathbf{\Pi}$ *and* E *are conserved quantities.*

We introduce the inertia tensor A for the body:

Definition 188. $\mathbf{A} := \sum \mathbf{A}_i$.

Then $\mathbf{\Pi} = \mathbf{A}(\mathbf{\Omega})$ and $E = \mathbf{A}(\mathbf{\Omega}, \mathbf{\Omega})$. Neither formula requires a summation over the particles: the shape of the rigid body has been encoded into $\mathbf{A}$. We sometimes use the identity

$$\mathbf{A}(\mathbf{\Omega}_1, \mathbf{\Omega}_2) = -\mathbf{\Omega}_1 \vee \mathbf{A}(\mathbf{\Omega}_2) \tag{9.18}$$

which is a consequence of the fact that the individual inertia tensors for each particle exhibit this property.

9.3.1 Inertia tensor of rigid body

Suppose the particle $\mathbf{R}_i = w_i\mathbf{E}_0 + x_i\mathbf{E}_1 + y_i\mathbf{E}_2 + z_i\mathbf{E}_3$. Then evaluating $\mathbf{A}(\mathbf{\Omega}, \mathbf{\Omega})$ via (9.15), multiplying out, summing over all particles in the body, and expressing the result in terms of the canonical basis for $\mathbf{P}(\bigwedge \mathbb{R}^{2*})$, the matrix for $\mathbf{A}$ is:

[1] We restrict ourselves to the case of a finite set of mass points, since extending this treatment to a continuous mass distribution presents no significant technical problems; summations have to be replaced by integrals.

$$\mathbf{A} = 2\sum_i m_i \begin{pmatrix} w_i^2+\kappa x_i^2 & \kappa x_i y_i & \kappa x_i z_i & -w_i y_i & w_i z_i & 0 \\ \kappa x_i y_i & w_i^2+\kappa y_i^2 & \kappa y_i z_i & w_i x_i & 0 & -w_i z_i \\ \kappa x_i z_i & \kappa y_i z_i & w_i^2+\kappa z_i^2 & 0 & -w_i x_i & w_i y_i \\ -w_i y_i & w_i x_i & 0 & x_i^2+y_i^2 & -y_i z_i & -x_i z_i \\ w_i z_i & 0 & -w_i x_i & -y_i z_i & x_i^2+z_i^2 & -x_i y_i \\ 0 & -w_i z_i & w_i y_i & -x_i z_i & -x_i y_i & y_i^2+z_i^2 \end{pmatrix} \tag{9.19}$$

Remark 189. In this form, the matrix represents a linear map $\mathbf{P}(\bigwedge \mathbb{R}^{2*}) \to \mathbf{P}(\bigwedge \mathbb{R}^2)$. To obtain a map $\mathbf{P}(\bigwedge \mathbb{R}^{2*}) \to \mathbf{P}(\bigwedge \mathbb{R}^{2*})$, multiply the result by $\mathbf{J}$. The entries we denote with $\{a_{ij}\}$.

Remark 190. Thm. 186 guarantees that we obtain all possible inertia tensors for a rigid body using particles with normalized positions.

Remark 191. By well known results of quadratic forms, we can choose a coordinate system in which $\mathbf{A}$ is diagonal. Then $\mathbf{A}$ reduces to a diagonal matrix with the entries

$$(M_{01}, M_{02}, M_{03}, M_{12}, M_{31}, M_{23})$$

where for example $M_{01} = \sum m_i(w_i^2 + \kappa x_i^2)$, $M_{02} = \sum m_i(w_i^2 + \kappa x_i^2)$, etc. These entries are called the *moments of inertia* of the rigid body. Note that regardless of the metric, all entries are positive. A negative value would only be possible in the hyperbolic case, but for a proper hyperbolic point, $w_i > x_i$, hence the inertia tensor is a positive definite form.

Remark 192. For the euclidean case, $M_{01} = M_{02} = M_{03} = m$, and the lower three entries are the familiar moments of inertia for the angular velocity, see for example [Arn78], Ch. 6. For the non-euclidean case, remembering that our points are normalized to unit length, one sees quickly that

$$\kappa M_{01} + M_{23} = \kappa M_{02} + M_{31} = \kappa M_{03} + M_{23} = m \tag{9.20}$$

9.3.1.1 The vector space of inertia tensors The inertia tensors obviously form a vector space $\mathcal{T}$, since the sum of two inertia tensors is again a valid inertia tensor, as is a scalar multiple of one. Not all symmetric bilinear forms can occur as inertia tensors, as (9.20). shows. A glance at (9.19) reveals that there are other constraints on the entries of the inertia tensor, besides (9.20). For example, the anti-diagonal is zero. Furthermore, the other off-diagonal entries only span a 6-dimensional space, since, for example, $a_{04} = -a_{15}$, etc. The diagonal entries represent a 4-dimensional space, so $dim(\mathcal{T}) = 10$, whereas the space of symmetric bilinear forms is 21. It is an open question, how one can characterize $\mathcal{T}$ in a geometrically meaningful way.

9.3.1.2 The four-particle representation of a rigid body It is possible from the six values $\{M_{ij}\}$ to find four positive values (m_0, m_1, m_2, m_3) so that $m_0\mathbf{E}_0 + m_1\mathbf{E}_1 + m_2\mathbf{E}_2 + m_3\mathbf{E}_3$ is a rigid body with the given inertia tensor. This is a rigid body consisting of points

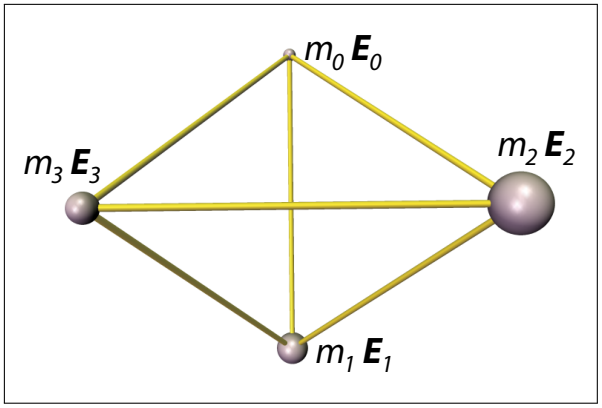

Fig. 9.3 Any rigid body has the same dynamic behavior as a four-particle body, whose particles are positioned at the basis which diagonalizes the inertia tensor.

at the vertices of the fundamental tetrahedron, with masses given by (m_0, m_1, m_2, m_3), presumably the simplest and most canonical one can construct. See Fig. 9.3. To find the required masses m_i: For simplicity assume $\kappa = 1$. From (9.20), $2\sum m_i(x_i^2) = M_{12} + M_{13} - M_{23}$. Define $m_1 := \sqrt{\dfrac{M_{12} + M_{13} - M_{23}}{2}}$, and similarly for the other masses. Verify that the resulting rigid body yields the inertia tensor with the given moments of inertia M_{ij}. Proceed similarly for other values of κ.

Remark 193. **The euclidean case.** For a euclidean-trained imagination it is challenging to imagine: three of the four particles lie at the ideal plane. This picture, however, is consistent with the degenerate form of the euclidean inertia tensor. The fact that $M_{01} = M_{02} = M_{03} = mw^2 = m$ can be seen in the figure in that the ideal vertices of the tetrahedron have vanishing *weight* relative to the single euclidean vertex $\mathbf{E}_0$ (their squares, after all, are 0). Among themselves, however, these ideal vertices determine the other three *non-degenerate* moments of inertia, the moments of inertia of a body rotating with a fixed point ($\mathbf{E}_0$). Once again, one sees remnants of the non-degenerate elliptic inner product on the ideal plane (Sect. 4.4.4).

9.3.2 A Clifford algebra for the inertia tensor

We define a Clifford algebra $\mathbf{C_A}$ based on $\mathbf{P}(\bigwedge^2 \mathbb{R}^{4*})$ by attaching the positive definite quadratic form $\mathbf{A}$ as the inner product.We denote the pseudoscalar of this alternative Clifford algebra by $\mathbf{I_A}$, and inner product of bivectors by $\langle , \rangle_{\mathbf{A}}$. We use the same symbols to denote bivectors in W^* as 1-vectors in $\mathbf{C_A}$. Bivectors in W are represented by 5-vectors in $\mathbf{C_A}$. Multiplication by $\mathbf{I_A}$ swaps 1-vectors and 5-vectors in $\mathbf{C_A}$; we use $\mathbf{J}$ (lifted to $\mathbf{C_A}$) to convert 5-vectors back to 1-vectors as needed. The following theorem, which we present without proof, shows how to obtain $\mathbf{\Pi}$ directly from $\mathbf{I_A}$ in this context:

Theorem 194. *Given a rigid body with inertia tensor* $\mathbf{A}$ *and velocity state* $\mathbf{\Omega}$*, the momentum state* $\mathbf{\Pi} = \mathbf{A}(\mathbf{\Omega}) = \mathbf{J}(\mathbf{\Omega I_A})$.

Conversely, given a momentum state $\mathbf{\Pi}$, we can manipulate the formula in the theorem to deduce:

$$\mathbf{\Omega} = \mathbf{A}^{-1}(\mathbf{\Pi}) = (\mathbf{J}(\mathbf{\Pi}))\mathbf{I}_{\mathbf{A}}^{-1}$$

In the sequel we denote the polarity on the inertia tensor by $\mathbf{A}(\mathbf{\Omega})$ and $\mathbf{A}^{-1}(\mathbf{\Pi})$, leaving open whether the Clifford algebra approach indicated here is followed.

9.3.3 Center of mass

The reader may have wondered why the center of mass has not been introduced into the discussion of the inertia tensor. This is due to the fact that the concept is metric-specific.

The process of diagonalizing the inertia tensor introduces a special coordinate system $\mathcal{M}$ closely tied to the mass distribution of the body. The existence of a *four-particle* representative for any rigid body (Sect. 9.3.1.2) is one consequence of this connection. The question of the center of mass is also related to this.

This coordinate system in the euclidean case is determined by the center of mass and the so-called principle axes: the axes of symmetry of the inertial ellipsoid. The latter can be thought of as ideal points (directions); the set of four orthonormal points then forms the fundamental tetrahedron of $\mathcal{M}$. The center of mass is the unique proper (non-ideal) vertex of this tetrahedron. The name fits since the mass points making up the body can in no way approach the other three vertices.

In the non-euclidean metrics, this special coordinate system cannot be so characterized. Particularly in elliptic space, the four corners of the fundamental tetrahedron are all proper and have equal right to be called the center of mass. The distribution of mass can just as well be said to be "centered" on one as on the other.

On the other hand, in the hyperbolic case, there is a unique time-like vertex $\mathbf{C}$ of the fundamental tetrahedron, such that $\mathbf{C}^2 < 0$. $\mathbf{C}$ can then be treated as the center of mass since clearly the mass distribution, similar to the euclidean case, cannot approach the other, space-like vertices of the tetrahedron.

9.4 Newtonian particles, revisited

Now that we have derived the inertia tensor for a rigid body in a metric-neutral way, it is instructive to return to consider the formulation of newtonian particles above (Sect. 9.2). We can see that in this formulation, particles exhibit properties usually associated to the ones we have discovered for rigid bodies. The following similarities can be identified:

- $E = -\frac{1}{2}\mathbf{\Gamma} \vee \mathbf{\Pi}$: The kinetic energy is the result of a dual pairing between the particle's velocity state and its momentum state in bivector space.
- $E = -\mathbf{\Omega} \vee \mathbf{\Pi}$: the same energy is obtained by using twice the global velocity state in place of the particle's velocity state. This follows from Thm. 181.
- $\mathbf{\Gamma} = \frac{1}{m}\mathbf{\Pi}\mathbf{I}$: The dual pairing is given by the polarity on the metric quadric, scaled by $\frac{1}{m}$. In the euclidean case only, this pairing is degenerate and only goes in one direction:

from the momentum state to produce the velocity state. In the non-euclidean case, the two states are true polar partners with respect to this scaled metric quadric.

In contrast, in the traditional approach to newtonian particles, such similiarities can only be found in a very disguised form, if at all. We consider it an advantage of the approach presented here, that the constituents out of which rigid bodies are composed behave in essentially the same way as the rigid bodies themselves. The idea that the inertia tensor of a particle is provided by the metric quadric is, to our knowledge, a new one.

9.5 The Euler equations for rigid body motion

In the absence of external forces, the motion of a rigid body is completely determined by its momentary velocity state or momentum state at a given moment. How can one compute this motion? First one needs to make essential use of the body and space coordinate systems introduced in Chapter 8.

The conservation laws of the previous section are generally valid only in the space coordinate system, for example, $\dot{\mathbf{\Pi}}_s = 0$. On the other hand, the inertia tensor will be constant only with respect to the body coordinate system, so, $\mathbf{\Pi}_c = \mathbf{A}(\mathbf{\Omega}_c)$. We need a definition of momentum dual to that of velocity.

Definition 195. The *momentum in the body* $\mathbf{\Pi}_c := \mathbf{A}(\mathbf{\Omega}_c)$, and the *momentum in space* $\mathbf{\Pi}_s := \mathbf{g}\mathbf{\Pi}_c\widetilde{\mathbf{g}}$.

9.5.1 Solving for the motion

Since $\mathbf{\Omega}_c = \widetilde{\mathbf{g}}\dot{\mathbf{g}}$, $\dot{\mathbf{g}} = \mathbf{g}\mathbf{\Omega}_c$, which is a first-order ODE. If we had a way of solving for $\mathbf{\Omega}_c$, we could solve for $\mathbf{g}$. If we had a way of solving for $\mathbf{\Pi}_c$, we could apply Theorem 194 to solve for $\mathbf{\Omega}_c$. So, how to solve for $\mathbf{\Pi}_c$?

We apply the corollary to the case of force-free motion. Then $\dot{\mathbf{\Pi}}_s = 0$: the momentum of the rigid body in space is constant. By Theorem 161,

$$0 = \dot{\mathbf{\Pi}}_s = \mathbf{g}(\dot{\mathbf{\Pi}}_c + 2(\mathbf{\Omega}_c \times \mathbf{\Pi}_c))\widetilde{\mathbf{g}} \tag{9.21}$$

The only way the RHS can be identically zero is that the expression within the outer parentheses is also identically zero, implying:

$$\dot{\mathbf{\Pi}}_c = 2\mathbf{\Pi}_c \times \mathbf{\Omega}_c \tag{9.22}$$

$$= 2\mathbf{\Pi}_c \times \mathbf{A}^{-1}\mathbf{\Pi}_c \tag{9.23}$$

The latter equation, the momentum form of Euler's equation of motion, involves only $\mathbf{\Pi}_c$. Writing $\mathbf{\Pi}_c = \sum_{ij} p_{ij}\mathbf{e}_{ij}$, and $m_{ij} := M_{ij}^{-1}$, (9.23) can be written as six separate equations:

$$\begin{aligned}
\dot{p}_{01} = &\quad 2(m_{02} - m_{03})p_{02}p_{03} + (\ m_{31} - m_{12})p_{12}p_{31} && (9.24a)\\
\dot{p}_{02} = &\quad 2(m_{03} - m_{01})p_{01}p_{03} + (\ m_{12} - m_{23})p_{12}p_{23} && (9.24b)\\
\dot{p}_{03} = &\quad 2(m_{01} - m_{02})p_{01}p_{02} + (\ m_{23} - m_{31})p_{23}p_{31} && (9.24c)\\
\dot{p}_{12} = &\quad 2(m_{01} - \kappa m_{31})p_{01}p_{31} + (\kappa m_{23} - m_{02})p_{02}p_{23} && (9.24d)\\
\dot{p}_{31} = &\quad 2(m_{03} - \kappa m_{23})p_{03}p_{23} + (\kappa m_{12} - m_{01})p_{01}p_{12} && (9.24e)\\
\dot{p}_{23} = &\quad 2(m_{02} - \kappa m_{12})p_{02}p_{12} + (\kappa m_{31} - m_{03})p_{03}p_{31} && (9.24f)
\end{aligned}$$

Remark 196. Note that for each coordinate $\dot{p_{ij}}$ depends on all the other coordinates with the exception of p_{kl}. For example, $\dot{p_{01}}$ involves all the other coordinates except p_{23}. For the euclidean case $\kappa = 0$, one also has $m_{01} = m_{02} = m_{03} = m^{-1}$, and one sees that the equations reduce to the familiar euclidean equations for linear and angular motion.

Remark 197. The form of the equations shows that an object with much symmetry will have less complex motion, since more of the 12 differences $m_{ij} - m_{kl}$ with vanish. When $m_{01} = m_{02} = m_{03}$ and $m_{12} = m_{31} = m_{23}$, for example, the inertia tensor maps $\mathcal{L}$ to $\mathcal{L}$, so simple momentum states give simple velocity states.

One can also express this ODE in terms of the velocity state alone. This yields the velocity form of Euler's equation:

$$\begin{aligned}
\dot{\mathbf{\Omega}}_c = \mathbf{A}^{-1}(\dot{\mathbf{\Pi}}_c) &= 2\mathbf{A}^{-1}(\mathbf{\Pi}_c \times \mathbf{A}^{-1}(\mathbf{\Pi_c}))\\
&= 2\mathbf{A}^{-1}(\mathbf{A}(\mathbf{\Omega}_c) \times \mathbf{\Omega}_c)
\end{aligned}$$

This equation can also be written as six separate equations. Here let $\mathbf{\Omega} = \sum_{ij} q_{ij}\mathbf{e}_{ij}$

$$\begin{aligned}
\dot{q}_{01} = &\quad -2m_{01}((M_{02} - \kappa M_{12})q_{02}q_{12} + (\kappa M_{31} - M_{03})q_{03}q_{31}) && (9.25a)\\
\dot{q}_{02} = &\quad -2m_{02}((M_{03} - \kappa M_{23})q_{03}q_{23} + (\kappa M_{12} - M_{01})q_{01}q_{12}) && (9.25b)\\
\dot{q}_{03} = &\quad -2m_{03}((M_{01} - \kappa M_{31})q_{01}q_{31} + (\kappa M_{23} - M_{02})q_{02}q_{23}) && (9.25c)\\
\dot{q}_{12} = &\quad -2m_{12}((M_{01} - \ M_{02})q_{01}q_{02} + (\ M_{23} - M_{31})q_{23}q_{31}) && (9.25d)\\
\dot{q}_{31} = &\quad -2m_{23}((M_{03} - \ M_{01})q_{01}q_{03} + (\ M_{12} - M_{23})q_{12}q_{23}) && (9.25e)\\
\dot{q}_{23} = &\quad -2m_{31}((M_{02} - \ M_{03})q_{02}q_{03} + (\ M_{31} - M_{12})q_{12}q_{31}) && (9.25f)
\end{aligned}$$

The complete set of equations for the motion g are given by the pair of first order ODE's:

$$\dot{\mathbf{g}} = \mathbf{g}\mathbf{\Omega}_c \tag{9.26}$$

$$\dot{\mathbf{\Omega}}_c = 2\mathbf{A}^{-1}(\mathbf{A}(\mathbf{\Omega}_c) \times \mathbf{\Omega}_c) \tag{9.27}$$

When written out in full, this gives a set of 14 first-order linear ODE's. The solution space is 12 dimensions; the extra dimensions corresponds to the normalization $\mathbf{g}\widetilde{\mathbf{g}} = 1$. At this point the solution continues as in the traditional approach, using standard ODE solvers. Our experience is that the cost of evaluating the Equations (9.26) is no more expensive than traditional methods.

9.5.2 The Euler top revisited

Equipped with the equations of motion (9.24) and (9.25), we can now return to the case of the Euler top as discussed in Chapter 1. We want to show that the Euler top appears in all the spaces under consideration.

What conditions on the velocity $\mathbf{\Omega}$ and momentum $\mathbf{\Pi}$ are necessary in order that the body behave as an Euler top, i.e., that the origin $\mathbf{E}_0$ remains fixed under the resulting motion? Assume we have chosen our coordinates so that the origin $\mathbf{E}_0$ is a center of mass of the object. Let $\{q_{ij}\}$ be the coordinates of $\mathbf{\Omega}$ and $\{p_{ij}\}$ be the coordinates of $\mathbf{\Pi}$. $\mathbf{E}_0$ remains fixed only if, for all time, $\mathbf{\Omega}$ is a line passing through it. We have shown previously that this implies that $q_{01} = q_{02} = q_{03} = 0$. The relation that $\mathbf{\Pi} = \mathbf{A}(\mathbf{\Omega})$ implies then that $p_{23} = p_{31} = p_{12} = 0$, i.e., $\mathbf{\Pi}$ is a line lying in $\mathbf{e}_0$, the polar plane of $\mathbf{E}_0$. Substituting these values into (9.25) reveals that they reduce to the 3-vector cross product form given in (1.1).

Remark 198. **Angular momentum.** In the derivation of the Euler top, we defined the angular momentum of a particle to be $\mathbf{M}_i := m_i\mathbf{R} \times \dot{\mathbf{R}}_i$ while in the discussion of newtonian particles in this chapter, the momentum took the form $m_i\mathbf{R}_i \vee \dot{\mathbf{R}}_i$. We want to show that these two definitions are compatible. Using affine coordinates for $\mathbf{R}_i$ and $\dot{\mathbf{R}}_i$ yields $\mathbf{\Pi}_i = (\dot{\mathbf{R}}; \mathbf{R}_i \times \dot{\mathbf{R}}_i)$ (here we use the notation of Sect. 7.4.3.2 to represent a bivector as a pair of 3-vectors). Hence

$$\begin{aligned}\mathbf{\Pi} &= \sum_i \mathbf{\Pi}_i \\ &= \sum_i (\dot{\mathbf{R}}; \mathbf{R}_i \times \dot{\mathbf{R}}_i) \\ &= (0; \sum_i \mathbf{R}_i \times \dot{\mathbf{R}}_i) \\ &= (0; \mathbf{M})\end{aligned}$$

Here we used the fact that $p_{23} = p_{31} = p_{12} = 0$ to go from the second to third equation, and we used the definition of the angular momentum in Chapter 1 to produce the final equation. Hence, the angular momentum $\mathbf{M}$ of the Euler top is related to the total momentum $\mathbf{\Pi}$ as follows: $\mathbf{M}$ is the normal direction of the plane obtained by joining $\mathbf{\Pi}$ to the fixed point $\mathbf{E}_0$ of the body.

9.5.3 Integrals of the motion

By Thm. 187, given an initial momentum bivector $\mathbf{\Pi}$, two quantities are conserved:

- **Energy:** $E = -\mathbf{\Pi}_c \vee \mathbf{\Omega}_c = \mathbf{A}(\mathbf{\Omega}_c, \mathbf{\Omega}_c)$, and
- **Momentum:** $\mathbf{\Pi}_s = \mathbf{\Pi}$.

Conservation of energy implies $\mathbf{\Omega}_c$ lies on the ellipsoid $Q_E : \mathbf{A}(\mathbf{\Omega}_c, \mathbf{\Omega}_c) = E$ during the motion. This ellipsoid is a positive definite quadric hypersurface of $\mathfrak{B}$. Conservation of momentum implies that $\mathbf{\Pi}_c$ lies on the quadric surface $\mathbf{\Pi}_c \cdot \mathbf{\Pi}_c = \mathbf{\Pi} \cdot \mathbf{\Pi} = L$ in $\mathfrak{B}$.

Converting to velocity states via $\mathbf{A}(\mathbf{\Omega}_c) = \mathbf{\Pi}_c$ implies that $\mathbf{\Omega}_c$ lies on the quadric surface $Q_M : \mathbf{A}(\mathbf{\Omega}_c) \cdot \mathbf{A}(\mathbf{\Omega}_c) = L$. Thus, $\mathbf{\Omega}_c$ lies on the intersection of Q_E and Q_M in $\mathfrak{B}$. Hence, the velocity state in the body is restricted to a $5-2 = 3$-dimensional quartic submanifold of $\mathfrak{B}$ (as is the momentum state in the body). Hence the *polhode*, the path of $\mathbf{\Omega}_c$ in $\mathfrak{B}$, lies in this submanifold. We return to this question in the results chapter in Sect. 11.4.4.

In every case, Q_E is an ellipsoid (positive definite), while the signature of Q_E depends on the metric quadric. And, since $\mathbf{A}$ is diagonal, the two quadric surfaces are confocal.

Remark 199. **Two-dimensional case.** In 2D, the two quadric surfaces intersect in a quartic curve. In light of Sect. 9.6, this agrees with classical results describing an Euler top, that the angular velocity moves along a closed quartic curve. In the hyperbolic plane, the surface Q_M is a hyperboloid of 2 sheets (consistent with the inner product $(2, 1, 0)$).

9.6 Isomorphism of dynamics in $\mathbf{Ell}^n$ with $\mathbb{R}^{n+1}$

We are now in a position to remark on a connection of the non-euclidean mechanics with a well-known part of euclidean dynamics. This connection depends on the fact that the isometry group of $\mathbf{Ell}^n$ is $PSO(n+1)$, the isometry group of $\mathbb{R}^{n+1}$ is $SO(n+1)$. $PSO(n+1) = SO(n+1)/\pm\mathbf{1}$.

Sect. 9.2.3.1 and, in particular, Thm. 186, established that any rigid body whose particles have non-normalized positions is equivalent to one which has normalized positions. So, we can assume that the positions of all particles in the rigid bodies in both $\mathbb{R}^{n+1}$ and $\mathbf{Ell}^n$ are normalized.

The two Clifford algebras $\mathbf{P}(\mathbb{R}_{n+1,0,0})$ (for $\mathbb{R}^{n+1}$) and $\mathbf{P}(\mathbb{R}^*_{n+1,0,0})$ (for $\mathbf{Ell}^n$ are isomorphic; one is the projectivized version of the other. The equations of motion are then identical for bodies with the same inertia tensor. It is straightforward to construct a canonical map from a rigid body B_R in $\mathbb{R}^{n+1}$ with inertia tensor $\mathbf{A}$, to a rigid body B_E in $\mathbf{Ell}^n$ with the same inertia tensor:

B_R and the antipodal body $-\mathsf{B}_R$ (the image of B_R under the antipodal map in $\mathbb{R}^{n+1}$) have the same inertial tensor. Then $\mathsf{B}_E := \mathbf{P}(\mathsf{B}_R)$ is a rigid body in $\mathbf{Ell}^n$ with the same inertia tensor. On the other hand, a rigid body B_E can be doubled by the antipodal map to produce a rigid body $\mathsf{B}_R \subset \mathbb{R}^{n+1}$ with twice the inertia tensor of B_E; multiplying all masses by $\frac{1}{2}$ produces a rigid body with the same inertia tensor.

Any solution of the equations (9.26) in $\mathbf{Spin}^n_{+1}$ gives simultaneously a solution for the elliptic body B_E in $PSO(n+1)$ and one for B_R in $SO(n+1)$. Any motion of the rigid body B_R induces a motion in the rigid body B_E by projectivization.

We use this isomorphism to translate known results about euclidean rigid body motion with a fixed point into results about elliptic motion. In particular the force-free dynamics of a rigid body in the elliptic plane are the same as a Euler top in $\mathbb{R}^3$. Clifford was the first to remark on this phenomenon in a short note from 1876, to be found in [Cli82a], pp. 236-240.

9.7 External forces

Until now, everything we have done is in the absence of external forces. It is relatively straightforward to go back and add them back in to the force-free results. The external force F acting on the rigid body is the sum of the external forces F_i acting on the individual mass points. In traditional notation, $F_i = m_i\ddot{\mathbf{r}}$. What is the homogeneous form for F_i? In analogy to the velocity state of the particle, we define the acceleration *spear* of the particle $\boldsymbol{\Upsilon}_i := \mathbf{R}_i \vee \ddot{\mathbf{R}}_i$, and the force state of the particle $\boldsymbol{\Delta}_i := m_i\boldsymbol{\Upsilon}_i$. Then the total force $\boldsymbol{\Delta}$ is the sum:

$$\boldsymbol{\Delta} = \sum \boldsymbol{\Delta}_i$$

The following theorem will be needed below in the discussion of work (Sect. 9.7.1):

Theorem 200. $\boldsymbol{\Delta} = \dot{\boldsymbol{\Pi}}$

Proof. Take the derivative of (9.17a):

$$\begin{aligned}\dot{\boldsymbol{\Pi}} &= \sum m_i \frac{d}{dt}(\mathbf{R}_i \vee \dot{\mathbf{R}}_i) \\ &= \sum m_i(\dot{\mathbf{R}}_i \vee \dot{\mathbf{R}}_i + \mathbf{R}_i \vee \ddot{\mathbf{R}}_i) \\ &= \sum m_i(\mathbf{R}_i \vee \ddot{\mathbf{R}}_i) \\ &= \boldsymbol{\Delta}\end{aligned}$$

□

Theorem 200 applied to (9.21) yields Euler equations for motion with external forces::

$$\begin{aligned}\boldsymbol{\Delta}_s = \dot{\boldsymbol{\Pi}}_s &= \mathbf{g}(\dot{\boldsymbol{\Pi}}_c + 2(\boldsymbol{\Omega}_c \times \boldsymbol{\Pi}_c))\widetilde{\mathbf{g}} \\ \widetilde{\mathbf{g}}\boldsymbol{\Delta}_s\mathbf{g} &= \dot{\boldsymbol{\Pi}}_c + 2(\boldsymbol{\Omega}_c \times \boldsymbol{\Pi}_c) \\ \boldsymbol{\Delta}_c &= \dot{\boldsymbol{\Pi}}_c + 2(\boldsymbol{\Omega}_c \times \boldsymbol{\Pi}_c) \\ \dot{\boldsymbol{\Pi}}_c &= \boldsymbol{\Delta}_c + 2(\boldsymbol{\Pi}_c \times \boldsymbol{\Omega}_c)\end{aligned}$$

Note that the forces have to be converted from world to body coordinate systems.

9.7.1 Work

As a final example of the projective approach, we discuss the concept of *work*. Recall that $\boldsymbol{\Pi} = \mathbf{A}(\boldsymbol{\Omega})$, so $\dot{\boldsymbol{\Pi}} = \mathbf{A}(\dot{\boldsymbol{\Omega}})$, and the definition of kinetic energy for a rigid body : $E = \mathbf{A}(\boldsymbol{\Omega}, \boldsymbol{\Omega})$.

Theorem 201. $\dot{E} = -\boldsymbol{\Omega} \vee \boldsymbol{\Delta}$

Proof.

$$\begin{aligned}\dot{E} &= \frac{d}{dt}\mathbf{A}(\mathbf{\Omega},\mathbf{\Omega}) \\ &= (\mathbf{A}(\dot{\mathbf{\Omega}},\mathbf{\Omega}) + \mathbf{A}(\mathbf{\Omega},\dot{\mathbf{\Omega}})) \\ &= \mathbf{A}(\mathbf{\Omega},\dot{\mathbf{\Omega}}) \\ &= -\mathbf{\Omega} \vee \mathbf{A}(\dot{\mathbf{\Omega}}) = -\mathbf{\Omega} \vee \dot{\mathbf{\Pi}} \\ &= -\mathbf{\Omega} \vee \mathbf{\Delta}\end{aligned}$$

where we apply Leibniz rule, the symmetry of $\mathbf{A}$, (9.18) and finally Thm. 200. □

In words: the rate of change of the kinetic energy is equal to the signed magnitude of the wedge product of force and velocity. This is noteworthy in that it does not involve the metric directly.

$\dot{E}$ is sometimes called the *power*. The *work* done by the force between time t_0 and t is the defined to be the integral:

$$\begin{aligned}w(t) = E(t) - E(t_0) &= \int_{t_0}^{t} \dot{E} ds \\ &= \int_{t_0}^{t} -\mathbf{\Omega} \vee \mathbf{\Delta} ds\end{aligned}$$

The integrand depends on the incidence properties of the force and the velocity, as points in $\mathfrak{B}$. If the two elements are in involution, then $\mathbf{\Delta} \vee \mathbf{\Omega} = 0$ and there is no work done; the "further away" $\mathbf{\Omega}$ lies from $\mathbf{\Delta}$, (in $\mathfrak{B}$!) the greater the power and hence the work done. The quantity $\mathbf{\Delta} \vee \mathbf{\Omega}$ is usually called the *virtual work* achieved by the force.

Remark 202. Ball ([Bal00]) introduced terminology for this situation which is widely-used in the English-speaking literature. He called a bivector representing a force or a momentum, a *wrench*; and a bivector representing a velocity, a *twist*. The bivector *qua* bivector, he called a *screw*. Then, the situation in the previous paragraph is described as "the virtual work achieved by the wrench $\mathbf{\Delta}$ acting upon the twist $\mathbf{\Omega}$".

9.7.2 Example

Imagine an ice skater who moving along the surface of a frozen lake with negligible friction; the single force is given by gravity. Assuming gravity is in the negative z-direction acting on the skater located at the origin, then $\mathbf{\Delta} = g\mathbf{e}_{12}$ (corresponding to the intersection line of the planes $x = 0$ and $y = 0$ with weight gravitation constant g). Consider two possible motions of the skater:

- The motion of the skater is a translation in the x-direction given by an ideal line of the form $\mathbf{\Omega} = d\mathbf{e}_{01}, d < 0$. $\mathbf{\Delta} \wedge \mathbf{\Omega} = 0$, so no work is required for the skater to skate!

- The skater spins around a fixed point. Then the velocity state relative to the natural diagonalized form of the inertia tensor has null ideal part $\boldsymbol{\Omega}_\infty = 0$ and the corresponding momentum state $\boldsymbol{\Pi} = \mathbf{A}(\boldsymbol{\Omega})$ has null euclidean part $\boldsymbol{\Pi}_o = 0$: it's a momentum couple: a momentum carried by an ideal line!
- As the skater spins, she stretches her arms out, then pulls her arms close to her body. This latter movement decreases the entries in the inertia tensor $\mathbf{A}$, increasing the entries in $\mathbf{A}^{-1}$; since $\boldsymbol{\Omega} = \mathbf{A}^{-1}(\boldsymbol{\Pi})$, her velocity increases proportionally in intensity: she spins faster.

One can see from this example the advantages of the projective approach: it unifies calculations, and handles exceptional cases, such as the translations and couples in the above example, at no extra cost.

9.8 The three metrics on $\mathfrak{B}$

The inertia tensor $\langle , \rangle_{\mathbf{A}}$ can be considered as a third quadratic form on $\mathfrak{B}$, in addition to the Plucker inner product $\langle , \rangle_P$ and the Killing inner product $\langle , \rangle_K$. The interaction of these three quadrics in $\mathfrak{B}$ gives rise to most of the phenomena associated to rigid body motion.

1. $\langle , \rangle_P$: $\langle \boldsymbol{\Omega}, \boldsymbol{\Omega} \rangle_P = 0 \iff \boldsymbol{\Omega}$ is a line; for two lines $\boldsymbol{\Omega}$ and $\boldsymbol{\Phi}$, $\langle \boldsymbol{\Omega}, \boldsymbol{\Phi} \rangle_P = 0 \iff$ the lines intersect. Furthermore, $\langle \boldsymbol{\Omega}, \boldsymbol{\Pi} \rangle_P$ expresses the kinetic energy of a rigid body with velocity $\boldsymbol{\Omega}$ and momentum $\boldsymbol{\Pi}$. Why is this so? In their pure forms, $\boldsymbol{\Omega} \in \mathbf{P}(\bigwedge \mathsf{V}^*)$ and $\boldsymbol{\Pi} \in \mathbf{P}(\bigwedge \mathsf{V})$ (see Sect. 9.3.1), and $E = \langle \boldsymbol{\Omega}, \boldsymbol{\Pi} \rangle$ where $\langle , \rangle$ is the evaluation operator of a vector and dual vector. However, as explained in Sect. 5.5.1, we carry out operations in $\mathbf{P}(\bigwedge \mathsf{V}^*)$ wherever possible. That is, we work with $\mathbf{J}(\boldsymbol{\Pi}) \in \mathbf{P}(\bigwedge \mathsf{V}^*)$ instead of with $\boldsymbol{\Pi}$. It is easy to verify that $\langle \boldsymbol{\Omega}, \boldsymbol{\Pi} \rangle = \langle \boldsymbol{\Omega}, \mathbf{J}(\boldsymbol{\Pi}) \rangle_P$.
2. $\langle , \rangle_K$ expresses the metric of the Cayley-Klein space in $\mathfrak{B}$; here we have considered the three cases $\kappa \in \{-1, 0, 1\}$. It is conserved by all isometries of the space, and expresses what a *rigid body* is.
3. The inertia tensor is the most individualized of the quadratic forms; the inertia tensors form a 10-dimensional vector space, as noted above in Sect. 9.3.1.1. Furthermore, the polarity it determines, in contrast to the Plücker and Killing forms, does not preserve $\mathcal{L}$. It also determines the form of the Euler equations (9.22), and therefore can rightfully be held responsible for the complex, unpredictable motion of the Euler top.

   See [Ada59], §41, for a related discussion.

9.9 The dual formulation of dynamics

For non-degenerate metrics, one can formulate the results of dynamics also dually. This formulation is obtained, just as in the case of kinematics Sect. 8.6, by applying the polarity

on the metric quadric to the complete dynamical configuration. As with kinematics, the resulting dynamics do not change; what changes is the descriptive framework.

Rather than newtonian point particles, one obtains newtonian plane particles. Since the velocity $\mathbf{\Gamma}$ and momentum $\mathbf{\Pi}$ of a point particle is described by $\mathbf{\Lambda I}$ and $m\mathbf{\Lambda}$, resp., the velocity $\widehat{\mathbf{\Gamma}}$ and momentum $\widehat{\mathbf{\Pi}}$ of the polar plane particle will be given by $\mathbf{\Lambda I}^2$ and $m\mathbf{\Lambda I}$, resp. These are easily seen to be $\kappa\frac{1}{m}\mathbf{\Pi}$ and $m\mathbf{\Gamma}$ (and one also sees why in a degenerate metric the process doesn't work). That is, the same weighted lines which represented the velocity and momentum of the point particle will in the dual formulation represent the momentum and velocity, resp., of the associated plane particle, with intensities depending on the mass m.

A rigid body consisting of particles will then be replaced by a rigid body consisting of the polar planes. If the midpoint of the body is $\mathbf{E}_0$, then the "mid-plane" of the dual body is $\mathbf{e}_0$. Using simple principles of projective geometry one can show that the concepts of "inside" and "outside" are reversed for such pairs of bodies. Consult Chapter 10 for an introduction to this line of reasoning; Fig. 10.2 shows how a 6-point body and its dual (polar) body appear.

Remark 203. **Polar momenta.** The figures in Chapter 11 make clear that the *polar* momentum $\mathbf{m}^\perp$ (a point in 2D and a line in 3D) play important roles in the the resulting forms of motion, even when the momentum is carried – as spear – completely by the original momentum line. For example, the center of mass of a symmetric rigid body in the hyperbolic plane under the influence of an improper momentum line rotates in a circle around $\mathbf{m}^\perp$ (see Fig. 11.2). On the other hand, the center of mass of the polar body is an improper line, the polar line of the standard center of mass. This polar center of mass moves then in a "circle" around the momentum line $\mathbf{m}$ (as elements of the dual hyperbolic plane).

Remark 204. **Quality of a dual force.** Dynamic concepts such as mass, force, and momentum, in contrast to purely kinematical concepts, are unthinkable without an associated bodily experience. In euclidean space a simple force reveals itself as a weighted spear, and its relationship to the experiencing human being is characterized by its point-wise nature; such a force acting on a human being is perceived as a more-or-less idealized point of pressure. In the dual formulation, possible in non-euclidean space, the same force may also appear as an *axis*; such a force naturally doesn't act on point-wise bodies, as a spear does, but on plane-wise bodies.

9.10 Comparison to traditional approach

The projective Clifford algebra approach outlined here exhibits several advantages over other approaches to rigid body motion. Considering to begin with just the euclidean case, the representation of kinematic and dynamic states as bivectors rather than as pairs of ordinary 3-vectors (linear and angular velocity/momentum/etc.) provides a framework free of the special cases which characterize the split approach (for example, translations

are rotations around an ideal line, a force couple is a single force carried by an ideal line, etc.). The Clifford algebra product avoids cumbersome matrix formulations and, as seen in Thm. 161, yields formulations which are valid for points, lines, and planes uniformly. The inertia tensor of a rigid body can be represented as a separate (positive definite) Clifford algebra defined on the space of bivectors. The treatment of Newtonian particles reveals an underlying velocity-momentum polarity in bivector space analogous to that of rigid bodies, an aspect which to our knowledge has not been discussed in the literature. Finally, very little extra work is required in the Clifford algebra approach, to establish metric-neutral results, valid for euclidean and non-euclidean rigid body mechanics. The non-euclidean results can then be directly polarized to yield a dual formulation of dynamics.

9.11 Guide to the literature

The treatment of rigid body motion in this chapter owes much to the spirit of [Arn78], Appendix 2. This school of thought, which has a wide literature (see also [Rat82] and [MR98]), defines a rigid body abstractly as a left-invariant metric on a Lie algebra. In our case, this is provided by the inertia tensor of the object, but the theory can be developed with reference to this more abstract formulation.

The fact that rigid body dynamics can be handled so elegantly using the algebras Cl^3_κ is not an accident. In many respects, Clifford algebras can be understood as a modern fruit on a mathematical tree whose roots reach back to the 19^{th} century investigations of Chasles, Möbius [Möb37], Plücker [Plu68], Klein [Kle27], and others into the mathematical formulation of rigid body dynamics. The impetus for the development of line geometry was given exactly by euclidean statics, see [Möb37], where the discovery of the linear line complex was reported. Consequently, the first mathematically sound formulation of rigid body motion using line geometry was achieved by Klein [Kle71].

Study himself worked mostly in kinematics rather than mechanics, despite the name of [Stu03]. His approach however was applied to mechanics in [vM24] and [Bla42]. The former was hampered by the awkward matrix notation required for stating transformation laws. These, on the other hand, are "built in" to the Clifford algebra approach and simplify the approach considerably. [Bla42] concentrated on the kinematics and rigid body motion in elliptic space.

The modern legacy of this work is varied. Some modern literature in rigid body mechanics, such as [Fea07], use *spatial vectors* to model rigid body motion; these are 6D vectors equivalent to our bivectors, but developed within a linear algebra framework reminiscent of [vM24]. This literature can also be seen as continuation of the work of Ball [Bal00], which has continued to have influence in the English-speaking literature, particularly in the area of kinematics and robotics.

Much contemporary work which applies Clifford algebra methods to physics and engineering uses the conformal model of Clifford algebra ([DL03], [Per09], [Hes10]) rather than the homogeneous model presented here. A euclidean extract of this thesis appears in [Gun11].

Non-euclidean literature. The extension of these euclidean results to non-euclidean spaces was first foreseen by Klein and Clifford independently. Klein's work led him to the insight that many of the principles of euclidean rigid body mechanics were in fact projective ones, and surmised that the same approach would also yield a theory for non-euclidean mechanics, when combined with the Cayley-Klein metric construction. This research was carried out at the end of the 19^{th} century and beginning of the 20^{th} in the work of Lindemann [Lin73], Clifford [Cli82b], Heath [Hea84], de Francesco [dF02], and others. Clifford, Heath, and Lindemann concentrated on the elliptic case; while de Francesco was the first to deal explicitly with rigid body motion in hyperbolic space. Explicit solutions of (9.25) were first provided by Heath in [Hea84] for elliptic space by the use of theta functions of two variables. These were later corrected and extended to hyperbolic space by de Francesco ([dF02]. [Bal00] contains a supplement devoted to elliptic rigid body motion based on his screw theory approach.

It is typical of the close connections of Clifford algebras with research into rigid body mechanics that Clifford's first research into the algebras which bear his name were done in the context of rigid body motion in elliptic space.

Chapter 10
Dual euclidean geometry

In Sect. 4.5 the choice of the three Cayley-Klein geometries featured in this research was discussed. On the other hand, an impartial observation of the methods and results which have been developed in the preceding chapters cannot overlook the ubiquitous role played by the projective principle of duality. This is particularly clear and unavoidable when one considers the non-degenerate metrics. The dual formulation of kinematics, (Sect. 8.6), or the fully equivalent roles of velocity and momentum in the formulation of dynamics, point to its importance.

Only in the euclidean case is this symmetry disturbed due to the degeneracy of the metric polarity, and the principle of duality appears to be lamed. For example, the dual formulation of kinematics is not valid here. One can however ask whether there is a larger context in which this euclidean exception nonetheless finds a dual partner. Recall that dualizing a Clifford algebra means to attach the same inner product to the dual Grassmann algebra, or equivalently, switching Q and Q^*. Furthermore recall (Thm. 25) that dualization of a non-degenerate algebra does not yield a new metric space, since Q and Q^* are equivalent, but dualizing a degenerate one does.

This leads us to introduce a fourth Clifford algebra to our standard trio. Consider Fig. 10.1. The three Cayley-Klein geometries studied til now correspond to the values -1, 0, and 1 of κ on the circle. Reflection in the horizontal line represents dualizing the corresponding Clifford algebra. Algebraically, this corresponds to inverting κ. As shown in Sect. 3.2, -1 and 1 are fixed points under dualization: the metric spaces which arise can be identified with the original metric spaces. However, 0 is mapped to ∞; euclidean geometry is mapped to dual euclidean geometry.

Considered geometrically, the limiting process which gave rise to euclidean space, described in Remark 45, can be pictured as expanding an oval quadric until it flattens out to a plane; the dual process, denoted here by ∞, goes in the other direction and shrinks the oval quadric to a point. Thus, the quadric Q of dual euclidean space is a single point; Q^* consists of the plane bundle in this point, all planes passing through this point. The three states (plane bundle in point, oval quadric, point field in plane) are shown in Fig. 7.7, where they arise in the process of continuously interpolating a polarity.

Thus, the addition of dual euclidean geometry to the three other geometries results in a mathematically self-dual configuration. Extending the circle of geometries from 3

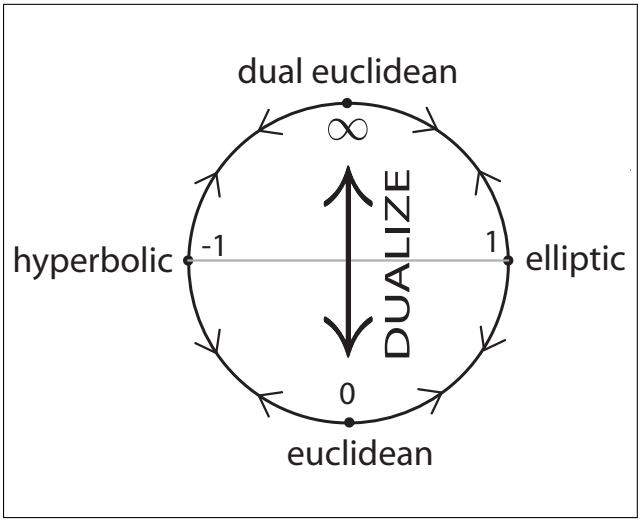

Fig. 10.1 The three Cayley-Klein geometries correspond to the values -1, 0, and 1 of κ. Dualization of the Clifford algebra Cl^n_κ is equivalent to inverting κ. -1 and 1 are fixed points, while euclidean geometry is mapped to dual euclidean geometry, and vice-versa.

to 4 means at the same time loosening the condition which leads to the restriction to these 3 (see Sect. 4.5). This condition is based on the notion of a manifold as a *point* set, an intrinsically non-self-dual concept. When one broadens this concept to allow spaces composed of *planes*, also, then one is led to include dual euclidean geometry as well as the other three. Elaboration of this idea lies outside the scope of the current work.

The rest of this chapter provides an introduction to dual euclidean geometry as a step towards a deeper understanding of how these four geometries form an organic whole, and closes with some references to current research into possible scientific applications of this unfamiliar geometry.

10.1 Introduction

The Clifford algebra for dual euclidean geometry is $\mathbf{P}(\mathbb{R}_{n,0,1})$, which is naturally isomorphic as *algebra* to $\mathbf{P}(\mathbb{R}^*_{n,0,1})$. We also denote this algebra as Cl^n_∞. The difference lies in the geometric *interpretation* of 1-vectors: as points or as hyperplanes. All the results obtained up til now for the euclidean plane and for euclidean space apply without exception to the dual euclidean plane and dual euclidean space, once they have been dualized. Space limitations make it impossible to make a detailed study. However, it is instructive to consider a few simple examples from these results in the areas of geometry, kinematics, and dynamics to provide a taste of what sort of geometry dual euclidean geometry is. Since mathematically-formally there is nothing new, we concentrate on noting the ways in which the geometry presents itself differently to human perception.

Write the metric space associated to $\mathbf{P}(\mathbb{R}_{n,0,1})$ as $\widehat{\mathbf{E}}^n$. Consider the dual euclidean plane and its Clifford algebra $\mathbf{P}(\mathbb{R}_{2,0,1})$. Just like the euclidean plane $\mathbf{E}^2$ has an ideal *line* represented by $\mathbf{e}_0$, $\widehat{\mathbf{E}}^2$ has an ideal *point* $\mathbf{e}^0$. Furthermore, in this ideal point there

is a elliptic metric on the ideal lines, which is in perspective to the elliptic metric on the ideal points of the ideal line of the euclidean plane. This means that the notion of angle measured in this ideal line pencil agrees with the angle measurement between euclidean lines in $\mathbf{E}^2$.

In order to compare these two metric geometries within the same plane, we assume the coordinates on W and W^* described in the previous chapters. Then we define an algebra isomorphism $P : \mathbf{P}(\bigwedge \mathsf{V}) \leftrightarrow \mathbf{P}(\bigwedge \mathsf{V}^*)$ by its action on the basis 1-vectors by $P(\mathbf{e}_i) = \mathbf{e}^i$ and extend by linearity. Using P, any configuration C in the euclidean plane can be interpreted as a configuration $\widehat{C}$, and vice-versa.

10.2 Example: hexagon and hexalateral

Fig. 10.2 shows a euclidean hexagon H and its polar counterpart $\widehat{H}$, a polar-euclidean hexalateral. The small star-form in the middle represents the ideal point $\mathbf{e}^0$. The 6 vertices of H correspond under P to the 6 bold lines forming $\widehat{H}$; the six boundary lines of H map to the 6 corners of $\widehat{H}$. The edges, as point sets, are line segments. The dual of a line segment (all the points between two given points on a line) is a *fan*: all the lines through a point between two given lines of the point. These 6 fans appear at the corners of the $\widehat{H}$.

Inside and outside. The *interior* of a euclidean polygon is the set of points which are separated from the ideal line by the edges of the polygon. Similarly, the interior of the polar polygon is the set of lines which are separated from the ideal point by the fans of the polar polygon. The dual line $\mathbf{E}^0 = P(\mathrm{e}0)$, the image of the ideal line of the euclidean plane, is clearly such a line; one can reach all other such lines by moving this line, as long as one is careful not to cross through one of the fans of the polar polygon. Hence, the *interior* of a polar polygon is a domain of lines that encloses the boundary of the polar polygon from *outside* (seen euclideanly). The interior of a euclidean domain is sometimes called a *kernel*; that of a polar-euclidean domain, a *hull*, to reflect this radically different quality it presents to the human perception.

The pattern of dots in the interior of H maps to the pattern of lines in the interior of $\widehat{H}$. The asymmetry of the way these geometries present themselves to human experience is clearly brought out by comparing these two patterns. The crossing points of the lines in $\widehat{H}$ correspond to joining lines of the points in $\widehat{H}$; the former are given to see while the latter must be thought.

The right-hand image shows the result of applying the "same" translation in each of the spaces. Here, *same* means that if T is the translation in $\mathbf{E}^2$, then PTP^{-1} is the translation of $\widehat{\mathbf{E}}^2$

10.2.1 Metric-neutralaspects

The duality between hexagon and hexalateral is not yet a metric one; the relation is based purely on projective principles. Only the application of a translation to both fig-

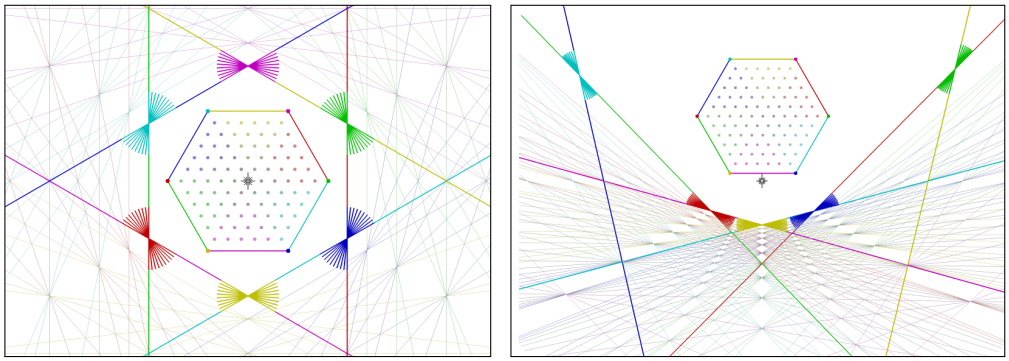

Fig. 10.2 A view of a euclidean hexagon and a polar-euclidean hexalateral. The right image shows the result of a translation applied in both spaces.

ures introduces a metric element. Consequently, the left-hand side of Fig. 10.2 can be considered also to apply as well to duality in non-euclidean geometries. In particular, if one considers the hexagon as representing a rigid body, then the hexalateral represents the dual rigid body (see Sect. 9.9), composed – in the plane – of mass lines instead of mass points. Then the center of mass of this particular dual rigid body is the polar line (in the particular metric being used) of the point-wise center of mass. The fact that inner and outer are reversed gives some inkling that dual dynamics presents challenges to the ordinary consciousness of space.

10.3 Euclidean and dual euclidean measurement

Clearly, the metric relations of points in the one geometry is mirrored by the metric relations of lines in the other, and vice-versa. That means that distances of points in dual euclidean geometry are calculated as angles are calculated in euclidean geometry, and distances of lines in dual euclidean geometry correspond to the distances of points in euclidean geometry.

To avoid confusion with terminology, the separation of two points in dual euclidean geometry is called the *shift* between the two points; the separation of two lines in dual euclidean geometry is called the *turn* between the two lines. Note that the shift, like euclidean angle, takes values in $[0, 2\Pi)$; while the turn, like euclidean distance, can become unboundedly large. The latter occurs when one of the lines approaches the ideal point. Two points are parallel when they lie on the same line through the ideal point. Two points are perpendicular when their joining lines to the ideal point meet at right angles.

We close our discussion of dual euclidean geometry by dualizing one euclidean concept, chosen from among many possible candidates.

10.3.1 Dual gravity

Objects in the neighborhood of the earth are attracted towards the earth according to Newton's law of gravitation. The force of attraction is carried by the line $\mathbf{\Sigma}_g$ joining the center of mass of the object and that of the earth (which can be considered to be the origin $\mathbf{E}_0$), and is proportional to the mass of each. If such an object is dropped from a position close to the surface of the earth, its center will move along the line $\mathbf{\Sigma}_g$ with essentially constant acceleration.

Dualize this situation. We have to consider both the object and the earth as being composed of planes which envelop their surfaces. The center plane of this dual earth can be considered to be the "origin plane" E^0. The center of the object is a plane close to the surface of the earth (which consists of tangent planes to this surface). The force of dual gravity will then be carried by a line $\mathbf{\Sigma}_d$ formed by the intersection line of the two center planes. Viewed with euclidean lenses, this will be an ideal line (since $\mathbf{E}^0$ is the euclidean ideal plane). If such an object is dropped, its center (plane) will rotate around $\mathbf{\Sigma}_d$ with essentially constant acceleration. Since $\mathbf{\Sigma}_d$ is euclidean ideal, the rotation will appear as a translation perpendicular to the normal direction of the plane, and (viewed euclideanly) *away* from the surface of the earth, towards the center plane $\mathbf{E}^0$ of the dual earth. The analogous 2D situation is illustrated in Fig. 10.3.

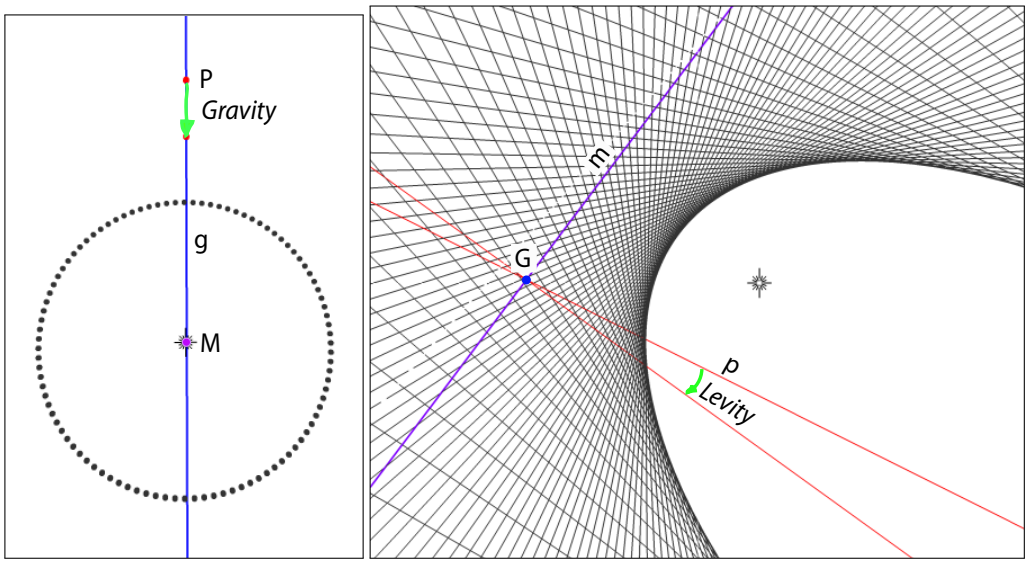

Fig. 10.3 The figure on the left illustrates the force of gravity acting on a point **P** along the line **G** towards the center **M** of a planet represented by a circle of points. On the right, the dual force acting on a line p around the intersection point **g** towards the center line **m** of a dual planet represented by a circle of lines. The star point represents the ideal point of the dual plane. In both cases the direction of the force is *away from* the ideal element.

Such is the phenomenology of dual gravity: planes moving away from the surface of the earth. Searching for a single word to express its nature, one is hard put to do better than *levity*. Whether such a force has a reality that expresses itself in the physical world is a second question. Certainly the success of predictive theories in the history of science teaches us that the chances of detecting something are greatly improved when one has first recognized it conceptually. The present work is limited to this conceptual "ground-breaking" which must precede any successful cultivation.

10.4 A circle of metric geometries

The focus of this work has been on the four discrete values $\kappa \in \{-1, 0, 1, \infty\}$ in Fig. 10.1. However, for all other values of κ there exists a non-degenerate Cayley-Klein geometry with that "curvature". We took advantage of the existence of such non-degenerate geometries in the limiting processes which led to euclidean and dual euclidean geometry in Sect. 3.2.1. With this expanded view, the object of study is a continuous family of geometries (and associated Clifford algebras). Without dual euclidean geometry, this family is parametrized by $\mathbb{R}$; with the addition of dual euclidean geometry $\kappa = \infty$ it is parametrized by $\mathbf{S}^1$, and hence is the 1-point compactification of $\mathbb{R}$, and has consequently the nice properties associated to compact objects. It is furthermore closed under dualization, which, in light of the importance of projective geometry in the foregoing exposition, is a further advantage of including dual euclidean geometry. The following literature guide shows that there is also a growing body of research supporting the inclusion of dual euclidean geometry within the standard mathematical toolkit of the natural scientist.

Since Riemann, the geometry of the physical universe has been accepted as an object of empirical research. Cosmologists typically model the universe as a general Riemannian manifold, with a variable curvature at each point. To first order, the above "circle" of constant-curvature geometries provide an approximation to the overall shape of the universe. The qualitative differences exhibited by this family is a valuable first step to understanding more complicated curved spaces. The Clifford algebras associated to this family provide a multi-purpose tool for exploring an d comparing geometry, kinematics, and dynamics in these spaces.

10.5 Guide to the Literature

Remark 205. **Terminology alert.** There is not yet a consistent terminology in the literature. What we call dual euclidean geometry is also known as *polar euclidean* geometry; its 3-dimensional version is also known as *counter-space*.

[Kow09], appendix to Ch. 6, contains a good introduction to this theme. Of particular interest is his discussion of areas of scientific research where dual euclidean geometry appears to provide promising advantages over euclidean geometry. For example, phe-

nomena of plant growth such as bud development, which proceeds around and out of an ideal point within; or, the central role of planar surfaces (leaves, flower petals) in plant morphology. A detailed account of the latter theme may be found in [AW80]; [Ada34] is a mathematical prequel by the same author that explores the vistas opened by projective geometry for the understanding of the human and natural worlds, and provides valuable background material for anyone interested in this theme.

See [Con08], pp. 71ff., for related discussions regarding the role of dual euclidean geometry in mechanics. [Tho09] represents an ambitious program to apply this concept to fundamental themes of physics such as gravity, light, electricity and magnetism, and more.

Chapter 11
Results

The results of Chapter 9 have been implemented in software. This chapter presents results based on this software, allowing a firstf look at the phenomenology of rigid body motion in elliptic and hyperbolic space. The chapter begins with an account of rigid body motion in the plane, since this context allows certain characteristic features to be identified most easily, before moving on to the three-dimensional case.

11.1 Comparison to Poinsot description of the Euler top

Recall the discussion of the Euler top in Chapter 1, in particular the discussion of the Poinsot description of the motion. The visualizations presented here also display the polhode (Sect. 9.5.3). The polhode in this case is the path of a bivector in $\mathfrak{B}$. Representing a general bivector in $\mathbb{R}P^3$ presents several challenges. As a first reduction, we use the ambient metric to represent a bivector via an axis pair (which is usually unique, see Sect. 7.7; resolving the non-unique case has to separately handled). Thus one obtains two paths in $\mathcal{L}$, representing these two axes. We currently investigate only one of these, which includes the proper axis if one exists. Each of these paths corresponds to a ruled surface in $\mathbb{R}P^3$. We sample the path in order to obtain an optimal representation.

There are some features of the $SO(3)$ Euler top which do not appear in our treatment of Cayley-Klein geometries. The inertia ellipsoid can be defined as the set of velocities that, for a given momentum and a given rigid body, preserve a given kinetic energy. This set is given by the level sets of the quadratic form $\mathbf{A}^{-1}$ in $\mathfrak{B}$. We have not found a simple way to visualize this in $\mathbb{R}P^3$. The herpolhode is contained in the invariant plane, which is a hyperplane of $\mathfrak{B}$. As noted in Sect. 7.2.1.3, such a hyperplane corresponds to a linear complex. The same analysis that Poinsot applied in the $SO(3)$ case regarding the interaction of the inertia ellipsoid and the invariant plane can also be applied here to show that the inertia ellipsoid rolls along the invariant plane in $\mathfrak{B}$, tracing out the polhode and the herpolhode on the two surfaces. We have not visualized these aspects, although there are no technical difficulties in visualizing the herpolhode in the same way as the polhode (see details below).

The current research does not provide a full Poinsot description for the rigid body motion studied here. Such a project would, like the Poinsot analysis described above, base itself on the moments of inertia and therefore have to be based in $\mathfrak{B}$, but at the same time translate the results obtained back into the 3D Cayley-Klein space. Due to the lack of such a theoretical understanding, the results presented here are mainly visual evidence accompanied by heuristic reasoning and conjectures. They will have served their purpose if they help to inspire interest in the subject which leads to a mathematical understanding.

11.2 Simulation Software

As noted in the previous chapter, the equations of motion have explicit solutions involving theta functions of two variables. The simulation does not use these exact solutions.

In the course of writing this thesis, two separate software simulations were written. First, non-interactive Mathematica packages and notebooks were developed for assistance in verifying all the calculations presented in the theoretic part. This code is focused on the 2- and 3-dimensional cases handled in the thesis. It is noteworthy that the code not only verified results but in many cases suggested new ones. However, since the code itself offers no innovative features, we do not discuss it further here.

This chapter focuses on the interactive software developed for visualizing the simulation results. We first give a short description of the software for the three-dimensional case. The two-dimensional version is essentially the restriction of the three-dimensional software to the $z = 0$ plane; its special features are defined separately below.

11.2.1 Specification of parameters

The software is designed to allow full control over parameters identified in the theoretical part of this work, for force-free rigid body motion. This includes:

1. **The inertia tensor of the body**. This is specified by giving the homogeneous coordinates (x, y, z, w) of a proper point. Then using the 4-particle representation discussed in Sect. 9.3.1.2, the rigid body consists of the four mass points $(x\mathbf{E}_1, y\mathbf{E}_2, z\mathbf{E}_3, w\mathbf{E}_0)$. The points must be proper points for the respective geometries; w is adjusted if necessary to bring it within range. The point (x, y, z, w) is normalized to have norm 1; any desired scaling can be interpreted as a mass, which is handled separately with the parameter m. The inertia tensor of the resulting body is proportional to the diagonal matrix

$$\mathbf{A} = m(w^2 + \kappa x^2, w^2 + \kappa y^2, w^2 + \kappa z^2, x^2 + y^2, x^2 + z^2, y^2 + z^2)$$

(Sect. 9.3.1). m, the mass, is a separate parameter controlled by a slider. Changing m speeds up or slows down the motion, but otherwise has no effect. Every valid inertia tensor can be created in this way (up to a rigid motion).

2. **The momentum in space.** A momentum line $\mathbf{\Pi}$ is specified by a distance $d \in [0, \infty]$ from the origin, and an 3D orientation, interactively entered using a virtual trackball. There is an additional real parameter $\alpha \in [0, 1]$. The actual momentum bivector used is then $\mathbf{\Xi} = (1 - \alpha)\mathbf{\Pi} + \alpha\mathbf{\Pi}^{\perp}$. α splits the momentum between $\mathbf{\Pi}$ and its polar line $\mathbf{\Pi}^{\perp}$. The instantaneous velocity $\mathbf{\Omega}$ is calculated as $\mathbf{\Omega} = \mathbf{A}^{-1}\mathbf{\Pi}$ and is likewise a non-necessarily simple bivector.

Remark 206. The momentum bivector $\mathbf{\Xi}$ plus the inertia tensor $\mathbf{A}$ fully determine the evolution of the body under Euler's equations (9.26).

11.2.2 3D Visualization

The visualization is implemented using jReality ([jr06], [WGH+09]), a metric-neutral 3D scene graph. jReality offers seamless support for visualization in all three geometries featuring the "insider's" view of these spaces. For a detailed description of the metric-neutral design and implementation issues involved, including a discussion of the insider's view, see [Gun10].

11.2.2.1 Visualization of bivectors Bivectors play a large role in this simulation. A simple bivector can be visualized as the line it represents – this does not depend on the metric. But for non-simple bivectors there is no convenient projective visualization. Such bivectors are displayed via an axis pair. This applies to simple bivectors, since the bivector itself is an axis then. The axis pair is generally unique (Remark 136), but any pair will do. Currently they are both displayed with the same color and intensity. There are plans in a future version of the software for color coding to be applied based on the homogeneous pitch of the bivector. Equal color on each axis would correspond to affine pitch 1 (Def. 137).

11.2.2.2 Visualization of ideal elements In the hyperbolic case, the ideal sphere of hyperbolic space is displayed using a semi-transparent textured map sphere, which allows one to see which parts of the momentum and velocity axes lie inside of hyperbolic space and which lie outside. This is not a realistic feature, but rather a informational one, which allows the user also to see "outside" of hyperbolic space, since important elements in the dynamic simulation may have their home there. See Fig. 11.1. Notice that only parts of one velocity axis and one momentum axis are within the sphere; the ends of these axes, and the improper axes, are visible more dimly outside the sphere.

11.2.2.3 Overview of 3D rigid body visualization The user chooses the desired metric from the 3 possibilities. The user can start and stop the rigid body motion simulation at any point. The underlying visualization strategy for rigid body motion is to display the following components:

1. **The body** is represented as a box (a right-angled hexahedron) centered on $\mathbf{E}_0$ with proportions determined by (x, y, z, w) above. In particular, the 8-particle body with unit-mass particles located at $\pm x\mathbf{E}_1 + \pm y\mathbf{E}_2 j + \pm z\mathbf{E}_3 + w\mathbf{E}_0$ has inertia tensor proportional to the 4-particle one described above. These 8 positions determine the

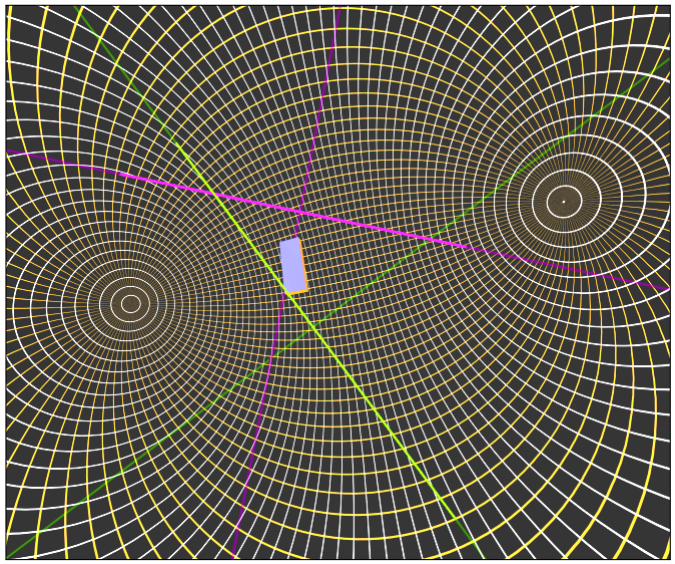

Fig. 11.1 The ideal sphere of hyperbolic space is displayed as a semi-transparent texture-mapped surface, allowing the user to see which parts of the configuration are proper and which are improper.

displayed box. The displayed size of the box can be scaled by the user, the default scale factor is .1. In the elliptic case, the choice of $\mathbf{E}_0$ is arbitrary, and any of the four points $\mathbf{E}_i$ can serve this function (Sect. 9.3.3); each has a corresponding box centered on a different $\mathbf{E}_i$. For example, the box around $\mathbf{E}_2$ consists of the 8 points $(\pm x, y, \pm z, \pm w)$ (which are projectively equivalent to $(\pm x, \pm y, \pm z, w)$. To distinguish the different boxes, to each axial direction is associated a color, so the four boxes each have 3 colors, 2 of which they share with any other one. Currently only the first is displayed.

2. **$\mathbf{\Pi}$ and $\mathbf{\Omega}$.** Both are calculated in the body coordinate system but displayed (naturally) in the space coordinate system. This provides a good check of the validity of the simulation, since the momentum in space is constant. If the displayed momentum appears to move, there is a problem with the simulation. $\mathbf{\Omega}$ in general is a non-simple bivector. Both axes of this bivector are then displayed. Currently the momentum axes are displayed in purple, and the velocity axes in bright green.
3. **The orbit of the center of mass.** As noted in Sect. 9.3.3, in elliptic dynamics there are four centers of mass. But regardless of the metric, the orbit (history of motion) of each of the points $\mathbf{E}_i$ is maintained and the user can choose which of these to display. In the euclidean case, they are not visible since they lie in the ideal plane; in the hyperbolic case they lie beyond the ideal sphere (but are nonetheless visible); only in the elliptic case are they all proper curves in the space.
4. **The polhode** (optional). A regular sampling of the velocity state $\mathbf{\Omega}_c$ as axis pair is collected in a list and then displayed. By Sect. 9.5.3, this is a closed curve for $n = 2$. One research goal of the software is to help suggest analogous results for the velocity

state in the body in the 3D case. The polhode is currently displayed as yellow lines which, for performance reasons, are rendered without shading.

11.2.3 2D Visualization

As indicated above, the 2D simulation and visualization is essentially the 3D one restricted to the plane $z = 0$. Hence we refers to points here as (x, y, w) triples. Since $\mathbf{m}$ lies in the $z = 0$ plane also, only three of the six moments of inertia have an influence on the motion: M_{01}, M_{02}, M_{12}. These can be calculated from (x, y, w) and the metric κ as follows:

$$M_{01} = \kappa y^2 + w^2$$
$$M_{02} = \kappa x^2 + w^2$$
$$M_{12} = x^2 + y^2$$

In the following, we often refer to (x, y, w) rather than (M_{01}, M_{02}, M_{12}) to identify the rigid body since the former is a metric-neutral identification, while the latter depends on the metric. This is useful for comparative studies of the same rigid body in different metrics. However, an exact analysis of the behavior in each metric is to be sought via $\{M_{ij}\}$, not (x, y, w).

The standard 2D simulation displays the rigid body as a small texture-mapped rectangle with the aspect ratio $\frac{x}{w} : \frac{y}{w}$. The momentum line $\mathbf{m} = \mathbf{e}_2 + d\mathbf{e}_0$ is a line parallel to the y-axis $\mathbf{e}_2$. Hence, $d = 1$ corresponds to an ideal hyperbolic momentum line. Since $d = \mathbf{m} \vee \mathbf{E}_0$, d is sometimes called the *moment* of the momentum with respect to the origin. The polar point of the momentum $\mathbf{M} := \mathbf{m}^\perp$ is also displayed and plays an important role in the non-euclidean setting. The boundary of the hyperbolic disk is displayed as a circle.

11.2.3.1 Compact mode In the two-dimensional version, there are optional "compact" display options for elliptic and hyperbolic planes. These compact views have the advantage that they offer full visibility of all components of the dynamical system, whereas the quality of the normal planar view (particularly for the elliptic case) is diminished by the frequent "disappearance" of one or the other moving element.

- Compact mode for the elliptic plane displays the simulation on the surface of $\mathbf{S}^2$, using the standard double-covering $\mathbf{S}^2 \to \mathbf{Ell}^2$. It replaces the rectangle representation of the body with a 3D box centered at the center of the sphere, representing the Euler top in $\mathbb{R}^3$ corresponding to the elliptic body, under the isomorphism defined in Sect. 9.6. Everything in the elliptic plane, except the rigid body itself, then appears twice in the compact view.
- Compact mode for the hyperbolic plane uses stereographic projection to map the hyperbolic plane onto the unit sphere, 1:1 except for the line $\mathbf{e}_0$ which is mapped to the "North pole" of the sphere. The boundary of the hyperbolic plane is mapped to the equator of the sphere. The momentum line is mapped to a circle.

See Fig. 11.2.

11.2.3.2 Flat 2D hyperbolic features For the flat model of the hyperbolic plane, the display has a number of unique features:

- A piece of "hyperbolic graph paper" is included, centered on the x-axis. See Fig. 11.2, lower right image. This "horizontal" markings on this surface are equidistant curves with respect to the x-axis; the "vertical" lines are hyperbolically equally-spaced, perpendicular lines to x-axis. Hence, the (x, y) position of a point lying on this graph paper gives its distance from the origin along the x-axis, then the perpendicular distance up to the point. This is useful in metrically assessing the orbit of a point.
- Related to the previous point, the orbit of the center of mass along this graph paper (and its virtual extension to the whole disk), is also presented in a euclidean view where the (x, y) coordinates are interpreted as euclidean coordinates. Hence the euclidean distances along the horizontal axis and along any vertical line are also hyperbolically correct; but the true hyperbolic distances between the vertical lines, as one leaves the x-axis, increase exponentially although in the euclidean picture they remain constant. See Fig. 11.6
- The momentum line is always positioned in *canonical* position. That means, when it is proper, it is the line $\mathbf{e}_2$. When it is improper, it is the line $\mathbf{e}_0$. To achieve this, a hyperbolic translation is applied to the whole scene (with the exception of the boundary and the graph paper described in the previous item).

11.3 2D rigid body mechanics

We now turn to a description of results obtained for planar rigid body motion. We discuss first bodies with (x, y) rotational symmetry, then turn to asymmetric bodies. Each of these topics in turn is discussed with regard to different choices of $\mathbf{m}$. The distinctions are somewhat artificial, since they only apply fully to hyperbolic case. And, other distinctions arise in the elliptic case which are handled separately. Note that due to the isomorphism of a rigid body moving in $\mathbf{Ell}^2$ to a Euler top in $\mathbb{R}^3$ (Sect. 9.6), all the results in the elliptic plane can be translated to the $\mathbb{R}^3$ setting where a mature theory exists to explain most of the phenomena demonstrated here. A full treatment based on this translation lies outside the scope of the current work.

11.3.1 General observations

Regardless of the choice of symmetry and position of $\mathbf{m}$, there are some distinctive features which can be observed, even before the object begins to move. Consider the three points $\mathbf{M}$, $\mathbf{V}$, and $\mathbf{E}_0$, the center of mass. Given initial conditions such that $\mathbf{V}$ lies between $\mathbf{M}$ and $\mathbf{E}_0$ for the elliptic plane, then $\mathbf{V}$ lies on the other side of $\mathbf{E}_0$ from $\mathbf{M}$ for the hyperbolic plane, and vice-versa. This follows directly from the fact that $\mathbf{M} = \mathbf{m}^\perp \equiv m_0\mathbf{E}_0 + \kappa m_1\mathbf{E}_1 + \kappa m_2\mathbf{E}_2$.

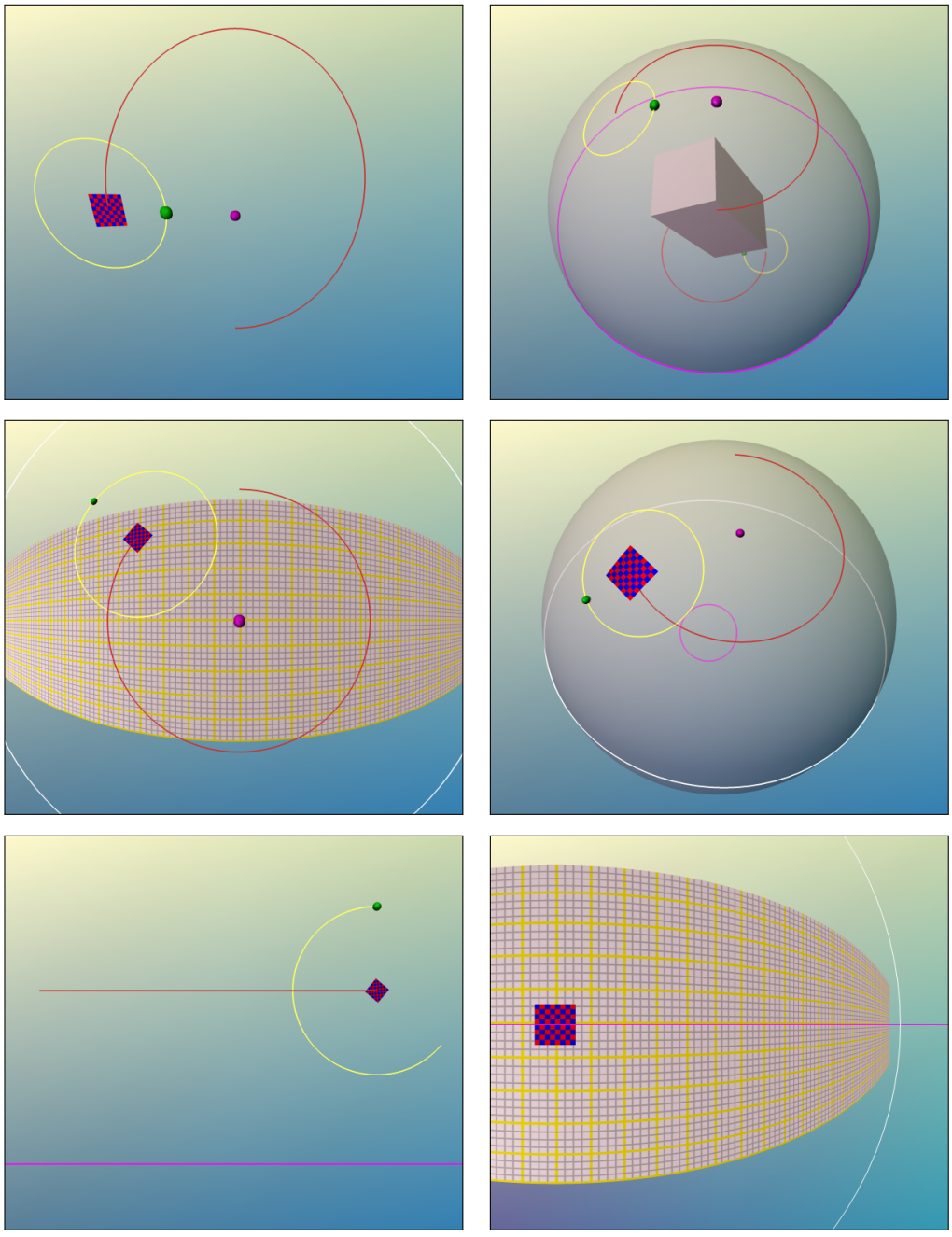

Fig. 11.2 A sampling of 2D visualizations of motion of (x-y) rotationally symmetric body in the three metrics elliptic, hyperbolic, and euclidean. The parameters were $(x, y, w) = (1, 1, 2)$, and $d = 4$. The non-euclidean cases include flat and compact views. The lower right picture shows the hyperbolic graph paper feature discussed in Sect. 11.2.3.2.

11.3.2 Rotationally symmetric body

By a rotationally symmetric body we mean one with $M_{01} = M_{02}$. This is equivalent in our setup to $x = y$. For the elliptic case, a body is rotationally symmetric if any two moments of inertia are the same (but, naturally, with a different axis for each pair). We leave this to the side since no qualitatively new behavior thereby arises.

11.3.2.1 With far momentum line By *far* we mean that $\mathbf{m}$ is improper in the hyperbolic metric. Then $\mathbf{M}$ is proper.

Fig. 11.2 illustrates the evolution of a symmetric rigid body ($(x, y, w) = (1, 1, 2)$) under the action of a momentum line with moment $d = 4$. The path of the center of mass $\mathbf{E}_0$ appears to be, in the non-euclidean case, a circle; and in the euclidean case, a straight line. That this is in fact the case can be deduced from the Euler equations (9.25). We show only that the polhode is a circle in all three cases. Set $q_{03} = q_{31} = q_{23} = 0$ (since $z = 0$ in the plane), $q_{12} = 1$ (homogeneous coordinates) and $M_{01} = M_{02} = M$ ($x - y$ symmetry of object). Then one obtains:

$$\begin{aligned}
\dot{q}_{01} &= -\frac{2q_{02}}{M}(M - \kappa M_{12}) \\
\dot{q}_{02} &= \frac{2q_{01}}{M}(M - \kappa M_{12}) \\
\dot{q}_{12} &= 0
\end{aligned}$$

This is a vector field that points perpendicular to the line connecting $\mathbf{V}$ with $\mathbf{E}_0$. Thus, regardless of the metric, the velocity point moves in a circle around the center of mass $\mathbf{E}_0$. One can then integrate the equation of motion $\dot{\mathbf{g}} = \mathbf{g}\boldsymbol{\Omega}_c$ to deduce that:

- **Euclidean.** The body moves on a straight line parallel to $\mathbf{m}$, and rotates around its center of mass with an angular velocity proportional to d.
- **Elliptic.** The body moves CCW around a circle which goes away from the momentum line, and undergoes an additional CCW rotation around its own center with signed angular velocity proportional to $M_{12} - M_{01} (= M_{02})$ (CCW when $M_{12} > M_{01}$, CW when $M_{12} < M_{01}$).
- **Hyperbolic.** The body moves CW around a circle which "heads" towards the momentum line, and undergoes an additional CCW rotation around its own center with angular velocity proportional to $M_{12} - M_{01}$. Since $M_{12} > M_{01}$ in the hyperbolic case, CW rotation is not possible.

11.3.2.2 With near momentum line By *near* we mean $\mathbf{m}$ is proper in the hyperbolic metric and $\mathbf{M}$ is improper: $d << 1.0$. The most dramatic change from the previous case occurs naturally for the hyperbolic case. See Fig. 11.3. Center of mass moves along equidistant curve to momentum line, and approaches but never arrives at the ideal point of this line in this direction. This is analogous to the behavior of the euclidean body, which also moves along an equidistant curve to the momentum line (which is a parallel line to the momentum line), and also approaches but never meets its ideal point.

In the other cases, the qualitative motion is the same as for far **m**. In the euclidean case, the object moves along the same line, but the linear velocity increases while the angular velocity is reduced. In the elliptic case, both the center of mass and the velocity state move along larger circles; the rotation around the center of mass is diminished. These behaviors can be deduced by elementary considerations arising from the relation $\mathbf{m} = \mathbf{A}(\mathbf{V})$; we leave that to the never-tiring reader.

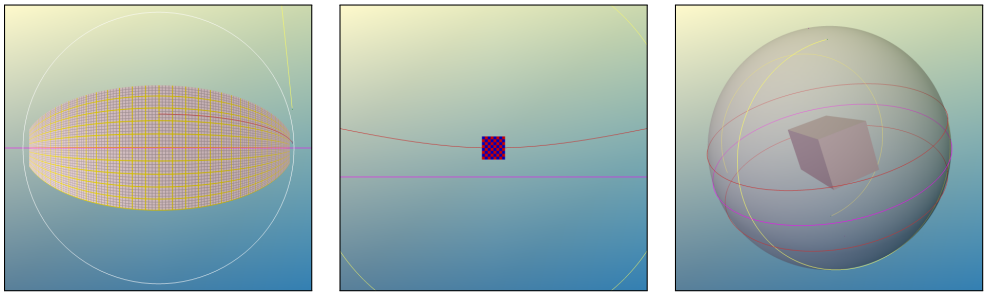

Fig. 11.3 A rotationally symmetric rigid body acted on by a "far" momentum line. Left picture shows flat view of hyperbolic case. Middle view shows flat elliptic plane, illustrating difficulties associated to flat view. Right view shows compact view of elliptic plane, here one clearly sees both path of center of mass and path of velocity are circles.

11.3.2.3 With ideal momentum line For a euclidean ideal momentum line, the resulting motion is pure rotation; the momentum line is obtained by integrating a force couple. For a hyperbolic ideal line, the center of mass moves along a *horocycle* passing through the ideal point of tangency of **m**. Fig. 11.4 shows two time values of this motion. The body never arrives at the ideal point. This behavior has no analog in the other metrics.

Remark 207. It would be conceivable to create a second kind of "horocyclic" graph paper for the hyperbolic disk which would demonstrate that this curve is actually a horocycle, just as the graph paper in Fig. 11.3 demonstrates that the curve is an equidistant curve.

11.3.3 Asymmetric body

Asymmetric means all moments of inertia are different. This is not possible for the euclidean case, since $M_{01} = M_{02} = m$. This leaves the non-euclidean cases to consider. We consider a body with $(x, y, w) = (.2, 1, 1.2)$.

11.3.3.1 Far momentum line We begin with the case of a far momentum line with $d = 4$. The two non-euclidean cases exhibit a similar behavior in this case. The motion of the center of mass describes a curve reminiscent of the *herpolhode* curve, the curve traced out by the angular velocity vector of an Euler top on the invariant plane.

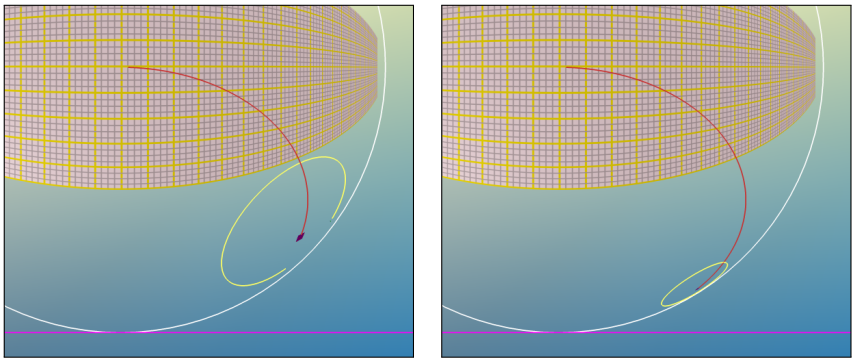

Fig. 11.4 A rotationally symmetric rigid body acted on by an ideal momentum line in the hyperbolic plane. The center of mass moves along a horocycle which shares a point with the momentum line, but never arrives at this point.

The body moves within a pair of circles centered on the center of mass. When it reaches the outer circle, it is oriented so that its long axis points at $\mathbf{E}_0$; when it reaches the inner circle, it has rotated so that its shorter axis points to the center. There are two frequencies involved: the angular velocity λ_1 around the momentum point $\mathbf{m}^\perp$, and the angular velocity λ_2 around the center of mass. When these two are commensurate, the curve is periodic; otherwise it fills the annulus bounded by the two circles.

When $\mathbf{m}$ moves further away (closer in), the circles shrink toward (expand around) $\mathbf{m}^\perp$.

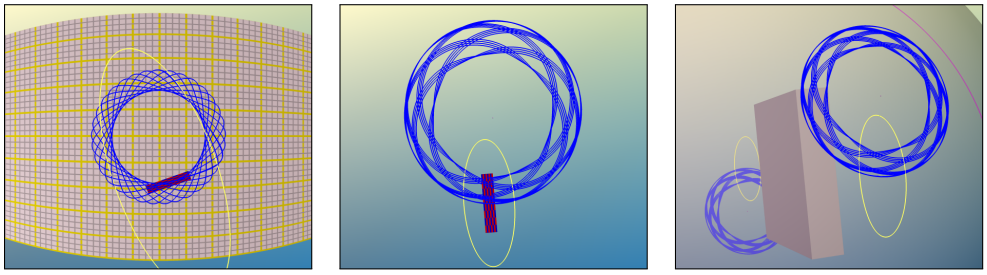

Fig. 11.5 An asymmetric rigid body acted on by a "far" momentum line. Left picture shows flat view of hyperbolic case. Middle view shows flat elliptic plane. Right view shows compact view of elliptic plane.

11.3.3.2 Near momentum line We begin with the case of a near momentum line with $d = .45$. The left image of Fig. 11.6 shows the motion for a hyperbolic body with $(x, y, w) = (.22, 1.0, 1.03)$. One observes that the body oscillates back and forth along $\mathbf{m}$ while moving in the direction of the ideal point of $\mathbf{m}$ to the right. The right image of

Fig. 11.6 provides the euclidean version of the graph paper (see above, Sect. 11.2.3.2). Close examination of this curve shows that it is not a pure sine curve, but obviously periodic. In any case, this oscillatory behavior with respect to a line has no analog in euclidean or elliptic space. It is a premonition, however, of the *screw motion* in three dimensions (Def. 125), as it combines an periodic motion in one direction with a translational one in the transverse one.

Remark 208. The values $(.2, 1.0, 1.03)$ in the previous example corresponds to very large hyperbolic body whose inertia tensor is $(0.06, 1.013, 1.05)$. M_{01} is very small. The oscillation becomes more pronounced, the smaller M_{01} becomes.

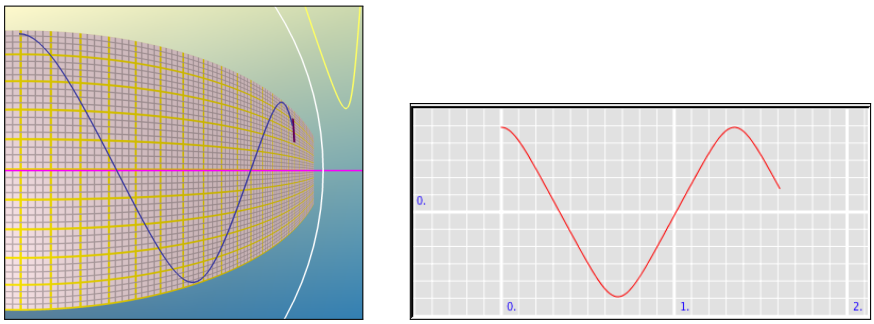

Fig. 11.6 The orbit of an asymmetric rigid body in the hyperbolic plane with $(x, y, w) = (.22, 1.0, 1.03)$ and $d = .45$. On the left, the view in the hyperbolic disk showing how the object moves from one side of the momentum line to the other. The velocity state curve consists of improper points (upper right yellow curve). On the right, the "euclidean" version of this path, redrawn on euclidean graph paper.

Finally, we consider the asymmetric elliptic case with a near momentum line. For some values of (x, y, w), the behavior is not qualitatively different from far momentum line. Decreasing d moves the pair of limiting circles away from the point $\mathbf{M}$ towards $\mathbf{m}$. However, it can also happen that there is only one limiting circle; the path of the rigid body crosses over $\mathbf{m}$ instead of remaining bounded away from it. See Fig. 11.7. The conditions under which this happens is a question requiring more robust mathematical tools than so far developed here.

11.3.3.3 With ideal momentum line For a hyperbolic ideal momentum line, the center of mass of an asymmetric body oscillates around a *horocycle* passing through the ideal point of tangency of $\mathbf{m}$. Fig. 11.8 shows two time values of this motion. The body never arrives at the ideal point. This behavior is a combination of the two behaviors already observed in hyperbolic plane: asymmetric with near momentum line (oscillation around $\mathbf{m}$), and symmetric with ideal momentum line (approach ideal point of horocycle).

This concludes our investigation of 2D rigid body motion. We have presented examples of all qualitatively different behaviors that have arisen in our simulations. The basic

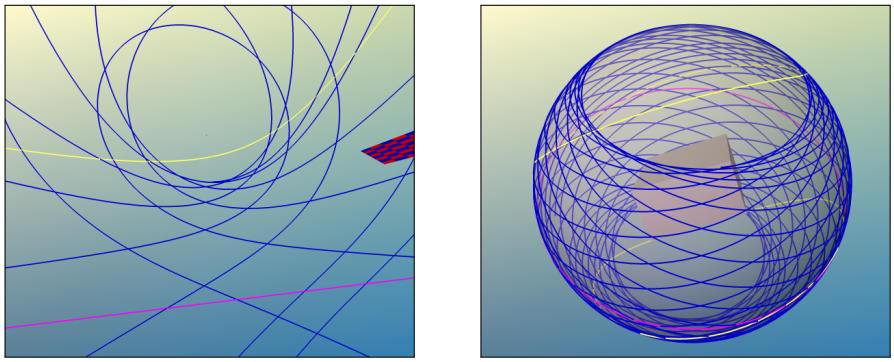

Fig. 11.7 The orbit of a center of mass of an asymmetric rigid body in elliptic space can also have only one limiting circle. Left picture shows flat view; right view shows compact view.

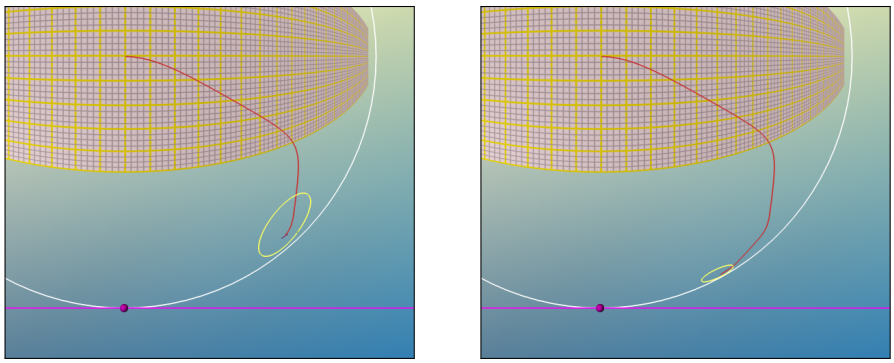

Fig. 11.8 An asymmetric rigid body with $(x, y, w) = (.25, 1.2, 2.0)$ acted on by a hyperbolic ideal momentum line. Two views of the same motion; the approach to $\mathbf{M}$ is clearly indicated.

vocabulary of behaviors which we have encountered will form the basis of our observations of the 3D case, which now follows.

11.4 3D rigid body mechanics

The main differences to the initial conditions specifying the motion include the extra coordinate z in the specification of the body and the fact that the momentum can be an arbitrary non-simple bivector.

This momentum $\mathbf{\Pi}$ then can be decomposed as the sum of two simple bivectors $\alpha\mathbf{\Pi}_s + \beta\mathbf{\Pi}_x$ where $\mathbf{\Pi}_s$ and $\mathbf{\Pi}_x$ are normalized, and $\mathbf{\Pi}_x = \mathbf{\Pi}_s^{\perp}$. The affine pitch of such a non-simple bivector is the ratio $\beta : \alpha$ (Def. 137).

The greatly enlarged parameter space of initial conditions for 3D rigid solid motion force this discussion to be less thorough and more anecdotal than the 2D discussion. We try to bring the attention to a selection characteristic behaviors without being able to offer a systematic survey of all possible combinations.

Since we restrict attention in this report the the center of mass $\mathbf{E}_0$, the w coordinate plays a special role in these considerations. The other three values (x, y, z) have equivalent roles to play. The evolution naturally also depends on the position of $\mathbf{\Pi}$. The situation is complicated by the fact that the default position of $\mathbf{\Pi}$ is aligned with the box coordinates and leads to an unstable planar orbit of the center of mass which is not interesting to us since it is isolated in orbit space.

11.4.1 Fully symmetric body

11.4.1.1 Simple momenta The extra dimension means that there are a range of symmetry conditions that give rise to distinctive behavior. We begin again with the study of spherically symmetric bodies, that is, ones for which $x = y = z$ with arbitrary (but valid) w. Then $M_{01} = M_{02} = M_{03} = k_1$, and $M_{12} = M_{31} = M_{23} = k_2$. When such a body is subjected to a simple far momentum $\mathbf{\Pi}$, it behaves like the 2D symmetric body above: in the euclidean case it moves along a line; in the non-euclidean it moves in a circle around $\mathbf{\Pi}^\perp$ whose radius depends on the distance of the initial position from $\mathbf{\Pi}^\perp$, with an angular velocity depending on k_1, while rotating around a parallel axis through its own center, with an angular velocity depending on k_2.

Remark 209. **Ideal momentum line.** An ideal momentum line leads in the euclidean case to pure rotation, as before; and to motion along a horocycle in the hyperbolic case. A near momentum line in the hyperbolic case leads to motion along an equidistant curve.

11.4.1.2 Non-simple momenta We next observe spherically symmetric bodies under the influence of non-simple momenta. Here the affine pitch (see above) is the distinguishing parameter. A pitch of 0 means that the momentum is carried by the line $\mathbf{\Pi}_s$; a pitch of ∞, that it is carried by the polar line $\mathbf{\Pi}_x$. Pitches close to 0 will lead to motion close to circular: helices with very gradual rise; larger values lead to steeper helices. Fig. 11.9 shows three examples of different pitches, one in hyperbolic space and two in elliptic. Note the path moves on an equidistant surface with respect to $\mathbf{\Pi}_x$; in hyperbolic space it is an ellipsoid; in elliptic space it is a one-sheeted hyperboloid. Also note that the path in elliptic space returns and fills in more of this surface unless the two frequencies are commensurate, in which case it is periodic orbit.

11.4.1.3 Clifford motion In elliptic space, when the affine pitch = 1, the body moves along a straight line which is right Clifford parallel (Sect. 7.4.1) to both $\mathbf{\Pi}$ and $\mathbf{\Pi}^\perp$. For pitch -1, the motion is along a left Clifford parallel. Besides the trivial case that $\mathbf{\Pi}$ is simple and passes through the center of mass, this is the only example of linear motion outside of euclidean space. Clifford motion puts particular strain on the simulation software since bivectors occur which have infinitely many axis pairs, so that the decomposition into an axis pair is not unique, resulting in visual anomolies that have no

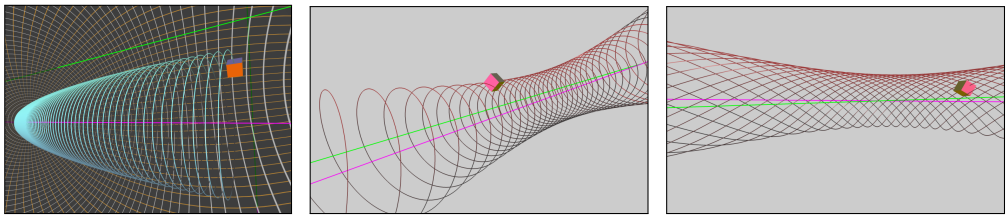

Fig. 11.9 A spherically symmetric body under the influence of a non-simple momentum. The left figure is hyperbolic with pitch .003; the middle is elliptic with pitch .03; the right is also elliptic with ptich .22.

physical significance. For example, the momentum in space may appear to wander, even though the bivector itself is constant.

We do not discuss non-simple momenta further in this chapter, since the resulting motions can be better handled by decomposing the motion into two motions, one due to $\mathbf{\Pi}_s$ and one due to $\mathbf{\Pi}_x$, and then recombining the results. This is essentially the strategy followed above in deducing the helical form of the polhodes in the case of spherically symmetric bodies.

11.4.2 Radially symmetric body

The next stricter condition on (x, y, z, w) is that at most two values are equal. The most striking aspect of this kind of rigid body is that, for simple $\mathbf{\Pi}$, the center of mass moves along an rotationally-symmetric invariant surface. The size and form of this invariant surface depends on the relative sizes of the values of (x, y, z, w).

The special case of two pairs of equal values is of interest only in the elliptic case and leads to an invariant surface close to a circular cone with axis $\mathbf{\Pi}^{\perp}$. See Fig. 11.10.

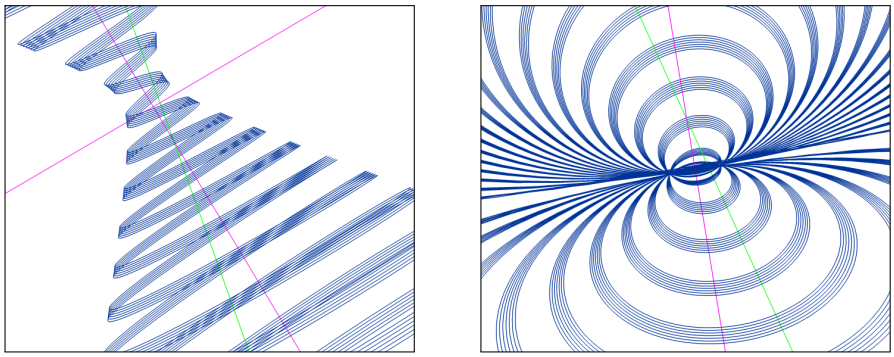

Fig. 11.10 A symmetric rigid body with $(x, y, z, w) = (1, 2, 1, 2)$ acted on by a simple far momentum line in elliptic space. Left view is silhouette view; right view shows view from surface towards "neck".

Leaving this special situation to the side, consider a single pair of equal values and two other unequal values, say $x = y$ and $z \neq w$. First consider the elliptic case. When w is largest of the values, then the invariant surface is convex, appearing to be a symmetric band cut from the outer surface of rotationally symmetric ellipsoid (symmetric means the top circular boundary is congruent to the bottom one); when w is the smallest value, the surface appears to be a similarly symmetric band cut from a hyperboloid of one sheet. The closer w approaches the next largest value, the more the spherical surface approaches the full sphere; in the other case, the more w approaches the next smaller value, the more the hyperboloid widens out and fills in the full surface mentioned in the previous paragraph. See sample pictures in Fig. 11.11.

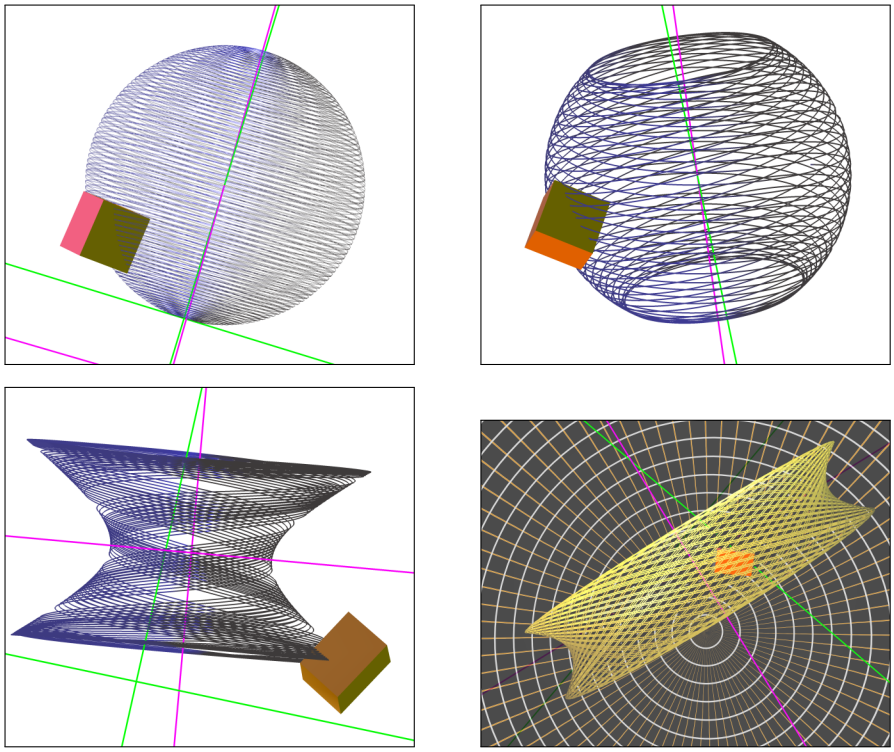

Fig. 11.11 Upper images: A rotationally symmetric body with $(x, y, z, w) = (.7, 1, 1, 1)$ acted on by a simple momentum line. Upper left; with a momentum line almost parallel with x-axis; upper right: with a momentum line far from axial. Lower left: $(x, y, z, w) = (.7, 1, 1, .55)$, with same momentum as UR. Lower right: hyperbolic with $(x, y, z, w) = (1, .6, .6, 1.25)$, with same (hyperbolic improper) momentum line as previous.

11.4.3 Asymmetric body

The final case is that all the values (x, y, z) are different. The resulting orbit of the center of mass tends then to fill out a volume in 3-space bounded by smooth surfaces. Fig. 11.12 shows a body with $x = y$ symmetry, whose orbit is a surface; then the same body where the $x = y$ symmetry has been broken. Notice that the orbit of the center of mass thickens out to fill a volume bounded by two similar hyperboloid-like surface pieces, joined top and bottom with a convex-appearing bridge surface.

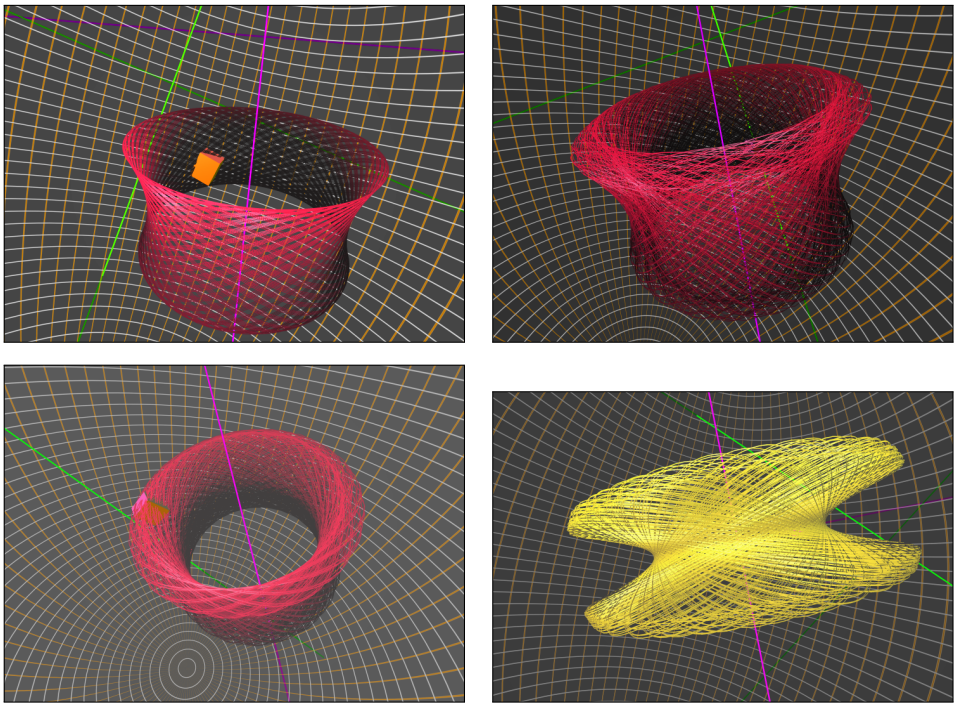

Fig. 11.12 Upper left: orbit of body with $x = y$ symmetry in hyperbolic space; upper right: same settings except $x \neq y$. Lower left: another view of UR; Lower right: similar orbit of another asymmetric body in hyperbolic space.

11.4.4 Polhode

As noted in Sect. 9.5.3, the polhode (the orbit of $\mathbf{\Omega}_c$) lies in a 3-dimensional quartic submanifold in $\mathfrak{B}$. And, as indicated above in Sect. 11.2.2.3, the simulation software collects the polhode in an array which can be, optionally, displayed. Samples of this display technique for a short orbit is shown in Fig. 11.13. Note the distinctive cusp singularities.

Watching the real-time development of this polhode reveals interesting temporal rhythms only partly expressed in the still frames shown.

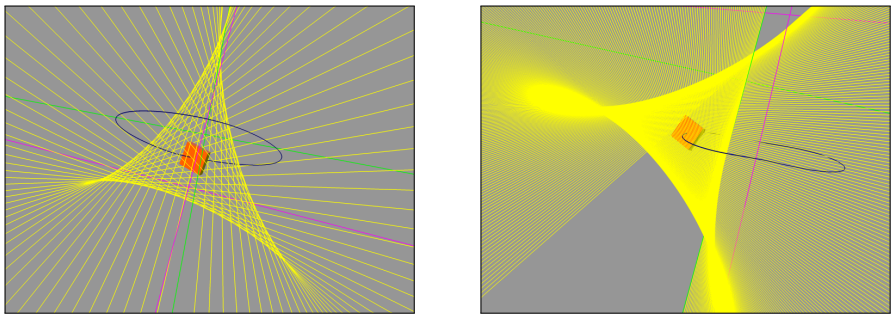

Fig. 11.13 Samples of polhode for rotationally symmetric body $(x, y, z, w) = (1, .25, 1, 1.3)$ in elliptic space. Figure on right is sampled 6 times more frequently than on left

.

After repeated observations of rotationally symmetric objects in hyperbolic space, the conjecture arose that the polhode (as a set of lines in $\mathbb{R}P^3$) envelops an egg-shaped surface centered on the center of mass and aligned with the inertial axes. Due to the rotational symmetry of the orbit, this egg shape also has rotational symmetry. We attempted to approximate this surface with an ellipsoid (interactively). Fig. 11.14 shows two views of the same approximation. The ratio of the axes of the approximating ellipsoid bear no immediately recognizable relationship to the moments of inertia of the object. It remains an open question, exactly which surface this is. Is it quadric or quartic, or neither? Here one requires probably methods for studying intersections of hypersurfaces in $\mathfrak{B}$ and the corresponding line set $\mathbb{R}P^3$.

11.5 Conclusion

This concludes the presentation of simulation and visualization results. In the survey presented here of rigid body motion, we have focused our attention on the varied behaviors which can be observed in force-free rigid body motion in non-euclidean space[1] As far as we know, these are the first such simulations and first such images that have been produced of non-euclidean rigid body motion. As noted in the introduction to this chapter, the corresponding Poinsot theory of motion is lacking. Such a phenomenological survey is nevertheless a useful research result if it stimulates others to activity towards such a theory. The visualization strategies presented here have been implemented without noteworthy difficulties using the metric-neutral scene graph provided by jReality. Among

[1] We have left the euclidean case to the side and used it mainly as a control for algorithm correctness.

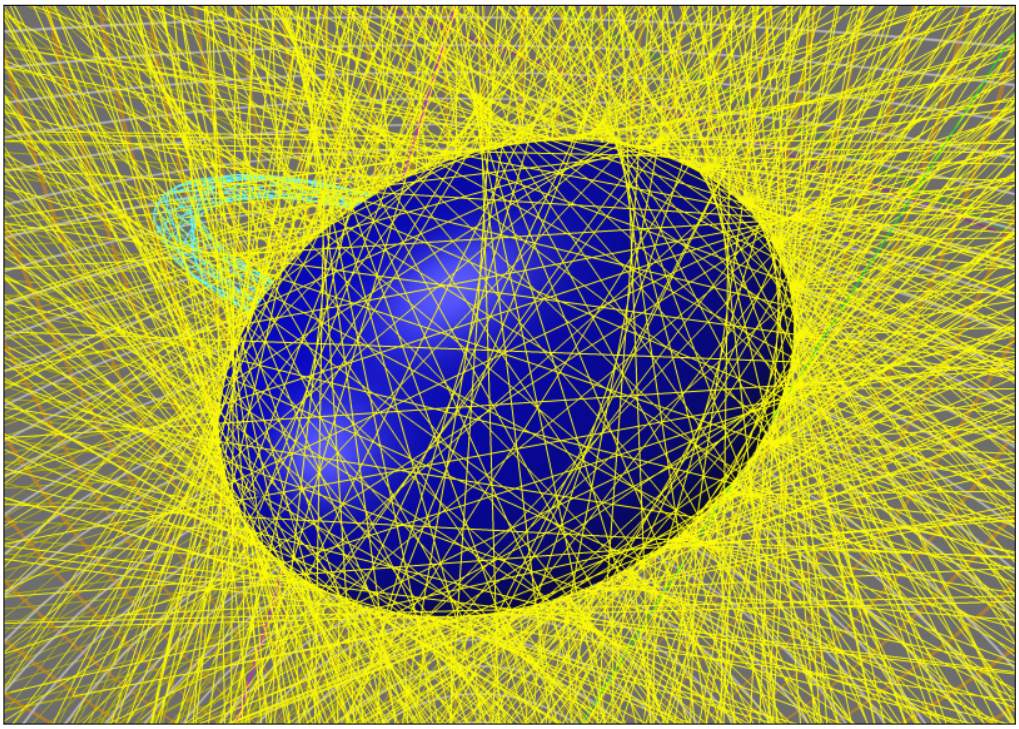

Fig. 11.14 A view of a the orbit of $\mathbf{\Omega}_c$ for a rotationally symmetric body in hyperbolic space with $(x, y, z, w) = (1, 1, .5, 1.2)$. The blue ellipsoid has been determined empirically to be tangent to all the yellow lines.

the visualization aspects, the theme of bivector visualization is particularly interesting. Much remains to be done in both the metric and projective setting.

Chapter 12
Conclusion

The goal, stated in the Forward, of modeling rigid body motion in spaces of constant curvature in dimensions 2 and 3, has been achieved. Based on this theory, simulations have been developed and images produced for the first time of how rigid bodies move in these non-euclidean spaces. Along the way to this goal, a series of related innovative results and tools, ranging from concrete to methodological, in a variety of geometric domains, have been established and discussed. In this chapter we provide an overview of these results.

12.1 Clifford algebras for Cayley-Klein geometries

Among other questions, Chapter 1 posed the question, whether it is possible to find algebraic structures similar to quaternions, for the Cayley-Klein geometries under consideration, and with possibly more powerful features.

We already noted in Remark 101 that Cl_1^2 contains the quaternions as an subalgebra, and furthermore extends the quaternions by including reflections via the operators $\underline{\mathbf{a}}$ for 1-vectors $\mathbf{a}$.

In fact, we have shown that the real, dual, projectivized Clifford algebras Cl_κ^n for $\kappa \in \{-1, 0, 1\}$ provide a faithful representation of the full (direct and indirect) isometry groups for the Cayley-Klein hyperbolic, euclidean, and elliptic geometries, resp. In Chapter 10 we saw that $\mathbf{P}(\mathbb{R}_{n,0,1})$ provides a similar structure for dual euclidean space, completing a family of four geometries that are closed under dualization. The resulting representations satisfy properties I-III of Sect. 1.3.1.

We noted in Chapter 4 that similar results can be obtained for the larger family of pseudo-euclidean geometries using the Clifford algebras $\mathbf{P}(\mathbb{R}^*_{p,m,1})$ and $\mathbf{P}(\mathbb{R}_{p,m,1})$. This class of geometries arose naturally from our definition in Chapter 3 of admissable quadric surfaces. A detailed treatment of all but the euclidean case, however, lies outside the scope of the current work.

12.2 Innovations

We also asked in Chapter 1 whether it is possible to generalize the quaternions in such a way that the resulting structures extend the functionality of the quaternions in other directions not related to the isometry group theory of the previous section. This study has established numerous such extensions. Here we give a brief review of the most important ones:

Geometry. The presence of the full exterior algebra allows the development of a rich metric geometric toolkit which the quaternion structure only offers in a restricted form. This representation exhibits a fundamental simplicity missing in linear algebra: the same entity that represents a geometric object (such as a plane) also represents the geometric transformation associated to it (in this case, the reflection in the plane). The detailed analysis of the geometric products in specific grades revealed a full gamut of geometric operations, both projective and metric. A series of examples were presented to show how these operations could be applied to familiar themes from metric geometry, such as orthogonal projection, distance and angle calculations, triangle centers, and more. In the euclidean case, particular attention was paid to the presence of a non-degenerate metric in the ideal plane. This fundamental aspect of euclidean geometry was shown to be faithfully represented in the algebra Cl_0^n.

Isometries. A further important theme was a thorough analysis of the pin and spin groups $\mathbf{Pin}_{+\kappa}^n$ and $\mathbf{Spin}_{+\kappa}^n$, which took advantage of the fact they consist of proper versors. For $n = 2$, the resulting exponential curves $e^{\boldsymbol{\Xi}}\mathbf{P}e^{-\boldsymbol{\Xi}}$ were illustrated and classified into six classes depending on metric and type of bivector (proper, ideal, improper). For $n = 3$, the concept of an *axis* of a rotor was defined, and led to a detailed algorithm for computing a logarithm of any rotor. Finally, an account of the continuous interpolation of the metric polarity was given.

Kinematics. Equipped with these powerful algebraic tools it was straightforward to produce a compact, metric-neutral representation of kinematics. One innovation was the decomposition of the vector field of a velocity state into a null polarity determined by the velocity state bivector, followed by the metric polarity. The derivation of the Lie bracket followed directly from the Leibniz rule applied to the geometric product form of the rotor operator $\underline{\mathbf{g}}$. One other innovation of the treatment was the discussion of dual kinematics, obtained in the non-euclidean spaces by polarizing the kinematic configuration on the metric quadric, and illustrating that in these spaces points and planes are equal citizens.

Dynamics. The treatment of dynamics followed standard approaches, such as found in [Arn78], but proceeded in a metric-neutral fashion, based in the dual, projectivized setting of the algebras Cl_κ^3. An innovative formulation of newtonian particles was presented, which we believe has much more in common with the theory of rigid bodies than existing treatments. A metric-neutral theory of rigid body motion was developed by building up rigid bodies out of such particles. Among the innovations presented was the handling of the inertia tensor as a separate Clifford algebra on the space of bivectors. The discussion of center of mass raised an important distinction with euclidean dynamics. This led to

another innovation, the "4-particle form" of the rigid body, a particularly simple canonical form for a rigid body. Finally, dual dynamics (analogous to the dual kinematics of the previous paragraph) was sketched out.

Visualization. Motivated by the example of Poinsot's work on the Euler top, one of the key visualization challenges addressed in this thesis is to provide 3-dimensional representations of the six-dimensional Lie groups and Lie algebras at work here. The theory of axes developed in Chapter 7 provided the key for representing both Lie group elements (rotors) and Lie algebra elements (bivectors). Further refinements of this approach were indicated in Chapter 11.

12.3 Advantages of our approach

Having established in the previous section the specific innovations contained in this thesis, in this section we change to focus to reflect on some *methodological* characteristics of this approach.

Advantages of the full algebra. While many of the results mentioned above can be also achieved within Cl^{n+}_{κ} alone (e. g., everything in [Stu03] belongs in this category), here the advantage of having the full algebra Cl^{3}_{κ} over the even subalgebra Cl^{3+}_{κ} reveals itself strongly. To begin with, the rotor operators $\underline{\mathbf{g}}$ operate uniformly on points, lines and planes. Furthermore, many of the fundamental entities and operations are defined in terms of points or planes:

- the null polarity: polar plane $\boldsymbol{\Xi} \vee \mathbf{P}$ and polar point $\boldsymbol{\Xi} \wedge \mathbf{a}$ (Sect. 7.3.1),
- the vector field associated to a bivector (Sect. 8.4), and
- the velocity and momentum of newtonian particles (Sect. 9.2).

Projective elements. The central position of the Cayley-Klein construction in this thesis implies naturally that projective geometry plays an important role. Over and above this necessary significance, we have striven to clearly delineate the role of projective geometry throughout the exposition. The use of Poincaré duality to implement the join operator in the Grassmann algebra can be seen as an aspect of these efforts. This departure from the prevailing metric approach was discussed in Sect. 5.10.

A specific, innovative thread in the investigation has been the role of purely projective elements within kinematics and dynamics. We mention here a few of the places where this projective principle reveals itself:

- the null polarity interpretation of the vector field associated to a global velocity state (Sect. 8.5),
- the condition for equilibrium of a force system (Sect. 9.1), and
- the definition of work (Sect. 9.7.1).

In all these cases, the underlying formula involves some purely projective condition in $\mathfrak{B}$. The first case features the composition of a skew polarity (the null polarity) and a

symmetric polarity (the metric polarity) to produce the vector field of a global velocity state. In the second case, the condition is that the set of weighted force bivectors sum to zero, regardless of metric. Finally, the last case asserts that the rate of change of the kinetic energy is equal to the wedge product ($\vee$) of the force bivector and the velocity bivector. This is, again, a non-metric value that depends only on the relative position of the bivectors in $\mathfrak{B}$.

A new light on euclidean geometry. Finally, this research throws a fresh and interesting light on euclidean geometry. By imbedding it in a continuous family of non-euclidean geometries (as described in Sect. 10.4), one is presented with the phenomena of euclidean geometry in a new, comparative setting. A certain class of phenomena, wider than commonly thought – as indicated in the previous paragraph – are projective and hence shared by the whole family. Against this projective background, one is confronted by a triad of qualitatively distinct geometries. On the one side there is hyperbolic geometry, with an ideal sphere separating it from the improper elements, which form, independently, polar hyperbolic geometry. On the other hand, elliptic geometry has neither ideal nor improper elements. In between, euclidean geometry has an ideal plane but no improper elements. And, in this ideal plane, we focused on the unexpected but crucial presence of an elliptic metric on ideal points (Sect. 4.4.4) and showed how it is accommodated by the Clifford algebras we use. Finally, to complete the family of geometries, Chapter 10 introduced dual euclidean geometry, characterized by an ideal point, along with an elliptic metric on its lines and planes.

Metric-neutral toolkit for geometric research and development. The main mathematical structures used to achieve the description of rigid body motion are the dual, projectivized real Clifford algebras $\mathbf{P}(\mathbb{R}^*_{n+1,0,0})$, $\mathbf{P}(\mathbb{R}^*_{n,1,0})$, and $\mathbf{P}(\mathbb{R}^*_{n,0,1})$ for $n = 2$ and $n = 3$. A wide variety of results for these algebras flowed into the earlier chapters of this thesis, providing the framework in which the solution of the rigid body motion challenge was possible in a compact, elegant, and metric-neutral fashion. Such a self-contained, integrated framework for metric geometry, kinematics, and dynamics of the classical Cayley-Klein geometries has no counterpart that we are aware of in the existing literature or praxis.

References

[Abl86] Rafel Ablamowitz. Structure of spin groups associated with degenerate clifford algebras. *J. Math. Phys.*, 27:1–6, 1986.

[Ada34] George Adams. *Strahlende Weltgestaltung*. Mathematisches-Astronomisches Sektion am Goetheanum, 1934.

[Ada59] George Adams. *Universalkräfte in der Mechanik*, volume 20 of *Mathematisch-astronomische Blätter*. Verlag am Goetheanum, Dornach, 1959.

[Arn78] V. I. Arnold. *Mathematical Methods of Classical Physics*. Springer-Verlag, New York, 1978. Appendix 2.

[AW80] George Adams and Olive Whicher. *The Plant Between Earth and Sun*. Rudolf Steiner Press, London, 1980.

[Bac59] F. Bachmann. *Aufbau der Geometrie aus dem Spiegelungsbegriff*. Springer, 1959.

[Bal00] Robert Ball. *A Treatise on the Theory of Screws*. Cambridge University Press, Cambridge, 1900.

[Bla38] Wilhelm Blaschke. *Ebene Kinematik*. Tuebner, Leibzig, 1938.

[Bla42] Wilhelm Blaschke. *Nicht-euklidische Geometrie und Mechanik*. Teubner, Leipzig, 1942.

[Bla54] Wilhelm Blaschke. *Analytische Geometrie*. Birkhauser, Basel, 1954.

[BM97] Garrett Birkhoff and Sanders MacLane. *A Survey of Modern Algebra*. A. K. Peters, Wellesley, Massachusetts, 1997.

[Bou89] Nicolas Bourbaki. *Elements of mathematics, Algebra I*. Springer Verlag, 1989.

[Cay59] Arthur Cayley. A sixth memoir upon the quantics. *Phil. Trans. Royal Soc. London, Series A*, 149:61–90, 1859.

[Cli82a] William Clifford. *Mathematical Papers*. MacMillan, London, 1882.

[Cli82b] William Clifford. Motion of a solid in elliptic space. In *Mathematical Papers*, pages 378–385. MacMillan, London, 1882.

[Cli82c] William Clifford. A preliminary sketch of biquaternions. In *Mathematical Papers*, pages 181–200. MacMillan, London, 1882.

[Con08] Oliver Conradt. *Mathematical Physics in Space and Counterspace*. Verlag am Goetheanum, 2008.

[Cox87] H.M.S. Coxeter. *Projective Geometry*. Springer-Verlag, New York, 1987.

[dF02] Domenico de Francesco. Sui moto di un corpo rigido in uno spazio di curvatura constante. *Mathematische Annalen*, 55:573–584, 1902.

[DFM07] Leo Dorst, Daniel Fontijne, and Stephen Mann. *Geometric Algebra for Computer Science*. Morgan Kaufmann, San Francisco, 2007.

[DL03] Chris Doran and Anthony Lasenby. *Geometric Algebra for Physicists*. Cambridge University Press, Cambridge, 2003.

[Fea07] Roy Featherstone. *Rigid Body Dynamics Algorithms*. Springer, 2007.

[Gie82] Oswald Giering. *Vorlesungen über höhere Geometrie*. Friedr. Vieweg, Braunschweig/Wiesbaden, 1982.

[Gra44] Hermann Grassmann. *Ausdehnungslehre*. Otto Wigand, Leipzig, 1844.
[Gre67a] W. H. Greub. *Linear Algebra*. Springer, 1967.
[Gre67b] W. H. Greub. *Multilinear Algebra*. Springer, 1967.
[Gsc91] Peter Gschwind. *Der lineare Komplex – eine überimaginäre Zahl*, volume 4 of *Mathematisch-astronomische Blätter*. Verlag am Goetheanum, 1991.
[Gun93] Charles Gunn. Discrete groups and the visualization of three-dimensional manifolds. In *SIGGRAPH 1993 Proceedings*, pages 255–262. ACM SIGGRAPH, ACM, 1993.
[Gun10] Charles Gunn. Advances in Metric-neutral Visualization. In Vaclav Skala and Eckhard Hitzer, editors, *GraVisMa 2010*, pages 17–26, Brno, 2010. Eurographics, `http://gravisma.zcu.cz/GraVisMa-2010/GraVisMa-2010-proceedings.pdf`.
[Gun11] Charles Gunn. On the homogeneous model of euclidean geometry. In Leo Dorst and Joan Lasenby, editors, *A Guide to Geometric Algebra in Practice*, chapter 15, pages 297–327. Springer, 2011.
[Hea84] R. S. Heath. On the dynamics of a rigid body in elliptic space. *Phil. Trans. Royal Society of London*, 175:281–324, 1884.
[Hes10] David Hestenes. New tools for computational geometry and rejuvenation of screw theory. In Eduardo Jose Bayro-Corrochano and Gerik Scheuermann, editors, *Geometric Algebra Computing in Engineering and Computer Science*, pages 3–35. Springer, 2010.
[Hit03] Nigel Hitchin. *Projective Geometry*. `http://people.maths.ox.ac.uk/hitchin/hitchinnotes/Projective_geometry/Chapter_3_Exterior.pdf`, 2003.
[HS87] David Hestenes and Garret Sobczyk. *Clifford Algebra to Geometric Calculus*. Fundamental Theories of Physics. Reidel, Dordrecht, 1987.
[HZ91] David Hestenes and Renatus Ziegler. Projective geometry with clifford algebra. *Acta Applicandae Mathematicae*, 23:25–63, 1991.
[jr06] jreality, 2006. `http://www.jreality.de`.
[Kle71] Felix Klein. Notiz, betreffend den Zusammenhang der Liniengeometrie mit der Mechanik der starrer Körper. *Mathematische Annalen*, 4:403–415, 1871.
[Kle72] Felix Klein. Über Liniengeometrie und metrische Geometrie. *Mathematische Annalen*, 5:106–126, 1872.
[Kle26] Felix Klein. *Vorlesungen Über Nicht-euklidische Geometrie*. Chelsea, New York, 1926. (Original 1926, Berlin).
[Kle27] Felix Klein. *Vorlesungen Über Höhere Geometrie*. Chelsea, New York, 1927.
[Kow09] Gerhard Kowol. *Projektive Geometrie und Cayley-Klein Geometrien der Ebene*. Birkhauser, 2009.
[LE70] Louis Locher-Ernst. *Geometrische Metamorphosen*. Verlag am Goetheanum, Dornach, Switzerland, 1970.
[Lin73] F. Lindemann. Über unendlich kleine Bewegungen und über Kraftsysteme bei allgemeiner projektivischer Massbestimmung. *Mathematische Annalen*, 7:56–144, 1873.
[Lou01] Pertti Lounesto. *Clifford Algebras and Spinors*. Cambridge University Press, 2001.
[McC90] J. Michael McCarthy. *An Introduction to Theoretical Kinematics*. MIT Press, Cambridge, MA, 1990.
[Möb37] A. F. Möbius. *Lehrbuch der Statik*. Göschen, Leibzig, 1837.
[MR98] Jerold Marsden and Tudor S. Ratu. *Introduction to Mechanics and Symmetry: A Basic Exposition of Classical Mechanical Systems*. Springer, New York, 1998.
[Per09] Christian Perwass. *Geometric Algebra with Applications to Engineering*. Springer, 2009.
[Plu68] Julius Pluecker. *Neue Geometrie des Raumes*. Düsseldorf, 1868.
[Poi51] Louis Poinsot. *Thorie nouvelle de la rotation des corps*. Bachelier, 1851.
[Poi84] Louis Poinsot. *Outlines of a new theory of rotatory motion*. Cambridge, 1884. Translation of Poinsot 1851.
[Por81] Ian Porteous. *Topological Geometry*. Cambridge University Press, Cambridge, 1981.
[PW01] Helmut Pottmann and Johannes Wallner. *Computational Line Geometry*. Springer, Berlin, 2001.
[Rat82] Tudor Ratiu. Euler-poisson equations on lie algebras and the n-dimensional heavy rigid body. *American Journal of Mathematics*, 104-2:409–448, 1982.

[Sel] Jon Selig. Personal communication.

[Sel00] Jon Selig. Clifford algebra of points, lines, and planes. *Robotica*, 18:545–556, 2000.

[Sel05] Jon Selig. *Geometric Fundamentals of Robotics*. Springer, 2005.

[Spe63] Emanual Sperner. *Einführung in die Analytische Geometrie und Algebra*, volume 2. Vandenhoeck & Ruprecht, Göttingen, 1963.

[SS04] Horst Struve and Rolf Struve. Projective spaces with cayley-klein metrics. *Journal of Geometry*, 81:155–167, 2004.

[Sto09] Hanns-Jörg Stoß. *Koordinaten im projektiven Raum*, volume 27 of *Mathematisch-astronomische Blätter*. Verlag am Goetheanum, Dornach, 2009.

[Stu91] Eduard Study. Von den Bewegungen und Umlegungen. *Mathematische Annalen*, 39:441–566, 1891.

[Stu03] Eduard Study. *Geometrie der Dynamen*. Tuebner, Leibzig, 1903.

[Tho09] Nick Thomas. *Space and Counterspace: A New Science of Gravity, Time and Light*. Floris Books, London, 2009.

[TL97] William Thurston and Silvio Levy. *Three-Dimensional Geometry and Topology: Volume 1*. Princeton University Press, 1997.

[vM24] Richard von Mises. Die Motorrechnung: Eine Neue Hilfsmittel in der Mechanik. *Zeitschrift für Rein und Angewandte Mathematik und Mechanik*, 4(2):155–181, 1924.

[Wei35] Ernst August Weiss. *Einführung in die Liniengeometrie und Kinematik*. Teubner, Leibzig, 1935.

[WGH+09] S. Weissmann, C. Gunn, T. Hoffmann, P. Brinkmann, and U. Pinkall. jreality: a java library for real-time interactive 3d graphics and audio. In *Proceedings of 17th International ACM Conference on Multimedia 2009*, pages 927–928, (Oct. 19-24, Beijing, China), 2009.

[Whi98] A. N. Whitehead. *A Treatise on Universal Algebra*. Cambridge University Press, 1898.

[Wik] Wikipedia. `http://en.wikipedia.org/wiki/Exterior_algebra`.

[Zie85] Renatus Ziegler. *Die Geschichte Der Geometrischen Mechanik im 19. Jahrhundert*. Franz Steiner Verlag, Stuttgart, 1985.